

Methods in  
Molecular Biology 1600

Springer Protocols

Otto Holst *Editor*

# Microbial Toxins

Methods and Protocols

*Second Edition*

 Humana Press

# METHODS IN MOLECULAR BIOLOGY

*Series Editor*  
**John M. Walker**  
**School of Life and Medical Sciences**  
**University of Hertfordshire**  
**Hatfield, Hertfordshire, AL10 9AB, UK**

For further volumes:  
<http://www.springer.com/series/7651>

# Microbial Toxins

## Methods and Protocols

### Second Edition

Edited by

**Otto Holst**

*Research Center Borstel, Leibniz-Center for Medicine and Biosciences,  
Borstel, Schleswig-Holstein, Germany*

 **Humana Press**

*Editor*

Otto Holst  
Research Center Borstel  
Leibniz-Center for Medicine and Biosciences  
Borstel, Schleswig-Holstein, Germany

ISSN 1064-3745                      ISSN 1940-6029 (electronic)  
Methods in Molecular Biology  
ISBN 978-1-4939-6956-2            ISBN 978-1-4939-6958-6 (eBook)  
DOI 10.1007/978-1-4939-6958-6

Library of Congress Control Number: 2017937053

© Springer Science+Business Media LLC 2017

This work is subject to copyright. All rights are reserved by the Publisher, whether the whole or part of the material is concerned, specifically the rights of translation, reprinting, reuse of illustrations, recitation, broadcasting, reproduction on microfilms or in any other physical way, and transmission or information storage and retrieval, electronic adaptation, computer software, or by similar or dissimilar methodology now known or hereafter developed.

The use of general descriptive names, registered names, trademarks, service marks, etc. in this publication does not imply, even in the absence of a specific statement, that such names are exempt from the relevant protective laws and regulations and therefore free for general use.

The publisher, the authors and the editors are safe to assume that the advice and information in this book are believed to be true and accurate at the date of publication. Neither the publisher nor the authors or the editors give a warranty, express or implied, with respect to the material contained herein or for any errors or omissions that may have been made. The publisher remains neutral with regard to jurisdictional claims in published maps and institutional affiliations.

Printed on acid-free paper

This Humana Press imprint is published by Springer Nature  
The registered company is Springer Science+Business Media LLC  
The registered company address is: 233 Spring Street, New York, NY 10013, U.S.A.

---

## Preface

In the year 2000, a first methods collection entitled *Bacterial Toxins: Methods and Protocols* was published which contained 20 chapters on protein toxins and endotoxin from bacteria and cyanobacteria. Then, in 2011, a next such collection was published, entitled *Microbial Toxins: Methods and Protocols*, which included both, protocols on (cyano)bacterial and mold fungus toxins, with some focus on aflatoxins. In both cases, the idea was to support researchers of various scientific disciplines with detailed descriptions of state-of-the-art protocols and, since the books turned out to be quite successful, it is quite obvious that this aim could be achieved. Based on this success, a second volume entitled *Microbial Toxins: Methods and Protocols* is presented now which contains protocols on (cyano)bacterial and mold fungus toxins, with a rather strong focus on Gram-negative endotoxins (lipopolysaccharides).

The interest of researchers across a broad spectrum of scientific disciplines in the field of microbial toxins is clearly unbroken. As many other fields do, this field makes use of a broad variety of biological, chemical, physical, and medical approaches, and researchers dealing with any microbial toxin should be familiar with various techniques from all these disciplines. It is our hope that the book *Microbial Toxins: Methods and Protocols, Second Edition* can strongly support researchers here.

*Microbial Toxins: Methods and Protocols, Second Edition* comprises 17 chapters presenting state-of-the-art techniques that are described by authors who have regularly been using the protocol in their own laboratories. Each chapter begins with a brief introduction to the method which is followed by a step-by-step description of the particular method. Also, and importantly, all chapters possess a Notes section in which e.g. difficulties, modifications and limitations of the techniques are exemplified. Taken together, our volume should prove useful to many scientists, including those without any previous experience with a particular technique.

*Borstel, Schleswig-Holstein, Germany*

*Otto Holst*

---

## Contents

<i>Preface</i> . . . . .	<i>v</i>
<i>Contributors</i> . . . . .	<i>ix</i>
1 Detection of Cholera Toxin by an Immunochromatographic Test Strip . . . . . <i>Eiki Yamasaki, Ryuta Sakamoto, Takashi Matsumoto, Biswajit Maiti, Kayo Okumura, Fumiki Morimatsu, G. Balakrish Nair, and Hisao Kurazono</i>	1
2 Electrochemical Aptamer Scaffold Biosensors for Detection of Botulism and Ricin Proteins . . . . . <i>Jessica Daniel, Lisa Fetter, Susan Jett, Teisha J. Rowland, and Andrew J. Bonham</i>	9
3 A Cell-Based Fluorescent Assay to Detect the Activity of AB Toxins that Inhibit Protein Synthesis . . . . . <i>Patrick Cherubin, Beatriz Quiñones, Salem Elkahoui, Wallace Yokoyama, and Ken Teter</i>	25
4 Molecular Methods for Identification of <i>Clostridium tetani</i> by Targeting Neurotoxin. . . . . <i>Basavraj Nagoba, Mahesh Dharne, and Kushal N. Gobil</i>	37
5 Label-Free Immuno-Sensors for the Fast Detection of <i>Listeria</i> in Food . . . . . <i>Alexandra Morlay, Agnès Roux, Vincent Templier, Félix Piat, and Yoann Roupiez</i>	49
6 Aptamer-Based Trapping: Enrichment of <i>Bacillus cereus</i> Spores for Real-Time PCR Detection . . . . . <i>Christin Fischer and Markus Fischer</i>	61
7 Detection of <i>Yersinia pestis</i> in Complex Matrices by Intact Cell Immunocapture and Targeted Mass Spectrometry. . . . . <i>Jérôme Chenau, François Fenaille, Stéphanie Simon, Sofia Filali, Hervé Volland, Christophe Junot, Elisabeth Carniel, and François Becher</i>	69
8 A Method to Prepare Magnetic Nanosilicate Platelets for Effective Removal of <i>Microcystis aeruginosa</i> and Microcystin-LR . . . . . <i>Shu-Chi Chang, Bo-Li Lu, Jiang-Jen Lin, Yen-Hsien Li, and Maw-Rong Lee</i>	85
9 An Immunochromatographic Test Strip to Detect Ochratoxin A and Zearalenone Simultaneously . . . . . <i>Xiaofei Hu and Gaiping Zhang</i>	95
10 Endotoxin Removal from <i>Escherichia coli</i> Bacterial Lysate Using a Biphasic Liquid System. . . . . <i>Janusz Boratyński and Bożena Szermer-Olearnik</i>	107

11	Fourier Transform Infrared Spectroscopy as a Tool in Analysis of <i>Proteus mirabilis</i> Endotoxins . . . . .	113
	<i>Paulina Żarnowiec, Grzegorz Czerwonka, and Wiesław Kaca</i>	
12	Laser Interferometry Method as a Novel Tool in Endotoxins Research . . . . .	125
	<i>Michał Arabski and Sławomir Wąsik</i>	
13	Endotoxin Entrapment on Glass via C-18 Self-Assembled Monolayers and Rapid Detection Using Drug-Nanoparticle Bioconjugate Probes . . . . .	133
	<i>Prasanta Kalita, Anshuman Dasgupta, and Shalini Gupta</i>	
14	A Bioassay for the Determination of Lipopolysaccharides and Lipoproteins . . .	143
	<i>Marcus Peters, Petra Bonowitz, and Albrecht Bufe</i>	
15	Capillary Electrophoresis Chips for Fingerprinting Endotoxin Chemotypes and Subclasses. . . . .	151
	<i>Béla Kocsis, Lilla Makszin, Anikó Kilár, Zoltán Péterfi, and Ferenc Kilár</i>	
16	Micromethods for Isolation and Structural Characterization of Lipid A, and Polysaccharide Regions of Bacterial Lipopolysaccharides . . . . .	167
	<i>Alexey Novikov, Aude Breton, and Martine Caroff</i>	
17	Mass Spectrometry for Profiling LOS and Lipid A Structures from Whole-Cell Lysates: Directly from a Few Bacterial Colonies or from Liquid Broth Cultures . . . . .	187
	<i>Béla Kocsis, Anikó Kilár, Szandra Péter, Ágnes Dörnyei, Viktor Sándor, and Ferenc Kilár</i>	
	<i>Index</i> . . . . .	199

---

## Contributors

- MICHAŁ ARABSKI • *Department of Microbiology, Jan Kochanowski University, Kielce, Poland*
- G. BALAKRISH NAIR • *World Health Organization, Mahatma Gandhi Marg, Indraprastha Estate, New Delhi, India*
- FRANÇOIS BECHER • *CEA, iBiTec-S, Service de Pharmacologie et d'Immunoanalyse, Gif-sur-Yvette, France*
- ANDREW J. BONHAM • *Department of Chemistry, Metropolitan State University of Denver, Denver, CO, USA*
- PETRA BONOWITZ • *Department of Experimental Pneumology, Ruhr University Bochum, Bochum, Germany*
- JANUSZ BORATYŃSKI • *Laboratory of Biomedical Chemistry - "Neolek," Ludwik Hirszfeld Institute of Immunology and Experimental Therapy, Polish Academy of Sciences, Wrocław, Poland*
- AUDE BRETON • *LPS-BioSciences, Institute for Integrative Biology of the Cell (I2BC), CEA, CNRS, Université Paris-Sud, Université Paris-Saclay, Orsay, France*
- ALBRECHT BUFE • *Department of Experimental Pneumology, Ruhr University Bochum, Bochum, Germany*
- ELISABETH CARNIEL • *Institut Pasteur, Unité de Recherche Yersinia, Paris, France*
- MARTINE CAROFF • *LPS-BioSciences, Institute for Integrative Biology of the Cell (I2BC), CEA, CNRS, Université Paris-Sud, Université Paris-Saclay, Orsay, France*
- SHU-CHI CHANG • *Department of Environmental Engineering, National Chung Hsing University, Taichung, Taiwan*
- JÉRÔME CHENAU • *CEA, iBiTec-S, Service de Pharmacologie et d'Immunoanalyse, Gif-sur-Yvette, France*
- PATRICK CHERUBIN • *Burnett School of Biomedical Sciences, College of Medicine, University of Central Florida, Orlando, FL, USA*
- GRZEGORZ CZERWONKA • *Department of Microbiology, Jan Kochanowski University, Kielce, Poland*
- JESSICA DANIEL • *Department of Chemistry, Metropolitan State University of Denver, Denver, CO, USA*
- ANSHUMAN DASGUPTA • *Department of Nanomedicine and Theranostics, Institute for Experimental Molecular Imaging, RWTH Aachen University Clinic, Aachen, Germany*
- MAHESH DHARNE • *NCIM Resource Centre, CSIR-National Chemical Laboratory (NCL), Pune, Maharashtra, India*
- ÁGNES DÖRNYEI • *Department of Analytical and Environmental Chemistry, University of Pécs, Pécs, Hungary*
- SALEM ELKAHOUI • *Laboratoire des Substances Bioactives, Le Centre de Biotechnologie à la Technopole de Borj-Cédria, Hammam-Lif, Tunisia*
- FRANÇOIS FENAILLE • *CEA, iBiTec-S, Service de Pharmacologie et d'Immunoanalyse, Gif-sur-Yvette, France*



- LISA FETTER • *Department of Chemistry, Metropolitan State University of Denver, Denver, CO, USA*
- SOFIA FILALI • *Institut Pasteur, Unité de Recherche Yersinia, Paris, France*
- MARKUS FISCHER • *Hamburg School of Food Science, Institute of Food Chemistry, University of Hamburg, Hamburg, Germany*
- CHRISTIN FISCHER • *Hamburg School of Food Science, Institute of Food Chemistry, University of Hamburg, Hamburg, Germany*
- KUSHAL N. GOHIL • *NCIM Resource Centre, CSIR- National Chemical Laboratory (NCL), Pune, Maharashtra, India*
- SHALINI GUPTA • *Department of Chemical Engineering, Indian Institute of Technology, Delhi, India*
- XIAOFEI HU • *Henan Academy of Agriculture Science/Key Laboratory of Animal Immunology, Ministry of Agriculture/Henan Key Laboratory of Animal Immunology, Zhengzhou, China*
- SUSAN JETT • *Department of Chemistry, Metropolitan State University of Denver, Denver, CO, USA*
- CHRISTOPHE JUNOT • *CEA, iBiTec-S, Service de Pharmacologie et d'Immunoanalyse, Gif-sur-Yvette, France*
- WIESŁAW KACA • *Department of Microbiology, Jan Kochanowski University, Kielce, Poland*
- PRASANTA KALITA • *Department of Chemical Engineering, Indian Institute of Technology, Delhi, India*
- FERENC KILÁR • *Institute of Bioanalysis, Faculty of Medicine and Szentágotthai Research Center, University of Pécs, Pécs, Hungary*
- ANIKÓ KILÁR • *MTA-PTE, Molecular Interactions in Separation Science Research Group, Pécs, Hungary*
- BÉLA KOCSIS • *Institute of Medical Microbiology and Immunology Faculty of Medicine, University of Pécs, Pécs, Hungary*
- HISAO KURAZONO • *Division of Food Hygiene, Department of Animal and Food Hygiene, Obihiro University of Agriculture and Veterinary Medicine, Obihiro, Hokkaido, Japan*
- MAW-RONG LEE • *Department of Chemistry, National Chung Hsing University, Taichung, Taiwan*
- YEN-HSIEN LI • *Department of Chemistry, National Chung Hsing University, Taichung, Taiwan*
- JIANG-JEN LIN • *Institute of Polymer Science and Engineering, National Taiwan University, Taipei, Taiwan*
- BO-LI LU • *Department of Environmental Engineering, National Chung Hsing University, Taichung, Taiwan*
- BISWAJIT MAITI • *Division of Food Hygiene, Department of Animal and Food Hygiene, Obihiro University of Agriculture and Veterinary Medicine, Obihiro, Hokkaido, Japan*
- LILLA MAKSZIN • *Institute of Bioanalysis, Faculty of Medicine, University of Pécs, Pécs, Hungary*
- TAKASHI MATSUMOTO • *R&D Center, NH Foods Ltd., Ibaraki, Japan*
- FUMIKI MORIMATSU • *Center for Regional Collaboration in Research and Education, Obihiro University of Agriculture and Veterinary Medicine, Obihiro, Hokkaido, Japan*
- ALEXANDRA MORLAY • *University Grenoble Alpes, SyMMES UMR 5819, CNRS, SyMMES UMR 5819, CEA, SyMMES UMR 5819, Grenoble, France*
- BASAVRAJ NAGOBA • *Maharashtra Institute of Medical Sciences & Research (Medical College), Latur, Maharashtra, India*

- ALEXEY NOVIKOV • *LPS-BioSciences, Institute for Integrative Biology of the Cell (I2BC), CEA, CNRS, Université Paris-Sud, Université Paris-Saclay, Orsay, France*
- KAYO OKUMURA • *Division of Food Hygiene, Department of Animal and Food Hygiene, Obihiro University of Agriculture and Veterinary Medicine, Obihiro, Hokkaido, Japan*
- SZANDRA PÉTER • *Department of Analytical and Environmental Chemistry, University of Pécs, Pécs, Hungary*
- ZOLTÁN PÉTERFI • *First Department of Internal Medicine, Infectology, Faculty of Medicine, University of Pécs, Pécs, Hungary*
- MARCUS PETERS • *Department of Experimental Pneumology, Ruhr University Bochum, Bochum, Germany*
- FÉLIX PIAT • *Prestodiag, Villejuif, France*
- BEATRIZ QUIÑONES • *USDA-ARS, Produce Safety and Microbiology Research Unit, Western Regional Research Center, Albany, CA, USA*
- YOANN ROUPIOZ • *University Grenoble Alpes, SyMMES UMR 5819, CNRS, SyMMES UMR 5819, CEA, SyMMES UMR 5819, Grenoble, France*
- AGNÈS ROUX • *University Grenoble Alpes, SyMMES UMR 5819, CNRS, SyMMES UMR 5819, CEA, SyMMES UMR 5819, Grenoble, France*
- TEISHA J. ROWLAND • *Cardiovascular Institute and Adult Medical Genetics Program, University of Colorado Denver Anschutz Medical Campus, Aurora, CO, USA*
- RYUTA SAKAMOTO • *R&D Center, NH Foods Ltd., Ibaraki, Japan*
- VIKTOR SÁNDOR • *Faculty of Medicine, Szentágotthai Research Center, Institute of Bioanalysis, University of Pécs, Pécs, Hungary*
- STÉPHANIE SIMON • *CEA, iBiTec-S, Service de Pharmacologie et d'Immunoanalyse, Gif-sur-Yvette, France*
- BOŻENA SZERMER-OLEARNIK • *Laboratory of Biomedical Chemistry - "Neolek," Ludwik Hirszföld Institute of Immunology and Experimental Therapy, Polish Academy of Sciences, Wrocław, Poland*
- VINCENT TEMPLIER • *University Grenoble Alpes, SyMMES UMR 5819, CNRS, SyMMES UMR 5819, CEA, SyMMES UMR 5819, Grenoble, France*
- KEN TETER • *Burnett School of Biomedical Sciences, College of Medicine, University of Central Florida, Orlando, FL, USA*
- HERVÉ VOLLAND • *CEA, iBiTec-S, Service de Pharmacologie et d'Immunoanalyse, Gif-sur-Yvette, France*
- SŁAWOMIR WAŚIK • *Department of Molecular Physics, Jan Kochanowski University, Kielce, Poland*
- EIKI YAMASAKI • *Division of Food Hygiene, Department of Animal and Food Hygiene, Obihiro University of Agriculture and Veterinary Medicine, Obihiro, Hokkaido, Japan*
- WALLACE YOKOYAMA • *USDA-ARS, Healthy Processed Foods Research Unit, Western Regional Research Center, Albany, CA, USA*
- PAULINA ŻARNOWIEC • *Department of Microbiology, Jan Kochanowski University, Kielce, Poland*
- GAIPING ZHANG • *Henan Academy of Agricultural Science/Key Laboratory of Animal Immunology, Ministry of Agriculture/Henan Key Laboratory of Animal Immunology, Zhengzhou, China*

# Chapter 1

## Detection of Cholera Toxin by an Immunochromatographic Test Strip

Eiki Yamasaki, Ryuta Sakamoto, Takashi Matsumoto, Biswajit Maiti, Kayo Okumura, Fumiki Morimatsu, G. Balakrish Nair, and Hisao Kurazono

### Abstract

As cholera toxin (CT) is responsible for most of the symptoms induced by *Vibrio cholerae* O1 or O139 infection, detection of CT is an important biomarker for diagnosis of the disease. The procedure for pathogenicity analysis of *V. cholerae* isolates must be carefully developed for the reason that the amount of CT produced by *V. cholerae* varies according to the medium used and culture conditions (i.e. temperature and aeration status) applied. Here we describe a reproducible rapid method for analysis of CT production by toxigenic *V. cholerae* with an immunochromatographic test strip that can detect as low as 10 ng/mL of purified recombinant CT.

**Key words** Immunochromatographic test strip, *V. cholerae*, Cholera toxin, Toxigenicity, Rapid diagnostic tests, AKI medium

---

## 1 Introduction

Cholera remains a major public health problem, especially in developing countries, and the seventh pandemic of cholera, which began in 1961 is still ongoing. In the case of diagnosis of cholera, after or along with the detection of the causative agent *Vibrio cholerae*, verification of cholera toxin (CT) production is of added significance, because only *V. cholerae* produces CT which is responsible for cholera symptoms such as acute “rice watery” diarrhea. Various methods, including immunoassays like immunochromatography (IC), enzyme-linked immunosorbent assay (ELISA), reversed passive latex agglutination (RPLA) etc., DNA-based assays like polymerase chain reaction (PCR), quantitative PCR (qPCR), loop mediated isothermal amplification (LAMP) etc., and bioassays including rabbit ileal loop test, rabbit skin test, cultured Chinese hamster ovary (CHO) cell assay, etc. for toxigenicity investigation of *V. cholerae* isolates have been established [1, 2]. Such immunoassays and DNA-based assays contribute to the rapid detection of CT and facilitate

timely, in some cases, on-site responses. While DNA-based assays may be more sensitive than immunoassays, the latter have an important advantage for the detection of extracellular bacterial toxin and analysis of the toxin expression level. Recently, some novel methodology of immunoassays with extremely high sensitivity has been reported [3, 4]. However, IC is still one of the most commonly utilized immunoassay because it is rapid and very easy to conduct. When IC is used, careful consideration has to be given to the way samples are prepared to allow an optimal production of the target protein.

Previously, we have established a toxigenic *V. cholerae*-specific immunochromatographic test strip (CT-IC) [5] which could detect CT in *V. cholerae* cultures in which at least 10 ng/mL of CT was expressed. The amount of CT produced in *V. cholerae* El Tor, which is the causative bacterium of the ongoing 7<sup>th</sup> cholera pandemic varies according to the medium used and culture conditions (i.e. temperature and aeration status), and the optimal condition is significantly different from that for the classical biotype which was responsible for the earlier cholera pandemics [6–9]. The AKI medium is one of the most efficient media to induce CT expression in *V. cholerae* El Tor. It was reported that if *V. cholerae* El Tor strains were cultured in AKI medium under biphasic culture conditions, i.e. 4 h cultivation in a stationary phase followed by 16 h cultivation in a shaking flask at 37 °C, most of the strains produced more than 10 ng/mL of CT [8]. Therefore, the combination of CT-IC with AKI medium is advantageous in analyzing the ability of *V. cholerae* isolates to produce CT.

---

## 2 Materials

Prepare all media and solutions using ultrapure water (deionized) at room temperature.

### 2.1 Culture Media

1. 5% NaHCO<sub>3</sub>: Weigh 1.5 g NaHCO<sub>3</sub> and transfer to the cylinder. Add distilled water to a volume of 20 mL. Dissolve all powder of NaHCO<sub>3</sub> completely. Make up to 30 mL with additional distilled water. Filter the solution by using DISMIC Mixed Cellulose Ester Syringe Filter Unit (25AS Type) having a pore size of 0.45 μm (Advantec Co. Ltd.) immediately before use (*see Note 1*).
2. AKI medium: Weigh 4.5 g of Bacto™ Peptone, 1.2 g of yeast extract and 1.5 g of NaCl and transfer to 300 mL glass beaker containing about 200 mL of distilled water. Dissolve all powder completely. Transfer the solution to 300 mL graduated cylinder and make up to 282 mL with distilled water. Transfer the solution into the autoclavable container and sterilize the

solution with autoclave unit at 121 °C for 15 min. After cooling the sterilized medium to room temperature, add 18 mL of 5% NaHCO<sub>3</sub> aseptically (*see Note 2*).

3. Luria-Bertani (LB) agar plate: Weigh 4.0 g of Bacto™ Tryptone, 2.0 g of Bacto™ Yeast extract and 4.0 g of NaCl and transfer to 500 mL beaker containing about 350 mL of distilled water. Dissolve all powder completely. Transfer the solution to 500 mL graduated cylinder and make up to 400 mL with distilled water. Transfer the solution into the autoclavable container containing 6.0 g of agar (powder). After mixing the solution, sterilize with autoclave unit at 121 °C for 15 min. After cooling the sterilized medium to 50–55 °C, pour it into sterile Petri plates.

## 2.2 Immuno-chromatographic Test Strip

1. The test strip was prepared with rabbit polyclonal antibodies raised against recombinant purified CT as reported previously [5, 10].

---

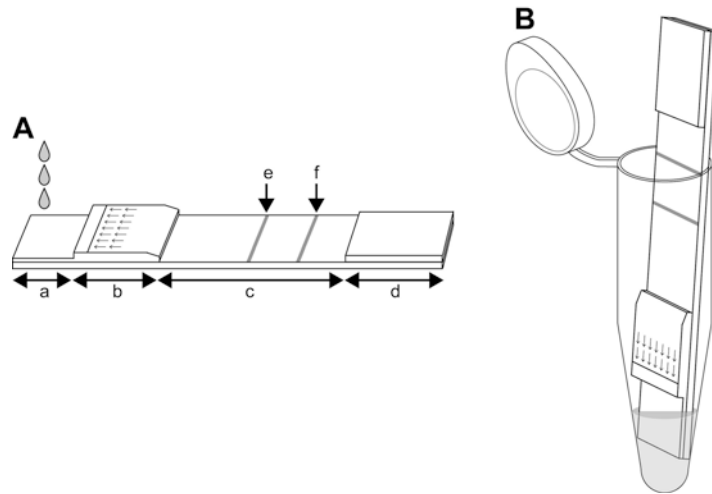
## 3 Methods

### 3.1 Bacterial Cell Culture Preparation for Immuno-chromatographic Analysis

1. Inoculate a *V. cholerae* isolate (isolated by the established procedures) onto a non-selective agar medium such as LB agar plate (*see Note 3*).
2. Incubate the LB agar plate at 37 °C for 18–24 h until colonies can be observed.
3. Pick a well isolated colony and inoculate a culture tube containing 10 mL of AKI broth (*see Note 4*).
4. Let the tube stand at 37 °C for 4 h.
5. Transfer entire culture into a sterilized 100 mL Erlenmeyer flask (*see Note 5*).
6. Incubate in the shaking incubator at 37 °C for about 16 h (*see Note 6*).
7. The obtained bacterial cell culture is used in the analysis with CT-IC (*see Note 7*).

### 3.2 Cholera Toxin Detection by Immuno-chromatographic Test Strip

1. Place CT-IC on horizontal table (*see Note 8*).
2. Apply 100 µL of the bacterial cell culture obtained in **step 7** in Subheading 3.1 to the sample application section (Fig. 1a) (*see Note 9*).
3. Leave the strip for about 15 min at room temperature.
4. Observe the test result. A positive result shows reddish purple lines in the test position and control position. A negative result shows a reddish purple line only in the control position. If no reddish purple line appears in the control position, the result is considered to be invalid.



**Fig. 1** Illustration of an immunochromatographic test strip for detection of CT (CT-IC). CT-IC can be used either on a flat bench (**a**) or in a test tube (**b**). *a*, Sample application section. *b*, Reagent containing section. *c*, Detection section. *d*, Absorbent pad. *e*, Test line for CT detection position. *f*, Control line appearance position

### 3.3 Cholera Toxin Detection by Immuno- chromatographic Test Strip (Alternative Procedure)

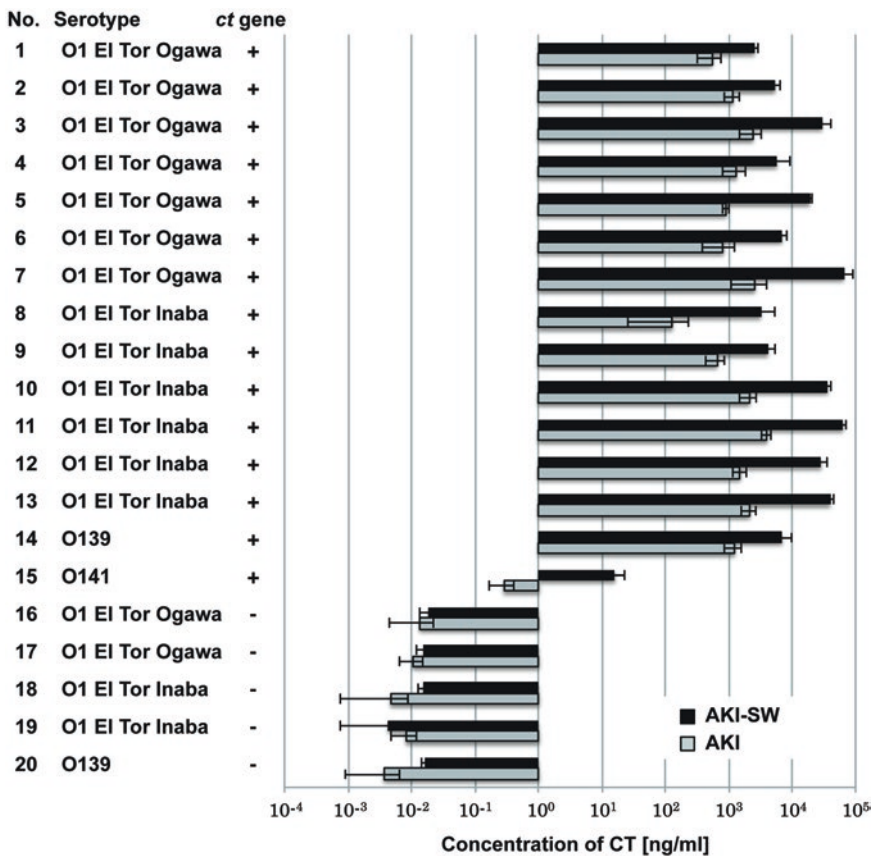
1. Transfer 150  $\mu\text{L}$  of the bacterial cell culture obtained in **step 7** in Subheading 3.1 to fresh 1.5 mL micro tube.
2. Put the CT-IC in the micro tube to immerse the sample application section in the cell culture (Fig. 1b) (*see Note 10*).
3. Leave the strip for about 15 min at room temperature.
4. Observe the test result. Criteria for result judgment are same as above (*see Subheading 3.2, step 4*).

---

## 4 Notes

1. The filtration step is done for the purpose of sterilization. Therefore, the filtered solution must be collected and stored in a sterilized bottle. If the sterilized solution cannot be used immediately, store the solution in a sealed bottle at 4  $^{\circ}\text{C}$ .
2. It is better to prepare the medium immediately before use. If the prepared medium cannot be used immediately, store the medium in a sealed bottle at 4  $^{\circ}\text{C}$ . The medium must be brought to room temperature before use.
3. Selective or differential media such as TCBS agar, Vibrio agar or CHROMagar™ Vibrio can be used for isolation of *V. cholerae*. Before the analysis with CT-IC, it is better to do subcultivation on non-selective agar medium to obtain completely isolated colony.

4. For the stationary cultivation phase, a small sterilized container such as 15 mL centrifuge tube (height, 150 mm; diameter, 15 mm) can be used. Degassing is not needed.
5. For the shaking cultivation phase, Erlenmeyer flask with the volume more than 100 mL (i.e. more than 10 times of volume of the culture) must be used to enforce adequate aeration.
6. Expression of CT not only in *V. cholerae* O1 El Tor but also in other serotypes is known to vary depending on the culture conditions. AKI medium is known as an effective medium to induce CT expression. Two culture conditions are known for effective induction of CT expression in AKI medium: AKI-SW condition (4 h cultivation in a stationary test tube followed by >16 h cultivation in a shaking flask at 37 °C) and AKI condition (>20 h cultivation in a stationary test tube at 37 °C) [6–9]. Quantitative analysis with 15 independent *ct*-gene positive *V. cholerae* strains revealed that CT expression under AKI-SW condition was considerably higher than under AKI condition (Fig. 2). We strongly recommend AKI-SW condition for use in


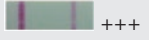



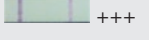





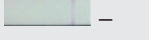


**Fig. 2** Expression of CT under AKI-SW and AKI conditions. Concentration of CT in the culture supernatant were obtained after cultivation of various *V. cholerae* isolates under AKI-SW (black bar) or AKI (gray bar) and were then analyzed by bead-ELISA for CT quantification [11]. Data are mean  $\pm$  SD of values from three independent experiments

the analysis with CT-IC. Among the 15 isolates we analyzed, one isolate (strain No. 15 in Fig. 2) expressed CT at a concentration of substantially lower than the detection limit of CT-IC (10 ng/mL) under AKI condition. However, CT expression could be detected by CT-IC with AKI-SW condition (concentration of CT was  $0.28 \pm 0.12$  ng/mL in AKI condition whereas  $16.1 \pm 6.97$  ng/mL in AKI-SW condition).

7. We confirmed that centrifugation to remove bacterial cells did not affect CT-IC results as indicated in Table 1. In case No. 1 (moderate CT expression with low cell density), case No. 2 (high CT expression with high cell density) and case No. 3 (low CT expression with high cell density), whole cell cultures and cleared supernatants that were obtained after centrifugation ( $900 \times g$ , 5 min) gave the same results in CT-IC analysis. These results indicated that bacterial cells did not inhibit reactions developing on the immunochromatographic test strip. In addition, in case No. 4, *ct* gene-negative *V. cholerae* El Tor Ogawa strain with high cell density did not give false-positive results even if the whole cell culture was applied to the immunochromatographic test strip.
8. The test strips are normally provided with light shielding package and stored at 4 °C. Allow the test strips to come to room temperature (20–25 °C) before opening the package to prevent moisture absorption. Do not touch with bare fingers on

**Table 1 Effect of centrifugation before immunochromatographic analysis on CT-IC results**

Case No.	Strain No.*1	ct gene	Culture condition	CT expression [ng/mL]*2	Cell density*3	Centrifugation	CT-IC result*4
1	8	+	AKI	$127.5 \pm 102.1$	Low 	+	 +++
						–	 +++
2			AKI-SW	$2009.6 \pm 77.3$	High 	+	 +++
						–	 +++
3	15	+	AKI-SW	$16.1 \pm 7.0$	High 	+	 +
						–	 +
4	16	–	AKI-SW	< 0.1	High 	+	 –
						–	 –

\*1: The strain No. are matched with the number in Fig. 2

\*2: The concentration of CT in the clear supernatant of the cultures measured with bead-ELISA are indicated. Data are mean  $\pm$  SD of values from three independent experiments

\*3: Relative cell density and pictures of cell cultures in cuvettes are shown

\*4: Results of CT-IC analyses are shown. The “+++”, “+” or “–” symbols are placed on the left side of the strips developing “strong”, “faint” or “no” bands at test lines respectively. T: test line, C: control line



the sample application section and detection section (Fig. 1). It is better to hold the absorbent pad with tweezers or gloved fingers when handling the test strips.

9. Be careful not to overload the sample application zone to prevent spillage. Apply the culture in two batches as appropriate.
10. Any type of the container can be used in **step 1** in Subheading 3.3. Adjust the volume of cell culture to keep the surface of the sample below the reagent containing sections of the test strips.

---

## Acknowledgements

This study was supported in part by a Grant-in-Aid of Ministry of Health, Labor and Welfare (H26-Shinkou-Shitei-002).

## References

1. Dick MH, Guillerm M, Moussy F et al (2012) Review of two decades of cholera diagnostics—how far have we really come? *PLoS Negl Trop Dis* 6:e1845
2. CDC (1999) Laboratory methods for the diagnosis of *Vibrio cholerae*. Chapter VII
3. Palchetti I, Mascini M (2008) Electroanalytical biosensors and their potential for food pathogen and toxin detection. *Anal Bioanal Chem* 391:455–471
4. Shlyapnikov YM, Shlyapnikova EA, Simonova MA et al (2012) Rapid simultaneous ultrasensitive immunodetection of five bacterial toxins. *Anal Chem* 84:5596–5603
5. Yamasaki E, Sakamoto R, Matsumoto T et al (2013) Development of an immunochromatographic test strip for detection of cholera toxin. *Biomed Res Int* 2013:679038
6. Iwanaga M, Kuyyakanond T (1987) Large production of cholera toxin by *Vibrio cholerae* O1 in yeast extract peptone water. *J Clin Microbiol* 25:2314–2316
7. Iwanaga M, Yamamoto K (1985) New medium for the production of cholera toxin by *Vibrio cholerae* O1 biotype El Tor. *J Clin Microbiol* 22:405–408
8. Iwanaga M, Yamamoto K, Higa N et al (1986) Culture conditions production for stimulating cholera toxin by *Vibrio cholerae* O1 El Tor. *Microbiol Immunol* 30:1075–1083
9. Sánchez J, Medina G, Buhse T et al (2004) Expression of cholera toxin under non-AKI conditions in *Vibrio cholerae* El Tor induced by increasing the exposed surface of cultures. *J Bacteriol* 186:1355–1361
10. Yonekita T, Fujimura T, Morishita N et al (2013) Simple, rapid, and reliable detection of *Escherichia coli* O26 using immunochromatography. *J Food Prot* 76:748–754
11. Uesaka Y, Otsuka Y, Kashida M et al (1992) Detection of cholera toxin by a highly sensitive linked immunosorbent assay. *Microbiol Immunol* 36:43–53

## Electrochemical Aptamer Scaffold Biosensors for Detection of Botulism and Ricin Proteins

Jessica Daniel, Lisa Fetter, Susan Jett, Teisha J. Rowland, and Andrew J. Bonham

### Abstract

Electrochemical DNA (E-DNA) biosensors enable the detection and quantification of a variety of molecular targets, including oligonucleotides, small molecules, heavy metals, antibodies, and proteins. Here we describe the design, electrode preparation and sensor attachment, and voltammetry conditions needed to generate and perform measurements using E-DNA biosensors against two protein targets, the biological toxins ricin and botulinum neurotoxin. This method can be applied to generate E-DNA biosensors for the detection of many other protein targets, with potential advantages over other systems including sensitive detection limits typically in the nanomolar range, real-time monitoring, and reusable biosensors.

**Key words** Biosensors, Toxins, Electrochemical, Aptamer, Botulism, Ricin, Voltammetry, E-DNA, Gold electrodes, Proteins

---

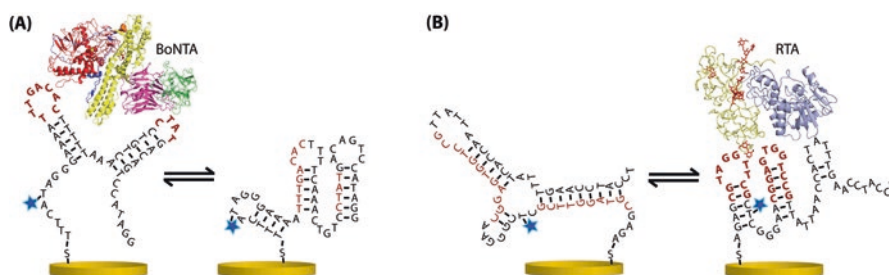
### 1 Introduction

Accurate and rapid detection of biomarkers is useful in many applications, ranging from food safety [1] and environmental sampling to medical diagnostics [2] and small-molecule drug discovery. Biosensors, which are devices that incorporate biological interactions as the basis of their sensing mechanisms [3], are uniquely suited to overcoming challenges associated with detecting a specific biomolecule in dense, complex, biological liquid matrices [4] (e.g., whole blood or river water samples). In addition, biosensors have several other appealing features that allow them to be used successfully in unique and challenging situations, including high specificity of detection, high reproducibility, relative ease of manufacturing and affordability, rapid throughput, direct readout, and minimal invasiveness.

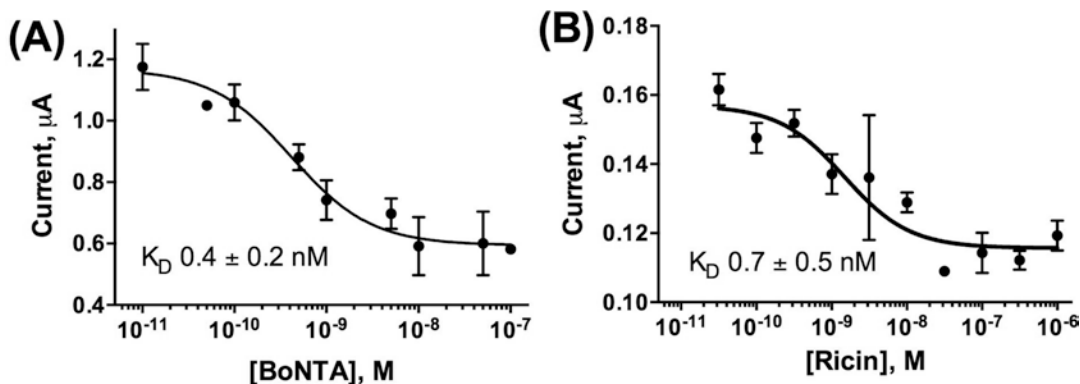
One prominent and successful class of biosensors is electrochemical DNA (E-DNA) biosensors [5]. E-DNA biosensors rely on the changing conformational dynamics of a synthetic

deoxyoligonucleotide (DNA) scaffold containing an aptamer or transcription factor-binding motif that recognizes the target biomolecule [6–9] (Fig. 1). The DNA scaffold is modified with functional groups to enable attachment to an electrode surface (typically through a thiol-gold bond) and to an electrochemically active reporter molecule (e.g., methylene blue) [10, 11]. When the biosensor is subjected to voltammetric analysis, the scaffold conformation changes depending on whether or not it is bound to its target biomolecule, and this affects the dynamics and the position (and thus observed current) of the electrochemically active reporter molecule relative to the electrode surface [12] (Fig. 1). This principle enables E-DNA biosensors to effectively function in complex matrices [4], including real-time monitoring in animal blood [2], and be successfully used against a range of targets, including oligonucleotides [6], small-molecule drugs [13], heavy metals [14], antibodies [15], DNA-binding proteins [16], and protein toxins [9].

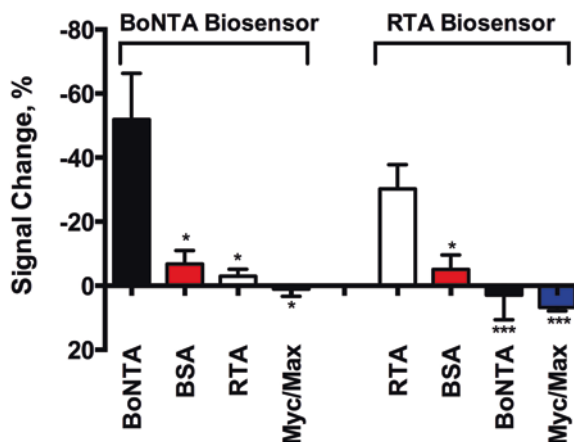
In theory, E-DNA biosensors can be designed to detect any molecule for which oligonucleotide-binding interactions are known or discoverable (such as via systematic evolution of ligands by exponential enrichment [SELEX]). Recently, our group generated E-DNA biosensors for the detection of protein toxins responsible for ricin and botulism toxicity [9]. Here we describe the design and use of novel E-DNA biosensors against these and similar targets. The biosensors described here can detect nanomolar concentrations of ricin chain A and botulinum neurotoxin variant A (Fig. 2), with high specificity and negligible off-target signals, and function when challenged with complex matrices such as blood serum albumin or other proteins (Fig. 3).



**Fig. 1** Schematic of E-DNA biosensor, illustrating the change in position and dynamics of the reporter molecule (methylene blue, represented by a *blue star*) attached to the DNA scaffold in response to binding of the biomolecule target. Shown are biosensors directed toward the biomolecular targets (a) botulinum neurotoxin variant A (BoNTA) and (b) ricin toxin chain A (RTA). The gold electrode surface (*yellow disc*) is passivated with a monolayer of 6-mercapto-1-hexanol (not shown) to prevent nonspecific binding of biomolecules (Reproduced from ref. [9] with permission of the Royal Society of Chemistry)



**Fig. 2** Representative dose-responsive curves of peak current vs. toxin concentration for botulinum neurotoxin variant A (BoNTA, **a**) and ricin toxin chain A (RTA, **b**). Both E-DNA biosensors display robust equilibrium signal change in response to target concentration, with apparent dissociation constant ( $K_D$ ) values of  $0.4 \pm 0.2$  nM for BoNTA and  $0.7 \pm 0.5$  nM for RTA (Reproduced from ref. [9] with permission of the Royal Society of Chemistry)



**Fig. 3** The botulinum (BoNTA) and ricin (RTA) biosensors display minimal off-target responses when challenged with off-target proteins, including bovine serum albumin (BSA) and other biomolecular targets, such as the unrelated DNA-binding protein complex Myc/Max. Student's *t*-test was performed to compare on-target to off-target response (\* for  $p < 0.05$ , \*\*\* for  $p < 0.0001$ ) (Reproduced from ref. [9] with permission of the Royal Society of Chemistry)

## 2 Materials

Prepare all solutions using ultrapure water (prepared by purifying deionized water, to attain a sensitivity of  $18 \text{ M}\Omega\text{-cm}$  at  $25 \text{ }^\circ\text{C}$ ) and analytical grade reagents. Prepare and store all reagents at room temperature (unless indicated otherwise). Diligently follow all waste disposal regulations when disposing of waste materials.

## 2.1 Biosensor Design and Synthesis

1. Biosensor DNA: Synthetic DNA scaffold with 5' terminal disulfide (e.g., 5'' thio C6 modifier/trityl-6-thiohexyl amidite) and internal thymidine-methylene blue to be used as an electrochemically active reporter molecule (methylene blue succinimidyl ester coupled to amino modifier C6 T amidite/5''-DMT-T[acrylamido-C6-NH-TFA]) (*see Note 1*). Resuspend DNA in ultrapure water at 100  $\mu$ M. Store aliquoted at  $-20\text{ }^{\circ}\text{C}$  wrapped in aluminum foil. The ricin biosensor sequence used here is 5'- AGAG CGT AGG TTC G C[T(Methylene Blue)]C GGG AA CGG AGT GGT CCG TTATTA ACC ACT ATTT GAA CCT ACC -3', and the botulinum toxin biosensor sequence is 5'- TTT CA[T(Methylene Blue)] AGG GA AA ATTTGACACT TT TCAAAC T GTCCTATGAC A GTCCA TAGG -3' [9].
2. Quickfold application from the DINAMelt web server, hosted by the RNA Institute at the State University of New York at Albany [17], available at <http://unafold.rna.albany.edu/?q=DINAMelt/Quickfold> (*see Note 2*).
3. OPTIONAL: Fealden DNA biosensor algorithm [8], available at [http://www.bonhamlab.com/wp-content/uploads/2016/05/Fealden-0.2\\_04232016.zip](http://www.bonhamlab.com/wp-content/uploads/2016/05/Fealden-0.2_04232016.zip) (*see Note 3*).
4. PCR tubes: 0.5 mL flat-cap PCR tubes, RNase- and DNase-free, polypropylene.

## 2.2 Electrode Preparation

1. Pine Research Instrumentation WaveNano USB Potentiostat (*see Note 4*).
2. Pine Research Instrumentation Compact Voltammetry Cell Grip Mount.
3. Pine Research Instrumentation WaveNano Shielded Cell Cable.
4. Pine Research Instrumentation Compact Voltammetry Cable.
5. Pine Research Instrumentation Ceramic Patterned Gold Electrode.
6. Pine Research Instrumentation AfterMath Scientific Data Organizer Software.
7. Alkaline cleaning solution: 0.5 M NaOH.
8. Acid cleaning solution: 0.5 M H<sub>2</sub>SO<sub>4</sub>.
9. Etch solution: 0.1 M H<sub>2</sub>SO<sub>4</sub>, 0.01 M KCl.
10. Evaluation solution: 0.05 M H<sub>2</sub>SO<sub>4</sub>.

## 2.3 Biosensor Attachment and Surface Passivation

1. TCEP solution: 1 M Tris(2-carboxyethyl)phosphine hydrochloride. Store aliquoted at  $-20\text{ }^{\circ}\text{C}$ .
2. Phosphate-buffered saline (PBS): 8 g NaCl, 0.2 g KCl, 1.44 g Na<sub>2</sub>HPO<sub>4</sub>, 0.24 g KH<sub>2</sub>PO<sub>4</sub>, and pH adjusted to 7.4 with HCl, adjusted to 1 L with ultrapure water.

3. Mercaptohexanol solution: 0.001 M 6-mercapto-1-hexanol in PBS. Prepare and work with solution in a chemical fume hood. Store at 4 °C for up to 1 month.
4. PCR tubes: 0.5 mL flat-cap PCR tubes, RNase- and DNase-free, polypropylene.
5. Petri dish: 100 mm × 15 mm, polystyrene.

#### **2.4 Botulism and Ricin Protein Preparation**

1. PBS: *see* Subheading 2.3.
2. Ricin solution: Ricin A chain from *Ricinus communis* (castor-bean or castor-oil-plant, from Sigma-Aldrich). Resuspend at 1 mg/mL in PBS. Store aliquoted at 4 °C.
3. Botulism solution: Botulinum neurotoxin variant A1 atoxic derivative [18]. Resuspend at 1 mg/mL in PBS. Store aliquoted at −80 °C.

#### **2.5 Electrochemical Biosensing Experiment**

1. PBS: *see* Subheading 2.3.
2. Target biomolecule solution: *see* Subheading 2.4.
3. Prepared electrode: *see* Subheading 2.3.
4. AnyPeakFinder software program (source code available at <http://www.bonhamlab.com/tools/code/>) or AfterMath program with built-in peak height analysis functions (*see* Note 5).

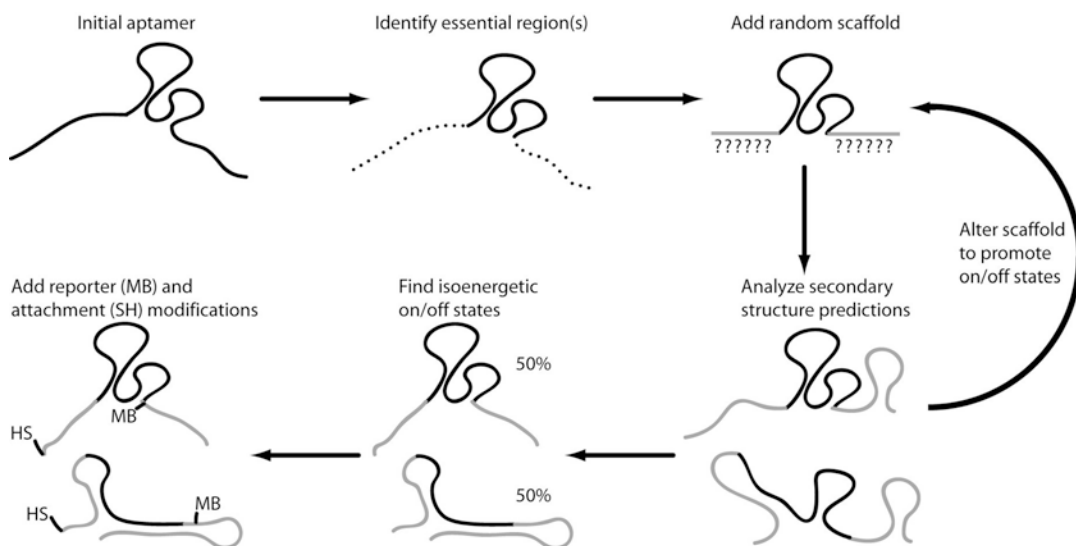
---

### **3 Methods**

Carry out all procedures at room temperature unless otherwise specified.

#### **3.1 Sensor Design and Synthesis**

1. Identify a DNA-binding motif that recognizes your biomolecule target of interest. We have used previously identified transcription factor binding sites [16] or aptamers [2, 9] or aptamers that we identified in-house [9].
2. Identify regions of the motif that are presumed to be “essential” for target binding interactions (Fig. 4). For aptamers, detailed mechanistic binding studies are often available in the literature; the regions of interest will typically be predicted to form “loops” in their secondary structure. Confirmation via Quickfold may be useful.
3. Design a synthetic DNA scaffold that incorporates the motif region(s) identified to be essential for target binding interactions and allows for potential disruption of these binding interactions. To do this, design the essential regions to be flanked on either or both of its 5′ and 3′ ends with deoxyoligonucleotides that are partially complementary to the essential regions, facilitating the formation of secondary structures



**Fig. 4** Schematic of biosensor design workflow process. An initial aptamer is truncated to essential regions and then flanked by a random scaffold of novel oligonucleotides. Secondary structure predictions are used to guide changes to the scaffold sequence to promote the formation of isoenergetic states that either present or obscure the aptamer essential regions. The addition of a reporter molecule (e.g., methylene blue, “MB”) and surface attachment modifications (i.e., thiol-gold bond, “HS”) leads to a completed biosensor design

or folding patterns that likely disrupt target binding. Multiple rounds of confirmation via Quickfold or other secondary structure prediction services may be useful (*see Note 6*).

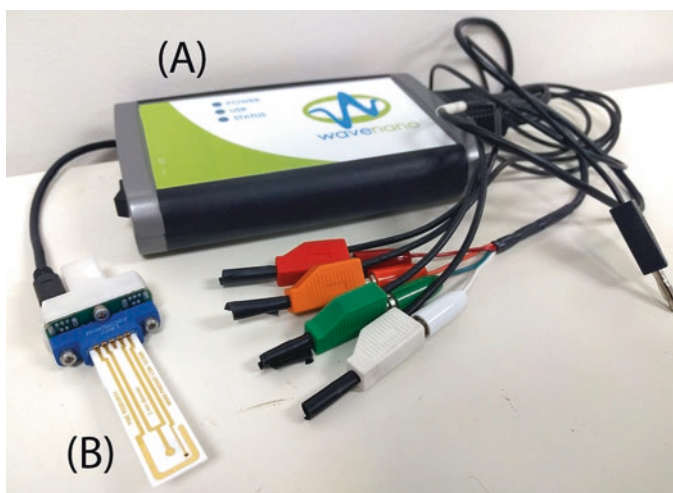
4. Continue designing the scaffold by iteratively adding, removing, or changing oligonucleotides in the nonessential regions to ultimately create a scaffold with two potential, equally favorable (i.e., isoenergetic) states: one state in which the essential regions are available for target binding interactions (i.e., in their native form) and one in which the essential regions are unavailable due to being base paired with nonessential regions (Fig. 4) [8]. The Fealden DNA biosensor algorithm is a designing tool that may be used to help automate this process.
5. Once a scaffold has been designed with the two desirable isoenergetic states, modify the scaffold design to include an electrode attachment point. A thiol group located at the 5' terminus of the entire scaffold should serve as the attachment point by forming a thiol-gold bond between the scaffold and the gold electrode surface.
6. Further modify the scaffold design to include an electrochemically active reporter molecule; here a methylene blue is used. The methylene blue can be easily covalently appended to a modified thymine. Examine the scaffold's two isoenergetic states to identify a thymine that is nonessential in a significantly different folded environment and has significant distance

change from the 5' terminus between the two folded states (Fig. 1). Again, Fealden may be used to help automate this selection process (*see Note 6*).

7. Synthesize the designed scaffold using a DNA synthesis company or in-house phosphoramidite deoxyoligonucleotide synthesis.
8. Resuspend the DNA in ultrapure water upon receipt at a concentration of 100  $\mu\text{M}$ , aliquot it into PCR tubes (typically 4  $\mu\text{L}$  per tube), and store aliquots at  $-20\text{ }^{\circ}\text{C}$ .

### 3.2 Electrode Preparation

1. Connect the WaveNano USB Potentiostat to a computer via a USB cable.
2. Connect the Compact Voltammetry Cell Grip Mount to the potentiostat using the WaveNano Shielded Cell Cable and Compact Voltammetry Cable, being sure that the alligator clips of the Shielded Cell Cable do not touch each other.
3. Place the Ceramic Patterned Gold Electrode face up in the grip mount, and add a plastic adaptor spacer (included with electrode) at the bottom of the grip mount to ensure solid contact between the grip mount and electrode. Ensure that the black ground electrode of the Shielded Cell Cable is connected to outlet ground (*see Fig. 5*).
4. Power on the potentiostat and ensure that the status light is green.
5. Open and log in to the AfterMath Scientific Data Organizer Software. Ensure that the WaveNano Potentiostat is recognized



**Fig. 5** Image of Pine Research Instrumentation (a) WaveNano instrument with correct cables and (b) ceramic-patterned electrode with exposed gold electrode surfaces. The biosensor attaches to the central, circular gold electrode



and communicating with AfterMath; the potentiostat's status should be listed as "idle" (see AfterMath support site for guidance; <http://wiki.voltammetry.net/pine/aftermath>).

6. Insert the electrode into a 30 mL beaker, and add 15 mL of alkaline cleaning solution, ensuring that the exposed gold surfaces of the electrode are submerged and the grip mount and contacts on the electrode remain dry.
7. Create and run a new cyclic voltammetry experiment to perform 100 scans from  $-0.4$  V to  $-1.35$  V at a sweep rate of 2 V/s. This will reductively desorb any sulfur-linked molecules on the electrode surface.
8. Remove the electrode from the alkaline cleaning solution, rinse with ultrapure water, and repeat **step 6** using 15 mL of acid cleaning solution (instead of alkaline cleaning solution).
9. Create and run a new bulk electrolysis experiment to perform oxidation using 2 V applied for 5 s followed by reduction using  $-0.35$  V applied for 10 s. This will oxidize any organic contaminants and then reduce any gold oxide formed.
10. Create and run a new cyclic voltammetry experiment to perform cyclic oxidation and reduction voltammetric scans, performing 20 scans with a scan rate of 4 V/s, followed by a further 4 scans at 0.1 V/s, from 0.35 V to 1.5 V. This step will sequentially oxidize and then reduce any remaining contaminants on the electrode surface.
11. Remove the electrode from the acid cleaning solution, rinse with ultrapure water, and repeat **step 6** using 15 mL of etch solution (instead of alkaline cleaning solution).
12. Create a new cyclic voltammetry experiment, and perform scans over four different potential ranges, each for ten scans at scan rate of 0.1 V/s: 0.2–0.75 V, 0.2–1.0 V, 0.2–1.25 V, and 0.2–1.5 V. This will etch away the surface layer of the electrode as gold chloride complexes, resulting in a substantially cleaned surface.
13. Remove the electrode from the etch solution, rinse with ultrapure water, and repeat **step 6** using 15 mL of evaluation solution (instead of alkaline cleaning solution).
14. Create a new cyclic voltammetry experiment, and perform four scans from  $-0.35$  V to 1.5 V at a scan rate of 0.1 V/s. This will oxidize a gold oxide layer on the electrode and then completely reduce it. The area under the reduction peak can be used to calculate the available surface area of the electrode [10, 19].
15. Store the cleaned electrode submerged in evaluation solution for up to 1 h before proceeding with using it in Subheading 3.3.

### 3.3 Biosensor Attachment and Surface Passivation

1. While performing the electrode preparation protocol (Subheading 3.2), thaw aliquots of sensor DNA (prepared in Subheading 3.1) and TCEP solution at room temperature. Avoid exposing the sensor DNA to light.
2. To a clean PCR tube, add 3  $\mu\text{L}$  sensor DNA and 3  $\mu\text{L}$  TCEP solution. Allow the sensor DNA/TCEP mixture to react for at least 15 min, until it has changed from light blue to clear in color [10] (*see Note 7*).
3. Mix 44  $\mu\text{L}$  of PBS with the sensor DNA/TCEP mixture.
4. Remove the electrode from the evaluation solution (from **step 15** of Subheading 3.3) and rinse it with ultrapure water. Using a clean, delicate task wiper (e.g., a Kimwipe), dry the electrode by wicking it dry, touching only the ceramic portions of the electrode and taking care not to touch the exposed gold surfaces.
5. Add the entire 50  $\mu\text{L}$  of sensor DNA/TCEP/PBS mixture to the electrode's surface, being careful to cover the entire exposed gold surface. Place the electrode inside a closed petri dish for 60 min, which will minimize evaporation and allow the reaction to proceed. In arid climates, we have found it is important to also add 250  $\mu\text{L}$  of PBS to the bottom of the petri dish and rest the electrode on top of a small, upside-down weigh boat in the dish to help prevent premature drying (*see Note 8*).
6. Using a delicate task wiper, dry the electrode as described in **step 4**. Immediately proceed with the next step to prevent the electrode from completely drying.
7. Add 100  $\mu\text{L}$  of mercaptohexanol solution [20] to the electrode, being careful to cover the entire exposed gold surface. Place the electrode inside a petri dish. Allow the reaction to proceed for 1–24 h at 4  $^{\circ}\text{C}$  (*see Note 9*).
8. Equilibrate the prepared biosensor in PBS for at least 20 min before use (in Subheading 3.5). This can be accomplished by repeating **step 6** of Subheading 3.2 using 15 mL of PBS (instead of alkaline cleaning solution).

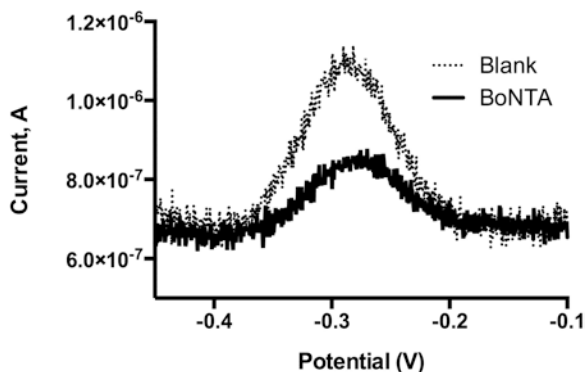
### 3.4 Botulism and Ricin Protein Preparation

1. Remove aliquoted protein solution (either ricin or botulinum solution, depending on desired target biomolecule) from storage and place on ice.
2. In microcentrifuge tubes, prepare a total of approximately ten serial dilutions of the protein solution in PBS, each dilution containing 100  $\mu\text{L}$ , ranging from 0.01 nM to 1  $\mu\text{M}$ . Keep the dilutions on ice and use them within 2 h.

### 3.5 Electrochemical Biosensing Experiment

1. Following PBS equilibration at the end of Subheading 3.3, remove the electrode from the PBS. Using a delicate task wiper, dry the electrode as described in **step 4** of Subheading 3.3.

- Place the grip mount and electrode in a horizontal position with the exposed gold surfaces facing up.
- Cover the electrode's exposed gold surfaces with 100  $\mu\text{L}$  of PBS, being careful to cover the working, counter, and reference elements of the electrode. Allow the electrode to equilibrate for at least 10 min. *Note:* Instead of PBS, bovine blood serum or whole bovine blood may alternatively be used (*see Note 10*).
- Ensure that the Compact Voltammetry Cable and Shielded Cell Cable are correctly attached to the grip mount and that the potentiostat's status in the AfterMath software is shown as "idle."
- Create a new square wave voltammetry experiment in the AfterMath program, with voltage ranging from  $-0.5$  to  $0.1$  V, an amplitude of 50 mV, and a step size of 1 mV. The optimal square wave frequency should be experimentally derived as it can dramatically affect the signaling of the biosensor [21]; 100 Hz is a typically useful frequency for a wide variety of biosensors.
- Run the experiment; a rounded peak in current at approximately  $-0.3$  V should be present, due to the redox potential of the methylene blue modification (*see Fig. 6*). The peak height is proportional to the effective efficiency of electron transfer between the surface and the methylene blue modification [22] (*see Note 11*).
- Rinse electrode with ultrapure water. Using a delicate task wiper, dry the electrode as described in **step 4** of Subheading 3.3.
- Cover the electrode's exposed gold surface with 100  $\mu\text{L}$  of 0.01 nM ricin or botulinum solution (prepared in Subheading 3.4), being sure to cover the working, counter, and reference



**Fig. 6** Square wave voltammograms of BoNTA biosensor equilibrated in PBS with 100 nM BoNTA (BoNTA) or with PBS only (Blank) (Reproduced from ref. [9] with permission of the Royal Society of Chemistry)

elements of the electrode. Allow the electrode to equilibrate for at least 10 min.

9. Create a new square wave voltammetry experiment from  $-0.5$  to  $0.1$  V with an amplitude of  $50$  mV and a step size of  $1$  mV using the experimentally determined optimal frequency.
10. Run the experiment; the methylene blue-derived peak in current at approximately  $-0.3$  V should remain present. The magnitude of any change in peak height reflects changes in biosensor signaling due to the presence of the target biomolecule.
11. Repeat **steps 7–10** using the other prepared serial dilutions (prepared in Subheading 3.4), using them in order of increasing concentration. For each dilution, measure the peak in current using AfterMath's peak height tool, or export the data as a comma-separated value (csv) file format, and use the AnyPeakFinder program to determine the peak heights.
12. Using the peak current observed in **step 6** as the baseline current, calculate the relative change in current for each dilution as a percentage increase or decrease in signal. For example, for each dilution, the baseline peak height could be subtracted from the dilution's peak height, and this value could be divided by the baseline peak height to calculate the percentage change.
13. Use the resulting data to construct a saturation binding curve, allowing visualization of the apparent dissociation constant for the target.
14. Following establishment of the target concentration dependent response, this section's procedure can be repeated using samples of unknown protein concentration to allow for quantification of the protein concentration in solution, enabling biosensing applications.

---

## 4 Notes

1. DNA synthesis is performed by standard phosphoramidite coupling on a solid support, which is available from many companies, such as Biosearch Technologies or Integrated DNA Technologies. Briefly, a 5' dimethoxytrityl (DMT)-protected deoxynucleotide phosphoramidite is attached to a controlled pore glass support through the 3' hydroxyl. Acid treatment is then used to remove DMT, followed by coupling to the next deoxynucleotide phosphoramidite, protective acetylation, and oxidation and then a repeated cycle of deprotection and coupling. Modified deoxynucleotide phosphoramidites can be easily included in this synthesis process.

2. The online Quickfold module is convenient, but there are several other tools available that predict DNA secondary structure folding, and any of these other tools should, in principle, be sufficient for the necessary analysis. Examples include RNAstructure from the University of Rochester Medical Center (<http://rna.urmc.rochester.edu/RNAstructureWeb/Servers/Predict1/Predict1.html>) and Integrated DNA Technologies' OligoAnalyzer Hairpin module (<https://www.idtdna.com/calc/analyzer>).
3. The Fealden software significantly automates the task of evaluating predicted DNA secondary structures for correct biosensor conformational states, but it is optional and may require Python programming experience to customize it for new applications. Fealden requires a UNIX-like environment and has been confirmed to work on Ubuntu Linux and Mac OSX.
4. Potentiostats and analysis software are available from several vendors; here we use Pine Research Instrumentation. Other vendors that could provide suitable instrumentation packages include CH Instruments, Inc., and Metrohm Autolab Nova.
5. Analysis of square wave voltammetric data requires accurately measuring the height of observed current peaks (when plotting current vs. voltage). AfterMath software includes a manual tool for this measurement, and as the data can be exported in csv format, a variety of computational tools can be used to identify and measure current peaks, including Mathematica and Matlab. Our lab provides source code for AnyPeakFinder, a Python program that can automatically read csv formats and extract peak height values; see <http://www.bonhamlab.com/tools/code/any-peak-finder-interactive/>.
6. The core principles of selecting correct regions and optimizing folded structures have been explored in a number of studies [7–9, 23–26] and demonstrate that an iterative, trial-and-error approach can often yield good results. Generally, structures with predicted free energies within 1 kJ/mol are more likely to be meaningful. Minimizing the number of predicted states helps avoid inconsistent results.
7. For sensor DNA solutions, the DNA sensor concentration is known to affect biosensor performance [12, 27]. The added TCEP solution must be sufficient to fully reduce the disulfide modification present in the sensor DNA solution, and consequently in this protocol the amount of TCEP solution added is in high excess. The observed color change is due to reversible reduction of the methylene blue modification. Although this change has no impact on the final performance of the biosensor, it is a convenient marker for the progress of reduction of the solution.

8. This process allows the sensor DNA to attach to the surface in an incomplete monolayer, with average spacing between molecules that minimizes or eliminates interactions between neighboring sensors, which is important for reproducible performance. Optimizations of this surface packing have been previously explored [12, 28].
9. The mercaptohexanol solution addition acts to form a stable, mixed surface monolayer with the attached sensor DNA. While 6-mercapto-1-hexanol is the most common of these “passivation” chemicals, our lab has additionally found success with the use of (11-mercaptopundecyl)tetra(ethylene glycol), which presents a more biocompatible monolayer for studies in complex matrices. The monolayer formed prevents nonspecific interactions of the biomolecule target with the electrode’s gold surface and provides a more reproducible current response. Typically, 100  $\mu\text{L}$  is added to the electrode surface and allowed to adhere for 1 h. Using larger volumes, such as 200  $\mu\text{L}$ , followed by sealing the electrode in a petri dish and storing it overnight at 4  $^{\circ}\text{C}$ , has also been successful. Our lab has also attempted to briefly wash the mercaptohexanol-passivated electrodes with saline sodium citrate (SSC) buffer or 1% bovine serum albumin (BSA) buffer with minimal successes. This was performed by allowing the mercaptohexanol to adhere to the electrode overnight, then removing it with a pipette, and adding 50  $\mu\text{L}$  of either the SSC or BSA. The solution was allowed to sit for 10 min before beginning trials.
10. To serve as a test bed for complex matrices uses of these sensors, we have employed both adult bovine serum and bovine whole blood (citrate stabilized) in place of PBS. In both matrices, sensors still performed well, although the magnitude of current changes is often reduced.
11. The precise voltage where the peak in current is found for methylene blue will vary based on solution conditions (e.g., pH and ionic content). Different reporter dyes will have a different characteristic voltage for peak current.

---

## Acknowledgment

This work would not be possible without ideas from Kevin Plaxco, University of California Santa Barbara, and Ryan White, University of Maryland Baltimore County. Support for this work was provided by the Metropolitan State University of Denver’s College of Letters, Arts, and Sciences Dean’s office, Provost’s office, and the Applied Learning Center.

## References

1. Miranda-Castro R, de-los-Santos-Álvarez N, Lobo-Castañón MJ (2016) Aptamers as synthetic receptors for food quality and safety control. *Compr Anal Chem* 74:155–191. doi:10.1016/bs.coac.2016.03.021
2. Ferguson BS, Hoggarth DA, Maliniak D et al (2013) Real-time, aptamer-based tracking of circulating therapeutic agents in living animals. *Sci Transl Med* 5:213ra165
3. Lee TM-H (2008) Over-the-counter biosensors: past, present, and future. *Sensors* 8:5535–5559
4. Lubin AA, Lai RY, Baker BR et al (2006) Sequence-specific, electronic detection of oligonucleotides in blood, soil, and foodstuffs with the reagentless, reusable E-DNA sensor. *Anal Chem* 78:5671–5677
5. Hasanzadeh M, Shadjou N (2016) Electrochemical nanobiosensing in whole blood: recent advances. *TrAC Trends Anal Chem* 80:167–176
6. Lubin AA, Plaxco KW (2010) Folding-based electrochemical biosensors: the case for responsive nucleic acid architectures. *Acc Chem Res* 43:496–505
7. Vallée-Bélisle A, Bonham AJ, Reich NO et al (2011) Transcription factor beacons for the quantitative detection of DNA binding activity. *J Am Chem Soc* 133:13836–13839
8. Schaffner SR, Norquest K, Baravik E et al (2014) Conformational design optimization of transcription factor beacon DNA biosensors. *Sens Bio-Sensing Res* 2:49–54
9. Fetter L, Richards J, Daniel J et al (2015) Electrochemical aptamer scaffold biosensors for detection of botulinism and ricin toxins. *Chem Commun (Camb)* 51:15137–15140
10. Rowe AA, White RJ, Bonham AJ, Plaxco KW (2011) Fabrication of electrochemical-DNA biosensors for the reagentless detection of nucleic acids, proteins and small molecules. *J Vis Exp* 52:e2922
11. Ricci F, Plaxco KW (2008) E-DNA sensors for convenient, label-free electrochemical detection of hybridization. *Microchim Acta* 163:149–155
12. Xiao Y, Uzawa T, White RJ et al (2009) On the signaling of electrochemical aptamer-based sensors: collision- and folding-based mechanisms. *Electroanalysis* 21:1267–1271
13. Liu J, Wagan S, Dávila-Morris M et al (2014) Achieving reproducible performance of electrochemical folding aptamer-based sensors on microelectrodes: challenges and prospects. *Anal Chem* 86:11417–11424
14. Xiao Y, Rowe AA, Plaxco KW (2007) Electrochemical detection of parts-per-billion lead via an electrode-bound DNzyme assembly. *J Am Chem Soc* 129:262–263
15. Vallée-Bélisle A, Ricci F, Uzawa T et al (2012) Bioelectrochemical switches for the quantitative detection of antibodies directly in whole blood. *J Am Chem Soc* 134:15197–15200
16. Bonham AJ, Hsieh K, Ferguson BS et al (2012) Quantification of transcription factor binding in cell extracts using an electrochemical, structure-switching biosensor. *J Am Chem Soc* 134:3346–3348
17. Markham NR, Zuker M (2005) DINAMelt web server for nucleic acid melting prediction. *Nucleic Acids Res* 33:W577–W581
18. Vazquez-Cintron EJ, Vakulenko M, Band PA et al (2014) Atoxic derivative of botulinum neurotoxin a as a prototype molecular vehicle for targeted delivery to the neuronal cytoplasm. *PLoS One* 9:e85517
19. Xiao Y, Lai RY, Plaxco KW (2007) Preparation of electrode-immobilized, redox-modified oligonucleotides for electrochemical DNA and aptamer-based sensing. *Nat Protoc* 2:2875–2880
20. Creager SE, Olsen KG (1995) Self-assembled monolayers and enzyme electrodes: progress, problems and prospects. *Anal Chim Acta* 307:277–289
21. White RJ, Plaxco KW (2009) Exploiting binding-induced changes in probe flexibility for the optimization of electrochemical biosensors. *Anal Chem* 82:73–76
22. Uzawa T, Cheng RR, White RJ et al (2010) A mechanistic study of electron transfer from the distal termini of electrode-bound, single-stranded DNAs. *J Am Chem Soc* 132:16120–16126
23. Vallée-Bélisle A, Ricci F, Plaxco KW (2012) Engineering biosensors with extended, narrowed, or arbitrarily edited dynamic range. *J Am Chem Soc* 134:2876–2879
24. Vallée-Bélisle A, Plaxco KW (2010) Structure-switching biosensors: inspired by Nature. *Curr Opin Struct Biol* 20:518–526
25. White RJ, Plaxco KW (2009) Engineering new aptamer geometries for electrochemical aptamer-based sensors. In: Fell NF, Jr, Swaminathan VS (eds) *Proc Soc Photo Opt Instrum Eng. SPIE, Department of Chemistry and Biochemistry University of California, Santa Barbara, Santa Barbara, CA 93106-9510*, p 732105
26. Schoukroun-Barnes LR, Wagan S, White RJ (2014) Enhancing the analytical performance of electrochemical RNA aptamer-based sensors for sensitive detection of aminoglycoside antibiotics. *Anal Chem* 86:1131–1137

27. White RJ, Phares N, Lubin AA et al (2008) Optimization of electrochemical aptamer-based sensors via optimization of probe packing density and surface chemistry. *Langmuir* 24:10513–10518
28. Huang K-C, White RJ (2013) Random walk on a leash: a simple single-molecule diffusion model for surface-tethered redox molecules with flexible linkers. *J Am Chem Soc* 135:12808–12817



## A Cell-Based Fluorescent Assay to Detect the Activity of AB Toxins that Inhibit Protein Synthesis

Patrick Cherubin, Beatriz Quiñones, Salem Elkahoui, Wallace Yokoyama, and Ken Teter

### Abstract

Many AB toxins elicit a cytotoxic effect involving the inhibition of protein synthesis. In this chapter, we describe a simple cell-based fluorescent assay to detect and quantify the inhibition of protein synthesis. The assay can also identify and characterize toxin inhibitors.

**Key words** AB toxin, Ricin, Shiga toxin, Toxin detection, Toxin inhibitors, Toxicity assay, Vero cells

---

### 1 Introduction

AB-type protein toxins are produced by numerous bacterial pathogens and some plants [1]. These toxins contain a catalytically active A subunit and a cell-binding B subunit. The A and B moieties can encompass different regions of a single polypeptide chain or may represent distinct proteins in various stoichiometries (e.g., AB, AB<sub>2</sub>, AB<sub>5</sub>, A<sub>3</sub>B<sub>7</sub>). Many AB toxins inhibit protein synthesis through inactivation of elongation factor 2 or the 28S rRNA [2–5].

Several methods can detect the toxin-induced inhibition of protein synthesis or resulting cell death. A common procedure measures the viability of intoxicated cells by dye exclusion, MTT/MTS assay, or similar protocols [6–11]. This strategy can require several days of toxin exposure and often involves additional processing steps for data collection. Furthermore, as discussed later, there is a temporal disconnect between the inhibition of protein synthesis and the loss of cell viability. A direct method to quantify the toxin-induced inhibition of protein synthesis measures the incorporation of radiolabeled amino acids into newly synthesized proteins [12, 13]. This requires the handling of radioisotopes, which is laborious, potentially hazardous, and can only accommodate a limited number of samples. Quantitative luciferase-based

assays have been described that are similar to the system reported here, but these systems require several preparatory and/or processing steps to enact the detection method [14, 15]. A recently described assay that monitors the production and secretion of acetylcholinesterase likewise requires additional processing steps for data acquisition [16].

As an alternative to existing technologies, we developed a simple and quantitative cell-based assay for the detection of toxins that inhibit protein synthesis. A Vero cell line with constitutive expression of a destabilized variant ( $t_{1/2} = 2$  h) of the enhanced green fluorescent protein (d2EGFP) is challenged with toxin for 18–24 h. Intoxicated cells degrade d2EGFP and do not replenish the lost protein due to the toxin-induced block of protein synthesis. The fluorescent signal from Vero-d2EGFP cells is accordingly lost in proportion to the applied dose of toxin. This assay provides reproducible data with minimal hands-on effort (*see Note 1*). The procedure does not require radioisotopes, commercial kits, or additional processing steps. A plate reader is required for reading fluorescent samples, but the only major recurring cost is the use of black-walled, clear-bottom 96-well tissue culture microplates. As described below, the noninvasive nature of the fluorescent measurement allows the Vero-d2EGFP cells to be used for additional purposes. Furthermore, the protocol can be adapted to screen for toxin inhibitors.

---

## 2 Materials

### 2.1 Cell Culture

1. Parental Vero cells (ATCC #CCL-81) and a clonal population of Vero-2dEGFP cells with stable, constitutive expression of the d2EGFP reporter (*see Notes 2–5*).
2. Complete Dulbecco's Modified Eagle Medium (DMEM) for carrying cells: DMEM, high glucose (4.5 g/L D-glucose) with 584 mg/L L-glutamine and 110 mg/L sodium pyruvate (GIBCO), supplemented with 10% fetal bovine serum (Atlanta Biologicals, Flowery Branch, GA), 1% antibiotic-antimycotic solution, and 1 mg/mL Geneticin (G-418).
3. Intoxication medium: F-12 + GlutaMAX-I nutrient mixture (Ham's F-12; GIBCO) (*see Note 6*).
4. HyClone antibiotic-antimycotic 100× solution: 10,000 U/mL penicillin, 10,000 µg/mL streptomycin, and 25 µg/mL amphotericin B (GE Healthcare).
5. Trypsin-EDTA 1× solution containing 0.25% trypsin, 0.9 mM EDTA, and phenol red (GIBCO).
6. HyClone phosphate-buffered saline (PBS) 1× solution: 6.7 mM PO<sub>4</sub> without calcium or magnesium (GE Healthcare).

7. Costar® black-walled 96-well polystyrene plates with a clear, flat bottom (Corning Inc., Kennebunk, ME) (*see Note 7*).
8. Geneticin/G-418 (GIBCO) (*see Note 8*).
9. 100 × 20 mm tissue culture dishes (Techno Plastic Products).
10. Fisherbrand 25 mL sterile disposable divided well pipette basins (Fisher Scientific).
11. Eppendorf Research® plus 8-channel variable 30–300 µL pipette (p300) (Eppendorf).
12. Costar® 8-channel adapter vacuum aspirator (Corning Inc.).

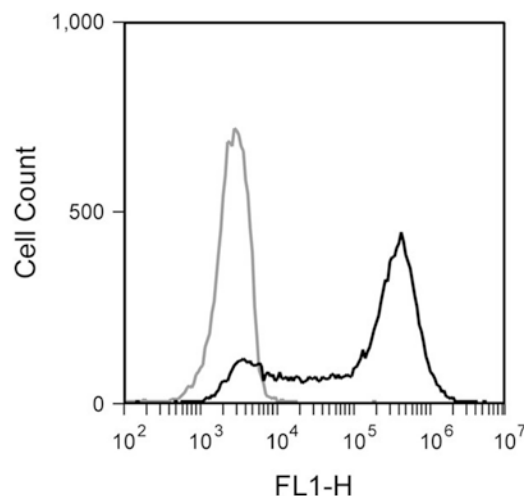
## 2.2 Toxins

1. Ricin (Vector Laboratories, Burlingame, CA).
2. Cell-free culture supernatant containing Shiga toxin 1 (Stx1) and Shiga toxin 2 (Stx2) (*see Notes 9 and 10*).

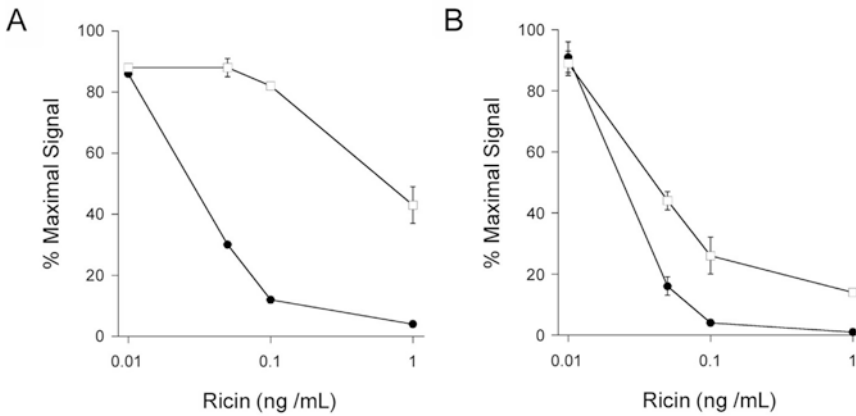
---

## 3 Methods

We generated a Vero cell line that stably expresses d2EGFP-N1, an EGFP variant that contains a C-terminal PEST sequence for rapid degradation by the ubiquitin-proteasome system [17, 18]. Steady-state fluorescence in the Vero-d2EGFP cell line is easily detected by cytofluorometry (Fig. 1) and microscopy or with a plate reader [17, 19]. When challenged with a toxin that inhibits protein synthesis, toxin-susceptible cells will degrade d2EGFP and will not produce more of the protein. Productive intoxication accordingly results in the loss of d2EGFP fluorescence. As shown in Fig. 2, ricin reduced the Vero-d2EGFP fluorescent signal in a dose-dependent manner (*see Note 11*). The loss of EGFP fluorescence



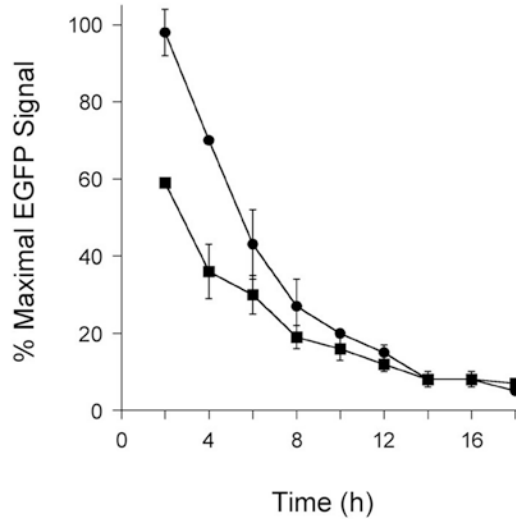
**Fig. 1** Fluorescent output from the Vero-d2EGFP cells. 20,000 parental Vero (*gray*) or Vero-d2EGFP (*black*) cells were subjected to cytofluorometry



**Fig. 2** Effect of ricin on protein synthesis and cell viability. Fluorescence (*filled circles*) and cell viability via MTS assay (*open squares*) were measured in the same population of Vero-d2EGFP cells after an 18 h (**a**) or 42 h (**b**) incubation with serial dilutions of ricin. Results were expressed as percentages of the maximal signal obtained from unintoxicated Vero-d2EGFP cells. The means  $\pm$  standard errors of the means of at least four independent experiments with six replicate samples for each condition are shown

was much more dramatic than the loss of cell viability after an 18 h intoxication: a half-maximal effective ricin concentration ( $ED_{50}$ ) of 0.03 ng/mL was recorded by the Vero-d2EGFP assay, whereas the MTS cell viability assay reported an  $ED_{50}$  of 0.7 ng/mL (Fig. 2a). Both fluorescence and viability were measured in the same cell population (*see Note 12*). The loss of viability eventually mirrored the loss of fluorescence after 42 h of toxin exposure, with both EGFP and MTS assays documenting an  $ED_{50}$  of 0.02–0.04 ng/mL (Fig. 2b). These collective results highlight several advantages of the Vero-d2EGFP system, including (1) relatively rapid detection of toxin activity, (2) high sensitivity, (3) minimal sample handling for data acquisition, and (4) a noninvasive/nonterminal measurement that allows the cells to be used for other purposes such as an MTS assay.

To examine how quickly the Vero-d2EGFP assay can detect toxin activity, we monitored the time-dependent decay of EGFP fluorescence from intoxicated cells (Fig. 3, circles) (*see Note 13*). Using a single concentration of ricin (1 ng/mL), we found the EGFP signal begins to decay 4 h after toxin exposure and continues to decrease until 14 h when a minimal signal of 5–8% is achieved. With a 2 h half-life for d2EGFP, a signal strength corresponding to 6% of the unintoxicated control value could theoretically be reached 8 h after exposure to a toxin that inhibits protein synthesis. The longer time frame required to reach this point for ricin-treated cells reflects the temporal delay between toxin binding to the cell surface and A chain delivery to its site of action in the cytosol [2], as well as the asynchronous nature of intoxication in a population of cells. These cellular events also

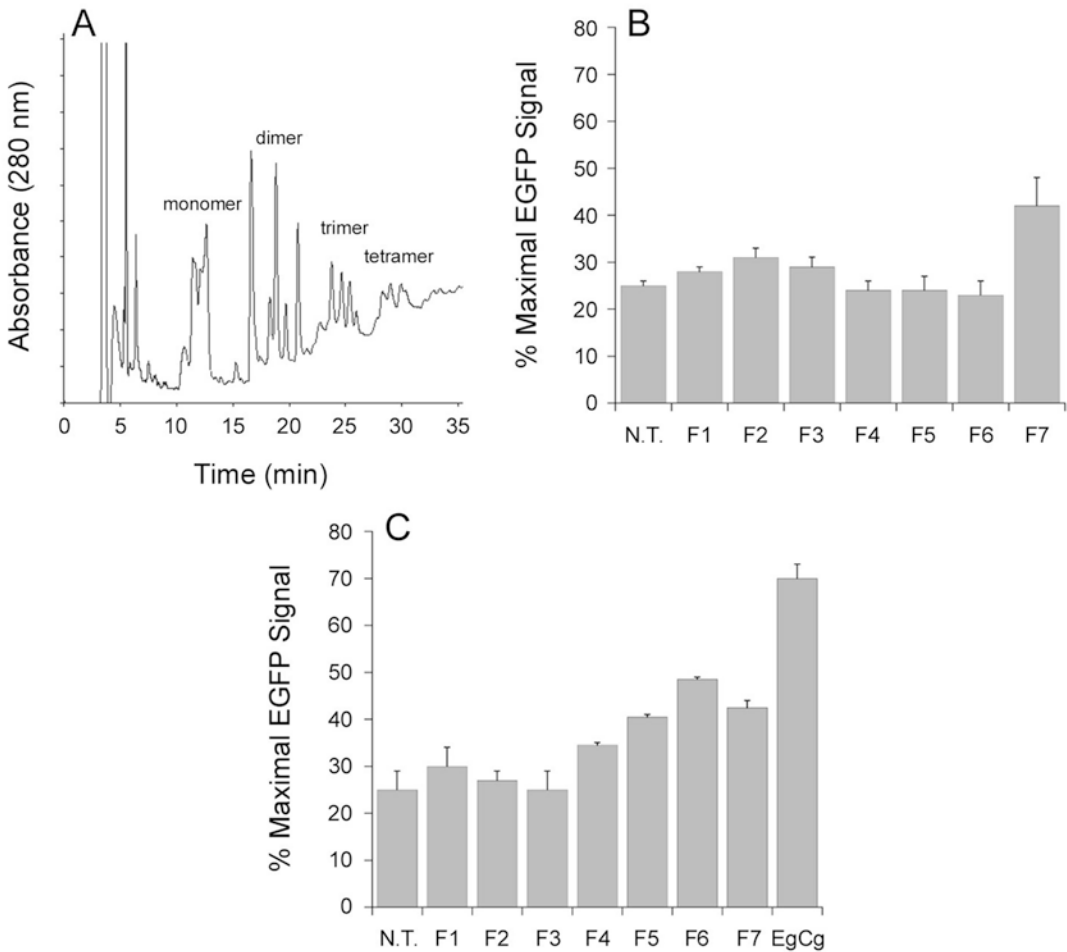


**Fig. 3** Time frame for loss of Vero-d2EGFP fluorescence. Measurements of fluorescent intensity were taken at 2 h intervals after incubation of Vero-d2EGFP cells with 1 ng/mL of ricin (*circles*) or 20  $\mu$ g/mL of the protein synthesis inhibitor cycloheximide (*squares*). Results were expressed as percentages of the maximal EGFP signal obtained from untreated Vero-d2EGFP cells. The averages  $\pm$  standard deviations of three independent experiments with six replicate samples per condition are shown

explain why the loss of EGFP fluorescence is slower in toxin-treated cells than in cells treated with cycloheximide, a membrane-permeant protein synthesis inhibitor (Fig. 3, squares). Nevertheless, our experiment demonstrated the cellular activity of ricin can be detected 4 h after toxin exposure and reaches its maximal effect on protein synthesis 14 h after toxin exposure.

Disruptions to the intoxication process will permit the continued synthesis of d2EGFP in toxin-treated cells. This principle was used to identify grape seed extract as a potent inhibitor of both Stx1 and Stx2 [17]. The antitoxin property of grape seed extract was then confirmed with an independent toxicity assay that monitored the overall level of protein synthesis in cells exposed to Stx2 [17] (*see Note 14*). In the presence of grape seed extract, the Vero-d2EGFP cells were also protected from ricin, diphtheria toxin, and exotoxin A [20].

Use of the Vero-d2EGFP assay to screen for toxin inhibitors is shown in Fig. 4. A previous screen of 26 purified polyphenolic compounds from grape extract failed to identify any individual inhibitor of Stx1/Stx2 [20], so we next screened fractions from the grape extract itself for antitoxin effects. Seven polyphenolic fractions, generated by using a modified normal-phase high-performance liquid chromatography method [21] (Fig. 4a), were mixed with a cell-free culture supernatant containing Stx1/Stx2 and applied to



**Fig. 4** Use of the Vero-d2EGFP assay to screen for toxin inhibitors. **(a)** A modified method using normal-phase high-performance liquid chromatography separated grape seed extracts into seven fractions enriched in polyphenol monomers (catechin and epicatechin), dimers, trimers, or tetramers as indicated. **(b)** Vero-d2EGFP cells were incubated with one of the extract fractions (5% final volume) and a 1:250 dilution of a cell-free culture supernatant from an *E. coli* strain that expresses both Stx1 and Stx2. After an 18 h incubation, EGFP fluorescence was measured with a plate reader. Results were expressed as percentages of the maximal EGFP signal obtained from a parallel set of unintoxicated Vero-d2EGFP cells. The means  $\pm$  standard errors of the means of at least four independent experiments with six replicate samples per condition are shown. **(c)** Vero-d2EGFP cells were incubated with 0.5 ng/mL of ricin and either one of the extract fractions (5% final volume) or 10  $\mu$ g/mL of epigallocatechin gallate (EgCg). After an 18 h incubation, EGFP fluorescence was measured with a plate reader. Results were expressed as percentages of the maximal EGFP signal obtained from a parallel set of unintoxicated Vero-d2EGFP cells. The averages  $\pm$  ranges of two to four independent experiments with six replicate samples per condition are shown. For panels B and C, fraction 1 (F1) represents material eluted from 0 to 5 min; F2 represents material eluted from 5 to 10 min; etc.

Vero-d2EGFP cells for 18 h (*see Note 15*). The fluorescent signal from cells exposed to toxin alone was reduced to 25% of the signal from unintoxicated Vero-d2EGFP cells (Fig. 4b). A similar loss of fluorescence was recorded for Vero-d2EGFP cells challenged with

toxin in the presence of fractions 1–6. However, intoxicated cells co-incubated with fraction 7 retained a stronger fluorescent signal, representing 42% of the unintoxicated control value and a statistically significant difference from the intoxicated control cells ( $p = 0.0217$ , Student's *t*-test). A similar screen indicated fractions 5–7 contain compounds that block ricin activity (Fig. 4c). In this screen, a known polyphenol inhibitor of ricin—epigallocatechin gallate (EgCg) [20, 22]—was used as a positive control. Further separation of the compounds in fractions 5–7, combined with additional Vero-d2EGFP assays, could potentially identify the specific polyphenols that confer resistance to Stxs and/or ricin.

### **3.1 Plating of Cells for the Fluorescence Assay**

1. Maintain the parental Vero and Vero-d2EGFP cells in a DMEM-based medium and passage when the cells form a >90% confluent monolayer on a 10 cm dish (*see Note 16*).
2. Working in a tissue culture hood, remove the spent medium from the tissue culture dish and wash the cells with 10 mL of sterile 1× PBS.
3. Detach cells from the dish by adding 1 mL of trypsin/EDTA for 10 min at room temperature (*see Note 17*).
4. Re-suspend detached cells in 9 mL of complete DMEM medium for a total volume of 10 mL.
5. Determine the cell concentration with a hemocytometer and alter it to a final concentration of 100,000 cells per mL. For the parental Vero cells, the final cell suspension should be in a 1.5 mL volume per 96-well plate. For the Vero-d2EGFP cells, the final cell suspension should be in a 9 mL volume per 96-well plate.
6. Pour each cell dilution (parental Vero and Vero-d2EGFP) into a separate sterile basin. Using a multichannel pipette (p300), transfer 100  $\mu$ L of the parental Vero cell suspension to the first row (12 wells) of a black-walled 96-well microplate with clear bottom. Again using a p300 multichannel pipette, transfer 100  $\mu$ L of the Vero-d2EGFP cell suspension to each of the remaining wells of the microplate.
7. Grow cells for ~24 h at 37 °C in a 5% CO<sub>2</sub> humidified incubator (*see Note 18*).

### **3.2 Treatment of the Cells with Toxin Inhibitors and/or Purified Toxin**

1. Prepare several ten- or twofold serial dilutions of toxin in serum-free Ham's F-12 medium. The final volume for each toxin dilution is 0.8 mL for 6 replicate samples or 1.5 mL for 12 replicate samples. For a screen of toxin inhibitors, prepare identical serial dilutions in Ham's F-12 medium containing the final concentration of inhibitor.
2. Remove medium from the Vero and Vero-d2EGFP cells with a multi-well vacuum aspirator.

3. Incubate Vero cells with 100  $\mu$ L per well of serum- and toxin-free Ham's F-12 medium, which is added with a p300 multi-channel pipette.
4. Incubate Vero-d2EGFP cells with 100  $\mu$ L per well of toxin serial dilutions in the absence or presence of inhibitor.
5. As an unintoxicated control condition, incubate Vero-d2EGFP cells with 100  $\mu$ L per well of serum- and toxin-free Ham's F-12 medium. When inhibitor screens are performed, incubate additional sets of unintoxicated Vero-d2EGFP cells with 100  $\mu$ L per well of the inhibitor alone.
6. As a positive control for the loss of fluorescence, treat one set of unintoxicated Vero-d2EGFP cells with the protein synthesis inhibitor cycloheximide.
7. Incubate cells with toxin for 18–24 h at 37 °C in a 5% CO<sub>2</sub> humidified incubator before fluorescence measurements are taken.

### **3.3 Fluorescence Measurements and Data Analysis**

1. Using a multi-well vacuum aspirator, remove 100  $\mu$ L of spent medium from each well (*see* **Notes 19** and **20**).
2. Using a p300 multichannel pipette, wash the cells with 200  $\mu$ L of 1 $\times$  PBS.
3. Using a p300 multichannel pipette, add another 100  $\mu$ L of 1 $\times$  PBS to the cells. Read measurements from cells bathed in 1 $\times$  PBS (*see* **Note 21**).
4. Measure the EGFP fluorescence on a Synergy H1 Multi-Mode Microplate Reader (BioTek, Winooski, VT) with bottom optics position using a 485 nm excitation and 528 nm emission filter set. Set the scale value for the automatic sensitivity adjustment to 20,000.
5. Readings taken from the parental Vero cells represent background levels of autofluorescence and are accordingly subtracted from the experimental measurements. After background subtraction, set the fluorescence value obtained from the unintoxicated (control) Vero-d2EGFP cells arbitrarily at 100%. Express all experimental data as percentages of this 100% control value. Examples of the results produced are shown in Figs. 2 and 3.
6. When screening toxin inhibitors, apply each inhibitor to Vero-d2EGFP cells in the absence of toxin to establish a separate control (100%) value for that condition. Express readings from Vero-d2EGFP cells incubated with both toxin and inhibitor as percentages of the corresponding control value from cells treated with the inhibitor alone. This procedure corrects for variability that could result from inhibitor autofluorescence and/or inhibitor effects on cell viability in the absence of toxin. Examples of the results produced are shown in Fig. 4.



---

## 4 Notes

1. In our experience, skilled high school and university undergraduates have been able to generate reproducible data with this system [20]. Another lab independently developed the Vero-d2EGFP toxicity assay and likewise reported highly reproducible data from ricin-treated cells [19].
2. Any cell type could be stably transfected with d2EGFP to generate a reporter cell line for this assay. We identified Vero cells as the most appropriate cell line for this work after several cell lines (Vero, BHK, CHO, Hep-2, HeLa, HEK 293, and COS-7) were characterized with dose-response curves to multiple plant and bacterial toxins. Of the cell lines tested, Vero cells displayed the highest level of sensitivity to a wide range of toxins.
3. Protocols for the generation of a Vero-d2EGFP cell line can be found in references [17, 19, 23].
4. The pd2EGFP-N1 plasmid (Clontech, Mountain View, CA) used to generate the Vero-d2EGFP cell line is no longer commercially available. Clontech offers a destabilized tetrameric green fluorescent protein (ZsGreen1) as an alternative to d2EGFP, although the construct is present in a promoterless plasmid (pZsGreen1-DR).
5. It is possible to run this or related assays with virally transduced cells [14, 24], but such a strategy requires additional preparatory steps for each experiment.
6. Tissue culture medium contributes a substantial background signal to the fluorescent measurement. The signal produced by F-12 medium is weaker than the DMEM signal and is minimized by washing the cells with PBS before measurement. An 18–24 h incubation in serum-free Ham's F-12 medium does not affect the viability of Vero or Vero-d2EGFP cells.
7. Black-walled microplates with clear, flat bottoms are required to prevent well-to-well bleeding of the fluorescent signal.
8. Geneticin was used as the selective pressure for isolation of the Vero-d2EGFP cell line. Maintaining drug selection (1 mg/mL) in the passage medium of the Vero-d2EGFP cells ensures continued, uniform expression of the EGFP reporter.
9. *Escherichia coli* O157:H7 strain RM1697, which expresses both Stx1 and Stx2 [25], was grown in Luria-Bertani broth at 37 °C with 200 rpm shaking. After a 15 min centrifugation at 3000 × *g*, the toxin-containing culture supernatant was filter sterilized with a 0.45 μm polyvinylidene fluoride syringe filter.
10. Purified Stx1 or Stx2, as well as other AB toxins, can be obtained from BEI Resources (Manassas, VA) or List Biological Laboratories (Campbell, CA).

11. The Vero-d2EGFP assay has also been used to generate dose-response curves for Stx1 and/or Stx2, *Pseudomonas aeruginosa* exotoxin A, and diphtheria toxin [17, 20].
12. It takes about 10 min to complete the steps outlined in Subheading 3.3 for a fluorescent measurement from living Vero-d2EGFP cells. Since the cells are viable and have not been modified by the measurement, they can subsequently be used for cell viability assays or other purposes. Thus, after recording the fluorescent intensity from our intoxicated cells, 20  $\mu$ L of the commercial MTS reagent (Promega, Madison, WI) was added to the 100  $\mu$ L of PBS in each well for a 2–3 h incubation at 37 °C. The MTS reagent is reduced by living cells to a colored product that is detected with a plate reader at an absorbance of 490 nm.
13. Separate sets of Vero and Vero-d2EGFP cells were used for each time point. All Vero or Vero-d2EGFP cells were seeded at the same time from a common basin of diluted cells (*see* Subheading 3.1, step 6). Toxin or cycloheximide was added simultaneously to five sets of cells for consecutive readings from 2–10 h. The remaining four sets of cells were challenged with toxin or cycloheximide at the end of the first day, which allowed measurements for the later time points to be collected on the second day. With this procedure, personnel were not required to remain in the lab for 18+ consecutive hours.
14. When screening for toxin inhibitors, compounds such as proteasome inhibitors that block the turnover of d2EGFP will produce a false-positive result: in these instances, the d2EGFP signal will persist despite the toxin-induced inhibition of protein synthesis. Screens for toxin inhibitors should accordingly include a secondary assay to validate the hit compounds.
15. Use of the Vero-d2EGFP system to detect toxins in cell-free bacterial culture supernatants is described in reference [26].
16. For passaging cells, a 1:10 dilution from a confluent 10 cm dish will take 3–4 days to again reach confluency in a fresh 10 cm dish. A 1:20 dilution from a confluent 10 cm dish will take about 4–5 days to again reach confluency in a fresh 10 cm dish. Cells passaged at either dilution will need fresh medium on the third day after transfer to a new dish.
17. Cells can be detached in less time ( $\leq 5$  min) by incubating them with trypsin/EDTA at 37 °C. A longer, room temperature incubation in the tissue culture hood permits time for preparation of the dishes and plates that will be used in the experiment.
18. Cell density will influence toxin sensitivity; highly confluent cells are more resistant to intoxication than subconfluent cells. For this reason, it is important to standardize from experiment to experiment the number of cells plated and the confluency of the cells at the time of toxin exposure.

19. If the experiment is terminal at this point, the PBS does not need to be sterile. In addition, the processing steps for a terminal experiment can be performed at the bench rather than in a tissue culture hood.
20. Always tilt the plate in the same orientation before aspirating or adding media to a defined point at the edge of each well. This will reduce the probability of cell loss during the processing steps.
21. To further reduce the background signal from cell culture media, final measurements are taken from cells bathed in PBS.

---

## Acknowledgments

This material is based upon work supported by the US Department of Agriculture, Agricultural Research Service, under the Non-Assistance Cooperative Agreement (NACA) No. 58-5325-4-024. Any opinions, findings, conclusions, or recommendations expressed in this publication are those of the authors and do not necessarily reflect the view of the US Department of Agriculture. The authors thank Dr. Lucia Cilenti for technical assistance with the Accuri flow cytometer (BD Biosciences, San Jose, CA).

## References

1. Sandvig K, van Deurs B (2005) Delivery into cells: lessons learned from plant and bacterial toxins. *Gene Ther* 12:865–872
2. Spooner RA, Lord JM (2015) Ricin trafficking in cells. *Toxins (Basel)* 7:49–65
3. Murphy JR (2011) Mechanism of diphtheria toxin catalytic domain delivery to the eukaryotic cell cytosol and the cellular factors that directly participate in the process. *Toxins (Basel)* 3:294–308
4. Lee MS, Koo S, Jeong DG et al (2016) Shiga toxins as multi-functional proteins: induction of host cellular stress responses, role in pathogenesis and therapeutic applications. *Toxins (Basel)* 8:E77
5. Michalska M, Wolf P (2015) *Pseudomonas* exotoxin A: optimized by evolution for effective killing. *Front Microbiol* 6:963
6. Konowalchuk J, Speirs JJ, Stavric S (1977) Vero response to a cytotoxin of *Escherichia coli*. *Infect Immun* 18:775–779
7. Paton JC, Paton AW (1998) Pathogenesis and diagnosis of Shiga toxin-producing *Escherichia coli* infections. *Clin Microbiol Rev* 11:450–479
8. Gamage SD, McGannon CM, Weiss AA (2004) *Escherichia coli* serogroup O107/O117 lipopolysaccharide binds and neutralizes Shiga toxin 2. *J Bacteriol* 186:5506–5512
9. Sekino T, Kiyokawa N, Taguchi T et al (2004) Characterization of a Shiga-toxin 1-resistant stock of vero cells. *Microbiol Immunol* 48:377–387
10. Pauly D, Worbs S, Kirchner S et al (2012) Real-time cytotoxicity assay for rapid and sensitive detection of ricin from complex matrices. *PLoS One* 7:e35360
11. Wahome PG, Bai Y, Neal LM et al (2010) Identification of small-molecule inhibitors of ricin and Shiga toxin using a cell-based high-throughput screen. *Toxicon* 56:313–323
12. Hovde CJ, Calderwood SB, Mekalanos JJ et al (1988) Evidence that glutamic acid 167 is an active-site residue of Shiga-like toxin I. *Proc Natl Acad Sci U S A* 85:2568–2572
13. Obrig TG, Louise CB, Lingwood CA et al (1993) Endothelial heterogeneity in Shiga toxin receptors and responses. *J Biol Chem* 268:15484–15488

14. Zhao L, Haslam DB (2005) A quantitative and highly sensitive luciferase-based assay for bacterial toxins that inhibit protein synthesis. *J Med Microbiol* 54:1023–1030
15. Gal Y, Alcalay R, Sabo T et al (2015) Rapid assessment of antibody-induced ricin neutralization by employing a novel functional cell-based assay. *J Immunol Methods* 424:136–139
16. Cohen O, Mechaly A, Sabo T et al (2014) Characterization and epitope mapping of the polyclonal antibody repertoire elicited by ricin holotoxin-based vaccination. *Clin Vaccine Immunol* 21:1534–1540
17. Quiñones B, Massey S, Friedman M et al (2009) Novel cell-based method to detect Shiga toxin 2 from *Escherichia coli* O157:H7 and inhibitors of toxin activity. *Appl Environ Microbiol* 75:1410–1416
18. Li X, Zhao X, Fang Y et al (1998) Generation of destabilized green fluorescent protein as a transcription reporter. *J Biol Chem* 273:34970–34975
19. Halter M, Almeida JL, Tona A et al (2009) A mechanistically relevant cytotoxicity assay based on the detection of cellular GFP. *Assay Drug Dev Technol* 7:356–365
20. Cherubin P, Garcia MC, Curtis D et al (2016) Inhibition of cholera toxin and other AB toxins by polyphenolic compounds. *PLoS One* 11:e0166477
21. Lazarus SA, Adamson GE, Hammerstone JF et al (1999) High-performance liquid chromatography/mass spectrometry analysis of proanthocyanidins in foods and beverages. *J Agric Food Chem* 47:3693–3701
22. Dyer PD, Kotha AK, Gollings AS et al (2016) An in vitro evaluation of epigallocatechin gallate (eGCG) as a biocompatible inhibitor of ricin toxin. *Biochim Biophys Acta* 1860:1541–1550
23. Massey S, Quiñones B, Teter K (2011) A cell-based fluorescent assay to detect the activity of Shiga toxin and other toxins that inhibit protein synthesis. *Methods Mol Biol* 739:49–59
24. Rasooly R, He X (2012) Sensitive bioassay for detection of biologically active ricin in food. *J Food Prot* 75:951–954
25. Quiñones B, Swimley MS, Taylor AW et al (2011) Identification of *Escherichia coli* O157 by using a novel colorimetric detection method with DNA microarrays. *Foodborne Pathog Dis* 8:705–711
26. Quiñones B, Swimley MS (2011) Use of a vero cell-based fluorescent assay to assess relative toxicities of Shiga toxin 2 subtypes from *Escherichia coli*. *Methods Mol Biol* 739:61–71

## Molecular Methods for Identification of *Clostridium tetani* by Targeting Neurotoxin

Basavraj Nagoba, Mahesh Dharne, and Kushal N. Gohil

### Abstract

Tetanus is a potentially fatal muscle spasm disease. It is an important public health problem, especially in rural/tribal areas of developing countries. Tetanus toxin, a neurotoxin (tetanospasmin), is the most important virulence factor that plays a key role in the pathogenicity of tetanus. Confirmation of virulence by confirming the production of tetanospasmin by infecting species forms the most important part in the diagnosis of tetanus. Various molecular methods have been devised for confirmation of diagnosis by targeting different genes. The most common molecular methods are tetanospasmin producing (*TetX*) gene-targeted methods using *TetX*-specific primers. Here, we describe various molecular methods targeting *TetX* gene such as polymerase chain reaction, pulsed-field gel electrophoresis, Southern blotting, loop-mediated isothermal amplification assay, etc. to confirm the virulence of *Cl. tetani*.

**Key words** Tetanus, Tetanospasmin, *TetX* gene, PCR

---

### 1 Introduction

*Clostridium tetani* is a motile, spore-forming, anaerobic Gram-positive bacillus causing tetanus—a potentially fatal muscle spasm disease [1]. Tetanus remains an important public health problem in developing countries, especially in rural/tribal areas [2–5].

Since the introduction of the vaccination program in 1961, there has been a significant decline in the number of cases in the Western world [6], and currently it is very rarely reported from the developed world [7]. Because of increased coverage of immunization, the incidence has also declined dramatically from the developing world. This is more true about the urbanized developing world where there is an increased coverage of immunization and where there is realization of the significance of immunization by population. However, in rural/tribal areas of the developing world, where the importance of immunization is not yet fully realized by population, tetanus still exists [8]. Hence, the isolated cases have

been frequently reported from developing countries, including India, especially in non-immunized and inadequately immunized individuals from rural/tribal areas [2–5, 9–12].

### **1.1 Importance of Laboratory Diagnosis**

In view of its existence, in isolated cases, isolation, identification, and to find out its virulence form an important part in the confirmation of infection by *Cl. tetani*. Although the diagnosis of tetanus is based on typical clinical features, laboratory methods are necessary to confirm the clinical diagnosis and to rule out certain conditions, which clinically mimic generalized tetanus [13]. These conditions include strychnine poisoning and dystonic reactions to antidopaminergic drugs. The most important part in the laboratory diagnosis is the confirmation of virulence to differentiate *Cl. tetani* from other morphologically similar nonpathogenic *Clostridia*, which include *Cl. tetanomorphum* and *Cl. sphenoides* [1].

Toxicity testing in guinea pigs or mice was the only method available in the past. Recently, a number of molecular methods have been developed to confirm the toxicity. In view of the strict rules governing the animal experiments, especially in countries like India, molecular methods are most suitable for the confirmation of virulence of the strain by detection of neurotoxin. Also these tests are very rapid and help in definitive diagnosis as well as in confirmation of virulence and to differentiate *Cl. tetani* from other morphologically similar nonpathogenic *Clostridia* mentioned above [14].

### **1.2 Importance of Molecular Methods**

As there is a wide variation in metabolic activities and nutritional requirements, it is difficult to identify bacteria belonging to genus *Clostridium* based on phenotypic characters [15]. Moreover, the confirmation of virulence is still more difficult, and no single test is available other than toxicity testing in animals, which is not feasible in most laboratories. Finally, because of ethical rules governing the use of animals for experimentation, it is very difficult to get permission to conduct such experiments.

In view of these problems, molecular methods are the best alternatives. Such molecular identification techniques are the most important tools for confirmation because they are species specific or to a particular bacterial phenotype, like genes for secondary metabolite production, degradation of certain pollutant, and endotoxin or exotoxin.

These techniques are highly sensitive and specific and help in accurate and rapid detection of microbial pathogens resulting in definitive diagnosis. They include polymerase chain reaction (PCR), fluorescent amplification-based specific hybridization (FLASH)-based PCR assay, loop-mediated isothermal amplification (LAMP) assay, pulsed-field gel electrophoresis (PFGE), and Southern blot analysis targeting neurotoxin gene (*TetX* gene). Other molecular methods targeting 16S rRNA and DNA typing can also be used for the confirmation of *Cl. tetani*.

The most commonly used molecular methods in the confirmation of diagnosis of tetanus are *TetX* gene-targeted methods using *TetX*-specific primers targeting the *Cl. tetani* neurotoxin.

### 1.3 *TetX* Gene-Targeted Methods

Tetanus is the result of production of powerful exotoxin (neurotoxin) known as tetanus toxin, also known as the tetanospasmin, which is released during spore germination. This toxin blocks release of neurotransmitter from the presynaptic membrane of inhibitory interneurons of the spinal cord and brainstem that regulate muscle contraction. Thus, the neurotoxin interferes with the normal nerve functioning, thereby causing continuous muscle contraction [16].

*Cl. tetani* contains a double-stranded circular DNA molecule of 2,799,250 bp in length as its genome. In addition to this chromosomal DNA, it shows the presence of an extra chromosomal plasmid of 74 kbp that encodes for an exotoxin [16]. The production of tetanus toxin is regulated by *TetR* (direct transcriptional activator of tetanus toxoid). The *TetX* (a gene of the tetanus toxin) and *TetR* are located on the 74 kbp plasmid (also known as megaplasmid) [17, 18]. This means that virulence of *Cl. tetani* is directly proportional to the presence of megaplasmid [19]. The size of the *TetX* gene is 1354 bp. For PCR amplification of this fragment of 1354 bp, the sequences of oligonucleotide primers are used. Polymerase chain reaction (PCR) is the most commonly used molecular technique for detection of tetanospasmin.

---

## 2 Materials

### 2.1 PCR Studies

#### 2.1.1 DNA Extraction

1. TE (Tris/EDTA) buffer: Prepare a stock solution of 1 M Tris by dissolving 60.57 g of Tris (hydroxymethyl) aminomethane in 500 mL of milli-Q water, and adjust the pH to 7.5 using HCl (*see* **Notes 1** and **2**). Prepare a stock solution of 0.5 M EDTA by dissolving 18.6 g diaminoethanetetraacetic acid in 100 mL of milli-Q water (*see* **Note 3**).

For DNA isolation, take 10 mL of 1 M Tris-HCl (pH 7.5) and 2 mL of 0.5 M EDTA (pH 8.0) from stock solution and fill up to the final volume of 1 L.

2. Sodium dodecyl sulfate (SDS): 10% solution in water (*see* **Note 4**).
3. Proteinase K: Required concentration is 20 mg/mL (stored in small single-use aliquots at  $-20^{\circ}\text{C}$ ).
4. Sodium chloride (NaCl): 5 M NaCl in water.
5. Cetyltrimethylammonium bromide (CTAB)/NaCl solution: Dissolve 4.1 g NaCl in 80 mL water and slowly add 10 g CTAB while heating and stirring. Heat to approximately  $65^{\circ}\text{C}$  to dissolve. Adjust volume to 100 mL with water. Store at room temperature.

6. Chloroform/isoamyl alcohol 24:1 (v/v, *see* **Notes 5** and **6**).
7. Water-saturated phenol/chloroform/isoamyl alcohol 25:24:1 (by vol., *see* **Notes 5** and **6**).
8. Isopropanol (*see* **Note 6**).
9. 70% ethanol (*see* **Note 6**).

Or

10. Bacterial DNA extraction kit (Merck-Genei).
11. TAE buffer: 1× TAE buffer containing 40 mM Tris, 20 mM acetate, and 2 mM EDTA (*see* **Note 7**).
12. 0.8% agarose horizontal gel electrophoresis: Dissolve 0.8 g of agarose in TAE buffer (*see* **Note 8**).
13. Load extracted DNA sample with 2 μL of GelRed™ dye. Perform the electrophoresis at approximately 100 V till the end of the gel, and observe the gel in protein simple gel documentation unit to visualize extracted DNA.
14. Check the quality of extracted DNA with NanoDrop Lite spectrophotometer (NanoDrop Biotechnologies). To check the concentration of extracted DNA, take the absorbance at 260 nm ( $A_{260}$ ). Quality of DNA can be checked by the ratio of absorbance at 260 and 280 nm. If the ratio is 1.8, then the DNA is pure, free from contamination of RNA and protein.

### 2.1.2 PCR Amplification and Sequencing

1. Primer (Eurofins): Primers are single-stranded short oligonucleotides which bind to the template strand and allow DNA polymerase to add complementary base pairs to its free 3'OH end. To amplify both strands of the template, two primers are required, i.e., forward primer and reverse primer which amplify the DNA in 5' → 3' direction. For PCR amplification add 10 nM concentration of each primer to the reaction tube. Primers used for the amplification of *TetX* gene are:

5' CTG GAT TGT TGG GTT GAT AAT G-3'

5' ATT TGT CCA TCC TTC ATC TGT AGG-3'

2. Deoxynucleoside triphosphate (dNTP) (Merck-Genei): dNTPs are the nitrogen bases which have to be added during the amplification reaction. Mixture of dNTPs contains purines, i.e., adenine (A) and guanine (G), and pyrimidines, i.e., cytosine (C) and thymine (T), in concentration of 200 μM/mL.
3. Taq polymerase (Genei): Taq polymerase is the DNA polymerase enzyme which adds dNTPs to the free 3'OH end of amplifying strand. Concentration required is 1 U/μL.
4. 10× reaction buffer (Genei) comprised of 100 mM Tris-HCl, 15 mM MgCl<sub>2</sub>, 500 mM KCl, and pH 8.3 (20 °C).



5. Exo-rSAP (New England Biolabs) method: PCR amplicons normally contain primer dimers and other impurities. To purify these amplicons, Exo-SAP method is used. PCR amplicons are mixed with Exo-Ant mix (*see Note 9*) and molecular grade PCR water.
6. ABI 3500xl genetic analyzer (Thermo Fisher): This is a sequencing instrument based on Sanger's sequencing principle. Sequencing is done according to the manufacturer's protocol.

### 2.1.3 Sequence Analysis

1. Sequence analysis software version 5.1 (Applied Biosystems): Use this software to check the quality of reads.

## 2.2 Materials

### Required for Pulsed-Field Gel Electrophoresis (PFGE) and Southern Blot Analysis

1. Agarose gel: 2% agarose gel (*see Note 8*).
2. Buffer I, a lysis buffer, used for the lysis of agar plugs: 6 mM Tris-HCl (pH 7.4), 1 M NaCl, 10 mM Na<sub>2</sub>EDTA, 0.5% Brij 58, 0.2% Na-deoxycholate, and 0.2% Na-lauroylsarcosine, supplemented with 5 mg/mL of lysozyme and 1 µg/mL of RNase.
3. Buffer II: 10 mM Tris-HCl (pH 7.4), 1 M Na<sub>2</sub>EDTA, 1% Na-lauroyl sarcosine, and 1 mg/mL proteinase K.
4. TE Buffer: 10 mM Tris-HCl, (pH 7.4), 0.1 mM Na<sub>2</sub>EDTA.
5. Restriction enzymes: 20 U of ApaI or SmaI. ApaI produces staggered end, while SmaI produces blunt ends.
6. Tris-borate, EDTA: 44.5 mM Tris-borate, 12.5 mM EDTA (pH 8.0).
7. Nylon membrane: Positively charged nylon membrane probed with digoxigenin (DIG)-labeled, double-stranded *TetX*-specific DNA fragment.
8. UV chamber: For fixation of transferred fragments on nylon membrane. Fixation is carried out at 312 nm.

### 2.3 Loop-Mediated Isothermal Amplification (LAMP) Assay

1. Primers: LAMP technique uses 4–6 pairs of primers, primers for conserved region and internal primer specific to gene of interest. For the identification of the presence of *TetX* gene in the sample are the following pairs of samples:

F3: 5'-GATAAAGATGCATCTTTAGGATT-3'.

B3: 5'-TCTTCTTCATTATCAACCCAAC-3'.

FIP:5'-AGTTGCTTGCAATTAATATATCCCTAGTAGGTA  
CCCATAATGGTCA-3.

BIP:5'-AACATGTGATTGGTACTTTGTACCTTATGTGT  
CTATGGTGTGTTG-3'.

2. *Bst* polymerase: The principle of LAMP is autocycling strand displacement DNA synthesis in the presence of *Bst* DNA polymerase with high strand displacement activity under

isothermal conditions between 60 and 65 °C resulting in 109 copies of target DNA as well as large amount of by-products (magnesium pyrophosphate) within an hour.

3. Water bath: For amplification. It is set at 60–65 °C.
4. Turbidometer: Measures the turbidity of by-product formed due to reaction of positive product with magnesium pyrophosphate.

---

## 3 Methods

### 3.1 PCR Studies

Use of PCR for the detection of the *TetX* gene is a rapid technique to confirm the presence of *Cl. tetani* in clinical samples as well as *Cl. tetani* grown in culture. The methodology used includes the following steps.

#### 3.1.1 DNA Extraction

Use a specimen obtained from a patient, collected in Robertson cooked meat broth, for DNA extraction [14]. Alternatively, suspend colonies of *Cl. tetani* grown on an agar plate in distilled water, and lyse these by incubation at 95 °C for 10 min, after centrifugation (76 rcf for 60 s). Use the supernatant of the lysate for DNA extraction [20]. Bacteria grown in broth culture can also be used for DNA extraction [21]. Extract bacterial DNA applying a standard procedure [22], i.e., incubate the cells in a CTAB solution at 65 °C followed by chloroform extraction and isopropanol precipitation.

1. Inoculate 5 mL of liquid culture with the bacterial strain and incubate under suitable conditions for 24 h.
2. Centrifuge 1.5 mL of the culture in a microcentrifuge for 2 min or until a compact pellet forms. Discard the supernatant.
3. Re-suspend the pellet in TE buffer by repeated pipetting, and add 30 µL of 10% SDS and 3 µL of 20 mg/mL proteinase K to a final concentration of 100 µg/mL proteinase K in 0.5% SDS. Mix thoroughly and incubate for 1 h at 37 °C.
4. Add 100 µL of 5 M NaCl and mix thoroughly. This step is very important as CTAB–nucleic acid precipitate will form, if salt concentration drops below about 0.5 M at room temperature. The aim here is to remove cell wall debris, denatured protein, and polysaccharides complexed to CTAB, while retaining the nucleic acids in solution.
5. Add 80 µL of CTAB/NaCl solution. Mix thoroughly and incubate 10 min at 65 °C.
6. Add an approximately equal volume (0.7–0.8 mL) of chloroform/isoamyl alcohol, mix thoroughly, and spin 4–5 min in a microcentrifuge. This extraction removes CTAB–protein/polysaccharide complexes.

7. Remove aqueous, viscous supernatant to a fresh microcentrifuge tube. Add an equal volume of phenol/chloroform/isomyl alcohol, extract thoroughly, and spin in a microcentrifuge for 5 min.
8. Transfer the supernatant to a fresh tube. Add 0.6 volume of isopropanol to precipitate the nucleic acids. Shake the tube back and forth until a stringy white DNA precipitate becomes clearly visible.
9. Wash the DNA with 70% ethanol to remove residual CTAB and respin for 5 min at room temperature to re-pellet it. Carefully remove the supernatant and briefly dry the pellet in a vacuum concentrator.
10. Re-dissolve the pellet in 100  $\mu$ L TE buffer. This may take some time (up to 1 h) since the DNA is of high molecular mass. 15  $\mu$ L of this DNA will typically be fully digested by 10 U of *EcoRI* in 1 h, which is sufficient to be clearly visible on an agarose gel.

### 3.1.2 PCR Amplification and Sequencing

1. Use the *Cl. tetani*-specific primers targeting a 1354 bp fragment of the *TetX* gene to amplify the DNA extracted from the specimen. The PCR reaction containing 10 nM (each) primer (Eurofins), 200  $\mu$ M (each) deoxynucleoside triphosphate (dNTP) (Genel), 1 U of *Taq* polymerase (Genel) in the appropriate reaction buffer, and 50 and 100 ng of DNA extracts as the templates are carried out in 50  $\mu$ L of reaction mixture.
2. Use as cycling conditions: 95  $^{\circ}$ C for 10 min, followed by 25 cycles each consisting of 1 min at 94  $^{\circ}$ C, 1 min at 52  $^{\circ}$ C, and 1.5 min at 72  $^{\circ}$ C.
3. Document positive PCR amplicons.
4. Purify using Exo-rSAP (New England Biolabs) method. Mix 5  $\mu$ L of PCR product with 2  $\mu$ L of Exo-Ant mix (*see Note 9*). Heat reaction tube in thermocycler at 37  $^{\circ}$ C for 30 min and 80  $^{\circ}$ C for 20 min. Then, cool at 4  $^{\circ}$ C in thermocycler only. Check the purity and store samples at -20  $^{\circ}$ C. Sequence both strands using 3500xl genetic analyzer (Thermo Fisher) [23].

### 3.1.3 Detection of PCR Products

The specific PCR amplification product (amplicons) containing the target nucleic acid can be detected by using different techniques such as agarose gel electrophoresis, Southern blot analysis, dot blot analysis, and other methods. Agarose gel electrophoresis is the most commonly used method.

### 3.1.4 Sequence Analysis and Interpretation

1. Assemble and edit the obtained sequences using sequence analysis software version 5.1 (Thermo Fisher).
2. Submit edited sequences to BLASTN and BLASTX using default parameters for analysis [24], followed by comparison with closest homologous sequences retrieved from the GenBank database.

3.1.5 *Fluorescent Amplification-Based Specific Hybridization (FLASH)-Based PCR Assay*

This is a FLASH based PCR assay. This PCR assay used for rapid identification of cultured isolates of *Cl. tetani* appears to be more suitable and rapid [21]. This method is also a *TetX* gene-targeting method. The steps used are the same as in PCR assay, except for the last step:

1. Analyze the PCR products by agarose gel electrophoresis.
2. Save the images with the help of the fluorescence detector gene.
3. Analyze the obtained fluorescence data using gene software. This method gives clear and unambiguous results [21].

**3.2 Other Molecular Methods Used for Detection of *Cl. tetani* by Targeting *TetX* Gene (See Note 10)**

3.2.1 *PFGE and Southern Blot Analysis*

1. Grow *Cl. tetani* on solid media, collect, adjust to  $2 \times 10^8$  CFU/mL, and then mix 1:1 with 2% agarose to prepare agarose plugs.
2. Lyse the embedded cells in buffer I solution supplemented with 5 mg/mL lysozyme and 1  $\mu$ g/mL RNase for 5 h at 37 °C.
3. Incubate the plugs overnight in 1 mL of buffer II.
4. Wash the plugs thoroughly with TE buffer.
5. Digest agarose plugs overnight at 25 °C with 20 U of *ApaI* or *SmaI*.
6. Perform electrophoresis on 1% PFGE-grade agarose using a CHEF Mapper XA system. Running conditions are 0.5–20 s for both enzymes, using switch times of 0.5–20 s for 27 h at 6.0 V/cm, 14 °C, in 0.5 $\times$  TBE (Tris-borate, EDTA).
7. Stain gels either with ethidium bromide and analyze using a Gel Doc 1000 system (BIO-Rad labs) or prepare Southern blots, which are subsequently probed with a 1354 bp digoxigenin (DIG)-labeled, double-stranded probe specific for *TetX* gene. Prepare this probe by PCR using the DIG Chem-Link labeling and detection set kit as recommended by the manufacturer.
8. Fix the DIG-labeled probe specific to *TetX* gene on a nylon membrane.
9. Transfer the PFGE-separated DNA fragments to positively charged nylon membrane, and fix at 312 nm for 2 min.
10. Hybridize the blots against the DIG-labeled *TetX* probe.
11. Detect the hybridized *TetX* probe by using a DIG chemiluminescence detection system with chloroplastic drought stress protein as the substrate [23].

---

## 4 Notes

1. Having water at the bottom of the cylinder helps to dissolve Tris relatively easily, allowing the magnetic stir bar to go to work immediately. If using a glass beaker, Tris can be dissolved faster provided the water is warmed to about 37 °C. However, the downside is that care should be taken to bring the solution to room temperature before adjusting pH.

2. Concentrated HCl (12 N) can be used at first to narrow the gap from the starting pH to the required pH. However, it would be better to use a series of HCl (e.g., 6 N and 1 N) with lower ionic strengths to avoid a sudden drop in pH below the required pH. Use of safety wears is recommended while using corrosive reagents.
3. Note that EDTA will not be soluble until pH reaches to 8.0. Adjust the pH using NaOH. Use vigorous stirring, moderate heat to dissolve EDTA, if required.
4. SDS precipitates at 4 °C. Therefore, the lysis buffer needs to be warmed prior to use.
5. Always prepare fresh mixture.
6. It is advisable to use prechilled ( $\leq 4$  °C) reagents for good quality DNA isolation.
7. TAE buffer: Prepare 50× stock solution of TAE buffer. To prepare 50× TAE buffer, dissolve 242 g Tris base, 57.1 mL glacial acetic acid, and 100 mL of 0.5 M EDTA (pH 8.0) into 600 mL of deionized water. Adjust the final volume to 1 L with deionized water.

To prepare a 1× working solution from 50× stock buffer, mix 50× stock buffer with DNase-free deionized water 1:4 by vol.
8. Add agarose powder in buffer solution and boil it until all the agarose is melted. Cool it and pour it into casting tray. Allow it to solidify.
9. Preparation of Exo-Ant mix: Mix 0.2  $\mu\text{L}$  of antarctic phosphatase and ten times diluted 0.5  $\mu\text{L}$  of ExoI in 1.3  $\mu\text{L}$  of molecular-grade PCR water (HiMedia). Store the reagent at 4 °C.
10. The LAMP assay is another assay in which *TetX* gene of *Cl. tetani* is used as the target gene. LAMP is a rapid, highly specific, and sensitive technique for the identification of this bacterium. It is an amplification-based identification technique, but unlike PCR, LAMP does not require a thermal cycler and multiple steps for amplification. It amplifies the template strand under isothermal condition at 63–67 °C. LAMP assay uses two pairs of primers, namely, a pair of outer primers and a pair of inner primers which detect the conserved region of a gene, and amplification is done using Bst polymerase [25]. The reaction can be identified with the help of a turbidimeter. Turbidity is due to the formation of the by-product, magnesium dihydrogen phosphate. Alternatively, agarose gel electrophoresis can also be used or by applying appropriate chromogenic substances like hydroxynaphthol blue. Thus, special testing equipment is not required. Jiang et al. used tetanus toxin gene as target gene for the LAMP assay [25]. The accuracy and specificity of LAMP assay has been confirmed by comparison of LAMP assay with API 20A test [26].

## Acknowledgments

Authors wish to thank Dr. Milind Davane, Asst. Professor in Microbiology, and Mr. Vinod Jogdand, Asst. Librarian, MIMSR Medical College, Latur, for their help in the preparation of the manuscript.

## References

- Nagoba BS, Pichare AP (2016) Medical microbiology and parasitology, 3rd edn. Elsevier, New Delhi, pp 283–288
- Tullu MS, Deshmukh CT, Kamat JR (2000) Experience of pediatric tetanus cases from Mumbai. *Indian Pediatr* 37:765–771
- Lodha R, Sareen A, Kumar RM, Arora NK (2000) Tetanus in immunized children. *Indian Pediatr* 37:223–224
- Gibson K, Bonaventure UJ, Kiviri W, Parlow J (2009) Tetanus in developing countries: a case series and review. *Can J Anaesth* 56:307–315
- Alagbe-Briggs OT, Tinubu SA (2012) Tetanus - a case report with severe autonomic instability and: a review of the literature. *Niger J Med* 21:353–356
- Sanford JP (1995) Tetanus – forgotten but not gone. *N Engl J Med* 332:812–813
- Cook TM, Protheroe RT, Handel JM (2001) Tetanus: a review of the literature. *Br J Anaesth* 87:477–487
- Nagoba BS, Jahagirdar VL, Sheikh NK (2016) Tetanus is not the past – It still exists. *J Patient Safety Infect Control*. 4: (in press). doi:10.1016/j.jpsic.2015.11.006
- Chang SC, Wang CL (2010) Neonatal tetanus after home delivery: report of one case. *Pediatr Neonatol* 51:182–185
- Njiki Kinkela MN, Nguefack F, Mbassi Awa H, Chelo D, Enyama D, Mbollo Kobela M, Koki Ndombo PO (2012) Tetanus in older children in a pediatric hospital in Yaounde, Cameroon. *Pan Afr Med J* 11:37
- World Health Organization Report. Tetanus (total) reported cases from India. [http://apps.who.int/immunization\\_monitoring/global-summary/timeseries/tsincidencettetanus.html](http://apps.who.int/immunization_monitoring/global-summary/timeseries/tsincidencettetanus.html). Accessed on 19 May 2016
- Marulappa VG, Manjunath R, Mahesh Babu N, Maligegowda L (2012) A ten year retrospective study on adult tetanus at the epidemic disease (ED) hospital, Mysore in Southern India: a review of 512 cases. *J Clin Diagn Res* 6:1377–1380
- Longo DL, Fauci AS, Kasper DL, Hauser SL, Jameson JL, Loscalzo J (2012) Harrison's principles of internal medicine, vol Vol 1, 18th edn. The McGraw-Hill Companies, London, pp 1197–1200
- Madhu G, Sheikh N, Shah P, Mehetre G, Dharne MS, Nagoba BS (2015) Detection of *Clostridium tetani* in human clinical samples using *tetX* specific primers targeting the neurotoxin. *J Infect Public Health* 9:105–109
- Cato EP, Georgew L, Finegold M (1986) Genus *Clostridium prazmowski* 1880, 23AL. In: PHA S, Mair NS, Sharpe ME, Holt JG (eds) Bergey's manual of systematic bacteriology, vol vol. 2. Williams & Wilkins, Baltimore, pp 1141–1200
- Quantitation of *Clostridium tetani* genomes. Genesig Standard kit handbook HB10.04.08. Published Date: 26/04/2016
- Bruggemann H, Bauumer S, Fricke WF, Wiezer A, Liesegang H, Decker I et al (2003) The genome sequence of *Clostridium tetani*, the causative agent of tetanus disease. *Proc Natl Acad Sci U S A* 100:1316–1321
- Marvaud JC, Eisel U, Binz T, Niemann H, Popoff MR (1998) TetR is a positive regulator of the tetanus toxin gene in *Clostridium tetani* and is homologous to botR. *Infect Immun* 66:5698–5702
- Laird WJ, Aaronson W, Silver RP, Habig WH, Hardegnee MC (1980) Plasmid associated toxigenicity in *Clostridium tetani*. *J Infect Dis* 142:623
- Nagao K, Mori T, Sawada C, Sasakawa C, Kanezaki Y (2007) Detection of the tetanus toxin gene by polymerase chain reaction: a case study. *Jpn J Infect Dis* 60:149–150
- Mohammad S, Hossein E, Mohammad R, Mojtaba S, Saeid AJ (2011) Detection of *Clostridium tetani* by fluorescent amplification based specific hybridization. *Afr J Microbiol Res* 5:5489–5492
- Ausubel FM, Bren R, Kingston RE, Moore DD, Seidman JG, Struhl K (1988) Current protocols in molecular biology. John Wiley & Sons, Inc., New York, NY

23. Plourde-Owobi L, Seguin D, Baudin MA, Moste C, Rokbi B (2005) Molecular characterization of *Clostridium tetani* strains by pulsed-field gel electrophoresis and colony PCR. *Appl Environ Microbiol* 71:5604–5606
24. Altschul SF, Madden TL, Schaffer AA, Zhang J, Zhang Z, Miller W, Lipman DJ (1997) Gapped BLAST and PSI-BLAST: a new generation of protein database search program. *Nucleic Acids Res* 25:3389–3402
25. Jiang DN, Xiaoyun P, Jiehong W, Meng L, Ping L (2013) Rapid, sensitive and specific detection of *Clostridium tetani* by loop-mediated isothermal amplification assay. *J Microbiol Biotechnol* 23:1–6
26. Notomi T, Okayama H, Masubuchi H, Yonekawa T, Watanabe K, Amino N, Hase T (2000) Loop mediated isothermal amplification of DNA. *Nucleic Acids Res* 28:E63

## Label-Free Immuno-Sensors for the Fast Detection of *Listeria* in Food

Alexandra Morlay, Agnès Roux, Vincent Templier, Félix Piat, and Yoann Roupioz

### Abstract

Foodborne diseases are a major concern for both food industry and health organizations due to the economic costs and potential threats for human lives. For these reasons, specific regulations impose the research of pathogenic bacteria in food products. Nevertheless, current methods, references and alternatives, take up to several days and require many handling steps. In order to improve pathogen detection in food, we developed an immune-sensor, based on Surface Plasmon Resonance imaging (SPRi) and bacterial growth which allows the detection of a very low number of *Listeria monocytogenes* in food sample in one day. Adequate sensitivity is achieved by the deposition of several antibodies in a micro-array format allowing real-time detection. This label-free method thus reduces handling and time to result compared with current methods.

**Key words** *Listeria monocytogenes*, Food safety, Antibody microarrays, Immunosensor, Surface plasmon resonance (SPR), Bacterial growth

---

## 1 Introduction

*Listeria monocytogenes* is one of the five most frequent pathogens involved in death due to foodborne diseases (source CDC, <http://www.cdc.gov/foodborneburden/2011-foodborne-estimates.html>). Moreover, the incidence of listeriosis in the population has increased in recent years [1] with a mortality rate ranging from 20 to 30% [2]. So far, the standard method for *L. monocytogenes* detection in food products is time-consuming both in manipulations and for getting results. The major drawback of this cultural technique corresponds to the time necessary for bacterial enrichment, a step that is even longer for slow growing *L. monocytogenes* strains. In fact, according to the ISO 11290, the detection of this bacterial specie can take up to 6 days [3]. In the last decade, numerous researches have been investigated and a few alternatives methods have been developed for the detection of several important



food-borne pathogens such as *L. monocytogenes*. For instance, molecular techniques allowing bacterial DNA detection using Polymerase-Chain Reaction (PCR) after specific genetic sequence amplification have appeared as well as some immunoassays methods including Enzyme-Linked Immunosorbent Assay (ELISA), Enzyme-Linked Fluorescent Assay (ELFA) or lateral-flow assays [4]. Nevertheless, although faster than standards methods, these bacterial detection systems still require one or two enrichment steps which may last several days before the bacterial concentration has reached the limit of detection of the final analysis step. To our knowledge, only one example of *L. monocytogenes* detection led during the enrichment step has been described so far. It consists in incorporating antibody-functionalized nanoparticles [5]. In this work, the pathogen detection, using Surface Enhanced Raman Scattering (SERS), is based on an immunoassay which aggregates gold and magnetic labeling nanoparticles. In order to going one step further in the development of easy-to-operate techniques for the specific detection of *L. monocytogenes*, we designed a specific real-time antibody microarray allowing the detection label-free during the enrichment of food samples. This technology is based on the use of Surface Plasmon Resonance imaging (SPRi) of the bacterial growth [6].

---

## 2 Materials

### 2.1 Synthesis of *N*-Hydroxy-Succinimidyl-6-(1*H*-Pyrrole-1-yl)-Hexanamide (Pyrrole-NHS)

1. 2,5-Dimethoxytetrahydrofuran, mixture of cis and trans isomers (98%).
2. 6-Aminocaproic acid ( $\geq 99.0\%$ ) (Acros Organics).
3. Acetic acid.
4. 1,4-Dioxane (99.8%).
5. *N*-Hydrosuccinimide (98%).
6. *N,N*-Dicyclohexylcarbodiimide (99%).
7. *N,N*-Dimethylformamide (DMF) ( $\geq 99.0\%$ ).
8. Dichloromethane ( $\geq 99.8\%$ ).
9. Ethanol ( $\geq 99.8\%$ ).
10. Silicagel PF254 containing 15% CaSO<sub>4</sub> for chromatography (Sigma-Aldrich).

### 2.2 Coupling Antibodies to Pyrrole-NHS

1. Use four IgG type polyclonal antibodies, reacting with specific strains of *L. monocytogenes*: LIM 14 and LIM 16 (Prestodiag), Ab20506 (Abcam) and Ab78729 (Abcam). Re-suspend all antibodies are re-suspended in storage buffer (PBS-containing 0.1% sodium azide) at 0.5 mg/mL. Follow supplier recommendations regarding storage (4 °C for short term and -20 °C for long-term storage) (*see* **Notes 1** and **2**).

2. Use one monoclonal antibody, KLH (Keyhole Limpet Hemocyanin), which not reacts with bacterial models interesting for human health, as negative control (CEA Marcoule) (*see Note 3*).
3. 4 mM Pyrrole–NHS in dry DMSO (prepared as described in Subheading 3.1). Store at  $-20\text{ }^{\circ}\text{C}$ .
4. Phosphate buffered saline (PBS: 10 mM phosphate buffer, 2.7 mM KCl, 137 mM NaCl, pH 7.4). Dissolve under stirring 1 tablet in 200 mL of ultra-pure water. After preparation, sterilize by autoclaving at  $121\text{ }^{\circ}\text{C}$  during 15 min. Store at  $4\text{ }^{\circ}\text{C}$ .
5. Vivaspin 500  $\mu\text{L}$  ultracentrifugation spin columns with 30,000 MWCO cutoff membrane in polyethersulfone (Sartorius Stedim Biotech GmbH).
6. Electropolymerization buffer: 50 mM  $\text{NaH}_2\text{PO}_4$ , 50 mM NaCl, 10% (w/v) glycerol. The final pH is adjusted to 6.8 with NaOH. Store at  $4\text{ }^{\circ}\text{C}$ .
7. Spectrophotometer (NanoDrop, ND-1000, ThermoScientific).

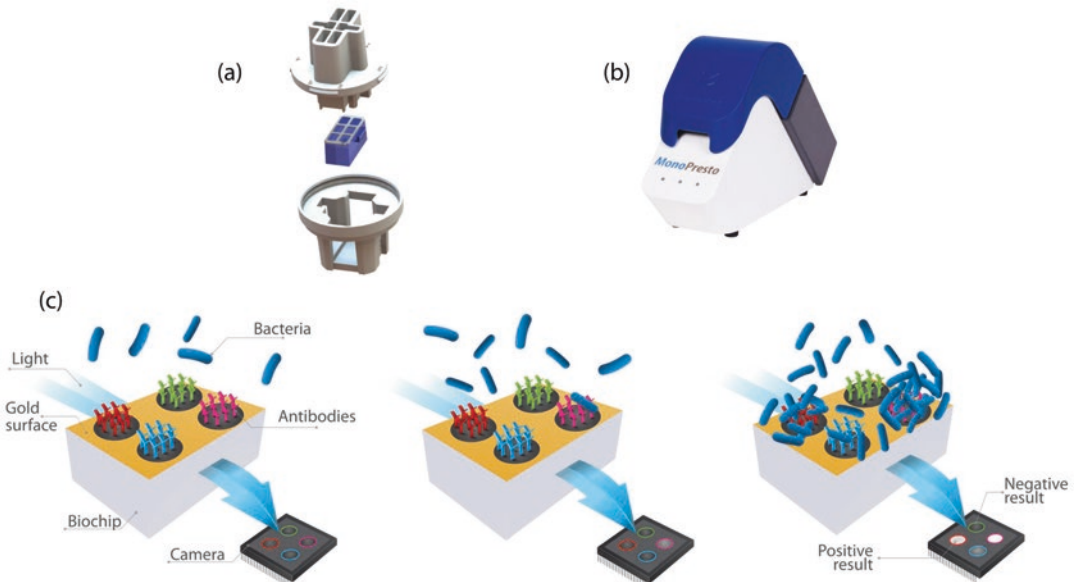
### **2.3 Electrochemical Deposition of Pyrrole–Antibody Conjugates on SPRI Biochip Surface**

1. Biochips: glass prisms coated with two metallic layers: 2 nm chrome and 50 nm gold (Prestodiag).
2. 1 M Pyrrole (Interchim) in acetonitrile. Store at  $-20\text{ }^{\circ}\text{C}$ .
3. 5  $\mu\text{M}$  Pyrrole–antibody conjugates (prepared as described in Subheading 3.2).
4. The microarrayer used for immobilizing Pyrrole-IgG conjugates on the prism is commercially available (OmniGrid Micro robotic Arrayer).
5. Bovine serum albumin (BSA), 0.1% in PBS.
6. 200  $\mu\text{L}$  small PCR tubes.

### **2.4 Sample Preparation and Detection of *L. monocytogenes* Strains Using SPRI**

1. Ready to use Demi-Fraser broth (Biokar diagnostics). Store protected from light at  $4\text{ }^{\circ}\text{C}$ .
2. Tryptic Soy Broth (TSB). Prepare according to manufacturer instructions.
3. Buffer peptone water (BPW, Biokar diagnostics). Prepare according to manufacturer instructions.
4. Tryptone Soy Agar (TSA), ready to use media in 200 mL bottle (bioMérieux). Prepare according to manufacturer instructions.
5. Compass *Listeria* Agar (Biokar diagnostics), ready to use. Store at  $4\text{ }^{\circ}\text{C}$ .
6. Two *L. monocytogenes* strains (A and B, serovars 1/2b and 4b respectively) were used in this study. They were isolated from natural contaminated food and provided by the Institut Scientifique d'Hygiène et d'Analyse (ISHA).

7. Stomacher® Bag containing 280  $\mu\text{m}$  filter membrane.
8. Peristaltic blender (Bag mixer, Interscience).
9. 14 mL sterile culture tubes.
10. Packaged salad (lettuce) bought in a local store.
11. Weighing scale.
12. Densitometer.
13. The SPRi system, called Monopresto™ (Prestodiag) allows the detection of pathogens in food samples. It is composed of two distinct parts: (1) the MonoPresto™ reader and the Bacterics™ software. Detection tests are carried by PlasmIA™ technology [7], and (2) the Prestokit comprising a six reaction chambers laid on the antibodies coated prism (Fig. 1). Each isolated chamber can contain 1000  $\mu\text{L}$  of solution. In order to prevent any leakage, a silicone gasket is placed between the prism and reaction chambers, all maintained tightened together by a clamping device (*see Note 4*). Moreover, temperature of the Monopresto™ system is regulated by the software allowing optimal growth of bacteria of interest (for *L. monocytogenes* a temperature of 37 °C is used) (*see Note 5*).



**Fig. 1** (a) Prestokit with biochip between the two plastic parts. The plastic parts on the **top** present six separated chambers. (b) The optical reader, MonoPresto. (c) Presentation of the PlasmIA technology. Viable cells grow in the wells and the binding of bacteria on specific antibodies is continuously monitored in a real-time and label-free manner

### 3 Methods

#### 3.1 Synthesis of Pyrrole-NHS

1. Heat under reflux for 4 h a mixture of 2,5-dimethoxytetrahydrofuran (490 mmol), 6-aminocaproic acid (430 mmol), acetic acid (450 mL) and 1,4-dioxane (600 mL).
2. Stir the previous mixture at room temperature overnight.
3. Remove the volatile compounds under reduced pressure and eliminate acetic acid by co-evaporation with ethanol ( $2 \times 100$  mL).
4. Dissolve the solid residues in 500 mL of dichloromethane and wash this solution with  $2 \times 250$  mL of ultrapure water to remove residual impurities and unreacted reagents. This solution is evaporated until dryness. The product (*N*-hydrosuccinimide) is obtained with a yield of 82%. Mass spectrometry: *N*-Hydrosuccinimide  $m/z$  182.1. It is purified by chromatography on silica gel ( $600 \times g$ ) column with a gradient of ethanol in dichloromethane. Start the elution with 500 mL of  $\text{CH}_2\text{Cl}_2$ , then 300 mL of a mixture of  $\text{CH}_2\text{Cl}_2/\text{EtOH}$  (98/2), 400 mL of  $\text{CH}_2\text{Cl}_2/\text{EtOH}$  (95/5) and finally 300 mL of  $\text{CH}_2\text{Cl}_2/\text{EtOH}$  (90/10) to elute *N*-hydrosuccinimide. After evaporation of the solvents, *N*-hydrosuccinimide looks like a brownish oil.
5. *N*-Hydrosuccinimide (144 mmol), and *N,N'*-Dicyclohexylcarbodiimide (159 mmol) are dissolved in DMF and stirred at room temperature overnight.
6. Filter the mixture on a sinter glass to eliminate *N,N'*-dicyclohexylurea.
7. Remove the volatile compounds as previously described under reduced pressure. The obtained product (Pyrrole-NHS) has the form of a white powder. It can be used directly or after purification by chromatography as in **step 4**.

#### 3.2 Coupling Antibodies to Pyrrole-NHS

The transamidification reaction between antibodies and the activated ester of Pyrrole-NHS involves the primary amine functions of antibody molecules. All buffers and antibody solutions are kept at 4 °C or on ice between each protocol steps.

1. Before starting the coupling reaction, wash the Vivaspin column membranes once with 200  $\mu\text{L}$  of PBS and centrifuge (all centrifugations are performed with the following settings: speed:  $15,000 \times g$ ; Temperature: 4 °C; Duration: 15 min). Then, load 200  $\mu\text{L}$  of IgG (0.5 mg/mL) on the columns and concentrate. In order to remove all traces of sodium azide, wash IgG then twice with 200  $\mu\text{L}$  of PBS. Finally, collect purified IgG with 200  $\mu\text{L}$  of PBS. Determine the IgG solution concentration by measuring the absorbance at 280 nm (molar

extinction coefficient 210,000 L/mol cm), with a spectrophotometer.

2. In the reacting solution, set the molar ratio of Pyrrole/IgG to 10. Then, adjust volumes of 200  $\mu\text{M}$  Pyrrole-NHS solution (prepare by dilution of the 4 mM solution in PBS) and PBS to reach this molar ratio in a final volume of 400  $\mu\text{L}$ . Typically for 200  $\mu\text{L}$  of an IgG solution at 3.3  $\mu\text{M}$  (= 0.5 mg/mL), add 34  $\mu\text{L}$  of Pyrrole-NHS and 166  $\mu\text{L}$  of PBS.
3. Incubate overnight at 4 °C. Protect tubes from light to minimize Pyrrole photo-oxidation.
4. Remove the unreacted Pyrrole-NHS by centrifugation. First of all, wash the column with 200  $\mu\text{L}$  of PBS. Then, load 400  $\mu\text{L}$  of the reacting solution and wash it twice with 200  $\mu\text{L}$  of PBS. Eventually, collect the Pyrrole-antibody conjugates in 80  $\mu\text{L}$  of electropolymerization buffer. Measure the protein concentration with a spectrophotometer and adjust the volume with the electropolymerization buffer to reach a 5  $\mu\text{M}$  final concentration (*see Note 6*). For short-term utilization, keep the solution at 4 °C, otherwise divide the solution in several aliquots and store at -20 °C.

### **3.3 Electrochemical Deposition of Pyrrole-Antibody Conjugates on SPRi Biochip Surface**

1. Remove any dust from the gold surface by argon flushing. The surface is then rinsed by running ultrapure water (18.2 M $\Omega$  cm), absolute ethanol and once again ultrapure water before being dried under argon flow.
2. Prepare a 100 mM Pyrrole solution by adding 10  $\mu\text{L}$  of the 1 M stock solution to 90  $\mu\text{L}$  of the electropolymerization buffer.
3. Prepare the spotting solutions by mixing 3  $\mu\text{L}$  of the 100 mM Pyrrole solution with 3  $\mu\text{L}$  of the antibody-Pyrrole conjugates (5  $\mu\text{M}$ ) and 9  $\mu\text{L}$  of electropolymerization buffer to reach a final volume of 15  $\mu\text{L}$ . The final concentrations in solution are 20 mM Pyrrole and 1  $\mu\text{M}$  antibody-Pyrrole conjugates (*see Note 7*).
4. Homogenize the spotting solutions by several pipetting before filling a 96-well plate with 11  $\mu\text{L}$  of each sample to be electrochemically grafted on the surface. Make sure that the solution reaches the bottom of the well and avoid air bubbles formation (*see Note 8*).
5. The electropolymerization of the spotting solutions is achieved using the microarrayer. Briefly, plunge a stainless steel needle in a specific well where it takes up about 5  $\mu\text{L}$  of solution. Then, direct it to a desired location on the prism and move it down to the surface. This step allows the deposit of a drop on the prism gold surface and the formation of an interface between two electrodes; the needle (counter electrode) and

the gold surface (working electrode). At that precise time, trigger an electrical pulse of a difference of potential ranging from 0.4 to 2.4 V, and maintain it for 100 ms (*see Note 9*), between the two electrodes. This step leads to Pyrrole polymerization and traps the antibodies onto the gold surface in a thin and solid polyPyrrole film. Once all the solutions of an antibody species are arrayed, rinse the needle and dry three times using ultra-pure water. Repeat the same procedure for all antibody species (*see Note 10*). Spot diameter is 350  $\mu\text{m}$ . A pitch of 450 nm between spots avoids their coalescence (*see Note 11*). Electrodeposition takes place in a closed chamber with a hygrometry level above 60%.

6. Passivate the functionalized prism then with 0.1% BSA solution for 20 min to prevent unspecific binding. After three washings with PBS, keep it finally in PBS at 4 °C before use.

### **3.4 Sample Preparation and Detection of *L. monocytogenes* Strains Using SPR Imaging**

All the steps described here are made using the two *L. monocytogenes* strains in parallel.

1. Streak bacteria from stock suspension conserved at  $-80$  °C on TSA plates. Incubate 24 h at 37 °C.
2. Take one isolated colony from the TSA plate using a sterile inoculation loop and re-suspend it in 6 mL of TSB placed in a 14 mL culture tube. Incubate overnight at 37 °C.
3. Dilute 1 mL of the culture in 9 mL of buffered peptone water. Measure the turbidity of the suspension using the densitometer and adjust it to  $1.0 \pm 0.2$  Mac Farland (approximately  $3 \times 10^8$  CFU/mL) by adding buffered peptone water. From this bacterial suspension, proceed to six tenfold serial dilutions in TSB (100  $\mu\text{L}$  of culture in 900  $\mu\text{L}$  TSB). Spread two TSA plates with 300  $\mu\text{L}$  of the last dilution ( $10^{-6}$ ), incubate at 37 °C and perform colony counting the next day (the number of CFU is usually around 30 CFU). In the same time, incubate a 14 mL tube with 3 mL of the TSB used for the serial dilution. The media sterility is guaranteed by the absence of bacterial growth in this tube.
4. Keep 150  $\mu\text{L}$  of the last dilution and incubate it at 37 °C for  $24 \pm 1$  h. This sample will serve as a positive control containing only the *Listeria* strain used for the seeding.
5. Two sample types containing salad are prepared: one negative control without bacteria and one artificially contaminated with bacteria of interest. For both bag types, weigh 25 g of lettuce, put it onto a Stomacher® Bag and add 250 mL of Demi-Fraser broth. This content is then blended for 1 min at maximal speed. Add 300  $\mu\text{L}$  of the last bacterial dilution ( $10^{-6}$  corresponding to 20–40 CFU) into dedicated bags. Incubate all samples  $24 \pm 1$  h at 37 °C.

6. Before the end of the food samples incubation, put up together the two parts of the Prestokit (including the prism) and add 900  $\mu\text{L}$  of TSB in each chambers. Place it inside the Monopresto reader. Follow the software instruction leading to the device calibration to launch the regulation at 37 °C. Let it stand there for at least 30 min before adding the food samples (*see Notes 11 and 12*).
7. After  $24 \pm 1$  h of the incubation, manually homogenize, then take out about 5 mL of each bag (in the filtered side) and place it in a 14 mL culture tube. With a 10  $\mu\text{L}$  inoculation loop, streak each sample onto Compass *Listeria* agar plates to ensure the presence (or absence) of the *L. monocytogenes* species. Put the plates at 37 °C for 24 h before interpretations. Also, proceed to seven tenfold serial dilutions of samples in TSB and spread 2 times 100  $\mu\text{L}$  of the two last dilutions with a sterile colony spreader onto TSA plates. Incubate 24 h at 37 °C and count the colony in order to estimate the initial number of bacteria in each chamber.
8. Once the TSB media presents in the Prestokit has warmed up sufficiently, add 100  $\mu\text{L}$  of each sample in each chamber. Typically, the same SPRi experiment monitors the presence of *L. monocytogenes* in a negative control (salad without bacteria) and in a test experiment (salad cultivated in the presence of 20–40 CFU of one of the *L. monocytogenes* specie). In the same time, launch analysis with a positive control chamber by adding 100  $\mu\text{L}$  of the pure culture of the same species of *L. monocytogenes* used for the salad contamination bag. Each sample should be tested at least in triplicates in two independent experiments.
9. When all the chambers of the Prestokit are filled with the different samples, start the SPRi experiment (*see Notes 13–15*). For *L. monocytogenes*, the run lasts 4 h at 37 °C.

---

## 4 Notes

1. Four antibodies have been tested for *L. monocytogenes* detection by SPRi after Pyrrole-NHS coupling. All of them enable the visualization of specific recognition. However, LIM 14 and LIM 16 showed a better sensibility than the two other antibodies as indicated by the time-to-results presented in Table 1.
2. Regarding the antibody choice, it is important to choose purified antibodies with a concentration of at least 0.5 mg/mL. Lower concentrations can result in important losses during centrifugation and concentration steps throughout the antibody conjugation to Pyrrole.

**Table 1**  
**Detection of *L. monocytogenes* in salad samples**

Medium	Bacterial strains	Initial inoculum (CFU/25 g of salad)	Bacterial concentration at the launch of the SPRi analysis (CFU/mL)	Time-to-results (min)				
				LIM 14 antibody	LIM 16 antibody	Ab 20506 antibody	Ab 78729 antibody	KLH antibody
Demi-Fraser & salad	A	27 ± 6	9 E6	25	20	30	20	NR
	A	27 ± 6	9 E6	35	30	45	30	NR
	A	23 ± 2	1 E7	45	40	115	50	NR
	B	23 ± 2	7 E6	45	45	55	55	NR
	B	33 ± 3	1.2 E7	65	55	170	65	NR
	B	33 ± 3	1.2 E7	65	55	30	25	NR
	None	NA	NA	NR	NR	NR	NR	NR
	None	NA	NA	NR	NR	NR	NR	NR
TSB	A	NA	7 E6	65	55	110	135	NR
	A	NA	5 E6	120	145	145	130	NR
	B	NA	1.7 E7	100	90	150	155	NR
	B	NA	2.3 E7	95	95	195	155	NR

The two *Listeria* strains in food samples are detected in less than 1 h. The time-to-result is obtained as soon as signals corresponding to one ROI exceeded the signal of the negative antibody (KLH) by one unit. NA means non applicable and NR means no recognition

- KLH antibody recognizes the keyhole limpet hemocyanin protein from *Megathura crenulata*. Therefore, it should not interact with *Listeria* species. However, it can be substituted by any antibodies that do not interact with *Listeria* species.
- The Prestokit, including the prism, is intended for single-use. This procedure avoids any risk of cross-contaminations between successive analyses and is easier and quicker.
- The SPRi device is devoid of any fluidic channels for sample injection. It eliminates the needs of complex sterilization procedure and risk of leakage.
- At the end of the coupling step, the antibody concentration can be below 5  $\mu\text{M}$  due to loss on the membrane. This is not a major problem since the solution will be later diluted to a final concentration of 1  $\mu\text{M}$  in the spotting solution.
- At the end of the **step 4** in Subheading 3.2, the final antibody–Pyrrole conjugates concentration of 1  $\mu\text{M}$  ensures a good balance between signal quality and quantity of antibodies used.



However, other concentrations have been tested with success (data not shown). Usually these solutions are prepared in small PCR tubes ensuring a sufficient level of liquid for pipetting.

8. Air bubbles in the spotting needle perturb the electric current flow, preventing a correct electropolymerization. If the electropolymerization process fails, it is necessary to wash and dry the needle three times before sucking up again the antibody solution.
9. These electropolymerization parameters ensure the formation of a thick poly-Pyrrole film (around 4 nm). Other electrochemical conditions regarding pulse intensity and duration can be tested. Nonetheless, reader should keep in mind that a thicker poly-Pyrrole film can be detrimental for SPR sensitivity. Indeed, the intensity of the evanescent wave, necessary for the SPR phenomenon, decreases exponentially with thicker layers.
10. Spots are arrayed in triplicate to ensure a good reproducibility of the interaction. In order to confirm the specificity of the recognition, at least one spot line should be composed of an irrelevant antibody (here KLH).
11. During the electrodeposition, the hygrometry level is a crucial parameter to take into account. In fact, if it is not set up correctly, the antibody spots could dry too quickly or be spread on the gold surface which would cause mixes of antibodies.
12. In order to avoid refractive index changes caused by the medium temperature rise during the detection, the TSB is heated at 37 °C for 30 min before the experiment beginning.
13. The interactions between bacteria and regions of interest (ROI) corresponding to each antibody spot are viewable in real time through the MonoPresto™ interface. These ROI corresponding to an established spotting array are automatically defined by the software at the beginning of the experiment.
14. As the interactions between antibody spots are reproducible, a mean signal can be calculated.
15. Once the incubation in the SPRi is ended, we subtract the KLH signal from other antibodies. This post-treatment analysis eliminates the non-specific signal impacting all antibodies which can be induced by media changes (acidification) or interactions with the sample endogenous bacteria.

---

## Acknowledgements

The work is part of a PhD thesis (A. M.) funded by the National Association for Research and Technology (ANRT n° 624/2013). This project was also partly supported by the Labex ARCANE program (ANR-11-LABX-0003-01).

## References

1. Magalhães R, Mena C, Ferreira V et al. (2014) Bacteria: *Listeria monocytogenes*. Encyclopedia of food safety, Oxford, UK, Elsevier
2. Todd ECD, Notermans S (2011) Surveillance of listeriosis and its causative pathogen, *Listeria monocytogenes*. Food Control 22:1484–1490
3. Pusztahelyi T, Szabó J, Dombrádi Z et al (2016) Foodborne *Listeria monocytogenes*: a real challenge in quality control. Scientifica (Cairo) 2016:5768526
4. Välimaa T-A, Tilsala-Timisjärvi A, Virtanen E et al (2015) Rapid detection and identification methods for *Listeria monocytogenes* in the food chain—a review. Food Control 55:103–114
5. Weidemaier K, Carruthers E, Curry A et al (2015) Real-time pathogen monitoring during enrichment: a novel nanotechnology-based approach to food safety testing. Int J Food Microbiol 198:19–27
6. Bouguelia S, Roupioz Y, Slimani S et al (2013) On-chip microbial culture for the specific detection of very low levels of bacteria. Lab Chip 13:4024–4032
7. Morlay A, Piat F, Mercey T et al (2016) Immunological detection of *Cronobacter* and *Salmonella* in powdered infant formula by plasmonic label-free assay. Letter Appl Microbiol 62:459–465

## Aptamer-Based Trapping: Enrichment of *Bacillus cereus* Spores for Real-Time PCR Detection

Christin Fischer and Markus Fischer

### Abstract

Aptamer-based trapping techniques are in general suitable to replace common antibody-based enrichment approaches. A time-consuming isolation or clean-up is often necessary during sample preparation, e.g. for the detection of spores. For the development of bioanalytical routine approaches, aptamers with a high affinity to *B. cereus* spores were applied for the establishment and validation of an aptamer-based trapping technique in milk with fat contents between 0.3 and 3.5%. Thereby, enrichment factors of up to sixfold were achieved. The combination of an aptamer-based enrichment by magnetic separation and the subsequent specific real-time PCR detection represents a reliable and rapid detection system.

**Key words** Aptamer, *Bacillus cereus*, Spore trapping, Real-time PCR, Milk, Food poisoning

---

### 1 Introduction

*Bacillus cereus* is a common food poisoning microorganism, which is closely related to *Bacillus anthracis*, and *Bacillus thuringiensis* [1–6]. The spore-forming *B. cereus* is a Gram-positive food pathogen which can be found in milk and dairy products. The pathogenicity is based on two different types of toxins, the diarrhea-inducing and the emetic toxin [7–10].

These toxins are harmful, especially for young, old, pregnant and immunocompromised persons (YOPIs). Thus, it is very important to prevent food from *B. cereus* contaminations under aspects of consumer protection and quality assurance. Concerning the pathogenicity (toxin producers) various legal regulations are available. According to article 3 section 1 in conjunction with annex 1 chapter 2 process hygiene criteria (chapter 2.2 milk and dairy products) of Commission Regulation (EC) No. 2073/2005 on microbiological criteria for foodstuffs, microorganisms and the corresponding toxins are strictly regulated so that rapid and reliable analytical assays are mandatory [11].

The detection of *B. cereus* spores in milk could be fulfilled by the utilization of in vitro generated aptamers (i.e. receptors) in combination with various readout techniques (i.e. PCR or others like LFD, or sensor chips) [12]. To establish a rapid and cost-efficient trapping and detection method for routine analysis without the necessity to perform a time-consuming microbiological enrichment, an aptamer-based trapping procedure was developed. In order to validate the trapping technique, a specific optimized real-time PCR method for detection of *B. cereus* was applied [13]. The trapping was developed in milk simulating buffer and tested in sterilized milk (containing 0.3, 1.5, and 3.5% fat) for verification of suitability under real conditions.

---

## 2 Materials

All solutions have to be prepared under the use of ultrapure water and analytical grade reagents. Prepare and store all reagents at room temperature (unless it is indicated otherwise). Diligently follow all waste disposal regulations when disposing waste materials. Generally, we work under sterile conditions thus there is no need to add sodium azide to the solutions (unless it is indicated). Pathogenic microorganisms were autoclaved and disposed afterwards.

### 2.1 Preparation of Aptamer-Linked Magnetic Beads

1. SiMAG-Carboxyl beads: 10 mg/mL (chemicell GmbH, Berlin, Germany).
2. MES-buffer: 0.1 M 2-(*N*-morpholino)ethanesulfonic acid, pH 5.0.
3. Aminated aptamers: 100  $\mu$ M (Integrated DNA Technologies, Inc., Leuven, Belgium) with an affinity towards the selected target molecule (Table 1).
4. PBS buffer: 137 mM NaCl, 2.7 mM KCl, 12 mM Na<sub>2</sub>HPO<sub>4</sub>, pH 7.4.
5. Blocking and Storage-buffer: PBS buffer containing 0.1% BSA, 0.05% sodium azide (*see* Note 1).

### 2.2 Aptamer-Based Trapping

1. Milk simulating buffer: 55 mM NaCl, 20 mM MgCl<sub>2</sub>, 67 mM CaCl<sub>2</sub>, 80 mM KCl, 40 mM Tris-HCl, pH 6.6 (*see* Note 2).
2. Milk samples: three commercial available milk samples with different fat contents (0.3, 1.5, and 3.5%).
3. *B. cereus* spores: strains MHI M1 and two wild types [10<sup>7</sup> CFU/mL received from Lehrstuhl für Hygiene und Technologie der Milch (Oberschleißheim, Germany)].

### 2.3 Spore Lysis

1. Glass beads: acid-washed, diameter = 0.5 mm.
2. TissueLyser: use for mechanical treatment to lyse the spores (Qiagen GmbH, Hilden, Germany).

**Table 1**  
**Sequences with the regarding calculated dissociation constants for aptamers towards *B. cereus* spores. Primer regions are *italicized* [14]**

<b>Aptamer</b>	<b>Aptamer sequence (5'–3')</b>	<b><math>K_D</math> [nM]</b>
BacApt3	<i>CATCCGGTCACACCC</i> TGGTGCAGACCCCATAGGGGGGGCGTCCGGATGTAGGAGTAGGGTGTGGCTCCCCGTATC	35.5
BacApt4	<i>CATCCGGTCACACCC</i> TGCTCCAGCGTCCAGCCGTGCGTCCAGCCCGGACCCCTGTCAAGCCCTCGCCGGTGTGGCTCCCCGTATC	44.6
BacApt5	<i>CATCCGGTCACACCC</i> TGCTCCAGGTGGGGGGCGTATTACTGAGGCAGAGTAGTTGGCCCGGGTGTGGCTCCCCGTATC	19.1

### **2.4 Real-Time PCR Detection**

1. Real time PCR: iCycler iQ5 (BioRad Laboratories, Inc.; Hercules, CA).
2. DreamTaq buffer: DreamTaq buffer (10×), unknown composition (Fisher Scientific-Germany GmbH, Schwerte, Germany).
3. dNTPs: equimolar Mix of dGTP, dCTP, dATP, dTTP, each 10 mM (Bioline GmbH, Luckenwalde, Germany).
4. DreamTaq polymerase: 5.0 U/μL (Fisher Scientific-Germany GmbH, Schwerte, Germany).
5. Primer: mp3L1R1for and mp3L1R1rev (Invitrogen Life Technologies GmbH, Darmstadt, Germany) [13].
6. SYBR Green: SYBR Green I nucleic acid gel stain (10,000×, Invitrogen GmbH, Karlsruhe, Germany).

---

## **3 Methods**

### **3.1 Preparation of Aptamer-Linked Magnetic Beads**

1. Wash 200 μL SiMAG-Carboxyl beads twice with 1 mL MES-buffer and discard the supernatant.
2. Suspend the resulting bead-pellet in 250 μL MES-buffer containing 10 mg EDC [1-ethyl-3-(3-dimethylaminopropyl)carbodiimide hydrochloride] and incubate for 10 min under agitation to active the carboxylated bead surface.
3. Add 50 μL of aminated aptamer (100 μm) with an affinity towards the selected target molecule (here: *B. cereus* spores) and incubate the solution for 2 h at room temperature under slow agitation.
4. Wash SiMAG-Carboxyl beads three times with 1 mL PBS-buffer, dissolve the beads in 1 mL Blocking and Storage-buffer, and store at 4 °C (*see Note 2*).

### **3.2 Aptamer-Based Trapping**

1. Refold the aptamer-linked magnetic beads in milk simulating buffer for 5 min at 95 °C with subsequent cooling to 4 °C to avoid heteroduplexes and to ensure correct aptamer folding (*see Note 3*).
2. Dilute 10 μL of aptamer-linked magnetic bead mixture with 990 μL (1) milk simulating buffer, (2) milk with 0.3% fat, (3) milk with 1.5% fat, and (4) milk with 3.5% fat containing the target molecules (here: *B. cereus* spores up to 10<sup>7</sup> CFU/mL). Incubate the resulting solution for 30 min under agitation (*see Note 4*).
3. Centrifuge the sample for 2 min at 10,000 × *g* and remove the supernatant. Wash the resulting bead pellet three times with 1 mL ddH<sub>2</sub>O each and finally re-suspend it in 100 μL ddH<sub>2</sub>O.

4. Elute the aptamer-bound spores 5 min at 96 °C. Transfer the reaction tube in a magnetic separator and collect the hot supernatant, which contains the enriched spores, in a new reaction tube. Ensure that the magnetic beads remained in the first reaction tube and get not collected with the supernatant, which contains the enriched spores. Storing of the samples at –20 °C until further use is advisable (*see Note 5*).

A suitable detection method for quantification is subsequent necessary. Due to the enrichment by reduction of sample volume (from 1000 µL to 100 µL) and the clean-up by removal of matrix, a recently published *B. cereus* specific real-time PCR assay could be used. The general process is applicable for a broad range of other spores or targets, solely the used aptamers and the subsequent method of quantification should be adjusted (in the present study real-time-PCR or in other studies e.g. LC-MS/MS).

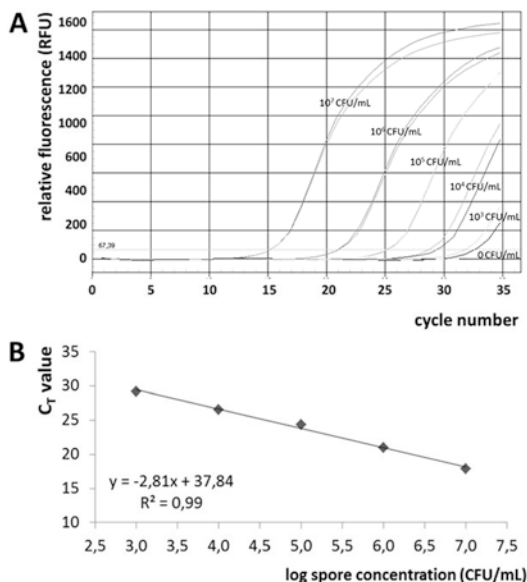
### 3.3 Spore Lysis

The primers used for spore quantification via real time PCR target the hbID gene of *B. cereus* [13]. To obtain the bacterial DNA as template for PCR, the spore shell was lysed mechanically as following:

1. Add 250 mg glass beads to the enriched spore solutions (*see Subheading 3.2*) to generate a spore lysate.
2. Lyse the solution by mechanical treatment (5 min at 30 Hz, twice) using a TissueLyser (Qiagen GmbH, Hilden, Germany). The supernatant with fragmented spores was subsequently used for real-time PCR (*see Note 6*).

### 3.4 Real-Time PCR Detection

1. Real-time PCR assay (template: lysed spore solution) was performed using a iCycler iQ5 (*see Note 7*).
2. Set up a reaction mixture consisting of following components: 1× DreamTaq buffer, 0.8 mM dNTPs, 0.25 units DreamTaq polymerase, 0.25 µM of each primer, 0.3125× SYBR Green I, 3 µL enriched and lysed spore solution and fill up to 20 µL with ddH<sub>2</sub>O [13].
3. Perform the real-time PCR with the following temperature program: initial denaturation at 95 °C for 10 min, 35 cycles (95 °C for 15 s, 60 °C for 10 s, and 72 °C for 10 s each), final elongation for 10 min at 72 °C [13].
4. For quantitation and comparison, an external calibration with *B. cereus* spores (wild type, 10<sup>3</sup> to 10<sup>7</sup> CFU/mL) should be carried along (Fig. 1, *see Note 8*).



**Fig. 1** (a) Example of amplification curves during real time PCR with different *B. cereus* MHI M1 spore concentrations (from left to right): 10<sup>7</sup> CFU/mL, 10<sup>6</sup> CFU/mL, 10<sup>5</sup> CFU/mL, 10<sup>4</sup> CFU/mL, 10<sup>3</sup> CFU/mL and 0 CFU/mL. (b) Resulting calibration line during real time PCR with  $R^2 = 0.99$ . Spore concentration (from left to right): 0 CFU/mL, 10<sup>3</sup> CFU/mL, 10<sup>4</sup> CFU/mL, 10<sup>5</sup> CFU/mL, 10<sup>6</sup> CFU/mL, 10<sup>7</sup> CFU/mL. Reprinted with permission from (Fischer, C.; Hünninger, T.; Jarck, J.-H.; Frohmeyer, E.; Kallinich, C.; Haase, I.; Hahn, U.; Fischer, M. *Food Sensing: Aptamer-Based Trapping of Bacillus cereus* Spores with Specific Detection via Real Time PCR in Milk. *J Agric Food Chem* 63:8050–8057). Copyright (2015) American Chemical Society

## 4 Notes

1. BSA was added to the Blocking and Storage buffer to prevent unspecific interactions by activated but not covalent linked carboxyl-groups on the bead surface [15].
2. Milk-simulating-buffer was used during aptamer selection, to mimic the ionic milieu of milk. To simplify the aptamer selection, a milk simulating buffer was chosen for selection process. The buffer excludes some ingredients like e.g. milk sugar or fat, but corresponds to milk in terms of ionic composition and pH value. Trapping was also performed in milk-simulating buffer as a positive control, as it was expected that aptamers exhibit their highest affinity towards the target in the corresponding selection buffer.
3. Before each trapping experiment, the required volume of magnetic beads was transferred to a new reaction tube, the supernatant was removed in a magnetic field and the beads were taken up in the initial volume of milk simulating buffer.



**Table 2**

Obtained enrichment factors for aptamer-based trapping in milk simulating buffer and milk with different fat contents. The maximal trapping factor was determined mathematically to 10. Reprinted (adapted) with permission from (Fischer, C.; Hünninger, T.; Jarck, J.-H.; Frohnmeyer, E.; Kallinich, C.; Haase, I.; Hahn, U.; Fischer, M. *Food Sensing: Aptamer-Based Trapping of Bacillus cereus Spores with Specific Detection via Real Time PCR in Milk*. Journal of agricultural and food chemistry. 2015. 63, 8050–8057). Copyright (2015) American Chemical Society

Matrix strain	Milk-simulating buffer	Milk 0.3% fat	Milk 1.5% fat	Milk 3.5% fat
<i>B. cereus</i> wild type	5.2	3.5	4.3	4.0
<i>B. cereus</i> wild type	5.7	3.1	6.7	4.8
<i>B. cereus</i> MHI M1	7.1	3.9	3.2	7.5
Mean value	6.0 ± 1.0	3.5 ± 0.4	4.7 ± 1.8	5.4 ± 1.9
Mean value 2	4.91 ± 1.07			

4. The spore surface due to its dimension probably offers several different binding sites [16]. To cover a maximum range of potential binding sites, and enable a binding of a multitude of the heterogenous spores, a mixture of aptamer-linked magnetic beads (BacApt3, BacApt4 and BacApt5) was used for the presented aptamer-based trapping.
5. The resulting enrichment factor (up to 10×, Table 2) is limited due to the volume reduction (1000 µL to 100 µL) which is performed during trapping. You may choose a higher initial volume or a lower end volume to increase your enrichment factor and to improve the trapping efficiency. Please consider, that this might mean that a higher aptamer-linked bead concentration is needed for trapping.
6. The lysed spore solution should be used quickly to prevent enzymatic DNA degradation or similar reactions [17].
7. The lysed spores were diluted prior to measurement 1:10 with ddH<sub>2</sub>O.
8. Milk simulating buffer/milk samples spiked at a concentration equal to pre-enrichment were used as control samples. The assay was additionally performed using *B. subtilis* and *B. thuringiensis* spores as template to demonstrate the specificity of the protocol. It was shown, that the protocol with the subsequent real-time detection was specific for *B. cereus* spores.

---

## Acknowledgement

This research project was supported by the German Ministry of Economics and Technology (via AiF) and the FEI (Forschungskreis der Ernährungsindustrie e. V., Bonn, Germany); Project AiF 331 ZN.

The author's thank Dr. Tim Hünninger, Jan-Hinnerk Jarck, and Esther Frohnmeyer for practical support and discussion.

## References

1. Helgason E, Økstad OA, Caugant DA, Johansen HA, Fouet A, Mock M, Hegna I, Kolstø A-B (2000) *Bacillus anthracis*, *Bacillus cereus*, and *Bacillus thuringiensis*—one species on the basis of genetic evidence. *Appl Environ Microbiol* 66:2627–2630
2. Drobniewski F (1994) The safety of *Bacillus* species as insect vector control agents. *J Appl Bacteriol* 76:101–109
3. Bruno JG, Ulvick SJ, Uzzell GL, Tabb JS, Valdes ER, Batt CA (2001) Novel immunofluorescence assay method for *Bacillus* spores and *Escherichia coli* O157:H7. *Biochem Biophys Res Commun* 287:875–880
4. Bennet RW, Harmon SM (1990) *Bacillus cereus* food poisoning. Laboratory diagnosis of infectious diseases: principles and practice. Bacterial, mycotic and parasitic diseases. Springer-Verlag, New York
5. Lambert B, Peferoen M (1992) Insecticidal promise of *Bacillus thuringiensis*. *Bioscience* 42:112–122
6. de Maagd RA, Bravo A, Crickmore N (2001) How *Bacillus thuringiensis* has evolved specific toxins to colonize the insect world. *Trends Genet* 17:193–199
7. Setlow P (1994) Mechanisms which contribute to the long-term survival of spores of *Bacillus* species. *J Appl Bacteriol* 76:49S–60S
8. Beutling D, Böttcher C (1998) *Bacillus cereus*: ein Risikofaktor in Lebensmitteln. *Arch Lebensmittelhyg* 49:90–96
9. Mahler H, Pasi A, Kramer JM, Schulte P, Scoging AC, Bar W, Krahenbuhl S (1997) Fulminant liver failure in association with the emetic toxin of *Bacillus cereus*. *N Engl J Med* 336:1142–1148
10. Dufrenne J, Bijwaard M, Te Giffel M, Beumer R, Notermans S (1995) Characteristics of some psychrotrophic *Bacillus cereus* isolates. *Int J Food Microbiol* 27:175–183
11. Regulation C (2005) No. 2073/2005 of 15 November 2005 on microbiological criteria for foodstuffs. *Official J Eur Union L* 338:1–26
12. Tombelli S, Minunni M, Mascini M (2007) Aptamers-based assays for diagnostics, environmental and food analysis. *Biomol Eng* 24:191–200
13. Wehrle E, Didier A, Moravek M, Dietrich R, Märtlbauer E (2010) Detection of *Bacillus cereus* with enteropathogenic potential by multiplex real-time PCR based on SYBR green I. *Mol Cell Probes* 24:24–130
14. Fischer C, Hünninger T, Jarck J-H, Frohnmeyer E, Kallinich C, Haase I, Hahn U, Fischer M (2015) Food sensing: aptamer-based trapping of *Bacillus cereus* spores with specific detection via real time PCR in milk. *J Agric Food Chem* 63:8050–8057
15. Hünninger T, Wessels H, Fischer C, Paschke-Kratzin A, Fischer M (2014) Just in time-selection: a rapid semiautomated SELEX of DNA aptamers using magnetic separation and BEAMing. *Anal Chem* 86:10940–10947
16. Hünninger T, Fischer C, Wessels H, Hoffmann A, Paschke-Kratzin A, Haase I, Fischer M (2015) Food sensing: selection and characterization of DNA aptamers to *Alicyclobacillus* spores for trapping and detection from orange juice. *J Agric Food Chem* 63:2189–2197
17. Hünninger T, Felbinger C, Wessels H, Mast S, Hoffmann A, Schefer A, Martlbauer E, Paschke-Kratzin A, Fischer M (2015) Food targeting: a real-time PCR assay targeting 16S rDNA for direct quantification of *Alicyclobacillus* spp. Spores after aptamer-based enrichment. *J Agric Food Chem* 63:4291–4296

## Detection of *Yersinia pestis* in Complex Matrices by Intact Cell Immunocapture and Targeted Mass Spectrometry

Jérôme Chenu, François Fenaille, Stéphanie Simon, Sofia Filali, Hervé Volland, Christophe Junot, Elisabeth Carniel, and François Becher

### Abstract

We describe an immunoaffinity-liquid chromatography-tandem mass spectrometry (immuno-LC-MS/MS) protocol for the direct (i.e., without prior culture), sensitive and specific detection of *Yersinia pestis* in complex matrices. Immunoaffinity enables isolation and concentration of intact bacterial cells from food and environmental samples. After protein extraction and digestion, suitable proteotypic peptides corresponding to three *Y. pestis*-specific protein markers (murine toxin, plasminogen activator and pesticin) are monitored by targeted LC-MS/MS using the selected reaction monitoring (SRM) mode. This immuno-LC-MS/MS assay has a limit of detection of  $2 \times 10^4$  CFU/mL in milk or tap water, and  $4.5 \times 10^5$  CFU in 10 mg of soil.

**Key words** Bacteria, Mass spectrometry, Immunoaffinity, Targeted proteomic, Detection, Matrices

---

### 1 Introduction

*Yersinia pestis* is the causative agent of bubonic and pneumonic plague, an acute and often fatal disease. Due to its prevalence and high lethality, *Y. pestis* is classified as a category A bioterror agent by the Centers for Disease Control and Prevention (CDC), the highest rank of potential bioterrorism agents (<http://www.bt.cdc.gov/agent/agentlist-category.asp>). Methods for rapid and sensitive detection of the presence of the bacteria in potentially contaminated matrices are essential. The high genetic similarity of the populations composing the *Yersinia pseudotuberculosis* complex e.g., 97% nucleotide identity reported between *Y. pestis* and *Y. pseudotuberculosis* [1], has to be taken into consideration for a specific detection of *Y. pestis*. The two plasmids pFra (or pMT1) and pPla (or pPst or pPCP1), which code for virulence factors, are unique to *Y. pestis* and thereby represents interesting targets for specific detection.

Nucleic acid-based assays and immunometric tests have been developed for *Y. pestis* detection by targeting respectively genes and proteins coded by pFra and pPla plasmids [2, 3]. Mass spectrometry (MS) offers a complementary approach for biodefense applications and detection of pathogenic microorganisms [4]. Beside the global bacterial protein fingerprints acquired by matrix-assisted laser desorption ionization time-of-flight MS (MALDI-TOF MS), targeted proteomics based on the selected reaction monitoring mode (SRM) [5] was proposed for direct bacteria detection. Selective SRM monitoring of bacteria markers was combined with affinity concentration of target cells for enhanced sensitivity and direct detection of bacteria in complex matrices without any time consuming bacterial culture [6, 7].

We describe here an immunoaffinity-LC-SRM protocol for the direct detection of *Y. pestis* in complex environmental and food samples. It combines the specificity and sensitivity of two complementary methods, immunoaffinity capture and targeted mass spectrometry detection of specific *Y. pestis* markers coded by pPla and pFra plasmids. Critical parameters for efficient immunocapture of intact *Y. pestis* cell and multiplex SRM detection of proteotypic peptides are emphasized.

---

## 2 Materials

Prepare all solutions using ultrapure water ( $\text{H}_2\text{O}$  mQ, resistivity of  $18 \text{ m}\Omega \text{ cm}$  at  $25^\circ\text{C}$ ) and analytical grade reagents. Ultrapure water used here was from a Milli-Q<sub>plus</sub> 185 purifier (Millipore, Bedford, MA).

### 2.1 Samples

1. Bacterial strains used in this study originated from the collection of Unité de Recherche Yersinia at the Institut Pasteur (Paris, France) (*see Note 1*).
2. Environmental and food samples used in this work: tap water, commercial milk powder (prepared at 5% v/w in  $\text{H}_2\text{O}$  mQ), soil (sampled in a field around the laboratory).

### 2.2 Immuno-purification

1. Magnetic beads: Dynabeads M-280 tosyl-activated (Life Technologies, Saint-Aubin, France), stored at  $4^\circ\text{C}$ .
2. Magnetic particle concentrator for microcentrifuge tubes, Dynal MPC-S (Life Technologies, Saint-Aubin, France).
3. Coupling buffer: 0.1 M sodium-phosphate buffer, pH 7.4. Add 2.62 g of  $\text{NaH}_2\text{PO}_4$  monohydrate (monobasic) and 14.42 g of  $\text{Na}_2\text{HPO}_4$  dihydrate (dibasic) to  $\text{H}_2\text{O}$  mQ to make a volume of 1 L. The pH of the final solution will be 7.4. This buffer can be stored for up to 1 month at  $4^\circ\text{C}$ .

4. Monoclonal antibody Pla35, stock solution at 1.2 mg/mL (*see Note 2*). Dilute the antibody to 422 µg/mL in coupling buffer.
5. Blocking buffer: phosphate-buffered saline (PBS), pH 7.4 with 0.5% (w/v) bovine serum albumin (BSA). Add 0.5 g of BSA (*see Note 3*) to 100 mL of PBS (DPBS without Ca<sup>2+</sup> and Mg<sup>2+</sup>, Lonza, Verviers, Belgium). This buffer can be stored for up to 1 month at 4 °C.
6. Washing and storage buffer: PBS, pH 7.4 with 0.1% (w/v) BSA. Dilute Blocking buffer fivefold in PBS. For example, add 10 mL of blocking buffer to 40 mL of PBS, pH 7.4. This buffer can be stored for up to 1 month at 4 °C.
7. Thermomixer compact for 1.5 mL microtubes (Eppendorf, Montesson, France).
8. PBS with 0.1% Tween-20: for 100 mL, add 0.5 mL of 20% Tween-20 (v/v) (*see Note 4*) to 99.5 mL of PBS. This buffer can be stored for up to 1 month at 4 °C.
9. PBS with 0.1% Tween-20 and 1 mg/mL BSA. Add 100 mg of BSA to 100 mL of PBS with 0.1% Tween-20. This buffer can be stored for up to 1 month at 4 °C.
10. Rotating wheel.
11. 1.5 mL microtubes LoBind (Eppendorf, Montesson, France).

### **2.3 *Y. pestis* Inactivation and Protein Extraction**

1. Prepare a 80% trifluoroacetic acid (TFA) solution. For 10 mL, add 8 mL of TFA (≥99% of purity, Sigma-Aldrich, St. Louis, MO) to 2 mL of H<sub>2</sub>O mQ.
2. Vortex mixer.
3. Laboratory centrifuge for microtubes enabling centrifugation up to 14,000 × *g* (ThermoFisher, Villebon sur Yvette, France).
4. Filter tubes of 0.22 µm pore size (Ultrafree MC filters, Millipore, Billerica, MA) (*see Note 5*).

### **2.4 Trypsin Digestion**

1. Centrifugal vacuum concentrator (ThermoFisher, Villebon sur Yvette, France).
2. pH indicator strips.
3. Ammonium bicarbonate solution, 1 M, pH 8.0. Dissolve 8 g of ammonium bicarbonate in 100 mL of H<sub>2</sub>O mQ. This buffer can be stored for up to 1 month at 4 °C.
4. Ammonium bicarbonate solution, 50 mM, pH 8.0 (AB50). Dilute 20-fold 1 M ammonium bicarbonate solution. For example, add 0.5 mL of 1 M ammonium bicarbonate to 9.5 mL of H<sub>2</sub>O mQ.
5. Dithiothreitol (DTT) solution, 45 mM. Add 6.9 mg of DTT to 1 mL of AB50. Make fresh before use.

6. Iodoacetamide (IAA) solution, 100 mM. Add 18.5 mg of IAA to 1 mL of AB50. Make fresh before use (*see Note 6*).
7. Trypsin solution (1 µg/µL). Reconstitute 20 µg of lyophilized trypsin (Sequencing Grade Modified Trypsin, Promega Cat# V5111, Fitchburg, WI) in 20 µL of re-suspension buffer (50 mM acetic acid) (*see Note 7*). Keep on ice before use.
8. Thermomixer for 1.5 mL microtubes (Eppendorf, Montesson, France).

### 2.5 Internal Standard Peptides

1. HPLC-grade acetonitrile (ACN) from SDS (Peypin, France).
2. Analytical-grade formic acid (FA).
3. Internal standards (IS): seven stable isotope-labeled peptides (synthesized by Bachem, Burgdorf, Switzerland) corresponding to the four targeted proteins, purity ≥95% (determined by HPLC), supplied as trifluoroacetate salt (*see Table 1*). Re-suspend each peptide in 30% ACN, 0.1% formic acid to have a stock solution at 4 mg/mL (*see Note 8*).
4. IS stock mixture (4×): Mix the seven peptides in 20% ACN, 0.4% formic acid at the following final concentrations: peptide 1 of Pla (Pla 1) at 400 ng/mL, peptide 2 of Pla (Pla 2) at 2000 ng/mL, peptide 1 of murine toxin (Ymt 1) at 40 ng/mL, and the four other peptides (Ymt 2, Psn 1, Ompa 1, Ompa 2) at 200 ng/mL (*see Note 9*).

### 2.6 LC and MS Conditions

1. HPLC polypropylen micro-vials (Supelco, France).
2. LC system: HP 1100 HPLC system (Agilent Technology, Les Ulis, France) (*see Note 10*).
3. LC column: Zorbax SB-C18 column (150 × 2.1 mm i.d., 5 µm particle size, 300 Å porosity) from Agilent Technology.
4. Use only analytical-grade reagents to constitute mobile phases. HPLC-grade acetonitrile was from SDS, and analytical-grade formic acid.
5. Mobile phase A: H<sub>2</sub>O mQ containing 0.1% (v/v) formic acid.
6. Mobile phase B: Acetonitrile containing 0.1% (v/v) formic acid.
7. Mass spectrometer: triple quadrupole TSQ Quantum Ultra mass spectrometer (Thermo Scientific, Les Ulis, France) (*see Note 11*).
8. XCalibur software (version 1.4 SR1, Thermo Scientific).

---

## 3 Methods

The overall immuno-LC-MS/MS procedure for sensitive detection of *Y. pestis* in complex environmental and food matrices is schematized in Fig. 1.

**Table 1**  
**Mass spectrometry settings for the multiplex SRM detection**

Protein	Peptide name	Peptide sequence	Peptide molecular mass (Da)	Precursor ion <i>m/z</i>	Product ion <i>m/z</i>	Collision energy (eV)	Tube lens (V)	Retention time (min)	Segment time range (min)
Plasminogen activator (Pla)	Pla1	NSGDSVSIIGGDAAGISNK	1647.77	825.0 ( <i>z</i> = 2)	889.6 ( <i>y</i> <sub>10</sub> <sup>1+</sup> )	27	80	3.2	2.0–3.8
	IS Pla1	NSGDS[ <sup>13</sup> C <sub>5</sub> <sup>15</sup> N]	1653.77	828.0 ( <i>z</i> = 2)	1089.9 ( <i>y</i> <sub>12</sub> <sup>1+</sup> )	27	80	3.2	2.0–3.8
					889.6 ( <i>y</i> <sub>10</sub> <sup>1+</sup> )	27	80	3.2	2.0–3.8
	Pla2	INDFELNALFK	1322.69	662.5 ( <i>z</i> = 2)	1089.9 ( <i>y</i> <sub>12</sub> <sup>1+</sup> )	27	80	3.2	2.0–3.8
					705.5 ( <i>y</i> <sub>6</sub> <sup>1+</sup> )	20	70	13.8	12.0–16.0
	IS Pla2	INDFELNA[ <sup>13</sup> C <sub>6</sub> ]LFK	1328.69	665.4 ( <i>z</i> = 2)	834.5 ( <i>y</i> <sub>7</sub> <sup>1+</sup> )	20	70	13.8	12.0–16.0
711.6 ( <i>y</i> <sub>6</sub> <sup>1+</sup> )					20	70	13.8	12.0–16.0	
Pesticin (Psn)	Psn1	ENEDILNNNR	1229.56	615.6 ( <i>z</i> = 2)	840.7 ( <i>y</i> <sub>7</sub> <sup>1+</sup> )	20	70	13.8	12.0–16.0
					630.3 ( <i>y</i> <sub>5</sub> <sup>1+</sup> )	20	80	2.8	2.0–3.8
	IS Psn1	ENEDILNNN[ <sup>13</sup> C <sub>6</sub> <sup>15</sup> N <sub>4</sub> ]R	1239.56	620.6 ( <i>z</i> = 2)	517.4 ( <i>y</i> <sub>4</sub> <sup>1+</sup> )	20	80	2.8	2.0–3.8
					640.3 ( <i>y</i> <sub>5</sub> <sup>1+</sup> )	20	80	2.8	2.0–3.8
Murine Toxin (Ymt)	Ymt1	ILIAFFFFTDK	1310.73	656.5 ( <i>z</i> = 2)	527.4 ( <i>y</i> <sub>4</sub> <sup>1+</sup> )	20	80	2.8	2.0–3.8
					901.5 ( <i>y</i> <sub>7</sub> <sup>1+</sup> )	18	80	17.8	16.0–19.0
	IS Ymt1	ILIAFFFFTD[ <sup>13</sup> C <sub>6</sub> <sup>15</sup> N <sub>2</sub> ]K	1318.73	660.5 ( <i>z</i> = 2)	1085.6 ( <i>y</i> <sub>9</sub> <sup>1+</sup> )	18	80	17.8	16.0–19.0
					972.5 ( <i>y</i> <sub>8</sub> <sup>1+</sup> )	18	80	17.8	16.0–19.0
					909.5 ( <i>y</i> <sub>7</sub> <sup>1+</sup> )	18	80	17.8	16.0–19.0
					1093.6 ( <i>y</i> <sub>9</sub> <sup>1+</sup> )	18	80	17.8	16.0–19.0
Ymt2	EIMQQSYLR	1166.58	584.1 ( <i>z</i> = 2)	980.5 ( <i>y</i> <sub>8</sub> <sup>1+</sup> )	18	80	17.8	16.0–19.0	
				666.4 ( <i>y</i> <sub>5</sub> <sup>1+</sup> )	20	70	4.4	3.8–6.0	
IS Ymt2	EIMQQSYL[ <sup>13</sup> C <sub>6</sub> <sup>15</sup> N <sub>4</sub> ]R	1176.58	589.1 ( <i>z</i> = 2)	538.3 ( <i>y</i> <sub>4</sub> <sup>1+</sup> )	20	70	4.4	3.8–6.0	
				925.5 ( <i>y</i> <sub>7</sub> <sup>1+</sup> )	20	70	4.4	3.8–6.0	
				676.4 ( <i>y</i> <sub>5</sub> <sup>1+</sup> )	20	70	4.4	3.8–6.0	
				548.3 ( <i>y</i> <sub>4</sub> <sup>1+</sup> )	20	70	4.4	3.8–6.0	
					935.5 ( <i>y</i> <sub>7</sub> <sup>1+</sup> )	20	70	4.4	3.8–6.0

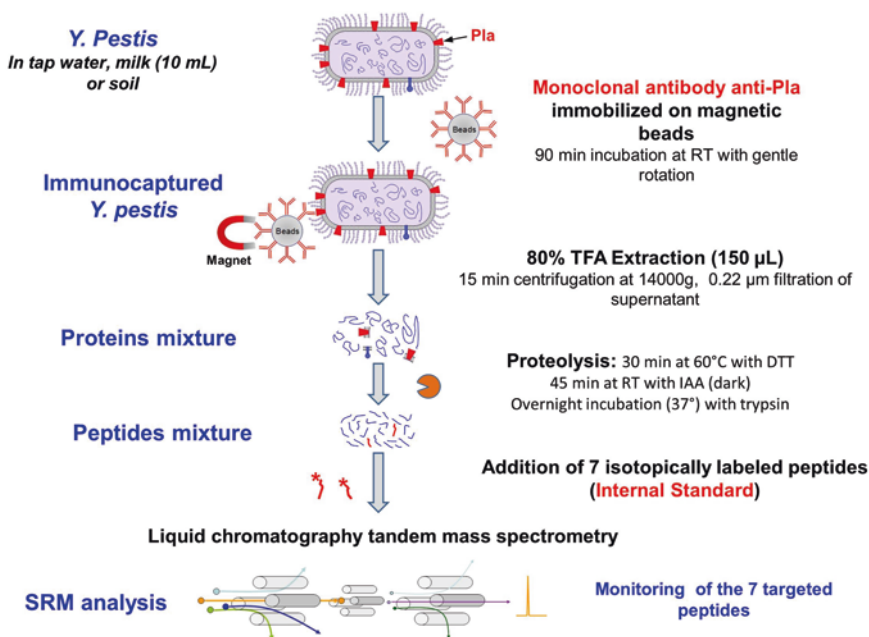
(continued)

**Table 1**  
(continued)

Protein	Peptide name	Peptide sequence	Peptide molecular mass (Da)	Precursor ion $m/z$	Product ion $m/z$	Collision energy (eV)	Tube lens (V)	Retention time (min)	Segment time range (min)
Outer membrane protein A (OmpA)	Ompa1	LSYPVAQDLDVYTR	1638.83	820.4 ( $z = 2$ )	638.8 ( $y_{11}^{2+}$ ) 1080.6 ( $y_9^{1+}$ )	25	80	3.0	2.0–3.8
	IS Ompa1	LSYPVAQDLDVYT [ $^{13}\text{C}_6,^{15}\text{N}_4$ ]R	1648.83	825.4 ( $z = 2$ )	720.1 ( $y_{12}^{2+}$ ) 643.8 ( $y_{11}^{2+}$ ) 725.1 ( $y_9^{1+}$ )	15 25 25	60 80 80	3.0 3.0 3.0	2.0–3.8 2.0–3.8 2.0–3.8
	Ompa2	GSPDGGGLDR	922.41	462.2 ( $z = 2$ )	1090.6 ( $y_{12}^{2+}$ ) 517.3 ( $y_5^{1+}$ )	25 18	80 60	3.0 10.0	2.0–3.8 6.0–12.0
	IS Ompa2	GSPDGGGLD[ $^{13}\text{C}_6,^{15}\text{N}_4$ ]R	932.41	467.2 ( $z = 2$ )	632.3 ( $y_6^{1+}$ ) 527.3 ( $y_5^{1+}$ ) 642.3 ( $y_6^{1+}$ )	18 18 18	60 60 60	10.0 10.0 10.0	2.0–3.8 6.0–12.0 6.0–12.0

Modified with permission from [7]. Copyright 2016 American Chemical Society





**Fig. 1** General workflow for *Y. pestis* detection. Modified with permission from [7]. Copyright 2016 American Chemical Society

The first step corresponds to the capture of *Y. pestis* intact cells using anti-Pla antibodies immobilized on magnetic beads. Proteins are then extracted from the immunocaptured bacteria with the 80% TFA protocol [8], which allows sample sterilization by total inactivation of bacteria. After acid neutralization, protein extracts are digested with trypsin, and the resulting proteotypic peptides corresponding to three *Y. pestis* specific targets (Pla, Ymt and Psn) are simultaneously monitored by SRM mass spectrometry for high robustness. These makers, coded by pPla and pFra plasmids, are unique to *Y. pestis*, and were selected by bottom-up proteomics (see Note 12).

### 3.1 Preparation of Pla35 Antibody-Coated Magnetic Beads

Preparation of 500  $\mu$ L Pla35 antibody-coated magnetic beads (see Note 13):

1. Re-suspend M-280 tosyl-activated magnetic beads by repeated gently pipetting until a homogeneous suspension is obtained and transfer 350  $\mu$ L of beads suspension to a new tube.
2. Place the tube on the magnet, allow the beads to pellet completely (liquid will turn clear) and remove supernatant.
3. Remove the tube from the magnet and wash the beads by adding 1 mL of Coupling Buffer. Mix by gently pipetting.
4. Place the tube on the magnet, allow the beads to pellet completely and remove supernatant.

5. Remove the tube from the magnet and add 520  $\mu\text{L}$  of monoclonal antibody Pla35 at 422  $\mu\text{g}/\text{mL}$  in Coupling Buffer (220  $\mu\text{g}$ ). Mix by gently pipetting and incubate at 37 °C overnight (12–18 h) using a thermomixer with shaking at 1200 rpm.
6. Place the tube on the magnet, allow the beads to pellet completely and remove supernatant.
7. Remove the tube from the magnet and add 1 mL of Blocking Buffer. Mix by gently pipetting and incubate at 37 °C for 1 h using a thermomixer with shaking at 1200 rpm (*see Note 14*).
8. Place the tube on the magnet, allow the beads to pellet completely and remove supernatant.
9. Remove the tube from the magnet and add 1 mL of Wash Buffer. Mix by gently pipetting.
10. Place the tube on the magnet, allow the beads to pellet completely and remove supernatant.
11. Repeat **steps 9–11**.
12. Re-suspend the beads in 500  $\mu\text{L}$  of Storage Buffer. These antibody-coated beads can be stored at 4 °C for up to 1 week.

### **3.2 *Y. pestis* Intact Cell Immunocapture from Complex Samples**

*Y. pestis* immunocapture is illustrated here in tap water sample. The protocol is adaptable to other complex samples: milk and soil (*see Note 15*).

1. Safety consideration: *Y. pestis* is a highly virulent species. All experiments performed with viable bacteria have to be performed in Biosafety Level 3 laboratory.
2. Withdraw 10 mL of artificially contaminated tap water (or suspect tap water sample) into a 50 mL tube.
3. Add 10 mL of PBS containing 0.1% Tween-20 and 1 mg/mL BSA (ratio 1:1, v/v) (*see Note 16*).
4. Add 50  $\mu\text{L}$  of IgG-coupled bead solution (prepared at step in Subheading 3.1) (*see Note 17*) and incubate for 90 min at room temperature with gentle rotation on a slowly rotating wheel (*see Note 16*).
5. Place the tube on the magnet, allow the beads to pellet completely and remove supernatant.
6. Remove the tube from the magnet and add 1 mL of PBS buffer to wash the beads-IgG-bacteria complex and remove weak non-specific binding. Mix by gently pipetting and transfer the solution into a 1.5 mL LoBind tube (Eppendorf) (*see Note 18*).
7. Place the tube on the magnet, allow the beads to pellet completely and remove supernatant.
8. Repeat **steps 4–6** once.

### 3.3 *Y. pestis* Inactivation and Protein Extraction

*Y. pestis* inactivation and protein extraction is performed directly on immunocaptured bacteria by using the TFA protocol for highly pathogenic microorganisms described by Lasch et al. [8].

1. After the last wash of beads-IgG-bacteria complex, place the tube on the magnet, allow the beads to pellet completely and remove supernatant.
2. Add 150  $\mu\text{L}$  of 80% TFA solution and mix by strong vortexing for 10 min.
3. Place the tube on the magnet, allow the beads to pellet completely and transfer supernatant (containing extracted proteins) into a new 1.5 mL LoBind tube.
4. Centrifuge at  $14,000 \times g$  and  $4\text{ }^\circ\text{C}$  for 15 min to pellet cellular debris.
5. Transfer the supernatant to Ultrafree MC filter tubes of 0.22  $\mu\text{m}$  pore size and spun at  $10,000 \times g$  for 5 min.
6. Transfer the filtrate containing the total protein extract into a new 1.5 mL LoBind tube. Protein extract is stored at  $-20\text{ }^\circ\text{C}$  until use.
7. The total inactivation and elimination of bacteria was checked by verification of the absence of colonies after culture on LBH agar as previously described [7, 8] (*see Note 19*).
8. Extracted samples were further processed outside the Biosafety Level 3 laboratory.

### 3.4 Protein Digestion by Trypsin

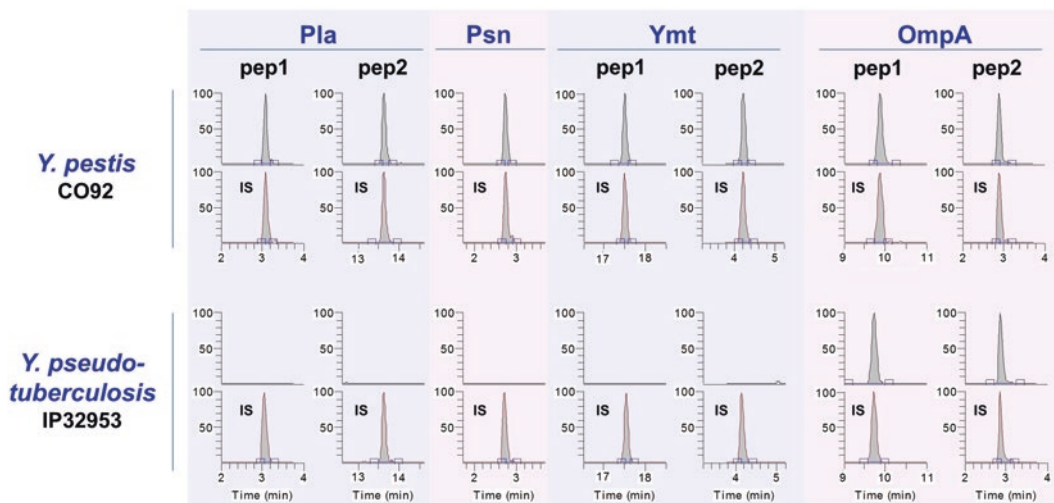
1. Dry protein extract by vacuum centrifugation to eliminate TFA.
2. After complete TFA elimination, re-suspend extracted proteins in 25  $\mu\text{L}$  of 50 mM ammonium bicarbonate. Check pH using pH indicator strips. The pH of the solution should be  $\sim 8.0$  (*see Note 20*).
3. Add 5  $\mu\text{L}$  of reducing agent (45 mM DTT) and incubate at  $60\text{ }^\circ\text{C}$  for 30 min using a thermomixer with shaking at 900 rpm.
4. Allow sample to cool at room temperature and spin briefly to collect condensation.
5. Add 5  $\mu\text{L}$  of alkylating agent (100 mM IAA) and incubate at room temperature for 45 min in the dark (*see Note 21*).
6. Add 1.5  $\mu\text{L}$  of 1  $\mu\text{g}/\mu\text{L}$  trypsin solution and incubate at  $37\text{ }^\circ\text{C}$  overnight (12–18 h) using a thermomixer with shaking at 900 rpm.
7. Allow sample to cool at room temperature and spin briefly to collect condensation.
8. Transfer 30  $\mu\text{L}$  of this trypsin digest in a HPLC vial containing 10  $\mu\text{L}$  of IS stock mixture  $4\times$  ( $1\times$  final). This sample mixture is used for LC-MS/MS analysis.

### 3.5 Multiplex SRM Assay

LC-MS conditions used in the original study are described below.

1. Thirty microliters of IS spiked sample were injected for LC-MS/MS analysis.
2. Data were acquired using the XCalibur software.
3. LC conditions:
  - (a) HP 1100 HPLC system
  - (b) Column: Zorbax SB-C18 maintained at 60 °C.
  - (c) Flow rate: 200  $\mu$ L/min.
  - (d) HPLC Gradient (total run time: 30 min): linear gradient from 15 to 40% B in 20 min, then a column wash at 95% B for 4 min and equilibration at 15% B for 6 min.
  - (e) Column effluent was directly introduced into the electrospray source of the MS system.
4. MS conditions:
  - (a) Triple quadrupole TSQ Quantum Ultra MS operated in the positive ion mode.
  - (b) Electrospray voltage at 3.9 kV and capillary voltage at 35 V.
  - (c) Sheat, ion sweep and auxiliary gas flow rates (nitrogen) optimized at 40, 20 and 15 (arbitrary units) respectively.
  - (d) Drying gas temperature: 350 °C.
  - (e) Proteotypic peptide detection in the SRM mode.
5. SRM method:
  - (a) Common parameters: 0.100  $m/z$  scan width, 0.1 s scan time, 0.4 Q1, 0.7 Q3, 1.5 mTorr Q2 pressure (using argon as the collision gas).
  - (b) SRM transitions: *see* Table 1 for the SRM transitions designed and monitored for each proteotypic peptide and the optimized parameters (tube lens and collision energy values). (*see* Note 22)
  - (c) SRM acquisition time was divided into five segments (*see* Table 1)
  - (d) A typical LC-SRM chromatogram of the monitored peptides is given in Fig. 2, including proteotypic and IS peptides.
  - (e) Data interpretation was performed using the XCalibur software (*see* Note 23).

Any modification to the protocol (LC-MS instrument, capture antibody, sample preparation conditions) could have an impact on the performance. Specification of the immuno-LC-MS/MS (SRM) assay in our conditions is described in Subheading 4 (*see* Note 24).



**Fig. 2** Typical LC–SRM chromatograms obtained for (a) *Y. pestis* C092 and (b) *Y. pseudotuberculosis* IP32953. Depicted SRM transitions are as follows: Pla (peptide 1 NSGDSVSIIGGDAAGISNK, 825 → 1089; peptide 2 INDFELNALFK, 662.5 → 834.5), Pesticin or Psn (ENEDLNNNR, 615.6 → 630.3), Plasminogen activator or Ymt (peptide 1 ILIAPFFFTDK, 656.5 → 972.5; peptide 2 EIMQQSYLR, 584.1 → 666.4), and OmpA (peptide 1 LSYPVAQDLVDYTR, 820.4 → 638.8; peptide 2 GSFDDGLDR, 462.2 → 517.3). In each case, the signal of the corresponding isotopically labeled peptide is indicated by IS (internal standard). Data were obtained using  $10^8$  bacteria. Reprinted with permission from [7]. Copyright 2016 American Chemical Society

## 4 Notes

1. *Y. pestis* is a highly virulent species. Strains were handled according to safety considerations applicable at the Institut Pasteur (Biosafety Level 3 laboratory).
2. The monoclonal antibody Pla35 used in our method was produced in mouse as previously described [3]. This antibody is directed against plasminogen activator (Pla) protein. This protein is a suitable target for intact cell immunocapture, as it is specific for *Y. pestis* (coded by the *Y. pestis* plasmid pPla) and is located at the bacterial surface. Other monoclonal antibody could be used but the impact on capture yield and specificity should be evaluated.
3. For all buffers containing BSA, use purified BSA Fraction V from Sigma-Aldrich,  $\geq 99\%$  purity.
4. Tween-20 is a highly viscous solution. Prepare a solution of 20% Tween-20 (v/v) in  $H_2O$  mQ. Hint: to prepare 1 mL of solution, cut off the extremity of pipet tips before attempting to pipet the 200  $\mu L$ . Pipet Tween-20 very slowly and disperse several times into 800  $\mu L$  of  $H_2O$  mQ.
5. Ultrafree filter tubes contain a Durapore PVDF (polyvinylidene fluoride) membrane which exhibits a low protein binding

capacity. The filter material was demonstrated to be resistant to highly concentrated TFA [8].

6. Iodoacetamide is light sensitive. Always prepare a fresh solution and protect it from light.
7. Trypsin solution (in 50 mM acetic acid) could be aliquoted and stored for up to 1 month at  $-80^{\circ}\text{C}$ .
8. Stock solutions at 4 mg/mL were prepared by dissolving 4 mg of powder peptide in 1 mL of 30% acetonitrile, 0.1% formic acid. Stock solutions were aliquoted and stored at  $-20^{\circ}\text{C}$ .
9. A simple method to obtain IS stock mixture (4 $\times$ ) consists in performing an intermediate dilution of each peptide at 40  $\mu\text{g}/\text{mL}$  (100-fold dilution). For 1 mL, add 10  $\mu\text{L}$  of stock peptide at 4 mg/mL to 990  $\mu\text{L}$  of 20% acetonitrile, 0.4% formic acid. Then use these diluted solutions to obtain IS stock mixture (4 $\times$ ) as following: add 100  $\mu\text{L}$  of Pla 1, 500  $\mu\text{L}$  of Pla 2, 10  $\mu\text{L}$  Ymt 1, 50  $\mu\text{L}$  Ymt 2, 50  $\mu\text{L}$  Psn 1, 50  $\mu\text{L}$  OmpA 1, 50  $\mu\text{L}$  OmpA 2, qsp 10 mL of 20% acetonitrile, 0.4% formic acid (9.24 mL). IS stock mixture (4 $\times$ ) could be aliquoted and stored at  $-20^{\circ}\text{C}$  until use.
10. Another LC system could be used. The critical parameters are: flow rate at 200  $\mu\text{L}/\text{min}$ , mobile phase gradient, and column compartment at  $60^{\circ}\text{C}$ .
11. Another triple quadrupole mass spectrometer can be used, but assay sensitivity will be dependent on the equipment. Tuning parameters defined for each monitoring transition should be adapted.
12. In a preliminary work, a bottom-up proteomics approach was performed and highlighted three relevant protein markers encoded by the *Y. pestis*-specific plasmids pFra (murine toxin) and pPla (plasminogen activator and pesticin). Suitable proteotypic peptides were thoroughly selected to monitor the three protein markers by targeted MS using the SRM mode. In addition, two peptides from outer membrane protein A (OmpA) were selected to evaluate the nonspecific capture of the closely related *Y. pseudotuberculosis* and *Y. similis* species. The reader could refer to Chenau et al. [7] where all details on identification and characterization of the selected markers are given.
13. The use of Dynabeads M-280 tosyl-activated (Life Technologies) is critical to obtain optimal capture conditions. Other magnetic beads with different diameters (300 nm and 2.8  $\mu\text{m}$ ) and chemistries for antibody coating (covalent binding with tosyl-activated beads or by protein G affinity) as well as different homemade monoclonal antibodies [3] directed against the specific membrane protein Pla were tested. Optimal recovery was achieved using Dynabeads M-280 tosyl-activated (2.8  $\mu\text{m}$  diameter) coated with Pla35 antibody [7].

14. Blocking of free tosyl-groups is a critical step to avoid non-specific capture during the immunocapture of intact *Y. pestis* cells.
15. Application to other environmental samples was demonstrated [7]. For milk samples, the same protocol could be used by replacing the 10 mL of tap water by 10 mL of milk containing bacteria. For soil analysis, 10 mg of soil sample was directly mixed with 10 mL of PBS with 0.1% Tween-20 and 1 mg/mL BSA.
16. Dilution of bacterial samples in PBS buffer containing 0.1% Tween-20 and 1 mg/mL BSA and incubation for 90 min at room temperature with gentle shaking on a wheel were required for a high and specific capture yield, weak nonspecific binding on the magnetic bead surface or wall tubes, and full integrity and low autoaggregation of *Y. pestis* cells. Under these conditions recovery was around 77% at  $5 \times 10^7$  CFU/mL, with CV of 6.8%.
17. Assay conditions are given for a sample volume of 10 mL. Assay performances were determined in these conditions. If needed, the volume of IgG-coupled bead solution could be adapted to lower sample volume. For example, use 35  $\mu$ L of IgG-coupled beads solution if detection is performed in 1 mL only of sample.
18. The use of 1.5 mL microtube LoBind (Eppendorf) allows to minimize protein loss on tube wall during the protein extraction step.
19. *Y. pestis* is a highly virulent species. In our initial study [7], the total inactivation and elimination of bacteria were systematically checked after neutralization of TFA with 9% Tween-80, 0.9% lecithin, 3% histidine in TSB and verification of the absence of viable bacteria in each extract after culture on LBH agar for 3 days, as described previously [8]. In Lasch et al. [8], it was demonstrated that *Bacillus* spores (highly resistant structure) were reliably sterilized in each of the 67 separate inactivation tests performed with the TFA inactivation protocol. They also demonstrated, for vegetative cells of the genera *Bacillus*, *Burkholderia*, *Escherichia*, and *Yersinia* (430 separate inactivation tests), a total bacteria inactivation after the first centrifugation, without the filtration step. We have confirmed the full efficiency of the TFA protocol for *Bacillus* spores inactivation on 55 strains of the *B. cereus* group (*B. anthracis*, *B. cereus* and *B. thuringiensis*) [9] and bacterial inactivation on 17 strains of the *Y. pseudotuberculosis* complex [7].
20. The main precaution is to ensure that the pH is around 8.0 for maximum proteolysis efficiency. If pH is too low, add 1  $\mu$ L of 1 M ammonium bicarbonate.

21. Aluminum foil can be used to cover the sample.
22. Two proteotypic tryptic peptides were selected (except for Psn) to unambiguously monitor each protein marker. Peptide selection was based on the recommendations for targeted proteomic experiments [5], regarding sequence uniqueness and amino acid composition.

At least two SRM transitions were monitored for each peptide to improve detection specificity. Product ions were preferentially selected with an  $m/z$  ratio higher than that of the parent ion. A signal was considered positive when peak intensity was three times above the noise level for both selected transitions. Additionally, two criteria should be met for a given peptide: (1) the variation of the retention time should be within 0.1 min in replicate injections with strict co-elution with the IS peptide and similar peak shape; (2) the relative ratio (i.e., for a given transition by dividing its peak area by the peak area of another transition) of the analyte compared with the relative ratio of the IS peptides should not be significantly different ( $\pm 30\%$ ).

23. At least two peptides were detected at the limit of detection. The monitoring of the most intense Pla (peptide Pla2) and Ymt (peptide Ymt1) peptides was sufficient to allow a robust, sensitive, and specific detection of *Y. pestis*.
24. Detection specificity for *Y. pestis* was demonstrated with 17 different strains. Seven *Y. pestis* strains from the three most common biovars were used as control for positive detection, and ten other strains from the *Y. pseudotuberculosis* complex were analyzed as negative samples. The first level of specificity is achieved by the specific antibody capture: immunocapture yield were determined at 77% for *Y. pestis* (mean for seven strains, range: 55–100%), at 1.8% for closely related *Y. pseudotuberculosis* (mean for eight strains, range: 0.02–7.4%) and 0.07% for closely related *Y. similis* (mean for two strains, range: 0.04–0.09%). In this experiment, OmpA proteotypic peptides were monitored to evaluate the efficiency of the Pla-dependent immunocapture of *Y. pestis* and its specificity toward the *Y. pseudotuberculosis* and *Y. similis* species. The second level of specificity is provided by the SRM monitoring of unique *Y. pestis* makers. Positive signals corresponding to the three markers were observed for *Y. pestis*. No signal was detected for any of these markers in *Y. pseudotuberculosis* or *Y. similis* strains (Fig. 2).

Assay sensitivity was evaluated in tap water, milk and soil samples. Limits of detection were as follow: tap water:  $2 \times 10^4$  CFU/mL, milk:  $2 \times 10^4$  CFU/mL, soil:  $4.5 \times 10^5$  CFU in 10 mg, with good linearity ( $r^2 > 0.98$ ) over a 4-log concentration range in tap water and milk ( $2 \times 10^4$  to  $2 \times 10^8$  CFU/mL).



The coefficient of variation (CV) was determined at 6.8% ( $n = 9$ ) with  $5 \times 10^7$  CFU/mL of CO92 strain in the PBS-BSA dilution buffer. Detection of *Y. pestis* was observed both for strains grown at 28 °C (optimal growth temperature) and 37 °C (temperature during infection).

## References

1. Chain PS, Carniel E, Larimer FW, Lamerdin J, Stoutland PO, Regala WM, Georgescu AM, Vergez LM, Land ML, Motin VL, Brubaker RR, Fowler J, Hinnebusch J, Marceau M, Medigue C, Simonet M, Chenal-Francisque V, Souza B, Dacheux D, Elliott JM, Derbise A, Hauser LJ, Garcia E (2004) Insights into the evolution of *Yersinia pestis* through whole-genome comparison with *Yersinia pseudotuberculosis*. Proc Natl Acad Sci U S A 101:13826–13831
2. Kenny JH, Zhou Y, Schriefer ME, Bearden SWJ (2008) Detection of viable *Yersinia pestis* by fluorescence in situ hybridization using peptide nucleic acid probes. J Microbiol Methods 75:293–301
3. Simon S, Demeure C, Lamourette P, Filali S, Plaisance M, Creminon C, Volland H, Carniel E (2013) Fast and simple detection of *Yersinia pestis* applicable to field investigation of plague foci. PLoS One 8:e54947
4. Duriez E, Armengaud J, Fenaille F, Ezan E (2016) Mass spectrometry for the detection of bioterrorism agents: from environmental to clinical applications. J Mass Spectrom 51:183–199
5. Domon B (2012) Considerations on selected reaction monitoring experiments: implications for the selectivity and accuracy of measurements. Proteomics Clin Appl 6:609–614
6. Chenau J, Fenaille F, Ezan E, Morel N, Lamourette P, Goossens PL, Becher F (2011) Sensitive detection of *Bacillus anthracis* spores by immunocapture and liquid chromatography-tandem mass spectrometry. Anal Chem 83: 8675–8682
7. Chenau J, Fenaille F, Simon S, Filali S, Volland H, Junot C, Carniel E, Becher F (2014) Detection of *Yersinia pestis* in environmental and food samples by intact cell immunocapture and liquid chromatography-tandem mass spectrometry. Anal Chem 86:6144–6152
8. Lasch P, Nattermann H, Erhard M, Stämmler M, Grunow R, Bannert N, Appel B, Naumann D (2008) MALDI-TOF mass spectrometry compatible inactivation method for highly pathogenic microbial cells and spores. Anal Chem 80:2026–2034
9. Chenau J, Fenaille F, Caro V, Haustant M, Diancourt L, Klee SR, Junot C, Ezan E, Goossens PL, Becher F (2014) Identification and validation of specific markers of *Bacillus anthracis* spores by proteomics and genomics approaches. Mol Cell Proteomics 13: 716–732

## A Method to Prepare Magnetic Nanosilicate Platelets for Effective Removal of *Microcystis aeruginosa* and Microcystin-LR

Shu-Chi Chang, Bo-Li Lu, Jiang-Jen Lin, Yen-Hsien Li, and Maw-Rong Lee

### Abstract

Algal toxin is a unique type of toxin generated with harmful algal blooms in water bodies. This phenomenon is worsened by eutrophication caused by excessive discharge of nutrients into surface water bodies. Since algal toxins are hard to remove after they enter the water treatment processes, an efficient method is required to inhibit the growth of algal cells, to settle the cells at the bottom of the water body and to remove the toxin from the water. We report an efficient way to prepare a novel nanohybrid material, i.e., magnetic nanosilicate platelet (MNSP), and its effects on the removal of microcystin toxins as well as the cells of *Microcystis aeruginosa*. MNSP was fabricated by a special treatment of a clay mineral, montmorillonite, and then its surface was decorated with magnetite nanoparticles by in situ synthesis. The nanohybrid can efficiently inhibit the growth of *M. aeruginosa*—a typical species that can generate one of the most notorious algal toxins, i.e., microcystins. Algal cells can be settled with minimal 500 ppm MNSP, and the turbidity can be reduced by more than 67%. The removal of microcystin-LR (MC-LR) was as high as 99.39% at a concentration of 100 ppm, while the pristine nanosilicate platelet could only remove 36.84% at the same dosage.

**Key words** Magnetic nanosilicate platelet, Harmful algal bloom, *Microcystis aeruginosa*, Microcystin-LR, Eutrophication

---

## 1 Introduction

On the earth, about 97.5% of the water is sea water. Only about 0.024% of the earth's water is available for human usage [1]. Due to global climate change and development of the modern human society, the ever-increasing water demand makes water a more and more scarce natural resource. According to United Nations, by 2050, more than one third of the world's projected population will live in river basins with severe water stress [2]. In addition, major water sources are facing enormous challenges due to algal blooms, such as Lake Taihu in China [3] or Lake Erie in the USA [4].

Algal growth in water bodies plays a positive role in nutrient cycling and fishery operation [5]. However, under special conditions, such as high nutrient inputs, low predation, and sufficient sunlight, their rapid proliferation can lead to severe consequences, like water discoloration, foul odor generation, and health impact on animals (including humans). Harmful algal blooms (HABs) occur when colonies of algae grow excessively while producing toxins or causing harmful effects on other organisms and the environment [6]. In the past, HABs have caused animal and human deaths and drinking water shortage problems [3, 7–9]. Among all these reported episodes, microcystins from *Microcystin aeruginosa* attracted much attention and have been most frequently studied [10].

Microcystins are generated by *M. aeruginosa* and can have more than 70 different types with similar molecular structures (Fig. 1) [11]. Among them, MC-LR is probably the most toxic one. In the past few decades, several methods have been proposed to remove microcystins in drinking water treatment processes, such as activated carbon, reverse osmosis, chlorination, ozonation, advanced oxidation, permanganate, hydrogen peroxide, photolysis, semiconductor, and photocatalysis [10, 12]. However, these methods either cause undesirable side effects or entail higher cost and treatment complexity. Here, we report a more environmental-friendly way to achieve high removal efficiency on both *M. aeruginosa* and its toxin, MC-LR.

In the past, clay has been applied to remove *Microcystis* spp. cells and toxins with moderate success. To remove the algal cells, within 6 h, clay particles at 750 mg/L can settle about 5000 cells with an initial concentration at ~70,000 cells/mL equivalent to a 7.1% removal [13]. To remove the MC-LR, higher than 833 mg/L of clay particles achieved 81% removal [14]. A most recent study showed that clay modified by hexadecyl trimethyl ammonium bromide (CTAB) can deactivate 92% of tested *M. aeruginosa* [15]. We have reported that nanosilicate platelet (NSP) can remove

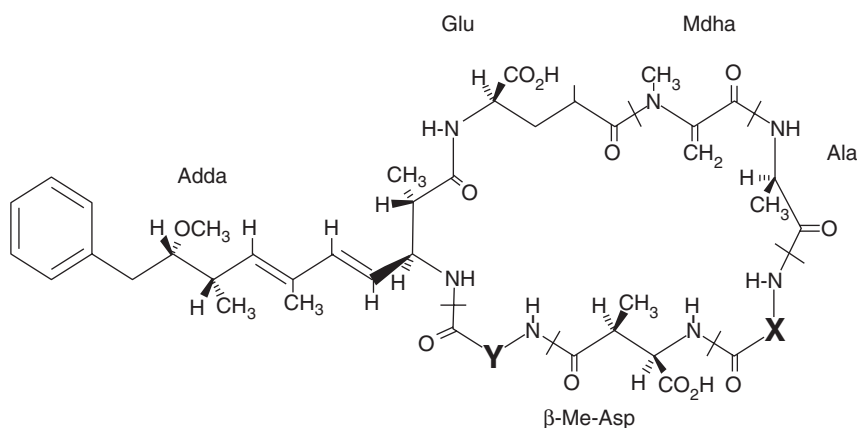


Fig. 1 Structural formula of microcystins [11]

MC-LR as high as 99% at a dosage of 500 ppm [16]. However, up to now, none of the studies has been performed on magnetic iron oxide nanoparticle-decorated nanosilicate platelet (MNSP) for HAB control regarding algal growth inhibition, settling enhancement, and toxin adsorption.

There are several advantages to development of this method by using such a nanohybrid material. First, most eutrophic water bodies are quite shallow, and a retrievable material (through magnetic attraction) can minimize the impact of particle deposit at the bottom. Second, MC-LR adsorbed on MNSP can be recovered physically upon magnetic separation since the uptake of MNSP may result in accumulation of toxin in predating organisms. Third, iron oxides themselves have been reported to be able to remove MC-LR through adsorption [17, 18].

---

## 2 Materials

### 2.1 Culture Preparation

1. *M. aeruginosa* PCC7820 was kindly provided by Prof. Tsair-Fuh Lin at National Cheng Kung University in Taiwan. This culture was originally obtained from Institut Pasteur (Paris, France). Growth medium was a BG-11 medium according to the literature [19].
2. Grow the culture in a 1-liter flask filled with BG-11 medium. Seal the flask using a sterile silicon stopper and shake it at 100 rpm on a shaker. Keep the temperature at 25 °C, and use a 23-W full-spectrum light bulb to provide lighting 12 h a day (e.g., CGB Full Spectrum Lighting, color temperature at 5500 K, Chang Gung Biotechnology, Taipei, Taiwan).
3. Transfer this culture to fresh media every month. Do not perform growth inhibition and settling tests until the cell density is higher than  $10^7$  cells/mL.

### 2.2 Nanosilicate Platelet Preparation

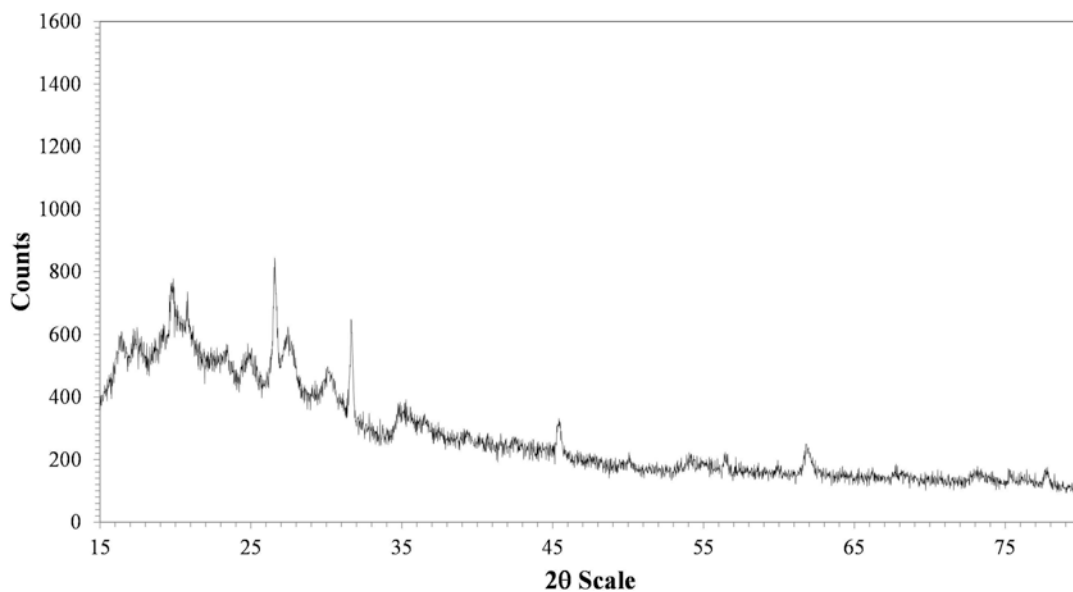
1. Prepare nanosilicate platelets, NSP, from the natural mineral of sodium form of montmorillonite (MMT) purchased from Nanocor Co. (Aberdeen, MS, USA). This clay mineral is the sodium counter ion form of the smectite silicates with 1.20 meq/g cationic exchange capacity. Use poly(oxypropylene)-tri-amine (Jeffamine T403, abbreviated as T403) with a molecular mass of 440 g/mol (Huntsman Chemical Co. or Aldrich Chemical Co.) and diglycidyl ether of bisphenol A (DGEBA, tradename BE-188) with an epoxy equivalent mass (EEM) of 188 (Nan-Ya Chemicals, Taiwan). Perform the exfoliation or delamination of the MMT layered structure in water according to [20, 21], as exemplified below.
2. Firstly, prepare the exfoliating agent, polyamines. Add to a 50-mL three-necked and round-bottomed flask, equipped with a mechanical stirrer, a thermometer, and a heating mantle,

T403 (7.15 g) and DGEBA (2.85 g). Mix these reactants by a mechanical stirrer at room temperature. Monitor the progress of epoxy/amine reaction by an FT-IR, showing the disappearance of  $910\text{ cm}^{-1}$  epoxide absorbance during the process. Stop the reaction after 4 h; the final product is a viscous, transparent liquid. After extracting out the unreacted T403, analyze the crude product by amine titration and gel permeation chromatography. In our experiment, the total amine content was 4.8 meq/g and gel permeation chromatography analysis identified two major peaks.

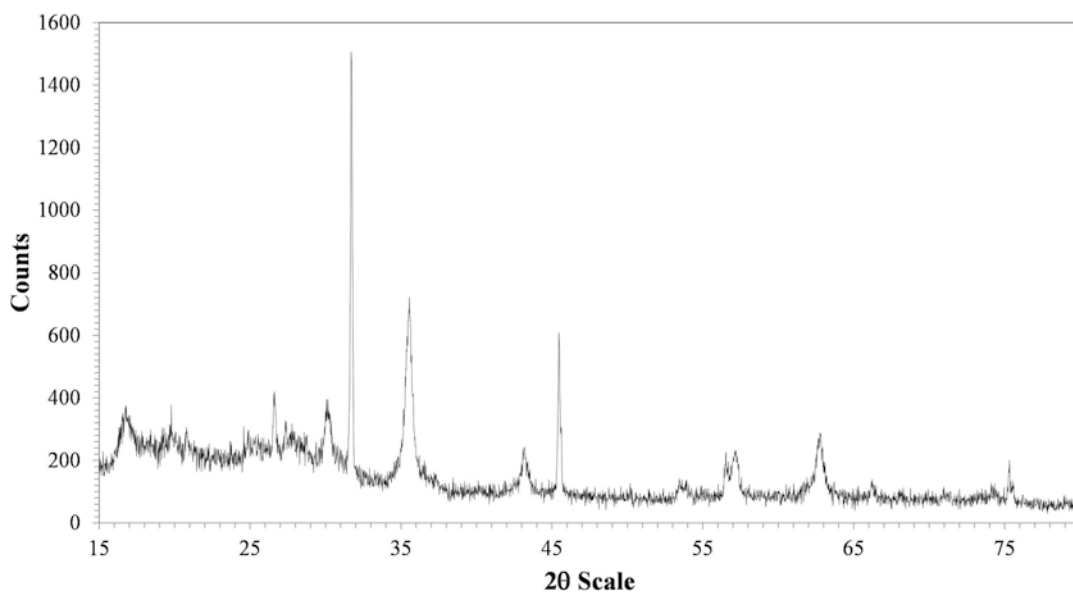
3. Secondly, disperse the clay of sodium MMT (1.0 g) in 100 mL of deionized water at  $80\text{ }^{\circ}\text{C}$  by overnight vigorous stirring to form a MMT slurry. Treat the prepared polyamines (4.50 g) separately at room temperature with a designated amount of hydrochloric acid (35 wt%, 0.71 g) to form the amine-HCl salts in water, and then add this to the silicate clay slurry. Stir this clay mixture at  $80\text{ }^{\circ}\text{C}$  for 3 h, and then filter, collect, and wash thoroughly with 40 mL of water/ethanol several times. Dry the raw NSP material and pulverize it to powder.
4. This raw NSP, as the form of water slurry of the exfoliated MMT, could be further modified by complexing with three alkyl R-dimethylbenzyl ammonium chloride surfactants (R represents 12:0, 14:0, and 16:0 alkyl groups, in a ratio of 63:30:7, respectively).
5. The final NSP represents a complex with the surfactants to form an organic silicate platelet. Confirm the physical size of NSP of about  $100 \times 100 \times 1\text{ nm}$  in lateral dimension by atomic force microscopy and transmission electron microscopy [20, 21]. A typical characterization using a high-resolution X-ray diffractometer (HRXRD D8 SSS, Bruker, Billerica, MA, USA) of NSP is shown in Fig. 2. Characteristic peaks are at 27.4, 31.8, 45.5, and 56.6 degrees on a  $2\theta$  scale.

### 2.3 MNSP Preparation

1. In order to synthesize magnetite nanoparticles (*see Note 1*), keep the environment anaerobic. To maintain the anaerobic synthetic conditions, perform all preparation steps for MNSP in a glove box (Coy Lab, Grass Lake, MI, USA). Subject all water used in this synthesis step to purging by nitrogen for at least 30 min, and then keep it in the anaerobic chamber for at least 1 day before use.
2. For a typical 0.5% of magnetite coverage of the surface area of the NSP, add 1.371 g of  $\text{FeCl}_2 \cdot 4\text{H}_2\text{O}$ , 3.731 g of  $\text{FeCl}_3 \cdot 6\text{H}_2\text{O}$ , 10.0 g of NSP (dry mass), and 2.208 g of NaOH into 70 mL of the water from the previous step. Seal the bottles to prevent oxygen aeration and then mix with a magnetic mixer for 10 min.
3. Add 2.208 g of NaOH to 18.4 mL of deoxygenated water to prepare a 3.0 N NaOH solution. A coprecipitation method was used to prepare MNSP. Put the mixture prepared in **step 2** into a sonication bath, and hold the temperature at  $85\text{ }^{\circ}\text{C}$  for a



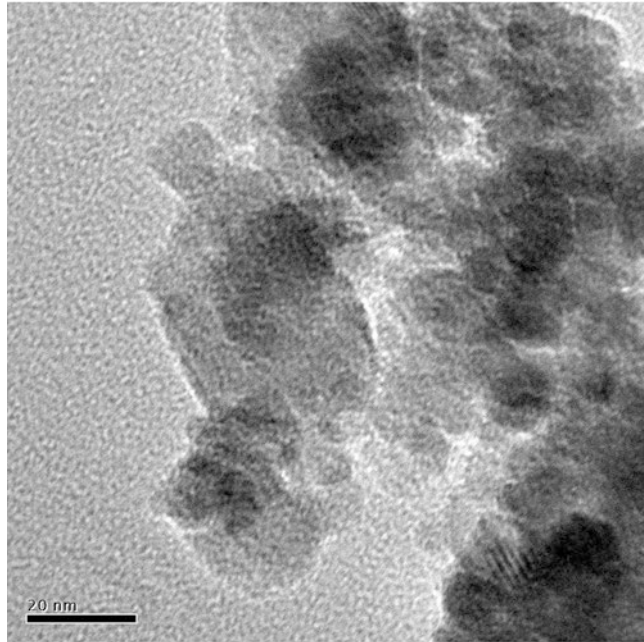
**Fig. 2** XRD characterization of final NSP



**Fig. 3** XRD characterization of MNSP

sonication period of 30 min. Then, add the 3.0 N NaOH solution (*see Note 2*). Cool the mixture to room temperature and transfer it into an anaerobic chamber.

4. In the anaerobic chamber, open the bottle, and wash the product using deoxygenated water three times. Hold all MNSP in place in the bottle by using a strong rare earth magnet. Thus, a clean batch of MNSP is ready for use (*see Note 3*). The HR XRD characterization of MNSP is shown in Fig. 3.



**Fig. 4** HRTEM characterization of MNSP (bar = 20 nm, magnification = 150,000 $\times$ )

The characteristic peaks for magnetite are 30.2, 35.5, 43.2, 57.1, and 62.6 degrees on a  $2\theta$  scale. Also, an electron micrograph of MNSP can be taken using a high-resolution transmission electron microscope (HRTEM) at a magnification of 150,000 folds (e.g., JEM-2010, JEOL, Tokyo, Japan. Fig. 4).

---

### 3 Methods

#### 3.1 Growth Inhibition Test

1. Perform the growth inhibition test of *M. aeruginosa* (PCC7820) by diluting the cells with BG-11 medium to different concentrations in order to see if MNSP could efficiently inhibit the growth of the *M. aeruginosa* within a high concentration range often encountered in an extremely eutrophic water body. Add MNSPs to final concentrations of 0, 10, 100, and 500 ppm.
2. Sample all test combinations at 0, 0.5, 2, 4, 12, 24, and 48 h. Enumerate all samples right away in a hemocytometer slide using a Carl Zeiss microscope (Axiovert 200, Carl Zeiss AG) and perform all tests in triplicates (*see Note 4*).
3. A typical result of growth inhibition test on  $2.06 \times 10^6$  cells/mL is shown in Fig. 5. The highest dosage at 500 mg/L of MNSP resulted in the best growth inhibition of *M. aeruginosa*.

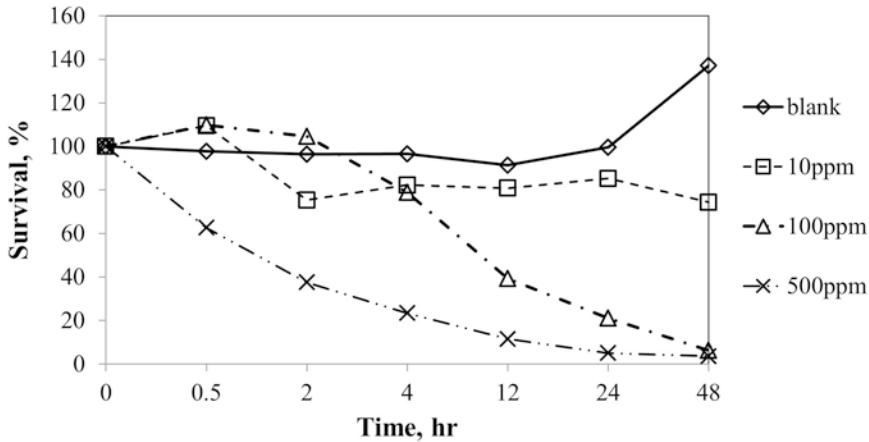


Fig. 5 Growth inhibition test results

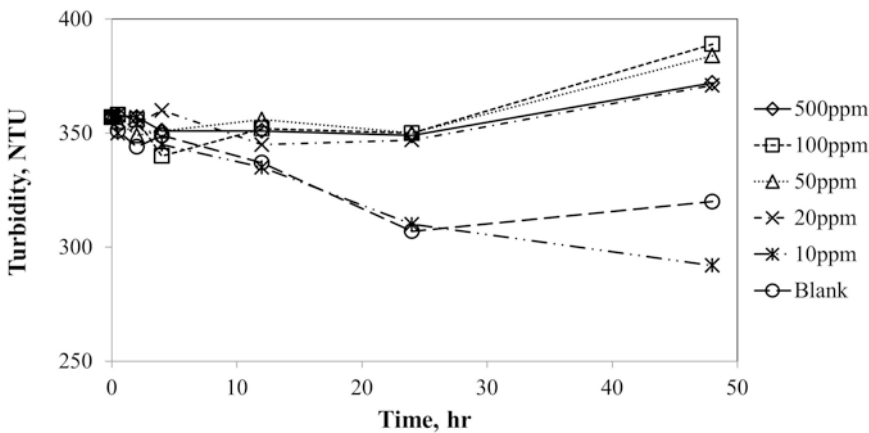


Fig. 6 Settling test on *M. aeruginosa* using MNSP

### 3.2 Settling Enhancement Test

1. Employ a jar test platform (e.g., JT-6S, Sun Great Technology Co, Ltd., Taipei, Taiwan) to test the settling-enhancing effect of NSP. In this test, cell concentration of *M. aeruginosa* should be above  $1.00 \times 10^7$  cell/mL because a higher concentration is more realistic in an algal bloom situation.
2. Add NSP to final concentrations of 0, 10, 20, 50, 100, and 500 ppm. After a 30-min mixing of cells and MNSP solutions at 30 rpm, leave all jars undisturbed for 1 h.
3. Then, sample the supernatants at 0.5, 2, 4, 12, 24, and 48 h to measure their turbidity using a turbidimeter (e.g., Hach 2100 N, Loveland, Colorado, USA).
4. A typical test result is presented in Fig. 6. The dosage of 10 ppm resulted in the best turbidity reduction. This is meaningful because typical eutrophication indices, like Carlson's index, include turbidity as an indicator, in terms of Secchi depth measurement.



### 3.3 Toxin Adsorption Test

1. The most toxic microcystin, MC-LR, in powder form, was purchased from Enzo Life Sciences, Inc. (New York, USA) with purity higher than 95%. Prepare a stock solution by adding methanol to a concentration of 500  $\mu\text{g}/\text{L}$  and store under  $-20\text{ }^\circ\text{C}$ .
2. Before the test, dilute it further by adding deionized water to 100  $\mu\text{g}/\text{L}$ , and add MNSP to each sample to final concentrations of 0, 10, 100, 500, and 1000 ppm. Rotate all samples at 120 rpm in a  $30\text{ }^\circ\text{C}$  warm room for 12 h. Take the supernatant after 30 min of settling, and filter it through a filter with 0.2  $\mu\text{m}$  pore size (Isopore<sup>TM</sup> Membrane Filters 0.2  $\mu\text{m}$  GTBP, Millipore, Billerica, Massachusetts, USA) (*see Note 5*).
3. Then, adjust the pH of the filtered samples to 10.5 before applying solid phase extraction (57030-U, Supelco) using an Oasis HLB column (Waters Corporation, Milford, Massachusetts, USA).
4. Then, elute MC-LR by methanol (containing 0.1% acetic acid), and concentrate it by purging with high-purity nitrogen (*see Note 6*).
5. A typical result of this step is shown in Fig. 7. At an initial 100  $\mu\text{g}/\text{L}$  MC-LR, the removal of a 100-ppm MNSP dosage was  $99.39 \pm 1.07\%$  (mean  $\pm$  standard deviation,  $n = 3$ ). This removal is significantly higher than our previously reported removal by using NSP without magnetite coating. The removal of 100  $\mu\text{g}/\text{L}$  of MC-LR using NSP (100 ppm dosage) is  $36.84 \pm 4.80\%$  (mean  $\pm$  standard deviation,  $n = 3$ ).

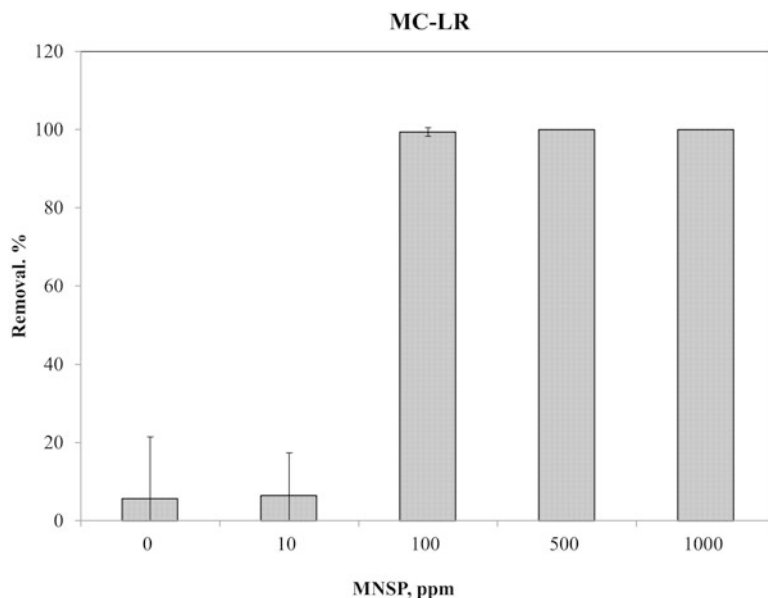


Fig. 7 Toxin removal by using MNSP

In addition, the 100-ppm MNSP dosage yielded higher removal than 500-ppm NSP. In other words, it saved about 80% of the dosage using MNSP to achieve a similar removal.

### 3.4 Toxin Quantification

1. Then analyze all samples using a Thermo Scientific Accela pump liquid chromatography system coupled to a Finnigan TSQ Ultra EMR mass spectrometer (Thermo Finnigan Corporation) with a Phenomenex ODS column (150 × 2.1 mm, 5 μm particle size, Phenomenex International).
2. The settings are H-ESI mode with spray voltage at 4.5 kV, heater temperature at 270 °C, capillary temperature at 270 °C, and sheath gas flow rate at 25 arbitrary units.
3. Quantitation transition ion was set at  $m/z$  from 995.5 to 135, and collision energy was at 60. The mobile phases were 0.1% formic acid in water (A) and 0.1% formic acid in methanol (B).
4. Set the elution condition at 90% A and 10% B for the first minute, and then ramp to 20% A and 80% B at 6 min, maintained at this ratio from 6 to 16 min.
5. At the 17th min, change the elution condition back to 90% A and 10% B, and then maintain at this ratio till the end of 25 min.

---

## 4 Notes

1. Magnetite synthesis is very sensitive to oxygen. Under aerobic conditions, magnetite cannot be obtained. Instead, hematite and maghemite will be formed, which are not as good as magnetite for magnetic recovery and phosphate removal.
2. The concentrated NaOH solution is very corrosive to glassware. Be careful when handling this reagent.
3. Magnetite nanoparticles are highly photolabile. They will be easily oxidized under light. The finished MNSP has to be stored in the dark before use.
4. For enumeration of algal cells using a hemacytometer slide, prior to counting, it is better to wait for at least 5.0 min after transferring the samples into the slide. In this way, the cells are more stable within the tiny space, and one can obtain more consistent results.
5. The filtration of samples from toxin adsorption can be accelerated by using a specialized vacuum chamber (Visiprep™ SPE Vacuum Manifold, #57044 Supelco, Sigma-Aldrich, St. Louis, MO, USA). The samples need to be evaporated to dryness before adding any eluent (methanol with 0.1% acetic acid).
6. The HLB columns need to be primed by 5.0 mL of methanol (twice) and then 5.0 mL deionized water (twice) before use. The flow rate of eluent needs to be carefully controlled at about two drops per second.

## Acknowledgments

The authors would like to thank Ministry of Science and Technology (Taiwan) of Republic of China (ROC) for the partial financial support of this research through a grant of MOST104-2221-E-005 -008.

## References

1. Miller J, Tyler G, Spoolman SE (2010) Environmental science, 13th edn. Cengage Learning, Belmont, CA
2. United Nations World Water Assessment Programme (2015) The United Nations world water development report 2015: water for a sustainable world. UNESCO, Paris
3. Qin B, Zhu G, Gao G, Zhang Y, Li W, Paerl H, Carmichael W (2010) A drinking water crisis in lake Taihu, china: linkage to climatic variability and lake management. *Environ Manag* 45:105–112
4. Rinta-Kanto JM, Konopko EA, DeBruyn JM, Bourbonniere RA, Boyer GL, Wilhelm SW (2009) Lake erie microcystis: relationship between microcystin production, dynamics of genotypes and environmental parameters in a large lake. *Harmful Algae* 8:665–673
5. Hallegraeff GM (1993) A review of harmful algal blooms and their apparent global increase. *Phycologia* 32:21
6. USEPA (2016) Harmful algal blooms. USEPA, Washington, DC
7. Teixeira MGLC, Costa MCN, Carvalho VLP, Pereira MS, Hage E (1993) Gastroenteritis epidemic in the area of the Itaparica dam, Bahia, Brazil. *Bull Pan Am Health Organ* 27:244–253
8. Jervis R, Welch WM, Hall C (2014) Ohio drinking water emergency 'not over yet'. USA Today. Gannett Satellite Information Network, Inc., McLean, VA
9. Trevino-Garrison I, DeMent J, Ahmed FS, Haines-Lieber P, Langer T, Ménager H, Neff J, van der Merwe D, Carney E (2015) Human illnesses and animal deaths associated with freshwater harmful algal blooms—Kansas. *Toxins (Basel)* 7:353–366
10. Westrick JA, Szlag DC, Southwell BJ, Sinclair J (2010) A review of cyanobacteria and cyanotoxins removal/inactivation in drinking water treatment. *Anal Bioanal Chem* 397:1705–1714
11. Hummert C, Dahlmann J, Reinhardt K, Dang HPH, Dang DK, Luckas B (2001) Liquid chromatography-mass spectrometry identification of microcystins in *Microcystis aeruginosa* strain from lake Thanh Cong, Hanoi, Vietnam. *Chromatographia* 54:569–575
12. Lawton LA, Robertson PKJ (1999) Physicochemical treatment methods for the removal of microcystins (cyanobacterial hepatotoxins) from potable waters. *Royal Soc Chem* 28:217–214
13. Verspagen JMH, Visser PM, Huisman J (2006) Aggregation with clay causes sedimentation of the buoyant cyanobacteria *Microcystis* spp. *Aq Microb Ecol* 44:10
14. Morris RJ, Williams DE, Luu HA, Holmes CFB, Andersen RJ, Calvert SE (2000) The adsorption of microcystin-LR by natural clay particles. *Toxicol* 38:303–308
15. Liu G, Fan C, Zhong J, Zhang L, Ding S, Yan S, Han S (2010) Using hexadecyl trimethyl ammonium bromide (CTAB) modified clays to clean the *Microcystis aeruginosa* blooms in Lake Taihu, China. *Harmful Algae* 9:413–418
16. Chang S-C, Li C-H, Lin J-J, Li Y-H, Lee M-R (2014) Effective removal of *Microcystis aeruginosa* and microcystin-LR using nanosilicate platelets. *Chemosphere* 99:49–55
17. Lee J, Walker HW (2011) Adsorption of microcystin-Lr onto iron oxide nanoparticles. *Colloids Surf A Physicochem Eng Asp* 373:94–100
18. Gao Y-Q, Gao N-Y, Deng Y, Gu J-S, Shen Y-C, Wang S-X (2012) Adsorption of microcystin-LR from water with iron oxide nanoparticles. *Water Environ Res* 84:562–568
19. Rippka R, Deruelles J, Waterbury JB, Herdman M, Stanier RY (1979) Generic assignments, strain histories and properties of pure cultures of cyanobacteria. *J Gen Microbiol* 111:1–61
20. Lin J-J, Chu C-C, Chiang M-L, Tsai W-C (2006) First isolation of individual silicate platelets from clay exfoliation and their unique self-assembly into fibrous arrays. *J Phys Chem B* 110:18115–18120
21. Chiu C-W, Chu C-C, Cheng W-T, Lin J-J (2008) Exfoliation of smectite clays by branched polyamines consisting of multiple ionic sites. *Eur Polym J* 44:628–636

## An Immunochromatographic Test Strip to Detect Ochratoxin A and Zearalenone Simultaneously

Xiaofei Hu and Gaiping Zhang

### Abstract

Lateral flow immunochromatographic assays are simple, useful tools for the detection of many different targets. In this format, a liquid sample containing target of interest moves along a strip of polymeric material adhered with various lines where molecules have been attached that exert specific interactions with the target. Here, we describe a colloidal gold-based immunochromatographic test strip for the simultaneous detection of ochratoxin (OTA) and zearalenone (ZEN) in corn and other cereals qualitatively and quantitatively.

**Key words** Immunochromatographic test strip, Colloidal gold, Mycotoxins, Ochratoxin A, Zearalenone

---

### 1 Introduction

Lateral flow immunoassays (LFIA) are simple, useful tools for a variety of point-of-care and field-use applications [1–3]. One typical LFIA format consists of a surface layer named sample pad to carry sample liquid via the conjugate pad along the strip encountering the detection zone up to the absorbent pad [4].

As with the ELISA method, there are two kinds of assay format of LFIA, namely, the direct (sandwich) or competitive one [5–8]. The sandwich LFIA is mainly used to detect macromolecular substance, as proteins, hormones, or enzymes. The competitive LFIA is mainly used to determine targets containing small molecules. Moreover, there are many kinds of labels which can be used for conjugates that attach on the conjugate pad, such as colloidal gold [9], latex, liposomes, fluorescent nanoparticles, quantum dots, or up-converting phosphor [4, 10]. Thus, lateral flow immunochromatographic test strips are currently widely used to detect veterinary drugs, pesticides, mycotoxins, prohibited additives, allergen, environmental pollutants, pathogens, hormones, and metabolites, because of their sensitivity, selectivity, speed, and ease of use [8, 10–13].

Conventional lateral flow strip only determines a single target per strip. Thus, we have labeled monoclonal antibodies for OTA and ZEN with colloidal gold and have subsequently developed a lateral flow immunoassay strip of the competitive format which can simultaneously detect OTA and ZEN.

---

## 2 Materials

All solutions were prepared using ultrapure water (the water has a sensitivity of  $18.2 \text{ M}\Omega \times \text{cm}$  at room temperature) or double-distilled water (DDW). All reagents are analytical grade or higher and prepared and stored at room temperature, unless otherwise specified. All the waste materials have been collected and disposed by professional company designated by the government.

### 2.1 Colloidal Gold Components

1. Gold chloride trihydrate, store at  $4 \text{ }^\circ\text{C}$  (*see Note 1*).
2. 1% gold chloride solution: dissolve 1 g gold chloride trihydrate (*see Note 2*) in 100 mL ultrapure water (*see Note 3*).
3. 1% trisodium citrate solution: dissolve 1 g trisodium citrate dehydrate in 100 mL ultrapure water.

### 2.2 Immuno-chromatographic Test Strips

1. Antibodies: anti-OTA and anti-ZEN monoclonal antibodies (*see Notes 4 and 5*) are prepared by Henan Key Laboratory, Henan Academy of Agricultural Sciences.
2. Buffer for sample pads of strips: 100 mM phosphate buffer (PB) containing 1% casein, 0.3% Tween 20, 5% trehalose, and 0.05% sodium azide (*see Notes 6 and 7*), store at  $4 \text{ }^\circ\text{C}$ .
3. Buffer for conjugate pads of strips: 20 mM borate buffer (*see Note 8*) containing 3% casein, 1% Triton X-100, and 0.03% sodium azide (*see Note 9*), store at  $4 \text{ }^\circ\text{C}$ .
4. Standard solutions of OTA and ZEN: diluting stock solutions (*see Note 10*) of OTA or ZEN with DDW, respectively.
5. Sodium chloride solution: dissolve 10 g sodium chloride in 100 mL DDW.

### 2.3 The Structural Components of the Immuno-chromatographic Test Strips

Nitrocellulose membrane, glass fiber, and absorbent pad were from Millipore, Bedford, MA, USA. The plastic supporting backbone was supplied by Jiening Biological Technology Co., Ltd., Shanghai, China.

### 2.4 Preparation of OTA-BSA and ZEN-BSA

1. Synthesize OTA-BSA by the method described by Wang et al. [14] with slight modification (*see Note 11*).
2. Prepare ZEN-BSA according to Sun et al. [12] (*see Note 12*).

### 3 Methods

All the procedures were carried out at room temperature unless specified otherwise.

#### 3.1 Preparation of Colloidal Gold Nanoparticles

1. Mix 1 mL 1% (w/v) gold chloride solution with 99 mL ultra-pure water in a very clean glassware (*see Note 13*) to prepare 0.01% gold chloride solution.
2. Add 1.6 mL of a 1% solution of trisodium citrate to 100 mL of boiling 0.01% gold chloride solution (*see Note 14*). The resulting solution, initially had a gray color which changed to lavender and then, with continued boiling, after 1–3 min developed a red hue. The resulting colloidal gold particle size was about 25 nm [15].

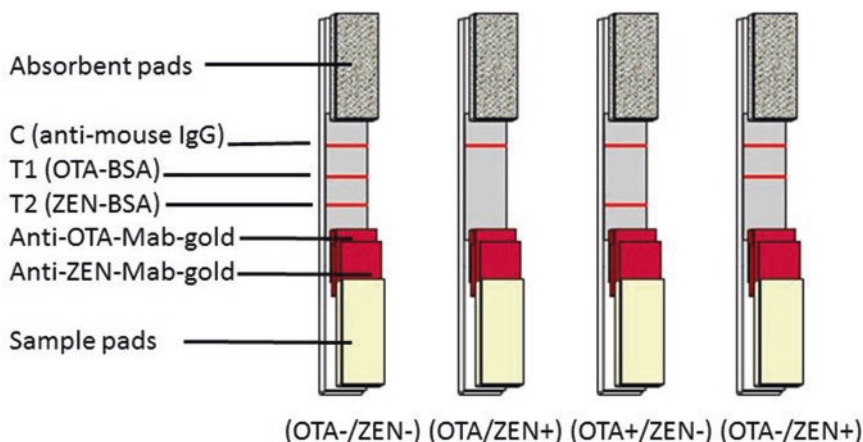
#### 3.2 Preparation of Colloidal Gold Conjugates of the Monoclonal Antibody

1. Adjust pH of the colloidal gold solution to 8.2 with 0.2 mol/L  $K_2CO_3$  (*see Note 15*).
2. Determine the most appropriate mAb protein concentration for conjugation: prepare twofold serial dilutions of the stock antibody solutions, anti-OTA or anti-ZEN (*see Note 16*). Mix 30  $\mu$ L of each dilution with 125  $\mu$ L of colloidal gold solution. After incubating for 5 min at room temperature, add 125  $\mu$ L of 10% NaCl solution. The color of the mixtures changes from brilliant red to blue as the concentration of mAb decreases. The optimum concentration of mAb for colloidal gold labeling is the lowest concentration of mAb solution at which there is a change in color [16] (*see Note 17*).
3. Drop the required volume of the optimal concentration of mAb protein into 100 mL colloidal gold solution (pH 8.2) (*see Note 18*). Gently mix for 70 min, then add 10 mL of 5% (w/v) casein, and incubate further for 10 min. Centrifuge the mixture at  $12,000 \times g$  for 30 min at 4 °C. Discard the supernatant, and re-suspend the sediment in 50 mL of gold conjugate suspension buffer (*see Note 19*).

#### 3.3 Assembly of Immuno-chromatographic Test Strips

The immunochromatographic test strip is based on the competitive immunoassay principle:

1. The strip structure contains the following elements: sample pads (*see Note 20*), conjugate pads (*see Note 21*), absorbent pads (*see Note 22*), nitrocellulose (NC) membranes (*see Note 23*), and plastic supporting backbone (*see Note 24*). Attach the sample pads, conjugate pads, NC membranes, and absorbent pads to the plastic supporting backbone sequentially (*see Note 25*) as shown in Fig. 1.
2. Coat the conjugate pads with colloidal gold-labeled anti-OTA and anti-ZEN mAbs with a XYZ Biostrip Dispenser separately. The volume of colloidal gold-labeled anti-OTA mAbs is 7  $\mu$ L/cm line, and of anti-ZEN 6  $\mu$ L/cm line. Dry the conjugate pads at 42 °C for 1 h.



**Fig. 1** Schematic diagram of simultaneous immunochromatographic strip test. C, control line; T1, OTA test line; T2, ZEN test line; +, mycotoxin positive; -, mycotoxin negative

- Spot test and control lines onto NC membrane (*see Note 26*) using XYZ Biostrip Dispenser at  $0.9 \mu\text{L}/\text{cm}$  line. Spot two test lines (*see Note 27*) with OTA-BSA at a concentration of  $0.25 \text{ mg}/\text{mL}$  and with ZEN-BSA at a concentration of  $0.30 \text{ mg}/\text{mL}$ , respectively (*see Note 28*). Spot the control line with staphylococcal protein A at a concentration of  $1.20 \text{ mg}/\text{mL}$ . Dilute all protein solutions for spotting with normal saline. The membrane is dried at  $42^\circ\text{C}$  for 4 h.
- Cut the assembled semirigid polyethylene sheet into strips ( $0.3 \text{ cm} \times 5 \text{ cm}$ ).

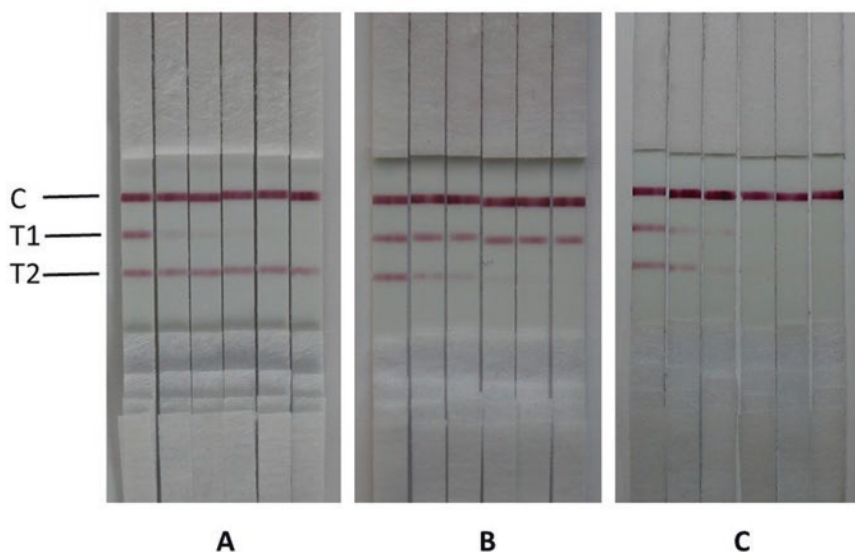
### 3.4 Sample Preparation

The samples included corn, barley, oat, rice, wheat, and other cereals:

- Ground the samples before mixing  $5 \text{ g}$  with  $2 \text{ mL}$  of  $1 \text{ M HCl}$  for 5 min.
- Add  $5 \text{ mL}$  of trichloromethane and shake the mixture violently for 15 min.
- Filter the mixture and abandon the upper aqueous phase.
- Add an equal volume of  $0.13 \text{ M NaHCO}_3$  to the remaining organic phase. Shake the mixture violently for 15 min.
- Centrifuge the mixture for 10 min at  $3300 \times g$ .
- The clear upper phase was used directly for analysis without further cleanup (*see Note 29*).

### 3.5 Assay Procedure and Determination of the Analytical Parameters

- Drop  $100\text{--}150$  microliters of spiked sample extracts onto the sample pad of a test strip.
- Observe the color of the test lines and control line 5–10 min later.
- Examine the strip with the naked eye to qualitatively detect OTA and ZEN presence (Fig. 2) (*see Note 30*).



**Fig. 2** Test strip of corn samples. Note: (a) OTA concentrations (from *left to right*), 0, 2, 3, 4, 5, and 6 ng/mL; (b) ZEN concentrations (from *left to right*), 0, 4, 8, 12, 16, and 20 ng/mL; (c) OTA/ZEN concentrations (from *left to right*), 0/0, 2/4, 3/8, 4/12, 5/16, 6/20, and 50/50 ng/mL; C line is the control line; T1 and T2 lines are the OTA and ZEN test lines, respectively

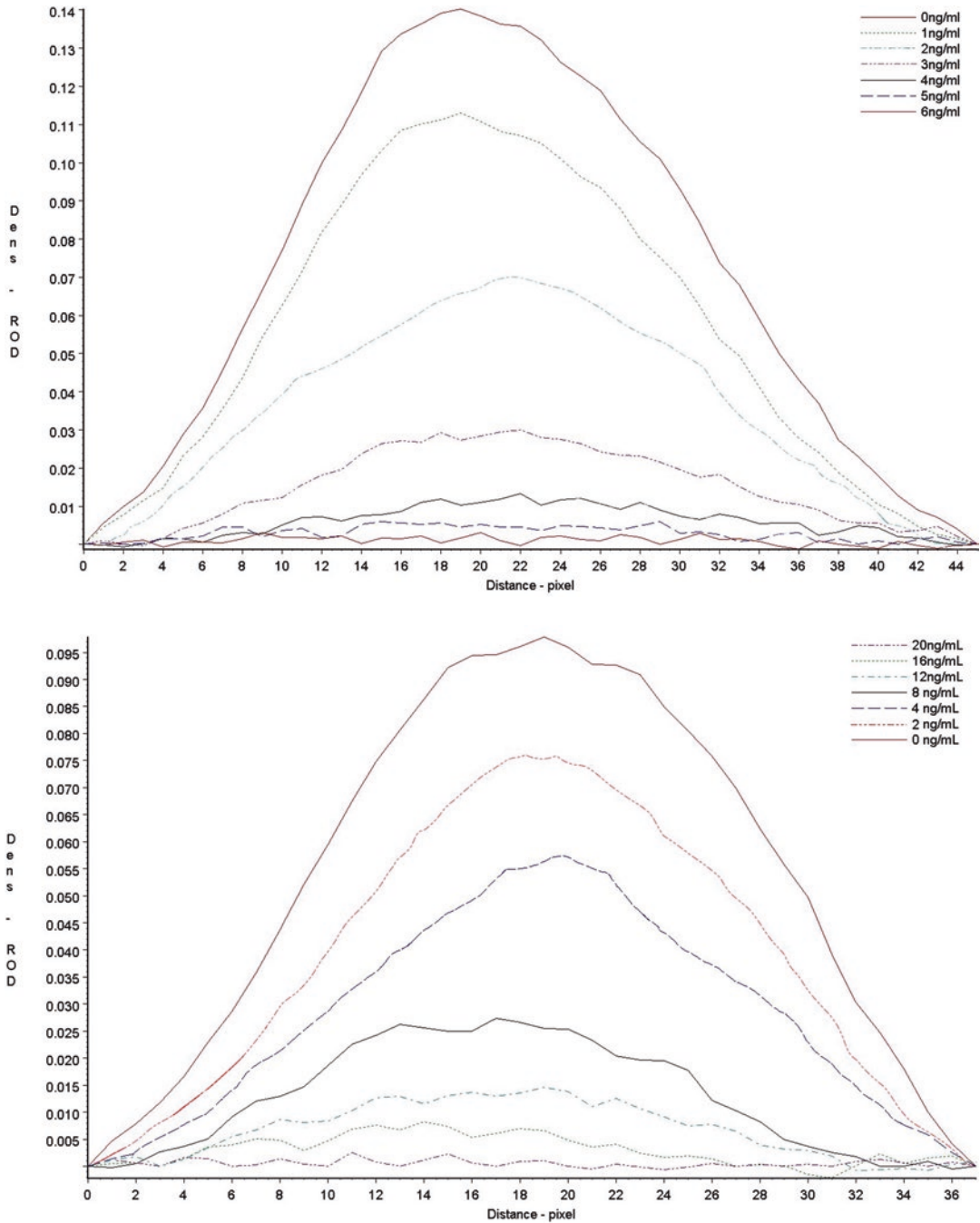
4. Detect OTA and ZEN quantitatively in samples (Figs. 3 and 4) by scanning the strips with the densitometer (*see Note 31*).

---

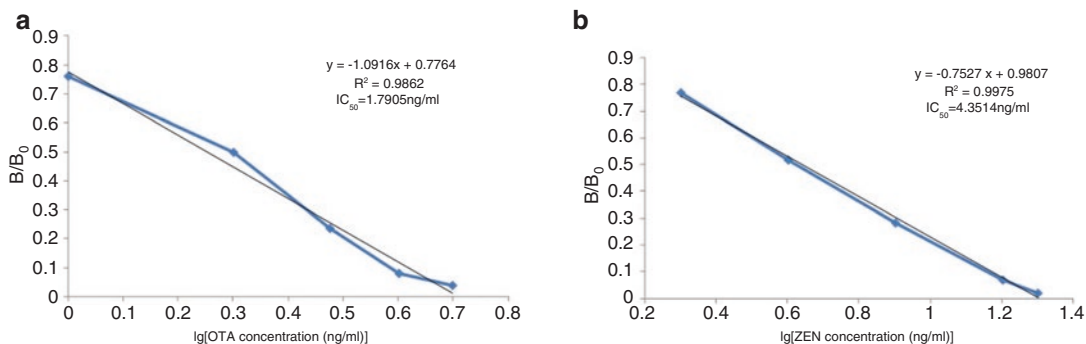
## 4 Notes

1. Gold chloride trihydrate readily absorbs water and should be kept in a sealed container and stored in a dry place. It can also be aliquoted and sealed under vacuum.
2. Gold chloride trihydrate should be weighed in a dry room, and the process should take as little time as possible.
3. The ultrapure water is prepared in our laboratory by PURELAB Classic UF water purifier (Veolia, UK) with purified water.
4. The OTA monoclonal antibody was prepared from ascitic fluid induced by the hybridoma secreting anti-OTA monoclonal antibody (cell line, 2A11). The immunological properties of OTA monoclonal antibody were determined: the 50% inhibitory concentration ( $IC_{50}$ ) for OTA was 0.163 ng/mL; the cross-reactivity was 16.3% with OTB and no more than 0.03% with compounds such as aflatoxin B1, fumonisin B, and zearalenone.
5. The ZEN monoclonal antibody was prepared from ascitic fluid from mice growing the hybridoma cell line 4A3-F9 secreting anti-ZEN monoclonal antibody. The immunological properties of ZEN monoclonal antibody were determined: the 50%





**Fig. 3** ROD curves in corn samples for OTA (a) and ZEN (b). Note: The corn extracts spiked with OTA (0, 1, 2, 3, 4, 5, 6 ng/mL) and ZEN (0, 2, 4, 8, 12, 16, 20 ng/mL<sup>-1</sup>) standard solutions were tested using the test strips. Test lines were scanned with a TSR3000 membrane strip reader



**Fig. 4** Standard curves in corn samples for OTA (**a**) and ZEN (**b**) using test strip detection. Note: The X-axis is expressed as log concentration.  $B/B_0$  represents the ratio of ROD of standards divided by that of the ROD at 0 ng/mL

inhibitory concentration ( $IC_{50}$ ) for OTA was 1.115 ng/mL; the cross-reactivity with zearalanone was 53.12% and less than 4% with other analogues such as  $\alpha$ -zearalenol,  $\beta$ -zearalenol,  $\alpha$ -zearalanol, and  $\beta$ -zearalanol.

6. 100 mM PB: mix 95 mL 0.2 M monosodium orthophosphate with 405 mL 0.2 M disodium hydrogen phosphate, then add DDW to the mixed solution to 1000 mL.
7. Sample pad buffer: mix 1 g casein, 5 g trehalose, 0.05 g sodium azide, and 0.3 mL Tween-20 in 100 mL PB.
8. 20 mM borate buffer: dissolve 7.63 g sodium tetraborate decahydrate in 1000 mL DDW.
9. Conjugate pad buffer: mix 3 g casein, 1 mL Triton X-100, and 0.03 g sodium azide in 100 mL 20 mM borate buffer.
10. Stock solutions: dissolve 1 mg OTA or ZEN in 1 mL methanol and store at  $-20^\circ\text{C}$ .
11. Preparation of OTA-BSA: 5 mg of OTA and 2.6 mg *N*-(3-dimethylaminopropyl)-*N'*-ethyl-carbodiimide (EDC) were dissolved in 1 mL dry *N,N*-dimethylformamide (DMF). The mixture was then added dropwise with mixing to 2 mL of a solution of 10 mg BSA in 130 mM sodium bicarbonate (pH 8.1). Mix at room temperature for 5 h, then add a further 1.2 mg EDC again. The final mixture was incubated overnight at  $4^\circ\text{C}$  with stirring. The conjugates were purified by dialysis against 0.01 M phosphate-buffered saline (PBS, pH 7.4) and stored at  $-20^\circ\text{C}$ .
12. Preparation of ZEN-BSA: 7 mg of BSA was dissolved in 1 mL of distilled water, and the pH adjusted to 10.8 using 1 M sodium hydroxide. Butane-1,4-diol diglycidyl ether (6  $\mu\text{L}$ ) was added, and the solution was incubated for 20 h at ambient temperature under a nitrogen atmosphere. 5 mg of ZEN dissolved in 1.5 mL of 0.5 M sodium hydroxide, degassed using

nitrogen, was then added to the epoxy-activated BSA solution. The reaction mixture was incubated for 20 h at ambient temperature under a nitrogen atmosphere. The conjugates were purified by dialysis against 0.01 M PBS and stored at  $-20\text{ }^{\circ}\text{C}$ .

13. Scratches on the inner surface of the glassware must be avoided, and a mild detergent can be used to clean the glassware and a soft cloth to scrub its inner surface. After cleaning, all detergent should be removed by rinsing thoroughly with ultrapure water, and then the glassware boiled with ultrapure water two or three times.
14. It is best to add trisodium citrate solution to the boiling gold chloride solution. The trisodium citrate solution should be added as quickly as possible into the boiling gold chloride solution with strong agitation.
15. The pH of prepared colloidal gold solution is about 6. Add  $12\text{ }\mu\text{L}$   $0.2\text{ M}$   $\text{K}_2\text{CO}_3$  to 1 mL of colloidal gold solution gives a final pH of 8.2.
16. Twofold serially diluted about 8–12 times in a row of wells.
17. In our experience, the lowest concentration of anti-OTA mAb protein that produced a change in color is  $15\text{ }\mu\text{g/mL}$  colloidal gold solution. For the anti-ZEN mAb protein, the amount is  $19.68\text{ }\mu\text{g/mL}$  colloidal gold solution.
18. For our experiment, we rounded up the optimum anti-ZEN mAb protein to  $20\text{ }\mu\text{g/mL}$  of colloidal gold solution. The optimum anti-OTA mAb protein concentration used was  $15\text{ }\mu\text{g/mL}$  of colloidal gold solution. Before conjugating the mAb protein to colloidal gold, we diluted the initial mAb protein to  $1\text{ mg/mL}$  with DDW; thus, to 100 mL of colloidal gold solution, 1.5 mL of the diluted anti-OTA mAb protein solution or 2 mL of the diluted anti-ZEN mAb protein solution was added.
19. Gold conjugate suspension buffer: add 1 g BSA, 0.03 g sodium azide to 100 mL of 20 mM borate buffer and store at  $4\text{ }^{\circ}\text{C}$ .
20. The sample pads are usually made of glass fiber, cross-linked silica, cellulose, or polyester cotton. In our laboratory, glass fiber is used, as a  $30\text{ cm} \times 1.5\text{ cm}$  strip previously soaked in sample pad buffer, then dried at  $42\text{ }^{\circ}\text{C}$  for 4 h.
21. Many materials can be used as conjugate pads, such as glass fiber, polyester film, and cellulose or non-woven fabrics. Our laboratory uses a glass fiber conjugate pad as a  $30 \times 0.8\text{ cm}$  strip previously soaked with conjugate pad buffer, then dried at  $42\text{ }^{\circ}\text{C}$  for 1 h.
22. The absorbent pads are made of white filter paper without any chemical additives as a  $30 \times 1.8\text{ cm}$  strip.

23. A 30 × 1.5 cm strip of nitrocellulose is used. Nitrocellulose can be replaced by cellulose acetate membrane, polyvinylidene difluoride membrane, or nylon membrane.
24. The plastic supporting backbone is made of semirigid polyethylene sheet, which specification is 30 × 6.5 cm.
25. The overlap for consecutive pads is 2 mm.
26. In our laboratory, the distance between the adjacent test lines 1 and 2 and control line is 0.45 cm.
27. If the strip is required to detect a single fungal toxin, then only one test line is put on the NC membrane.
28. The order of the conjugates in test line 1 and test line 2 can be changed.
29. The upper clear liquid should be diluted before analysis according to the detection sensitivity of strip and the limit set for the target in the foodstuff.
30. When both mycotoxins are absent (sample OTA<sup>-</sup>/ZEN<sup>-</sup>), all of the mAb-gold conjugates are trapped by the capture reagents resulting in three vivid red lines (T1, T2, and C line). Whereas if the sample contains both mycotoxins (OTA<sup>+</sup>/ZEN<sup>+</sup>), only one vivid red line appears at the C line. If two lines appear (C line and one T line), the sample is positive for either OTA or ZEA (OTA<sup>-</sup>/ZEN<sup>+</sup> or OTA<sup>+</sup>/ZEN<sup>-</sup>). The control line is colored red to ensure that the strip and the test procedure are correct. If no color appears at the control line, either the test procedure was improperly conducted or the strip was faulty and the sample should be tested again using a new strip [5]. The sensitivity of the test strip to the naked eye was set at the lowest concentration of OTA/ZEN giving no color at the corresponding test line. We found that the color of the OTA test lines and ZEN test lines disappeared at ≥6 ng/mL and ≥20 ng/mL, respectively. Therefore, the visual sensitivity for the test strip was found to be 6 ng/mL of OTA and 20 ng/mL of ZEN, respectively. In our laboratory, we consider a sample containing less than 6 ng/mL OTA as negative; for ZEN, this limit is 20 ng/mL.
31. With TSR3000 membrane strip reader (Bio-Dot), the immunochromatographic strip test can be used for a more quantitative analysis [6]. The higher the concentration of analyte in the sample the more it competes for the limited amount of mAb-gold conjugate. Hence, the color intensity of the appropriate test line is inversely related to the toxin concentration in the sample. A TSR3000 membrane strip reader was used to scan the strips and obtain the relative optical density (ROD) of the test line. The standard curve was constructed by plotting the G/D × A-ROD (pixel) values obtained from the standard sam-

ples against the log of the concentration. The  $IC_{50}$  and the lower detection limit (LDL) were calculated from the regression equation. The linearity was assessed by the coefficient of determination ( $R^2$ ). The sigmoidal dose–response curve produced by the OTA/ZEN standard samples against its logarithm concentrations and the  $G/D \times A$  (area), which had good linearity within the range of 0.62–5.14 ng/mL and 0.94–20.09 ng/mL for OTA and ZEN, respectively, and correlation coefficients of 0.9862 and 0.9975. The calculated regression equations were  $y = -1.0916x + 0.7764$  and  $y = -0.7527x + 0.9807$ . From these, the  $IC_{50}$  for OTA and ZEN were calculated to be 1.79 ng/mL and 4.35 ng/mL, and the LDL of OTA and ZEN were 0.77 ng/mL and 1.20 ng/mL, respectively. So the sensitivity of the test strip, using the Bio-Dot TSR3000 membrane strip reader, for cereal (extracts prepared by the aforementioned sample preparation method) was 0.77  $\mu\text{g}/\text{kg}$  and 1.20  $\mu\text{g}/\text{kg}$  of OTA and ZEN, respectively.

---

## Acknowledgment

This research was supported by the National Science & Technology Pillar Program of “12th Five-Year Plan” (2014BAD13B05) and the Distinguished Youth Fund Project of Henan Academy of Agricultural Sciences (2013YQ29). Norman Gregson, Professor at University of London, reviewed this manuscript and gave lots of good advice.

## References

1. Paek SH, Lee SH, Cho JH et al (2000) Development of rapid one-step immunochromatographic assay. *Methods* 22:53–60
2. Putalun W, Morinaga O, Tanaka H et al (2004) Development of a one-step immunochromatographic strip test for the detection of sennosides A and B. *Phytochem Anal* 15:112–116
3. Cho YJ, Lee DH, Kim DO et al (2005) Production of a monoclonal antibody against ochratoxin A and its application to immunochromatographic assay. *J Agric Food Chem* 53:8447–8451
4. Posthuma-Trumpie GA, Korf J, van Amerongen A (2009) Lateral flow (immuno) assay: its strengths, weaknesses, opportunities and threats. A literature survey. *Anal Bioanal Chem* 393:569–582
5. Zhao Y, Zhang G, Liu Q et al (2008) Development of a lateral flow colloidal gold immunoassay strip for the rapid detection of enrofloxacin residues. *J Agric Food Chem* 56:12138–12142
6. Song C, Liu Q, Zhi A et al (2011) Development of a lateral flow colloidal gold immunoassay strip for the rapid detection of olaquinox residues. *J Agric Food Chem* 59:9319–9326
7. Li X, Sun Y, Yang S et al (2015) Development of an immunochromatographic strip for antibody detection of pseudorabies virus in swine. *J Vet Diagn Invest* 27:739–742
8. Wang Y, Deng R, Zhang G et al (2015) Rapid and sensitive detection of the food allergen glycinin in powdered milk using a lateral flow colloidal gold immunoassay strip test. *J Agric Food Chem* 63:2172–2178

9. Zhang GP, Li QM, Yang YY et al (2005) Development of a one-step strip test for the diagnosis of chicken infectious bursal disease. *Avian Dis* 49:177–181
10. Song C, Zhi A, Liu Q et al (2013) Rapid and sensitive detection of beta-agonists using a portable fluorescence biosensor based on fluorescent nanosilica and a lateral flow test strip. *Biosens Bioelectron* 50:62–65
11. Zhi A, Li B, Liu Q et al (2010) Development of a lateral-flow immunochromatographic test device for the rapid detection of difloxacin residues. *Food Agric Immunol* 21:335–345
12. Sun Y, Hu X, Zhang Y et al (2014) Development of an immunochromatographic strip test for the rapid detection of zearalenone in corn. *J Agric Food Chem* 62:11116–11121
13. Yang X, Zhang G, Wang F et al (2015) Development of a colloidal gold-based strip test for the detection of chlorothalonil residues in cucumber. *Food Agric Immunol* 26:729–737
14. Wang XH, Liu T, Xu N et al (2007) Enzyme-linked immunosorbent assay and colloidal gold immunoassay for ochratoxin A: investigation of analytical conditions and sample matrix on assay performance. *Anal Bioanal Chem* 389:903–911
15. Frens G (1973) Controlled nucleation for the regulation of the particle size in monodisperse gold suspensions. *Nat Phys Sci* 241:20–22
16. Zhang G, Wang X, Zhi A et al (2008) Development of a lateral flow immunoassay strip for screening of sulfamonomethoxine residues. *Food Addit Contam Part A Chem Anal Control Expo Risk Assess* 25:413–423

## Endotoxin Removal from *Escherichia coli* Bacterial Lysate Using a Biphasic Liquid System

Janusz Boratyński and Bożena Szermer-Olearnik

### Abstract

Lipopolysaccharide (LPS, endotoxin, pyrogen) which is a component of the outer membrane of most Gram-negative bacteria is a troubling contaminant of crude bacteriophage suspension. Therefore, its removal is important for bacteriophage applications especially in preparations dedicated for use in therapy with bacterial infections treatment. The method presented here is used for extractive removal of endotoxins from bacteriophage preparations with a water immiscible solvent such as 1-octanol. During extraction most of the phage lytic activity is retained in the aqueous phase, while endotoxin accumulates in the organic solvent. The levels of endotoxin in the aqueous bacteriophage rich fraction are determined by *Limulus Amebocyte Lysate* or EndoLISA assay and are extremely low.

**Key words** Lipopolysaccharides, Bacteriophage, Extraction procedure

---

### 1 Introduction

Bacteriophage preparations are often contaminated by macromolecules derived from the host bacteria and culture medium. In the case of phages prepared on Gram-negative bacteria, the major pyrogen is lipopolysaccharide (endotoxin), which can be found in the outer membrane of these bacteria [1]. The amount of endotoxins is defined by an endotoxic unit (EU) which corresponds to activity of 100 pg of *Escherichia coli* lipopolysaccharide. Tolerated endotoxin levels depend on the route of the administration therefore the allowed threshold for most intravenous applications is 5 EU/kg/h [2]. Endotoxin is much more tolerated when administered orally [3, 4], additionally the endotoxin content of distilled water is ca. 20 EU/mL [5]. There is no general procedure for endotoxins removal which is the reason why many endotoxin elimination methods are tailored for specific bioproducts. [6]. For example, ultrafiltration is a common technique for purification biological macromolecules [7, 8]. Affinity techniques can be used to effectively remove lipopolysaccharides using immobilized ligands

such as polymyxin B [9, 10], L-histidine, poly-L-lysine, poly(ethyleneimine) [11], PEGylated polypeptides [12] and L-serine immobilized on polyvinylidene fiber [13]. A commercially available Endo-trap kit efficient at endotoxin removal is also applied to bacteriophage suspensions [14]. Here, we demonstrate a method for effective endotoxin removal from a bacteriophage crude suspension by extraction with water immiscible solvent namely 1-octanol [15]. The presented procedure allows for endotoxins removal from bacteriophage preparations with preserving antibacterial activity.

---

## 2 Materials

### 2.1 Media

Nutrient broth (pH  $7.2 \pm 0.2$ ): 0.4 g beef extract, 5.4 g enzymatic digest of casein, 1.7 g yeast extract, 4 g peptone, 3.5 g NaCl per liter. Dissolve the components in distilled water and sterilize in an autoclave. Add sterile glucose to a final concentration of 1%.

### 2.2 Bacterial Strains

1. *E. coli* B strain—e.g., from the Polish Collection of Microorganisms, Institute of Immunology and Experimental Therapy, Polish Academy of Sciences (PCM 1630). Keep the strain on MacConkey agar at 4 °C.
2. *Pseudomonas aeruginosa* strain—e.g., from the Polish Collection of Microorganisms, Institute of Immunology and Experimental Therapy, Polish Academy of Sciences (PCM 2720). Keep the strain on blood agar at 4 °C.

### 2.3 Bacteriophages

1. Bacteriophage T4—*E. coli*-specific bacteriophage from the American Type Culture Collection (Rockville, Maryland, USA).
2. Bacteriophage HAP1—*E. coli*-specific bacteriophage received from the phage collection of Laboratory of Bacteriophages, Institute of Immunology and Experimental Therapy, Polish Academy of Sciences [16].
3. Bacteriophage F8—*P. aeruginosa*-specific bacteriophage receive from the phage collection of Laboratory of Bacteriophages, Institute of Immunology and Experimental Therapy, Polish Academy of Sciences.

### 2.4 Determination of Endotoxins

1. Limulus Amebocyte Lysate test (Charles River Laboratories International).
2. EndoLISA (ELISA-based Endotoxin Detection Assay, Hyglos, Germany).



### 3 Methods

#### 3.1 Preparation of Crude Bacteriophage Suspension

1. Grow the bacterial culture in nutrient broth at 37 °C for 8–16 h, until the optical density (OD, 565 nm) reaches 1 McFarland units.
2. Infect the culture with bacteriophage (0.1 PFU/bacteria).
3. Grow this culture at 37 °C for further 8 h.
4. Filtrate the crude bacteriophage suspension using the filters with 0.22 µm pore size.

#### 3.2 Determination of Bacteriophage Titer

1. Determine the titer of phage, expressed as plaque forming units (PFU), using the double layer agar technique [17].

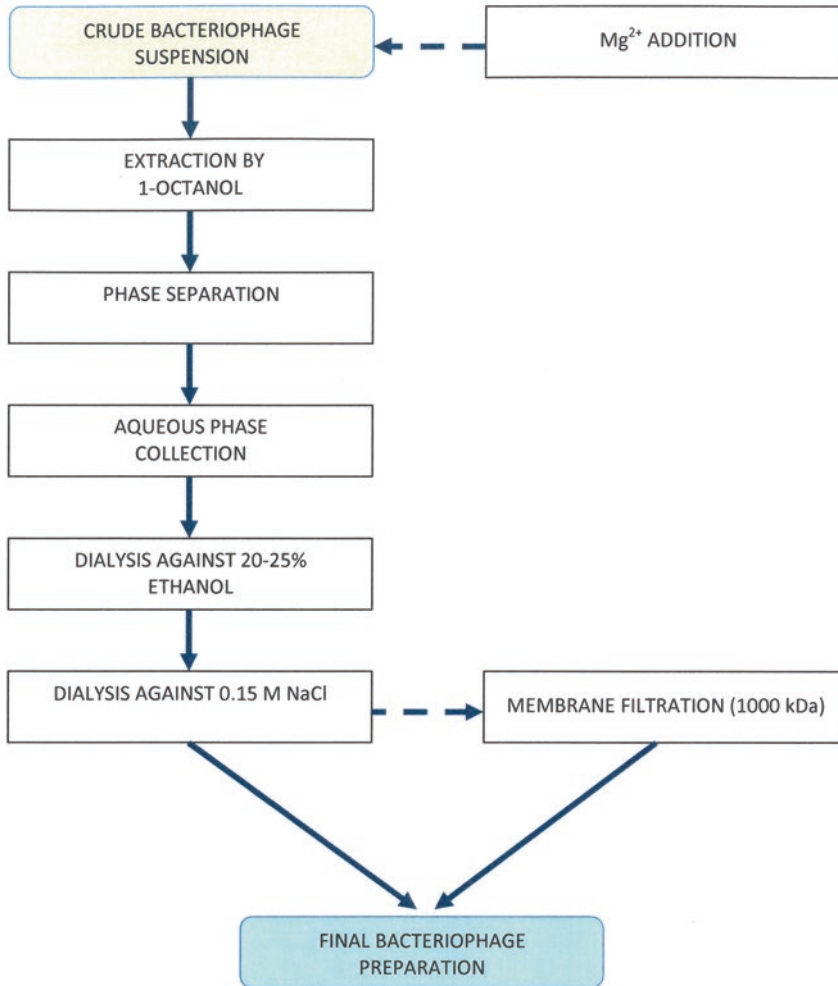
#### 3.3 General Purification Procedure

1. Supplement crude bacteriophage suspension by adding a 0.2 M solution of MgCl<sub>2</sub> to the final concentration of 0.02 M.
2. Incubate at 4 °C for 3–24 h.
3. Add the 10–20% of octanol (v/v) to the crude phage suspension and shake gently for 1–3 h at room temperature.
4. Cool the two-phase mixture to 4 °C for 1–3 h and separate using separatory funnel for liter-scale, or centrifugation at 4000 × g, 10 min for small samples.
5. Dialyze the collected aqueous phase using dialysis membrane (12–14 kDa), against 15–25% aqueous ethanol (5 × 4 h), and subsequently against aqueous 0.15 M NaCl sterile solution (4 × 4 h).
6. Optionally pass crude lysate through a Pellicon membrane (1000 kDa) EMD Millipore.
7. The fraction that does not pass through the membrane is the bacteriophage concentrate (Fig. 1).

#### 3.4 Determination of Endotoxins (Table 1)

##### 3.4.1 LAL Test

1. Use the end-point chromogenic Limulus Amebocyte Lysate test.
2. Quantification of endotoxins is achieved using the chromogenic technique—a standard curve, consisting of three measurement points, is performed for each determination.
3. Dilute samples serially with pyrogen-free water (supplied with the test) until the measurement is within the range of the standard curve.
4. Perform each data point in duplicate.
5. Maintain reaction conditions according to the manufacturer's recommendation [18].



**Fig. 1** Schematic illustration of purification protocol. *Dotted line* represents optional stages used for improved efficiency of the purification procedure

#### 3.4.2 EndoLISA Test

1. Mark the endotoxin levels of the T4 bacteriophage preparations after purification using EndoLISA according to the manufacturer's instructions.
2. Dilute the samples and standards with Binding Buffer prior to analysis.
3. Incubate samples on an assay plate overnight at room temperature with shaking.
4. Wash the plate with Washing Solution and add Assay Reagent.
5. Detect the fluorescent signal immediately in a fluorescence microplate reader (Synergy H4, BioTek, USA) [19, 20].

**Table 1**  
**Representative results of three different bacteriophages purification runs with 1-octanol extraction**

Entry	Bacteriophage strain	Titer of bacteriophage (10 <sup>9</sup> PFU/mL)		Endotoxin level (EU/mL) <sup>a</sup>		Relative endotoxin content (EU/10 <sup>9</sup> PFU)	
		Before <sup>b</sup>	After <sup>c</sup>	Before <sup>b</sup>	After <sup>c</sup>	Before <sup>b</sup>	After <sup>c</sup>
1	T4	110	50	34,000	0.9	310	0.02
2 <sup>d</sup>	T4	110	70	34,000	50	310	0.7
3	HAP1	6.0	2.0	60,000	14	10,000	7.0
4	F8	1.9	0.9	3800	8.0	2000	8.9

<sup>a</sup>Determined by chromogenic LAL test

<sup>b</sup>For crude bacterial lysate

<sup>c</sup>For bacterial lysate after purification but before ultrafiltration

<sup>d</sup>Phage culture not supplemented with MgCl<sub>2</sub> before extraction

## 4 Notes

1. The presence of magnesium ions increases the efficiency of pyrogen removal.
2. Other organic solvents use for extraction (1-butanol, olive oil, dichloromethane) also give good results nevertheless, we found 1-octanol to be the most practical due to easier phase separation. Another solvents such as olive oil or dichloromethane allowed for antibacterial activity preservation but they were not tested for endotoxin removal efficiency. 1-Butanol was tested for endotoxin removal and its efficiency is comparable with the use of 1-octanol. However, the solubility in water of 1-butanol is significantly higher than 1-octanol.
3. Determination of the endotoxin level directly after extraction is impossible, because the residual 1-octanol in the aqueous phase disable the LAL test. Thus, sequential dialyses against 15–25% ethyl alcohol and 0.15 M aqueous NaCl are employed.
4. The membrane filtration step (1000 kDa cut-off) is aimed to remove macromolecules originating from the culture medium and bacteria. The filtration also causes concentration of the bacteriophages but do not contribute to the removal of residual endotoxin (optionally).
5. The Limulus Amebocyte Lysate test and EndoLISA detect endotoxins with different sensitivity. In the obtained purified bacteriophages, the LAL test showed a higher level of endotoxin compared to the results received from EndoLISA.

6. During preparation of crude bacteriophage suspension the alternative method could be used to determine the number of bacteria. This method is using absorbance measurement 260/280 nm to estimate the number of bacteria in suspension [21].
7. The precise separation of the water phase is crucial for achieving low endotoxin level in the final product.

## References

1. Dofferhoff AS, Nijland JH, de Vries-Hospers HG, Mulder PO, Weits J, Bom VJ (1991) Effects of different types and combinations of antimicrobial agents on endotoxin release from gram-negative bacteria: an *in vitro* and *in vivo* study. *Scand J Infect Dis* 23:745–754
2. Daneshian M, Guenther A, Wendel A, Hartung T, von Aulock S (2006) In vitro pyrogen test for toxic or immunomodulatory drugs. *J Immunol Methods* 313:169–175
3. Bruttin A, Brussow H (2005) Human volunteers receiving *Escherichia coli* phage T4 orally: a safety test of phage therapy. *Antimicrob Agents Chemother* 49:2874–2878
4. Abedon ST, Kuhl SJ, Blasdel BG, Kutter EM (2011) Phage treatment of human infections. *Bacteriophage* 1:66–85
5. Gorbet MB, Sefton MV (2005) Endotoxin: the uninvited guest. *Biomaterials* 26:6811–6817
6. de Oliveira MP, Lopes AM, Mazzola PG, Rangel-Yagui C, Penna TC et al (2007) Methods of endotoxin removal from biological preparations: A review. *J Pharm Pharm Sci* 10:388–404
7. Petsch D, Anspach FB (2000) Endotoxin removal from protein solutions. *J Biotechnol* 76:97–119
8. Jang H, Kim HS, Moon SC, Lee YR, Yu KY, Lee BK et al (2009) Effect of protein concentration and detergent on endotoxin reduction by ultrafiltration. *BMB Rep* 42:462–466
9. Sato T, Shoji H, Koga N (2003) Endotoxin adsorption by polymyxin B immobilized fiber column in patients with systemic inflammatory response syndrome: the Japanese experience. *Ther Apher Dial* 7:252–258
10. Fiore GB, Soncini M, Vesentini S, Redaelli A (2010) Mechanisms of polymyxin B endotoxin removal from extracorporeal blood flow: hydrodynamics of sorption. *Contrib Nephrol* 167:55–64
11. Petsch D, Rantze E, Anspach FB (1998) Selective adsorption of endotoxin inside a polycationic network of flat-sheet microfiltration membranes. *J Mol Recognit* 11:222–230
12. Guo J, Meng F, Li X, Wang M, Wu Y, Jing X et al (2012) PEGylated click polypeptides synthesized by copper-free microwave-assisted thermal click polymerization for selective endotoxin removal from protein solutions. *Macromol Biosci* 12:533–546
13. Gao JP, Huang M, Li N, Wang PF, Chen HL, Xu QP (2011) Efficacy of a novel endotoxin adsorber polyvinylidene fluoride fiber immobilized with (L)-serine ligand on septic pigs. *J Zhejiang Univ Sci B* 12:264–272
14. Merabishvili M, Pirnay J-P, Verbeken G, Chanishvili N, Tediashvili M, Lashkhi N et al (2009) Quality-controlled small-scale production of a well-defined bacteriophage cocktail for use in human clinical trials. *PLoS One* 4:e4944
15. Szermer-Olearnik B, Boratyński J (2015) Removal of endotoxins from bacteriophage preparations by extraction with organic solvents. *PLoS One* 10(3): e0122672. doi:10.1371/journal.pone.0122672
16. Dabrowska K, Zembala M, Boratynski J, Switala-Jelen K, Wietrzyk J, Opolski A et al (2007) Hoc protein regulates the biological effects of T4 phage in mammals. *Arch Microbiol* 187:489–498
17. Adams MH (1959) *Bacteriophages*. Inter Science Publ, New York, USA, New York
18. Charles River Endosafe, Limulus Amebocyte Lysate – Endochrome. Available: [www.criver.com](http://www.criver.com).
19. Grallert H, Leopoldseder S, Schuett M, Kurze P, Buchberger B (2011) EndoLISA: a novel and reliable method for endotoxin detection. *Nature Methods* 8:i–v
20. Endolisa the world's first endotoxin detection system based on ELISA-technology. Available: <http://www.hyglos.de/en/products-services/products/elisa-based-endotoxin-detection-method.html>.
21. Szermer-Olearnik B, Sochocka M, Zwolińska K, Ciekot J, Czarny A, Szydzik J, Kowalski K, Boratyński J (2014) Comparison of microbiological and physicochemical methods for enumeration of microorganisms. *Postepy Hig Med Dosw* 68:1392–1396

# Chapter 11

## Fourier Transform Infrared Spectroscopy as a Tool in Analysis of *Proteus mirabilis* Endotoxins

Paulina Żarnowiec, Grzegorz Czerwonka, and Wiesław Kaca

### Abstract

Fourier transform infrared spectroscopy (FT-IR) was used to scan whole bacterial cells as well as lipopolysaccharides (LPSs, endotoxins) isolated from them. *Proteus mirabilis* cells, with chemically defined LPSs, served as a model for the ATR FT-IR method. The paper focuses on three steps of infrared spectroscopy: (1) sample preparation, (2) IR scanning, and (3) multivariate analysis of IR data (principal component analysis, PCA).

**Key words** Lipopolysaccharides, Fourier transform infrared spectroscopy, Multivariate analysis, ATR FT-IR spectroscopy, Principal component analysis

---

### 1 Introduction

Gram-negative bacterial endotoxins (lipopolysaccharides, LPS) are components of the outer membrane of the cell envelope and can be responsible for over-activation of the human immunological system and may lead to endotoxemia [1]. The positive outcomes of biological activity involve a humoral response and anti-LPS antibody generation. Anti-O-polysaccharide antibodies are useful for Gram-negative bacterial serotyping. Complete structures of LPS are important for understanding the biological activity of endotoxins.

Infrared spectroscopy is based on the principle that upon scanning with an infrared (IR) beam, the vibrational behavior of molecules in the sample changes energy quanta and modifying vibrational and rotational modes [2, 3]. Molecular bonds with an electric dipole moment within the sample will absorb the infrared radiation and vibrate in one of a number of ways, following patterns of either stretching, bending, deformation, or combination vibrations [2, 3]. Different chemical bonds absorb IR at different wavenumber ranges regardless of other structures in the molecule, and spectral peaks are derived from the absorption of bond vibrational energy changes in the IR region [3]. These vibrations can

then be correlated directly to the biochemical makeup of the sample, and the resultant infrared absorption spectrum provides a specific fingerprint that reflects the structure and composition of the sample. Infrared frequencies ( $4000\text{--}600\text{ cm}^{-1}$ ) were used due to the characteristic absorbance frequencies of organic molecules. Primary molecular vibrations are often divided into five windows, reflecting the predominant types of recorded class of organic components. The fatty acid region is  $2800\text{--}3000\text{ cm}^{-1}$ , the amide I and amide II (amide I/II) region is  $1500\text{--}1700\text{ cm}^{-1}$ , the mixed region is  $1200\text{--}1500\text{ cm}^{-1}$ , the wavenumber region  $1200\text{--}900\text{ cm}^{-1}$  is associated with the stretching vibrations of polysaccharides, and the  $600\text{--}900\text{ cm}^{-1}$  region is a true fingerprint region [2]. The principles of IR methods are presented in our and another recently published reviews [3, 4].

IR has been used to define the lamellar structures of lipid A, interactions with lysozymes and  $\text{Mg}^{2+}$ , and water content in LPS spectra [5, 6]. IR spectroscopy offers a direct view of the presence of LPS on bacterial cells, without preprocessing. This paper presents the IR spectra of *Proteus mirabilis* S1959 (O3) as well as of their two R mutant cells. The Ra type (strain R110) has its O-specific part deleted, and the Re type (R45) is deprived of its core oligosaccharide. Thus, they possess lipooligosaccharides (LOS). The acquisition of spectra and their mathematical analysis are given for whole *P. mirabilis* cells as well as for isolated LPS. IR spectroscopy in ATR mode and analysis were run in the following steps: (1) acquisition of IR spectra, (2) computer-based preprocessing, (3) mathematical analysis of preprocessed spectra, and (4) conclusions based on comparison with control samples.

---

## 2 Materials

1. *Proteus mirabilis* strains S1959, R110, and R45 can be obtained from the Institute of Microbiology and Immunology, University of Lodz, Lodz, Poland.
2. Ethanol (70% solution).

### 2.1 Equipment

1. Infrared spectrometer—Spotlight 400 FT-IR Imaging System (PerkinElmer).
2. Microcentrifuge.
3. Bacterial incubator.

### 2.2 Software

1. Spectrum One (PerkinElmer, Waltham, MA, USA) (*see Note 1*).
2. Statistica 12 (StatSoft Inc., USA).

### 3 Methods

#### 3.1 Sample Preparation

1. Cultivate the bacteria on Lysogeny broth (LB) plates at 37 °C for 18 h (*see Note 2*).  
Prepare samples were prepared following the steps listed in one of the options given below.
2. Transfer a single bacterial colony by a sterile plastic loop onto the crystal of the ATR device and leave at 18 °C for drying. Or scrape one loop of bacteria from the agar plate, suspend it in 100 µL of sterile deionized water, place 30 µL of the bacterial suspension on the crystal, and allow it to dry [7]. In the case of freeze-dried bacterial mass and LPSs, the water evaporation step is omitted.
3. For LPS samples, cultivate bacterial strains in nutrient broth supplemented with 1% glucose.
4. Harvest the bacterial cells at the end of logarithmic phase of growth, kill them by addition of 1% phenol (final concentration), and centrifuge ( $3000 \times g$ , 20 min, 10 °C) three times with distilled water, and then freeze-dry.
5. Extract smooth *P. mirabilis* S1959 (O3) LPS from freeze-dried bacterial mass by the phenol–water method [8].
6. Mix 20 g of freeze-dried bacterial cells with 600 mL distilled water, and immerse the glass container in a 65–67 °C water bath, for 30 min, with mixing till the suspension is homogenous.
7. Add 300 mL 90% phenol (from freshly prepared distilled crystalline phenol) and continue the extraction for 30 min at 65 °C.
8. Cool the mixture in an ice water bath approximately to 10 °C, and then centrifuge it for 30 min,  $300 \times g$ .
9. Separate the aqueous milky upper phase with the crude LPS.
10. Repeat extraction two times with sediment (phenol phase).
11. Combine all three water phases in a dialysis bag, and dialyze it in a cool room against tap water for 2 days and then against distilled water for another 2 days.
12. Concentrate dialyzed material by vacuum distillation, and then freeze-dry. The sample represents the crude LPS which may contain smaller amounts of protein and nucleic acids, which can be removed by enzymatic cleavage (*see below*).

Rough Ra- and Re-type LOS were obtained from strains R110 and R45, respectively, by the Galanos method (using phenol, chloroform, and light petroleum, 2:5:8 by vol., PCP) [9]:

1. To 10 g freeze-dried bacterial cells, add 200 mL PCP, and stir at 5–10 °C for 60 min.
2. Separate the cells as sediment by centrifugation for 15 min ( $4800 \times g$ ).
3. Repeat extraction of the sediment.
4. Combine the supernatants and evaporate chloroform and light petroleum by rotary evaporation (fume hood!).
5. Add to the remaining phenol phase dropwise distilled water, with gentle stirring until white LPS precipitation occurs.
6. Centrifuge in a refrigerated centrifuge at  $3000 \times g$  for 30 min, wash the sediment (= LPS) two times with acetone, and finally resolve it in distilled water and freeze-dry.
7. Purify aqueous 1% solutions of crude LPS and LOS from nucleic acids and proteins by ultracentrifugation (three times at  $105,000 \times g$ , 4 °C, 120 min).
8. For final LPS purification, perform treatment with nucleases [10], i.e., 2 mg/g LPS RNase and DNase (Merck) in 10 mM Tris–HCl buffer (pH 7.6) for 18 h at room temperature. Add one drop of toluene to prevent bacterial growth.
9. After overnight dialysis against distilled water, precipitate the LPS by ultracentrifugation ( $105,000 \times g$ , 4 °C, 120 min) and freeze-dry. Pure LPS/LOS should contain less than 2% proteins and only traces of nucleic acids) (*see Note 3*).

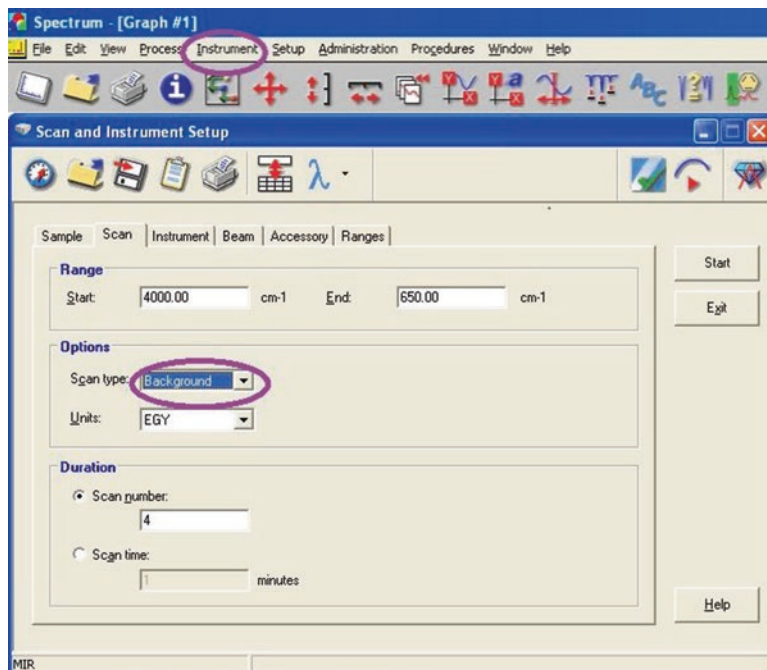
### 3.2 Acquisition of ATR FT-IR Spectra

1. Open the instrument-operating software by double-clicking the “Spectrum” icon.
2. Open instrumental settings.
3. Check the path to the location where files are to be saved.
4. Clean the ATR crystal with 70% ethanol or isopropanol and ensure the crystal is dry before background acquisition (*see Notes 4 and 5*).
5. Locate and click on “Instrument” in the panel. Select “Scan” and record a background spectrum (*see Note 6*) (Fig. 1).

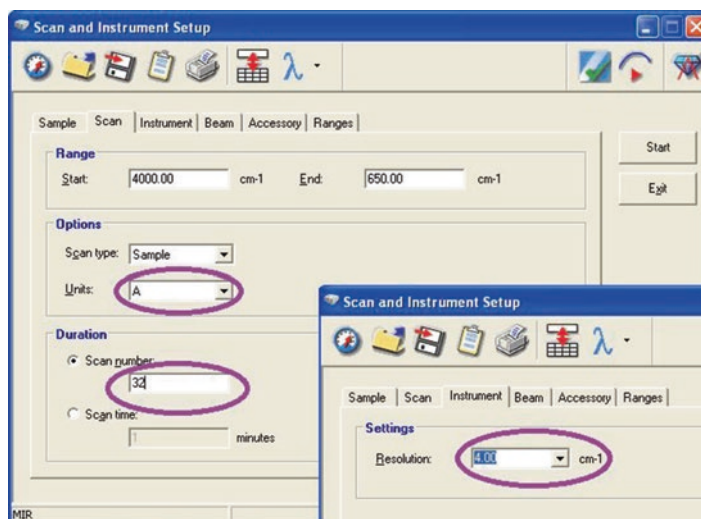
Prepare samples by following the steps listed in one of the options given below:

1. Place a colony of bacteria (*see Notes 7–9*) or a freeze-dried sample on the crystal of the ATR device and press with a pressure applicator [7, 11, 12], or place 30  $\mu\text{L}$  of a bacterial suspension on the crystal and allow to dry [13].
2. Acquire a sample spectrum with a resolution of 4  $\text{cm}^{-1}$  and 32 or 64 co-added scans. It is common to collect multiple technical and biological replicate samples; three biological replicates and three technical replicates are recommended (*see Note 10*) [11, 14] (Figs. 2 and 8a).





**Fig. 1** Background acquisition, screenshot from PerkinElmer's Spectrum FT-IR software



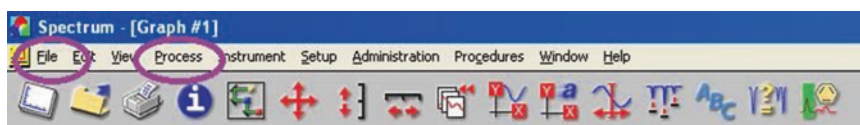
**Fig. 2** Sample acquisition, screenshot from PerkinElmer's Spectrum FT-IR software

### 3.3 Data Preprocessing

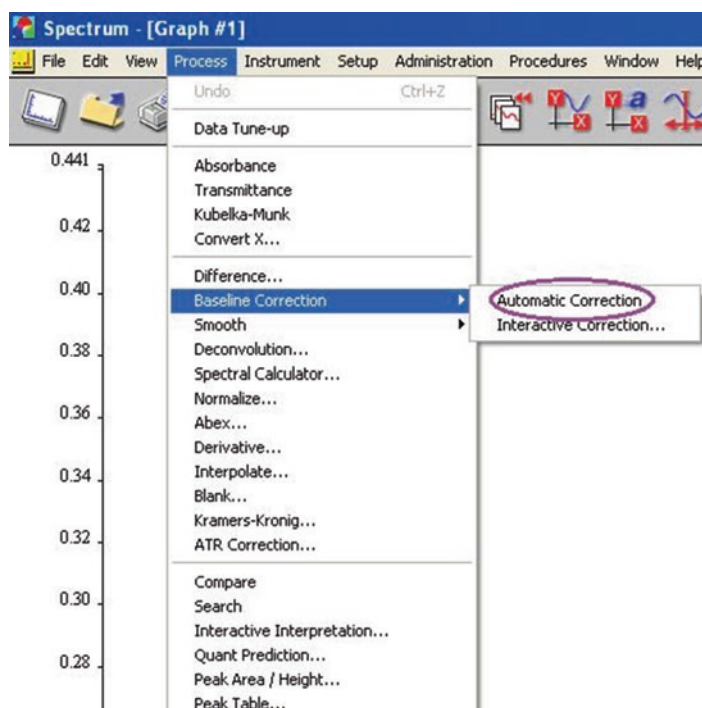
Preprocessing of spectra involves different options at each step; however, there are combinations of these steps that may be more or less appropriate than others, depending on the sample type, instrumentation setup, noise level, need for visualization of spectra, personal preferences, and classification performance, among other factors [3, 4].

#### 3.3.1 Preprocessing Using Spectrum One Software

1. Start “Spectrum” and click on “File...” and select “Open...” dataset (Fig. 3).
2. Locate and click “Process” in the top panel.
3. Locate and click “Baseline Correction → Automatic...” (see **Note 11**) (Fig. 4).
4. Locate and click on “Smooth” in the panel. Select “User selected smooth...” and choose the Savitzky–Golay algorithm and 9 points (see **Note 12**) (Fig. 5).



**Fig. 3** Preprocessing acquisition, screenshot from PerkinElmer’s Spectrum FT-IR software



**Fig. 4** Baseline correction, screenshot from PerkinElmer’s Spectrum FT-IR software

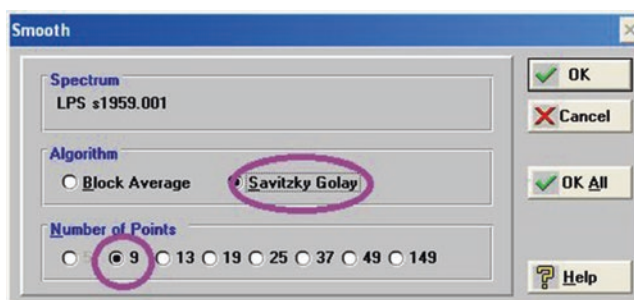


Fig. 5 Smooth, screenshot from PerkinElmer's Spectrum FT-IR software

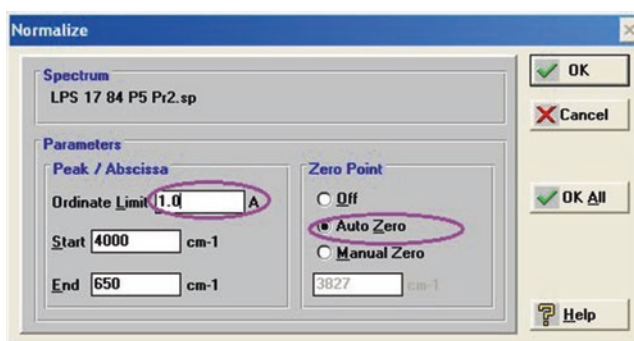


Fig. 6 Normalization, screenshot from PerkinElmer's Spectrum FT-IR software

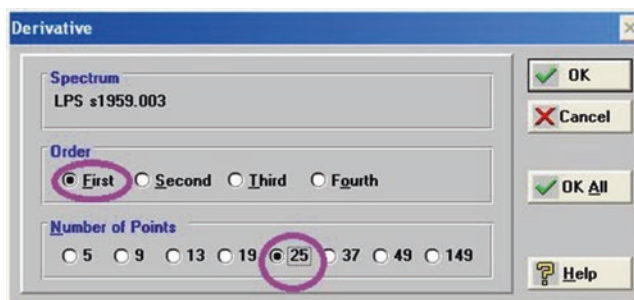
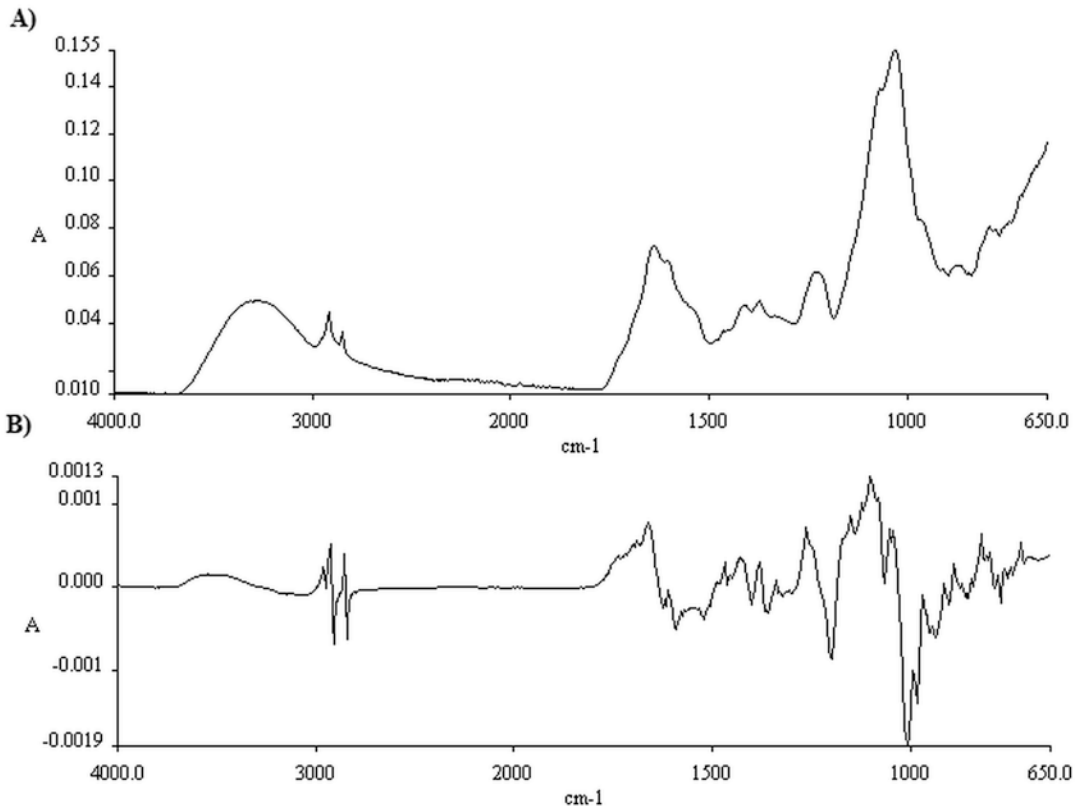


Fig. 7 Derivative, screenshot from PerkinElmer's Spectrum FT-IR software

5. Locate and click “Normalization” in the panel. Select “Auto zero” from the “Zero point” pop-up box for ordinate limit 1 (see Note 13) (Fig. 6).
6. Locate “Derivative” and perform Savitzky–Golay differentiation for the first derivative (most often used; second differentiation is also common) for 15 points (Fig. 7).
7. Open “File...” and “Save as...” to save normalized first derivative spectral data from the experiment to ASCII (Fig. 8b).



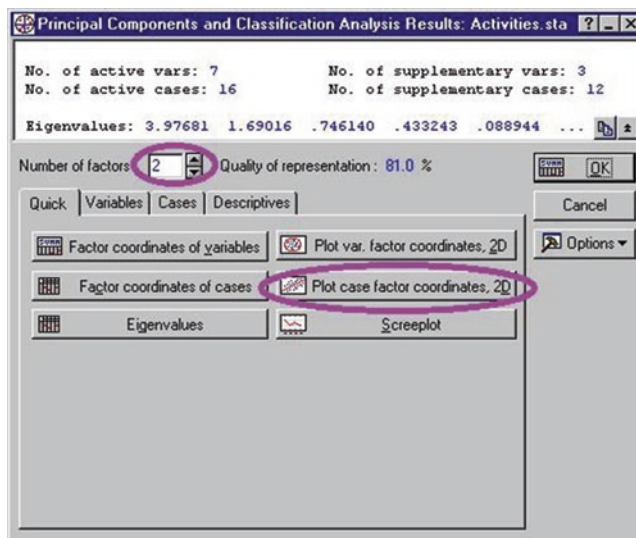
**Fig. 8** IR absorbance spectra for a *P. mirabilis* S1959 colony in the spectral range of 4000–650  $\text{cm}^{-1}$ . (A) Original absorbance spectrum; (B) first derivative

### 3.4 Multivariate Analysis

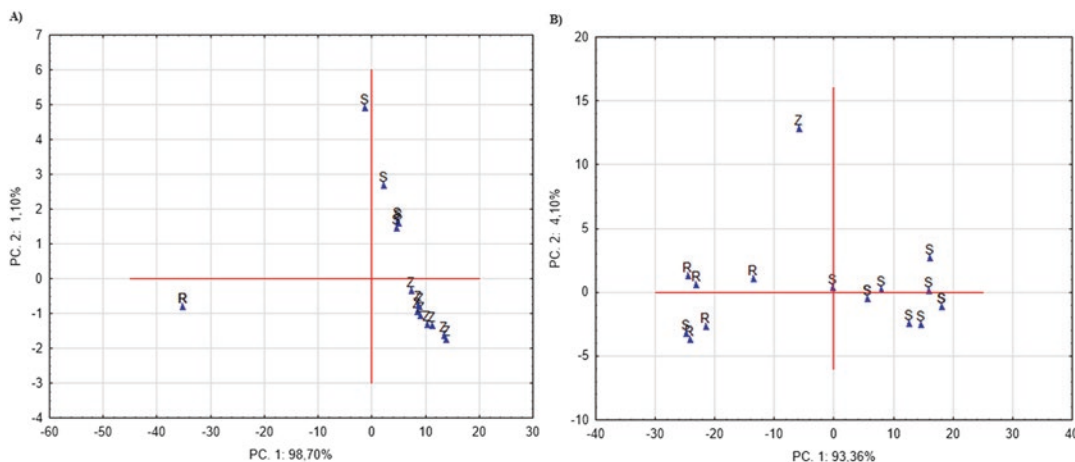
Choose a data analysis procedure appropriate to your analytical goal; this may be, e.g., clustering or principal component analysis (unsupervised classification) [7]:

1. Start STATISTICA, click on “Load...,” and select your dataset.
2. Locate and click on “Statistic” in the panel. Select “Multivariate...” and choose “Principal component analysis and classification analysis.”
3. Select the spectral range “1200–900  $\text{cm}^{-1}$ ” in the variables (*see Note 14*).
4. Click “OK” to perform initial computations, and then in the “Results” dialog box set the “Number of factors” to 2 (*see Note 15*) (Fig. 9).
5. Next, click “Plot case factor coordinates 2D” to display the results of observations (cases) (Fig. 10).

The presented PCA diagram of IR spectra (polysaccharide region 1200–900  $\text{cm}^{-1}$ ) shows the clustering of freeze-dried cells



**Fig. 9** “Principal component analysis and classification analysis,” screenshot from STATISTICA, StatSoft software



**Fig. 10** Diagram generated by PCA obtained from the 1200–900  $\text{cm}^{-1}$  spectral region (window 4—polysaccharides) (A) freeze-dried bacterial mass and (B) LPS extracted from three *P. mirabilis* strains: S1959 (S), R45 (Z), and R110 (R)

as well as of the isolated LPSs based on polysaccharide content. Smooth *P. mirabilis* S1959 (O3) are clustered away from the two R mutants lacking the O-polysaccharide part (Ra type, strain R110) or the core oligosaccharide (Re, strain R45). Differences inside the R and S groups may be due to natural preparation heterogeneity and the content of contaminants (nucleic acids, proteins, cations). This indicates ATR FT-IR sensitivity to recorded fingerprints of particular LPS sample preparations.

---

## 4 Notes

1. Spectral acquisition software is normally provided by the instrument manufacturer. Most of such programs also provide a number of preprocessing, and sometimes more advanced, data analysis options.
2. Throughout the experiment, it is advisable to use strictly controlled bacterial culture conditions, with the same type of nutrients. ATR FT-IR spectra of analyzed isolates should be acquired from an overnight subculture on an agar medium recommended for a given strain exactly after 18 h of growth at 37 °C (unless the analyzed strain has different culture conditions) to avoid spectral interferences due to colony age [7].
3. Even the same LPS IR spectra might differ due to the preparation method, LPSs heterogeneity, or traces of contaminants. Highly pure LPS preparation methods were described [15].
4. It is very important that a background spectrum is recorded for each sample! Also, a background spectrum should be taken if atmospheric changes occur (e.g., if a door has been suddenly opened).
5. The crystal surface must not be scratched under any circumstances! It is expected that some residual sample will be left. Isopropanol will remove most of the remaining residual film before and after each trial.
6. To acquire a background spectrum, the IR source should not be in contact with the sample, and it should be open to the surrounding environment.
7. The ATR crystal should be completely covered by the sample, and the minimum sample thickness should be three to four times the depth of penetration to ensure that there is no interference from the substrate.
8. The same pressure should be applied to all samples.
9. Intimate contact of the sample with the crystal is a very important parameter for ATR FT-IR analysis.
10. After the spectral acquisition of each sample, the crystal should be washed with isopropanol or 70% ethanol; the crystal should be left to dry.
11. Baseline should be corrected to zero in order to eliminate any differences between spectra due to shifts in baseline [3, 4].
12. Smoothing reduces instrumental noise and increases information content in the spectrum using one of the following algorithms: Savitzky–Golay de-noising [7, 16], PCA noise reduction, or minimum noise fraction [17].

13. Data can be normalized using MinMax [7] or vector normalization [18]. Scale the variables: this could be done by standardization (normalization of variables to zero mean and unit s.d.) or by normalization to a 0–1 range.
14. Wavenumbers from 1200 to 900  $\text{cm}^{-1}$  are characteristic for the polysaccharide region in the infrared spectrum and are associated with IR frequencies of O-specific (lipopolysaccharide) antigens from the bacterial cell envelope [7, 19–21].
15. As a result, “Quality of representation” should be computed as more than 80%.

---

## Acknowledgments

This study was supported by grant from the National Science Center, Poland granted on the basis of decision number DEC-2012/07/N/NZ6/04118 and grant no. 612 427 from the Jan Kochanowski University. Some of the experiments were run on apparatus purchased with European Union grant 307 under 2.2 Innovation Industry.

## References

1. Brunn GJ, Platt JL (2006) The etiology of sepsis: turned inside out. *Trends Mol Med* 12:10–16
2. Naumann D (2000) Infrared spectroscopy in microbiology. In: Meyers RA (ed) *Encyclopedia of analytical chemistry: applications, theory, and instrumentation*. John Wiley & Sons Ltd., Chichester, pp 102–131
3. Żarnowiec P, Lechowicz Ł, Czerwonka G, Kaca W (2015) Fourier Transform Infrared Spectroscopy (FTIR) as a tool for the identification and differentiation of pathogenic bacteria. *Curr Med Chem* 14:1710–1718
4. Davis R, Mauer L (2010) Fourier transform infrared (FT-IR) spectroscopy: a rapid tool for detection and analysis of foodborne pathogenic bacteria. *Curr Res Technol Educ Top Appl Microbiol Microb Biotechnol II*:1582–1594
5. Brandenburg K, Seydel U (1988) Orientation measurements on membrane systems made from lipopolysaccharides and free lipid A by FT-IR spectroscopy. *Eur Biophys J* 16:83–94
6. Seydel U, Koch C, Brandenburg K (1997) Investigations into lysozyme-endotoxin interactions with FT-IR spectroscopy and X-ray diffraction. *Spectrosc Biol Mol Modem Trends*:363–364
7. Zarnowiec P, Mizera A, Chrapek M et al (2016) Chemometric analysis of attenuated total reflectance infrared spectra of proteus mirabilis strains with defined structures of LPS. *Innate Immun* 22:325–335
8. Westphal O, Jann K, Himmelspach K (1983) Chemistry and immunochemistry of bacterial lipopolysaccharides as cell wall antigens and endotoxins. *Prog Allergy* 33:9–39
9. Galanos C, Luderitc O (1993) Isolation and precipitation of R-form of lipopolysaccharides: further applications of the PCP method. In: BeMiller J, Whistler R, Shaw D (eds) *Methods carbohydr. Chem*. John Wiley & Sons, Inc., pp 11–18
10. Gmeiner J (1975) The isolation of two different lipopolysaccharide fractions from various *Proteus mirabilis* strains. *Eur J Biochem* 62:621–626
11. Sousa C, Silva L, Grosso F et al (2014) Development of a FTIR-ATR based model for typing clinically relevant *Acinetobacter baumannii* clones belonging to ST98, ST103, ST208 and ST218. *J Photochem Photobiol B Biol* 133:108–114
12. Winder CL, Goodacre R (2004) Comparison of diffuse-reflectance absorbance and attenuated total reflectance FT-IR for the discrimination of bacteria. *Analyst* 129:1118–1122

13. Nagib S, Rau J, Sammra O et al (2014) Identification of *Trueperella pyogenes* isolated from bovine mastitis by fourier transform infrared spectroscopy. PLoS One:9–e104654
14. Muhamadali H, Weaver D, Subaihi A et al (2015) Chicken, beams, and *Campylobacter*: rapid differentiation of foodborne bacteria via vibrational spectroscopy and MALDI-mass spectrometry. Analyst 141:111–122
15. Pupo E (2011) Isolation of smooth-type lipopolysaccharides to electrophoretic homogeneity. In: Holst O (ed) Microbial toxins: methods and protocols, Methods in molecular biology, vol 739. Springer New York, Totowa, NJ, pp 101–112
16. Brandes Ammann A, Brandl H (2011) Detection and differentiation of bacterial spores in a mineral matrix by Fourier transform infrared spectroscopy (FTIR) and chemometrical data treatment. BMC Biophys 4:14
17. Baker MJ, Trevisan J, Bassan P et al (2014) Using Fourier transform IR spectroscopy to analyze biological materials. Nat Protoc 9:1771–1791
18. Bosch A, Miñán A, Vescina C et al (2008) Fourier transform infrared spectroscopy for rapid identification of nonfermenting gram-negative bacteria isolated from sputum samples from cystic fibrosis patients. J Clin Microbiol 46:2535–2546
19. Baldauf NA, Rodriguez-Romo LA, Männig A et al (2007) Effect of selective growth media on the differentiation of *Salmonella enterica* serovars by Fourier-transform mid-Infrared spectroscopy. J Microbiol Methods 68:106–114
20. Al-Qadiri HM, Lin M, Cavinato AG, Rasco BA (2006) Fourier transform infrared spectroscopy, detection and identification of *Escherichia coli* O157:H7 and alicyclobacillus strains in apple juice. Int J Food Microbiol 111:73–80
21. Kim S, Reuhs BL, Mauer LJ (2005) Use of Fourier transform infrared spectra of crude bacterial lipopolysaccharides and chemometrics for differentiation of *Salmonella enterica* serotypes. J Appl Microbiol 99: 411–417



## Laser Interferometry Method as a Novel Tool in Endotoxins Research

Michał Arabski and Sławomir Wąsik

### Abstract

Optical properties of chemical substances are widely used at present for assays thereof in a variety of scientific disciplines. One of the measurement techniques applied in physical sciences, with a potential for novel applications in biology, is laser interferometry. This method enables to record the diffusion properties of chemical substances. Here we describe the novel application of laser interferometry in chitosan interactions with lipopolysaccharide by detection of colistin diffusion. The proposed model could be used in simple measurements of polymer interactions with endotoxins and/or biological active compounds, like antibiotics.

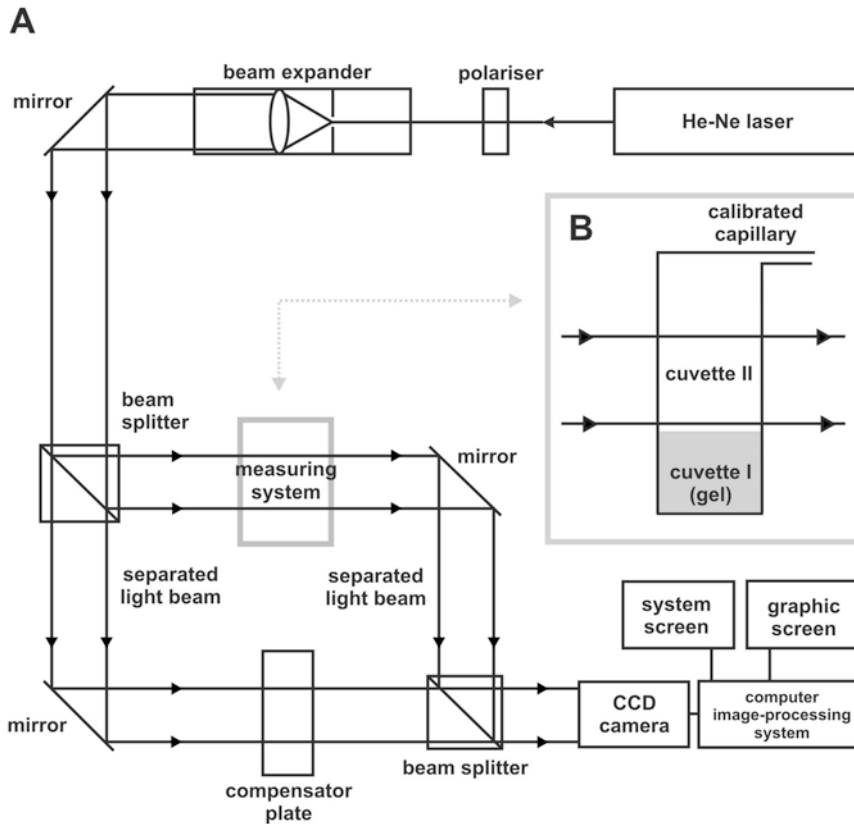
**Key words** Laser interferometry, Lipopolysaccharide, Chitosan

---

### 1 Introduction

Laser interferometry, based on the phenomenon of wave interference, enables quantitative substance assays by means of measurement of the difference between light refractive indexes for the studied and control substances. Properties of laser-generated radiation, i.e., low beam divergence, narrow spectral band, and high degree of coherence, positively influence the assay sensitivity.

Figure 1a depicts the interferometric setup used in our studies, which is basically suited for recording the refractive index modification inside the diffusion cell (Fig. 1b). A beam of monochromatic light ( $\lambda = 632.8 \text{ nm}$ ) is split into two beams, one of which passes through the diffusion cell. The other beam is directed by the mirror onto a compensator plate. The interferograms, which appear due to the interference of the two beams are recorded by a CCD camera and presented on a graphic screen (inserts in Fig. 3). A computer image-processing system, completed with a dedicated software, enables a mathematical analysis of interferograms shown on the system screen. The changes in solution concentration in the system involve variations  $\Delta n(x,t)$  of their refractive index.



**Fig. 1** Setup of the laser interferometry system used in this study (a) with diffusion cell (b)

The correlation coefficient  $a$  between concentration and refractive index of water solutions is refractometrically determined. The quantity of  $C(x,t)$  is calculated according to the formula

$$C(x,t) = C_0 + a\Delta n(x,t) \quad (1)$$

in which  $C_0$  is the initial substance concentration.

Recording the interferometric images with a given time step  $\Delta t$ , one can reconstruct the concentration profiles for different times. Moreover, the transport parameters, such as substance quantity  $N$ , substance flux  $J_s$ , the membrane permeability coefficient  $\omega_m$ , and the substance diffusion coefficient  $D$  after time  $t$  and in successive time intervals  $\Delta t$ , can be determined. These parameters are presented in Table 1.

The possibility of real-time diffusion analysis between unmixed systems and an analysis based on the change of the solution's refractive index favors the application of laser interferometry as analysis of biomolecular interactions based on the phenomenon of diffusion, for example, lipopolysaccharides (LPS) with antibiotics

**Table 1**  
**Transport parameters which can be determined by laser interferometry**

Transport parameter	Formula	
	After time $t$	In the time interval $\Delta t$ of number $i$
The amount of the transported substance	$N = S \int_0^{\delta} C_1(x,t) dx$	$N = S \int_0^{\delta'} C(x,t+i\Delta t) dx - S \int_0^{\delta} C(x,t+(i-1)\Delta t) dx$
The substance flux	$J_S = \frac{\int_0^{\delta} C(x,t) dx}{t}$	$J_S = \frac{\int_0^{\delta'} C(x,t+i\Delta t) dx - \int_0^{\delta} C(x,t+(i-1)\Delta t) dx}{\Delta t}$
Membrane permeability coefficient	$\omega_m = \frac{\int_0^{\delta'} C(x,t) dx}{RT [C_2(x=0,t) - C_1(x=0,t)] t}$	$\omega_m = \frac{\int_0^{\delta'} C(x,i\Delta t) dx - \int_0^{\delta} C_1(x,(i-1)\Delta t) dx}{RT [C_2(x=0,i\Delta t) - C_1(x=0,i\Delta t)] \Delta t}$
Diffusion coefficient	$D = \frac{\delta^2(t)}{4t(\operatorname{erfc}^{-1}(k))^2}$	$D = \frac{\delta^2(i\Delta t) - \delta^2((i-1)\Delta t)}{4\Delta t(\operatorname{erfc}^{-1}(k))^2}$

$C_1(x=0,t)$  and  $C_2(x=0,t)$  are the concentrations of the solutions on the membrane surfaces at time  $t$ ,  $\operatorname{erfc}$  is complementary error function defined as

$$\operatorname{erfc}(k) = \frac{2}{\sqrt{\pi}} \int_k^{\infty} e^{-\eta^2} d\eta \quad (5)$$

or polymers, analysis of antibiotics diffusion through bacterial biofilm, as well as biofilm degradation by bacteriophages [1–6].

In this study, the methodology focuses on laser interferometry measurements of chitosan interaction with LPS of *Pseudomonas aeruginosa* O10 in the presence of colistin.

## 2 Materials

Prepare all solutions using ultrapure water at room temperature by mixing for 2 h.

1. Laser interferometry system as depicted in Fig. 1.
2. Dissolve 0.5 g of chitosan in 25 mL of aqueous acetic acid (2% v/v, pH 3.0) and leave overnight at room temperature with continuous mechanical stirring to obtain a 2% (w/v) solution (*see Note 1*).
3. Dissolve 1 mg of LPS (in this study from *P. aeruginosa* O10) in 10 mL of water by sonication (20 kHz, 40%, 30 s) and mechanical stirring to obtain the LPS solution at 100  $\mu\text{g}/\text{mL}$ .

### 3 Methods

#### 3.1 Chitosan Hydrogel

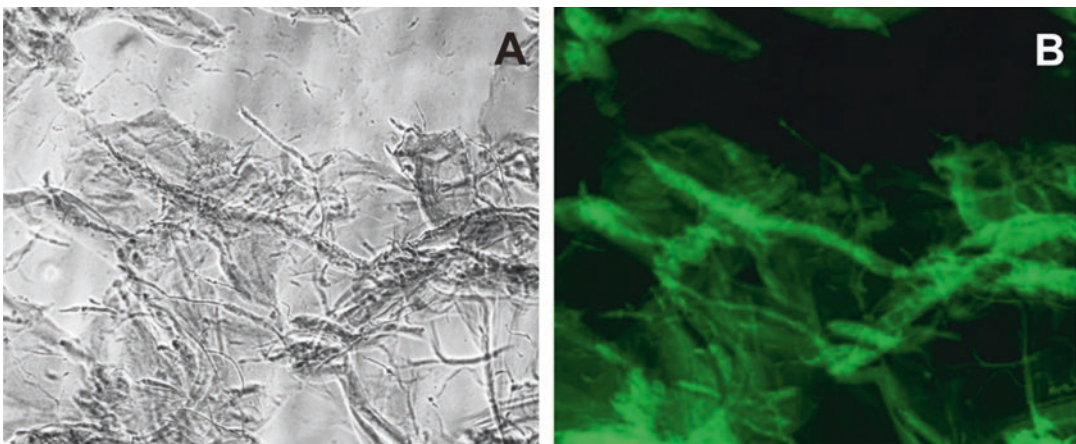
1. Take two glass beakers (each with capacity 250 mL) and prepare chitosan hydrogel particles in each of them: using a syringe, inject 5 mL of 2% chitosan solution in aqueous acetic acid drop by drop (10  $\mu$ L) to 50 mL of 2% NaOH water with continuous mechanical stirring, and leave for 3 h at room temperature (25 °C).
2. Centrifuge (15 min, 900  $\times g$ ) the hydrogel particles at room temperature (*see Note 2*).
3. Wash the chitosan hydrogel particle precipitates six times in 100 mL of water with centrifugation (15 min, 900  $\times g$ ) until a neutral pH is obtained.

#### 3.2 Incubation of Chitosan Hydrogel with LPS and/or Colistin

1. Incubate the washed chitosan hydrogel particle precipitates with 100  $\mu$ g/mL LPS in 10 mL of water for 18 h at 4 °C.
2. Wash the chitosan hydrogel particles three times in 20 mL of water with centrifugation (15 min, 2100  $\times g$ ).
3. Dissolve 2 mg of colistin sodium methanesulfonate in 1 mL of water by mechanical stirring.
4. Incubate the washed precipitates of chitosan hydrogel particles with 2 mg of colistin in 1 mL of water for 18 h at room temperature.

#### 3.3 Preparation of Agarose Gel with Colistin

1. Mix 1 mL of colistin/hydrogel suspension (pre-incubated with LPS or free from LPS) with 1 mL of 1.5% low melting point agarose gel at 40 °C by pipetting up and down, and add it to the bottom of the cuvette as element of the diffusion cell (Fig. 2; cuvette I).

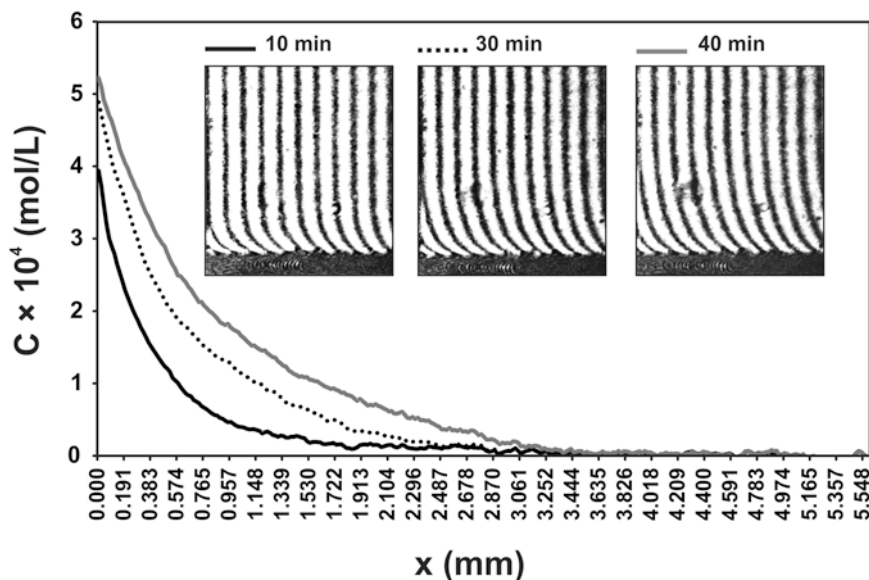


**Fig. 2** Images of chitosan hydrogel taken using optical (a) and fluorescence (b) microscopy (100 $\times$  magnification)

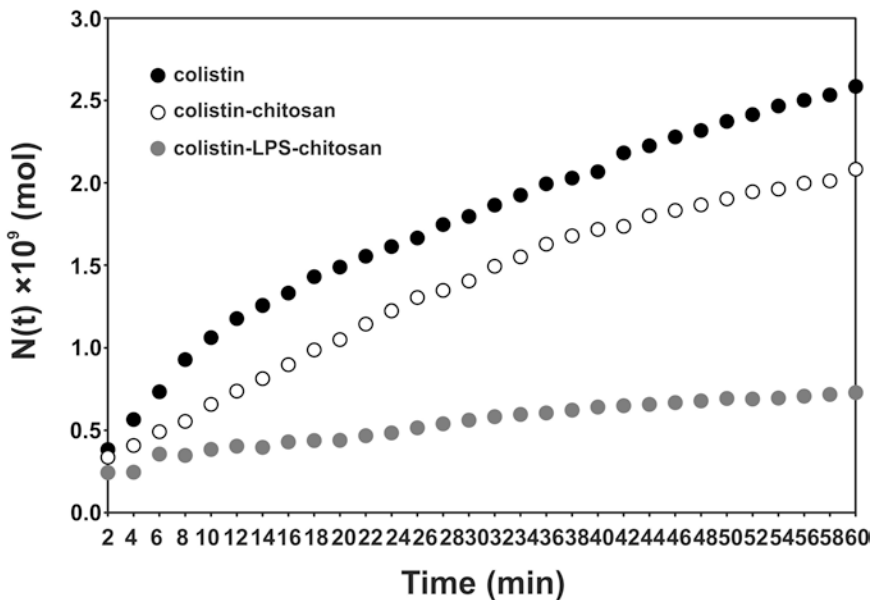
2. As control for laser interferometry analysis, prepare a third mixture 1 mL of colistin (2 mg/mL) with 1 mL of 1.5% low melting point agarose gel at 40 °C (*see Note 3*).
3. After 30 min (gelling process at room temperature), the samples are ready for analysis of free colistin diffusion from LMP agarose (in cuvette I) to water (in cuvette II, Fig. 2) by laser interferometry (*see Note 4*).

### 3.4 Laser Interferometry

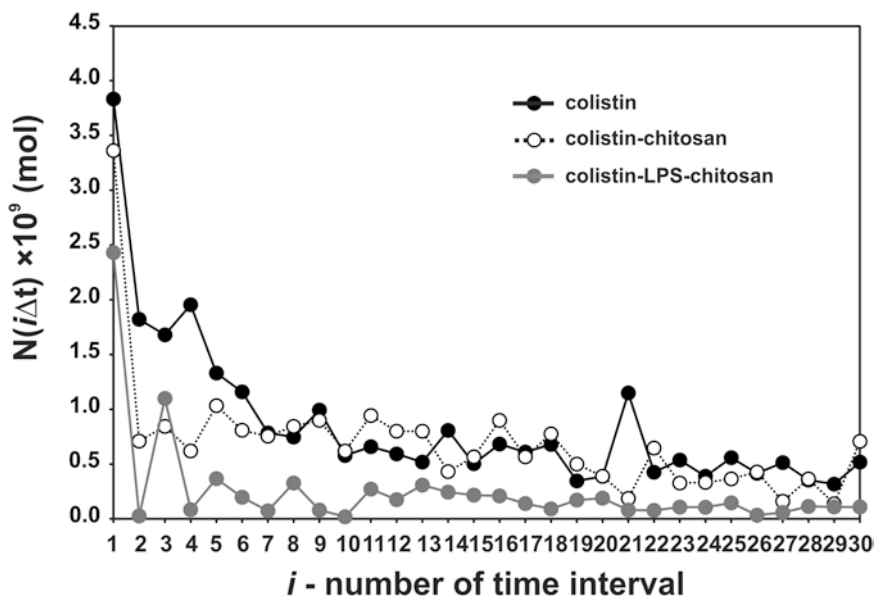
1. The prepared samples are placed in one of the arms of the interferometer (diffusion cell), and the interferometric images (time steps  $\Delta t = 120$  s) are recorded. Based on a computer analysis of the recorded interferograms, the spatio-temporal concentration distribution  $C(x,t)$  (i.e., concentration profile) of colistin is determined.
2. The selected transport parameters of colistin diffused to the water are calculated based on the obtained concentration profiles according the formulas presented in Table 1 (*see Note 5*). Figures 3, 4, 5, 6, and 7 show the diffusion parameters calculated for colistin released from agarose after pre-incubation with chitosan or chitosan-LPS complex. Generally, a higher amount of colistin released from agarose with an immobilized chitosan hydrogel in comparison to chitosan-LPS complexes indicates that LPS interacts with chitosan.



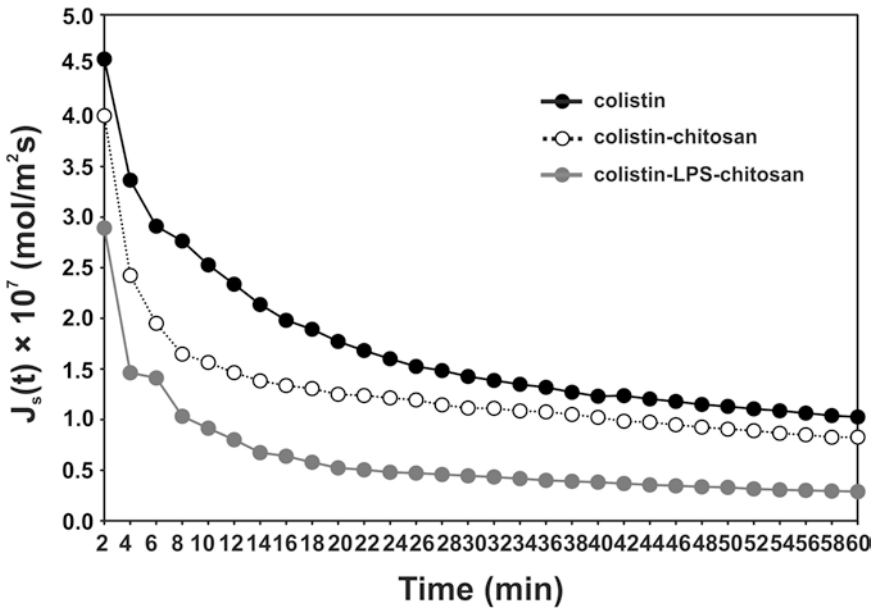
**Fig. 3** The concentration profiles of colistin released from 0.75% agarose gel after 10, 30, and 60 min, calculated on the base of interferograms using laser interferometry. Near the gel-water interface, the interferometric fringes are bent from a straight line, which means that the colistin was released from the gel to the water phase. The region of fringes curvature expands with time indicating that the thickness of concentration boundary layers (CBL) and the amount of released substance increase with time



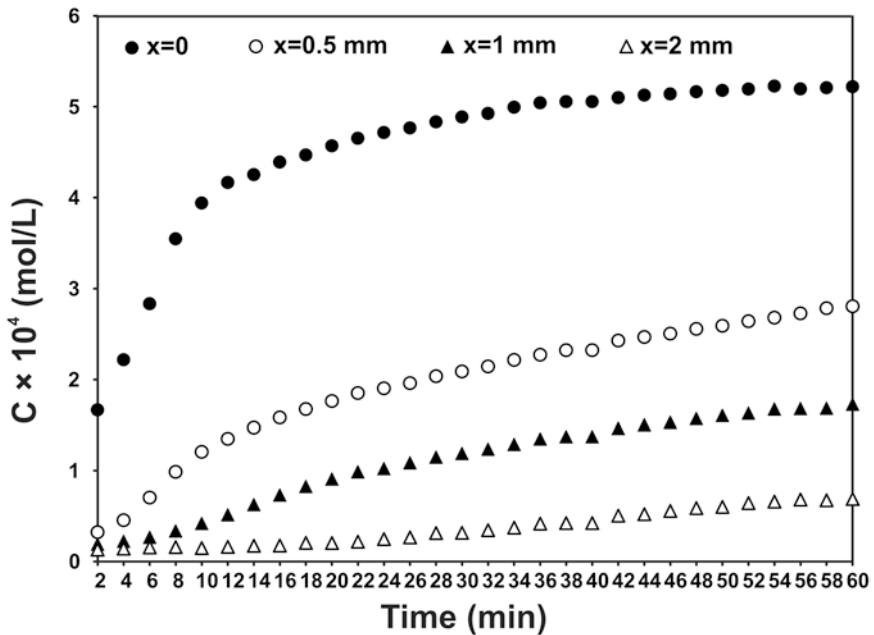
**Fig. 4** The amount (mol) of colistin alone (●), pre-incubated with chitosan (○) or LPS-chitosan complexes (●), released from 0.75% agarose measured by laser interferometry. The higher values (mol) of released colistin were observed after pre-incubation with chitosan ( $2.01 \times 10^{-9}$ ) than with chitosan-LPS complexes ( $7.29 \times 10^{-10}$ ) after 60 min



**Fig. 5** The amount (mol) of colistin alone (●), pre-incubated with chitosan (○) or LPS-chitosan complexes (●) released in successive time intervals from 0.75% agarose measured by laser interferometry system



**Fig. 6** Time dependency of diffusive flux of colistin alone (●), pre-incubated with chitosan (○) or LPS-chitosan complexes (●), released from 0.75% agarose measured by laser interferometry. The curves correspond to the curves shown in Fig. 3 and illustrate the kinetics of colistin transport from gel into the water phase. These curves are typical for the diffusion analyzed at the macroscopic level. In the initial stage of diffusion, we observe a rapid decrease of colistin flux due to increased concentration polarization



**Fig. 7** Time characteristics of concentration field evolution distances  $x_0 = 0, 0.5, 1,$  and  $2$  mm of the gel-water interface. The highest colistin concentration value occurs at the gel-water interface ( $x_0 = 0$  mm). A concentration near to zero indicates to be outside the CBL region; for example, the diffusing colistin reached the point  $x_0 = 2$  mm after time  $t > 20$  min. At the same time and at points  $x_0 = 0, 0.5$  and  $1$  mm, the concentrations were  $4.65 \times 10^{-4}, 2.19 \times 10^{-4},$  and  $1.85 \times 10^{-4}$  mol/dm<sup>3</sup>, respectively. From the plots results also that at points situated near the gel-water interface, the concentration evolves nonlinearly, whereas at points situated at longer distances from this interface, the concentration changes practically proportionally to the time

## 4 Notes

1. The chitosan solution can be stored at room temperature for 1 month.
2. Figure 2 shows chitosan hydrogel particles investigated by optical and fluorescence microscopy. Hydrogel was stained by 100 µg/mL fluorescein for 3 h at room temperature and six times washed in water.
3. A major advantage of the laser interferometry technique is the possibility of analyzing chemical compounds which form quasi-real solutions, such as amphiphilic colistin.
4. In the system presented here, only colistin is able to diffuse from agarose to the water phase. Chitosan particles or chitosan-LPS complexes are stabilized in agarose matrix.
5. While planning the interferometric experiment, it should be taken into account to study the transport of only one substance, due to the lack of identification of a substance in the multicomponent solutions. Moreover, using laser interferometry solutions can be studied with sufficient optical transparency.

## References

1. Arabski M, Wąsik S, Zych M et al (2013) Analysis of ciprofloxacin and gentamicin diffusion in *Proteus mirabilis* O18 biofilm by laser interferometry method. *Acta Biochim Pol* 60:707–711
2. Danis-Włodarczyk K, Olszak T, Arabski M et al (2015) Characterization of the newly isolated lytic bacteriophages KTN6 and KT28 and their efficacy against *Pseudomonas aeruginosa* biofilm. *PLoS One* 10(5):e0127603
3. Danis-Włodarczyk K, Vandenheuvel D, Jang HB et al (2016) A proposed integrated approach for the preclinical evaluation of phage therapy in *Pseudomonas* infections. *Sci Rep* 6:28115
4. Arabski M, Wąsik S, Dworecki K et al (2007) Laser interferometric determination of ampicillin and colistin transfer through cellulose bio-membrane in the presence of *Proteus vulgaris* O25 lipopolysaccharide. *J Membr Sci* 299: 268–275
5. Arabski M, Wąsik S, Dworecki K et al (2009) Laser interferometric and cultivation methods for measurement of colistin/ampicillin and saponin interactions with smooth and rough of *Proteus mirabilis* lipopolysaccharides and cells. *J Microbiol Methods* 77:179–183
6. Arabski M, Davydova VN, Wąsik S et al (2009) Binding and biological properties of lipopolysaccharide *Proteus vulgaris* O25 (48/57)-chitosan complexes. *Carbohydr Polym* 78: 481–487



## Endotoxin Entrapment on Glass via C-18 Self-Assembled Monolayers and Rapid Detection Using Drug-Nanoparticle Bioconjugate Probes

Prasanta Kalita\*, Anshuman Dasgupta\*, and Shalini Gupta

### Abstract

Bloodstream bacterial infections are known to illicit a systemic immune response that can lead to multi-organ failure and septic shock. The current endotoxin identification techniques in serum are expensive and elaborate requiring bulky benchtop instrumentation. We demonstrate a new route for endotoxin detection in which lipopolysaccharides (LPS) in solution are entrapped using C-18 silane-functionalized glass slides and tagged with polymyxin B sulfate (PMB) drug-conjugated gold nanoparticles. The signal from the particles is further amplified via the silver reduction approach to yield concentration-dependent colorimetric spots visible to the bare eye. The method is rapid, reliable, and cost-effective and fulfills an urgent unmet need in the healthcare industry for early septicemia diagnosis.

**Key words** Lipopolysaccharide (LPS), Endotoxin, Gold nanoparticle (GNP), Polymyxin B sulfate (PMB), Silver enhancement, C-18 silane

---

## 1 Introduction

Endotoxin, also referred to as LPS or pyrogen, is a conserved component of most Gram-negative bacterial cell envelopes [1]. Structurally, endotoxin can be segregated into three distinct components: (1) the repeating glycan polymer units known as O-antigen that are responsible for molecular immunogenicity, (2) a core oligosaccharide section, and (3) the (toxic) lipid-A region consisting of disaccharides and long fatty acid chains [2, 3]. Circulating endotoxins in the bloodstream are known to trigger an immunological cascade through the release of pro- or anti-inflammatory cytokines resulting in several pathological disorders such as hypotension, intravascular coagulation, multiple-organ failure, severe sepsis, and septic shock depending on the body's degree of imbalance [4, 5].

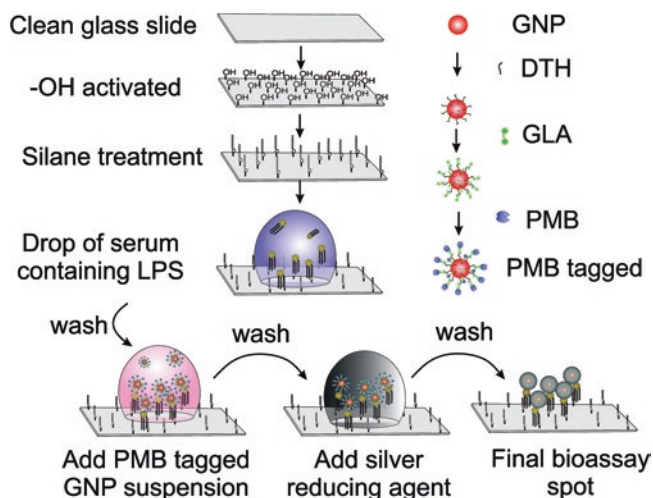
---

\*Prasanta Kalita and Anshuman Dasgupta these author contributed equally to this chapter.

In the other sectors too such as pharmaceuticals, agriculture, textile, defense, food, and water industry, the omnipresence of endotoxins as contaminants raises grave concerns [6–11]. Various endotoxin detection methods based on enzyme-linked immunosorbent assay (ELISA), clotting, absorbance, and chemiluminescence are commercially available to address the concerns of these sectors that demand rapid and affordable endotoxin monitoring [12–15]. Although some of these methods are now widely accepted, they come with their own drawbacks. For instance, the LAL test cannot be used to assay endotoxin in blood samples due to the presence of circulating inhibitors that prevent the coagulation reaction. Similarly, the ELISA detection kits are costly and require trained personnel to handle the microplate reader systems. Alternate approaches are therefore required that are simple, cost-effective and allow assaying complex milieu of biological analytes with high sensitivity and specificity.

Self-assembled monolayers (SAMs) offer a facile way of entrapping biomolecules or covalently attaching targeting moieties for their subsequent capture and are very popular in the field of bioassays and biosensors. For endotoxin detection specifically, thiolated organic molecules have been self-assembled onto gold surfaces for attaching different targeting ligands such as PMB and divalent cations like  $\text{Cu}^{2+}$  in order to identify trace amounts of endotoxin [16, 17]. In another ingenious example demonstrated by Peri and coworkers, LPS molecules were successfully self-assembled on the surface of hydrophobically functionalized magnetic nanoparticles in order to stimulate TLR4-dependent cell activation *in vitro* [18]. Our group has also recently reported a simple way to entrap and detect LPS molecules present in water and blood samples using silanized glass substrates [19]. The length of the alkane chains in the silane molecules was kept similar to the carbon atoms present in the fatty acid chains in the LPS (typically 16–18) in order to entropically drive the interdigitization and oriented binding of LPS on the hydrophobic surface, an approach motivated by the chromatographic separation techniques used for endotoxin purification of biological samples [20].

To detect the bound endotoxin on the glass surface, the molecules were tagged with gold nanoparticles (GNPs) coated with PMB drug (clinically known as colistin) known to have a high affinity for LPS molecules [21–23]. The use of drugs as targeting ligands is fast gaining popularity as it is superior to traditional moieties such as antibodies, peptides, or aptamers in terms of cost, thermal stability, resistance to denaturation, and ease of conjugation. The GNP conjugate probes were finally silver enhanced in order to amplify the signal multifold and get visual signal readout by the naked eye in the clinically relevant concentration range. A schematic of the assay is shown in Fig. 1, and a step-by-step experimental protocol to carry this out is discussed below. As one reads on, the simplicity of the assay and its suitability for clinical diagnostics will become apparent.



**Fig. 1** A schematic of the procedure used for the silver enhanced endotoxin bioassay using PMB-conjugated gold nanoparticles

## 2 Materials

All the items were purchased from Sigma-Aldrich and stored at room temperature unless otherwise stated. Refrigerated items were brought to room temperature before use. All the solutions were prepared using only pyrogen-free water (commercially available) and analytical grade reagents. For washing and other purposes, only ultrapure deionized (DI) water of high resistivity ( $\sim 18 \text{ M}\Omega \text{ cm}$ ) was used.

### 2.1 Glass Functionalization Components

1. Glass activation solution: Prepare 60 mL of piranha solution by slowly pouring  $\text{H}_2\text{O}_2$  over concentrated  $\text{H}_2\text{SO}_4$  in 3:1 v/v in a glass coplin jar. Alternately, use a basic piranha solution comprising of 1:1:5 v/v of  $\text{H}_2\text{O}_2$ : $\text{NH}_4\text{OH}$ : $\text{H}_2\text{O}$ .
2. 10 mM silane solution: Take 58 mL of dry toluene (water content  $\leq 0.001\%$ ) in a glass coplin jar and add 248  $\mu\text{L}$  of trichloro(octadecyl)silane solution to it while maintaining a dry environment using either a glove box or by purging nitrogen through a nozzle jet just above the working area in order to minimize any water vapor content (*see Note 1*).

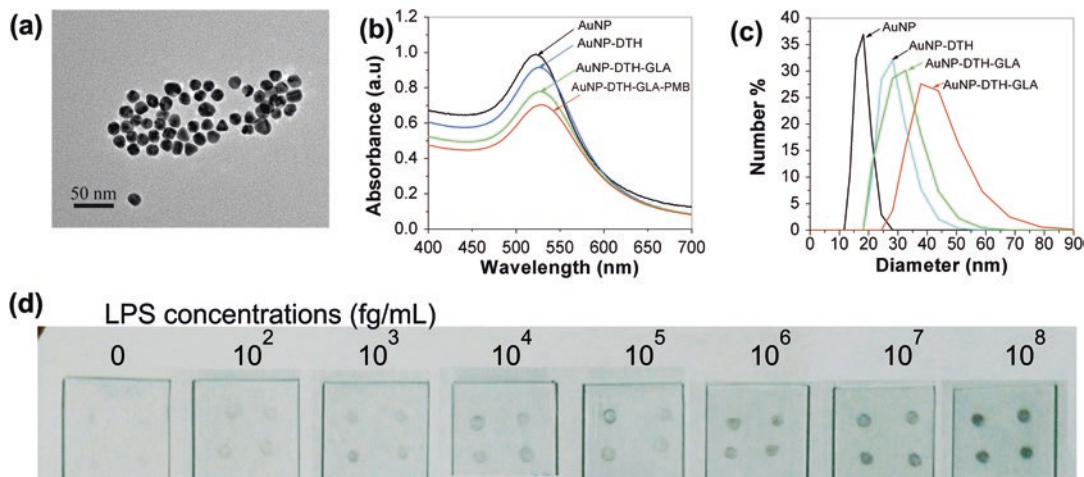
### 2.2 Sample Analyte Components

1. Serum: Take approx. 5 mL of whole blood in a pyrogen-free vial, and allow it to stand for 20 min at room temperature in order to coagulate. Centrifuge the coagulated blood at 10,380 rcf for 20 min. Collect the supernatant containing the serum, and store it at  $-20^\circ \text{C}$  in 95  $\mu\text{L}$  aliquots in pyrogen-free vials. Endotoxin-free frozen plasma/serum may alternately be purchased directly from a vendor.

2. LPS samples: Weigh 1 mg of lyophilized LPS powder (*Escherichia coli* serotype 055:B5) in depyrogenated glass vials, and add it to 1 mL of pyrogen-free water (Hyglos GmbH, Germany). Vortex the solution vigorously for at least 30 min and sonicate for another 5–10 min. Prepare multiple successive dilutions of this 1 mg/mL stock solution using pyrogen-free water until you reach 1 fg/mL concentration. Store at 4 °C. To prepare LPS samples in serum, bring the spiked aqueous LPS solutions to room temperature. Collect 5 µL from each of these samples, and add them separately to 95 µL serum aliquots to finally obtain 100 µL volume samples with varying LPS concentrations (*see Note 2*).

### 2.3 Detection Probe Components

1. 40 mM HEPES buffer, pH 7.4: Weigh about 4.766 g of HEPES salt, and add to 500 mL of ultrapure DI water kept in an autoclaved glass bottle. Shake the solution until all the salt disappears. Adjust the pH to 7.4 using 25 M NaOH solution. Store at 4 °C (*see Note 3*).
2. 9.3 mM dithiolalkane aromatic PEG-6 hydrazide (DTH) linker solution: Bring 50 g of DTH powder (Sensopath, USA) stored at –20 °C to room temperature, and add 2 mL of 99.9% (v/v) ethanol to obtain a 35.3 mM clear solution. Vortex vigorously for 10 min. Dilute a portion of this stock to 9.3 mM concentration using 99.9 v/v % ethanol, and prepare 10 µL aliquots in PCR tubes. Store the aliquots as well as the remaining stock at –20 °C.
3. Glutaraldehyde (GLA) solution: Prepare 10 mL of 2 w/v % GLA solution by adding 400 µL of 25 w/v % GLA stock to 9600 µL of 40 mM HEPES buffer at pH 7.4.
4. Polymyxin B sulfate (PMB) solution: Prepare 1 mL of 15.3 µM PMB solution by taking 1 µL of 15.3 mM stock solution and adding it to 999 µL of ultrapure DI water in a 1.5 mL Eppendorf tube. Homogenize the mixture using a vortexer. Store at 4 °C.
5. GNP suspension: Take approx. 16 nm citrate-stabilized GNPs suspended in ultrapure DI water, and adjust their concentration to 2 nM either by dilution or by centrifugation, and suspend the pellet in DI water. The GNPs may be purchased or synthesized by any of the known methods in the literature [24, 25]. Final volume of the suspension should be at least 10 mL. Store at 4 °C. The UV-visible spectrum of this suspension should peak around 522 nm (Fig. 2b). The size distributions of the particles are shown in Fig. 2a and c.



**Fig. 2** (a) Transmission electron microscopy image taken using Tecnai G2 (FEI) shows spherical particles approximately 16 nm in size. (b) UV-visible spectra and (c) DLS measurements of GNPs before and after chemical modification with DTH, DTH-GLA and DTH-GLA-PMB, respectively. A gradual right shift in peaks in both spectra indicates successful surface functionalization at each modification step. (d) Actual bioassay spots obtained after performing experiments in quadruplicate at each concentration. Images taken in ambient light using Nikon COOLPIX 310 CCD camera

### 3 Methods

All experiments are performed at room temperature unless otherwise stated. The described protocol for drug-modified GNP suspension preparation is sufficient to carry out multiple experiments. The excess stock can be stored at 4 °C for at least 3 months.

#### 3.1 PMB Conjugation to GNPs

1. Take 10 mL of 2 nM citrate-capped GNP suspension in a 15 mL conical glass flask. Add 20  $\mu$ L of 9.3 mM DTH solution to this suspension, and keep the mixture at 25 °C inside a shaker incubator at 200 rpm for 12 h.
2. Transfer the ligand-exchanged GNPs to a 15 mL falcon tube marked “1” and centrifuge it at 1660 rcf for 15 min. Transfer the supernatant to another falcon tube marked “2” and centrifuge it again at 5080 rcf for 15 min. Do not discard the pellet. Repeat the process at higher centrifugation speeds of 10,380 and 17,540 rcf. Collect all the pellets from the tubes marked 1–4, and mix them together in a single falcon tube. Re-suspend this final pellet in 40 mM HEPES buffer, pH 7.4 to a final volume of 10 mL. The UV-visible spectrum of this DTH-modified GNP suspension should give an approx. red-shift of 4 nm with respect to bare GNPs (Fig. 2b). The hydrodynamic size of the particles also increases by ~16 nm as measured by dynamic light scattering (DLS) (Fig. 2c).

3. Add 9 mL of 2% (w/v) GLA solution to an equal volume of the above DTH-modified GNP suspension in a clean conical glass flask. Keep the flask inside a shaker incubator for 8 h at 25 °C (*see Note 4*).
4. Repeat the same centrifugation steps involved during the removal of excess DTH from the GNP suspension. Finally suspend the pellet in 16 mL of 40 mM HEPES buffer, pH 7.4. The UV-visible spectrum of the GLA-modified particles should give a peak around 527.5 nm that is redshifted by 1.5 nm peak with respect to DTH-modified GNPs (Fig. 2b). The hydrodynamic size increases to 30 nm (Fig. 2c).
5. Transfer 16 mL of the GLA-modified GNP suspension (~1 nM) to a 50 mL glass conical flask. Add to this 10 µL of 15.3 µM PMB solution. Keep the solution in a shaker incubator at 200 rpm for 12 h at 25 °C.
6. Repeat the same centrifugation steps involved during the removal of excess DTH from the GNP suspension. Collect the final pellet and resuspend it in 14 mL of 40 mM HEPES buffer, pH 7.4 to bring the final concentration of the suspension to 1 nM. The UV-visible spectrum of PMB-modified particles should give a 1 nm peak shift with respect to GLA-modified GNPs (Fig. 2b). The final size of the particle becomes approx. 38 nm at this point (Fig. 2c). Store the particles at 4 °C (*see Note 5*).

### **3.2 Glass Silanization**

1. Clean a standard glass slide using a soft fiberless tissue (e.g., Kimwipes) soaked in acetone.
2. Soak the glass slide overnight in the acidic piranha solution to remove organic content and to activate the surface with hydroxyl (-OH) groups for subsequent reaction. Wash the slide with ample DI water and dry it under a purge of nitrogen (*see Note 6*).
3. Dip the dry glass slide in freshly prepared silane solution kept inside a glass coplin jar. Place the lid on the coplin jar and keep it inside a vacuum desiccator for at least 12 h. The desiccator should be pre-filled with nitrogen gas.
4. Take out the slide and dip it in another glass coplin jar filled only with dry toluene. Sonicate for 10 min to remove the excess unbound silane molecules. Repeat this step twice.
5. Take out the glass slide and keep it for drying in an oven at 70 °C for 1 h, and then store inside a desiccator until further use.

### **3.3 LPS Immobilization on Glass Substrates**

1. Wash the silanized glass slide with DI water just prior to beginning the LPS immobilization experiments (*see Note 7*).
2. Using a micropipette, adjacently drop cast two 10 µL droplets of serum/water on the surface of the silanized glass slide – one

containing and one without LPS (negative control). The distance between the droplets should be maintained at least 1 cm such that their contents do not mix. Keep the slide inside a pre-humidified water bath at 37 °C for 30 min (*see Note 8*).

3. Take the slide out of the water bath, and mark the area on which the LPS is immobilized on the bottom side of the glass slide using a permanent marker. Gently wash the area with DI water using a 1 mL micropipette (*see Note 9*).
4. Allow the slide to dry for 4–5 min under ambient conditions.

### **3.4 GNP Tagging and Silver Enhancement for Endotoxin Detection**

1. After LPS immobilization, add 100  $\mu\text{L}$  of the PMB-modified GNP suspension above the LPS-immobilized area (marked earlier). Keep the slide inside the pre-humidified water bath at 37 °C and incubate for 40 min.
2. Take the slide out and rinse it with DI water several times using a micropipette. Allow the slide to dry for 4–5 min under ambient conditions.
3. From the silver enhancement kit, take out 50  $\mu\text{L}$  each of solutions A and B in Eppendorf cups. Mix and vortex the two solutions together. Apply the entire mixture volume immediately to the LPS-immobilized area, and wait for 30–50 s for the spots to develop. Immediately wash the slide with copious amounts of ultrapure DI water (*see Note 10*).
4. A black spot should be visible to the naked eye where the LPS is immobilized. The rest of the glass slide remains clear (*see Note 11*) (Fig. 2d).

---

## **4 Notes**

1. Even trace amounts of water is sufficient to trigger self-polymerization of silane molecules leaving a whitish by product and incomplete functionalization of glass slides hampering the bioassay results.
2. Aqueous LPS solution when stored at 4 °C can be used up to 4 weeks without significant loss in activity. LPS samples prepared in serum should be used fresh (within 3 days) since serum proteins tend to get denatured and are liable to contamination. Avoid using plastic containers (e.g., polypropylene, polystyrene, polymethyl methacrylate, etc.) as LPS tends to stick to them irreversibly.
3. HEPES is a zwitterionic buffer with low ionic strength. It is more suitable for doing GNP experiments than other common buffers such as phosphate buffer saline (PBS) or borate in which the GNPs tend to aggregate.

4. In the GLA activation step, 360  $\mu\text{L}$  of 25% (w/v) GLA stock can also be added directly to 18 mL of 1 nM of GNP suspension. Use of six orders of magnitude higher molar concentration of GLA (than GNPs) is sufficiently high for restricting particle aggregation due to interparticle cross-linking. Since GNPs tend to stick to plastic surfaces upon conjugation with GLA, all vials or tubes used should be made out of glass to avoid particle loss.
5. The concentration of the GNP suspension may be calculated from its UV spectrum using the Beer-Lambert's law,  $A = \epsilon CL$ , where  $A$  is absorbance,  $\epsilon$  is particle-size-dependent extinction coefficient,  $C$  is sample concentration, and  $L$  is path length of the cuvette through which light travels. For 16 nm citrate-capped GNPs,  $\epsilon$  is reported as  $5.26 \times 10^8 \text{ M}^{-1} \text{ cm}^{-1}$  [26]. This  $\epsilon$  is assumed constant for all the ligand-modified GNPs in our study.
6. Base piranha solution is a mild reagent for  $-\text{OH}$  activation. If this is used, dip the glass slides in the solution at  $70^\circ \text{C}$  for at least an hour.
7. A silanized glass slide is highly hydrophobic. The success of the silanization procedure may be checked by putting a drop of water on the functionalized area; the water droplet should bead up and roll off without sticking to the underlying surface.
8. High humidity ( $>80\%$ ) aids LPS entrapment. Aqueous LPS solutions should always be vortexed vigorously prior to any experiment to break aggregates. Do not sonicate the serum samples.
9. The successful immobilization of LPS may be quickly confirmed by adding a drop of water to the functionalized area. When the slide is tilted, the droplet should not fall down since LPS immobilization makes the hydrophobic surface a hydrophilic one.
10. The silver enhancement mixture must be prepared fresh. This mixture is also sensitive to light, temperature, and the presence of salts.
11. The spot tends to gain more contrast once the slide is washed and dried.

*Special notes on LPS:* LPS is a pyrogenic material that requires strict safety guidelines to be followed inside the laboratory [27]. Experiments should only be performed inside a BSL-I class biosafety cabinet or fume hood using designated equipment disallowing contamination. All LPS-contaminated solutions, vials, and pipette tips should be discarded after dipping in 30% (v/v) sodium hypochlorite solution for 24 h at room temperature. Other utensils should be autoclaved for 1 h and discarded in disposable waste



bags in a designated place. All glassware should be depyrogenated by heating at 250 °C for 4 h. All the personnel involved in the experiments must be trained and should wear gloves, facial masks, and lab coats at all times. Hands must be washed with soap after performing the experiments.

LPS occurs naturally in the environment and does not harm healthy individuals but can exacerbate asthmatic symptoms in susceptible individuals. In such an event, visit a doctor immediately. In case of spills, wearing protective clothing and gloves, the area should be wiped up with an absorbent material and decontaminated with a freshly made bleach solution. In case of undue exposure, report to a doctor immediately.

---

## Acknowledgment

This work was supported by the grant received from DBT-BIRAC (BIG-II scheme) and the fellowship received from CSIR, New Delhi.

## References

1. Pearson FC, Dubczak J, Weary M et al (1985) Detection of endotoxin in the plasma of patients with gram-negative bacterial sepsis by the Limulus amoebocyte lysate assay. *J Clin Microbiol* 21:865–868
2. Ganesh V, Bodewits K, Bartholdson SJ et al (2009) Effective binding and sensing of lipopolysaccharide: combining complementary pattern recognition receptors. *Angew Chem Int Ed Engl* 48:356–360
3. Caroff M, Karibian D (2003) Structure of bacterial lipopolysaccharides. *Carbohydr Res* 338:2431–2447
4. Raetz CR, Whitfield C (2002) Lipopolysaccharide endotoxins. *Annu Rev Biochem* 71:635–700
5. David SA, Silverstein R, Amura CR et al (1999) Lipopolyamines: novel antiendotoxin compounds that reduce mortality in experimental sepsis caused by gram-negative bacteria. *Antimicrob Agents Chemother* 43:912–919
6. Turner AP (2013) Biosensors: sense and sensibility. *Chem Soc Rev* 42:3184–3196
7. Turner A (2013) Biosensors: then and now. *Trends Biotechnol* 31:119–120
8. Garcia J, Bennett DH, Tancredi D et al (2013) Occupational exposure to particulate matter and endotoxin for California dairy workers. *Int J Hyg Environ Health* 216:56–62
9. Pankhurst LJ, Deacon LJ, Liu J et al (2011) Spatial variations in airborne microorganism and endotoxin concentrations at green waste composting facilities. *Int J Hyg Environ Health* 214:376–383
10. Thorne PS, Perry SS, Saito R et al (2010) Evaluation of the limulus amoebocyte lysate and recombinant factor C assays for assessment of airborne endotoxin. *Appl Environ Microbiol* 76:4988–4995
11. Todi S, Chatterjee S, Sahu S et al (2010) Epidemiology of severe sepsis in India: an update. Paper presented at the 30th international symposium on intensive care and emergency medicine, Brussels, Belgium, 9–12 March 2010
12. Foster D, Derzko A, Romaschin A (2004) A novel method for the rapid detection of human endotoxaemia. *Clin Lab Int* 4:10–12
13. Bates DW, Parsonnet J, Ketchum PA et al (1998) Limulus amoebocyte lysate assay for detection of endotoxin in patients with sepsis syndrome. *Clin Infect Dis* 27:582–591
14. Grallert H, Leopoldseder S, Schuett M et al (2011) EndoLISA: a novel and reliable method for endotoxin detection. *Nat Methods* 8:i–v
15. Teng NN, Kaplan HS, Hebert JM et al (1985) Protection against gram-negative bacteremia and endotoxemia with human monoclonal IgM antibodies. *Proc Natl Acad Sci USA* 82:1790–1794
16. Zuzuarregui A, Arana S, Pérez-Lorenzo E et al (2013) Novel fully-integrated biosensor for endotoxin detection via polymyxin B immobilization onto gold electrodes. *J Sens Sens Syst* 2:157–164

17. Cho M, Chun L, Lin M et al (2012) Sensitive electrochemical sensor for detection of lipopolysaccharide on metal complex immobilized gold electrode. *Sens Actuators B Chem* 174:490–494
18. Piazza M, Colombo M, Zanoni I et al (2011) Uniform lipopolysaccharide (LPS)-loaded magnetic nanoparticles for the investigation of LPS-TLR4 signaling. *Angew Chem Int Ed Engl* 50:622–626
19. Kalita P, Dasgupta A, Sritharan V et al (2015) Nanoparticle–drug bioconjugate as dual functional affinity ligand for rapid point-of-care detection of endotoxin in water and serum. *Anal Chem* 87:11007–11012
20. Ongkudon CM, Chew JH, Liu B et al (2012) Chromatographic removal of endotoxins: a bioprocess engineer's perspective. *ISRN Chromatography* 2012:9
21. Schindler M, Osborn MJ (1979) Interaction of divalent cations and polymyxin B with lipopolysaccharide. *Biochemistry* 18:4425–4430
22. Mares J, Kumaran S, Gobbo M et al (2009) Interactions of lipopolysaccharide and polymyxin studied by NMR spectroscopy. *J Biol Chem* 284:11498–11506
23. Bhor VM, Thomas CJ, Surolia N et al (2005) Polymyxin B: an ode to an old antidote for endotoxic shock. *Mol Biosyst* 1:213–222
24. Slot JW, Geuze HJ (1985) A new method of preparing gold probes for multiple-labeling cytochemistry. *Eur J Cell Biol* 38:87–93
25. Tsai CY, Lee DS, Tsai YH et al (2004) Shrinking gold nanoparticles: dramatic effect of a cryogenic process on tannic acid/sodium citrate-generated gold nanoparticles. *Mater Lett* 58:2023–2026
26. Liu X, Atwater M, Wang J et al (2007) Extinction coefficient of gold nanoparticles with different sizes and different capping ligands. *Colloids Surf B Biointerfaces* 58:3–7
27. Chosewood LC, Wilson DE (2007) Biosafety in microbiological and biomedical laboratories. Diane Publishing, Washington

## A Bioassay for the Determination of Lipopolysaccharides and Lipoproteins

Marcus Peters, Petra Bonowitz, and Albrecht Bufe

### Abstract

The availability of convenient assays for the detection and quantification of pathogen-associated molecular patterns (PAMPs) is limited. In the case of lipopolysaccharide (LPS) the so-called LAL (limulus amebocyte lysate) test is available, an assay that is performed with the lysate of the blood of the horse shoe crab. Although a sensitive and convenient assay, it lacks specificity, since it is affected by other endotoxins like, for instance, fungal cell walls as well. Here, we describe a bioassay that can be used to detect and quantitate PAMPs in environmental samples. More specific we demonstrate the usage of TLR2 and TLR4/CD14/MD2 transfected Hek293 cells to quantitatively determine bacterial lipoproteins and LPS, respectively. We show the usefulness of these assays to measure LPS in tobacco before and after combustion.

**Key words** Lipopolysaccharide, Lipoprotein, Toll-like receptor, Bioassay, Pathogen-associated molecular patterns

---

### 1 Introduction

The sensitive and accurate measurement of pathogen-associated molecular patterns (PAMPs) is an important tool in many scientific fields, especially for immunologists, biochemists, and pharmacologists. However, the availability of high-quality methods is limited due to the lack of specific and sensitive immunoassays. Only in the case of lipopolysaccharide (LPS) there is an alternative in vitro assay with sensitivity comparable to ELISA, the limulus amebocyte lysate (LAL) test. This assay works well when the complexity of the sample is low, e.g., detection of LPS contamination in recombinant proteins isolated from bacterial expression systems. However with increasing complexity of the sample the LAL test suffers from its low specificity. In particular, fungal glycans can influence the outcome of the test [1–3]. Due to these limitations a more specific assay was released by the same company, the recombinant factor C (rFC) assay [4]. The rFC assay uses only the LPS binding protein from the clotting cascade of the LAL test as a biosensor. This assay

combines sensitivity and specificity but needs special equipment, that is, a fluorescence reader since it uses a fluorogenic substrate for development.

An alternative assay that is already in use to qualitatively give evidence for the presence or absence of PAMPs is a bioassay using TLR-transfected Hek293 cells [5]. HEK293 cells express genes for TLR1, TLR3, TLR5, TLR6, and NOD1. Therefore, these cells normally do not respond to LPS or bacterial lipoproteins. However when these cells are transfected with TLR4 or TLR2, respectively, they become reactive to these PAMPs. We have previously shown that transfected Hek293 cells can be used to detect LPS in environmental samples.

TLR4/MD2/CD14 transfected HEK293 cells are useful for the sensitive and specific quantification of LPS in complex samples such as dust extracts from the environment [6]. The procedure of PAMP detection is based on the stimulation of these cells with increasing concentration of highly purified *Escherichia coli* LPS leading to release of IL-8 in a dose-dependent manner. The resulting standard curve is used to determine LPS concentration in unknown samples.

Here, we extend the use of this assay to determine LPS in tobacco before and after combustion. Moreover, we describe a similar assay to determine TLR2 ligands by the use of TLR2-transfected HEK293 cells.

Tobacco for production of cigarettes is dried after harvesting the leaves. During the drying process microbes propagate on the drying tobacco leaves. Therefore, it is not surprising that tobacco products contain PAMPs. There are some studies determining the LPS content of tobacco via LAL test [7] and one study that is using the specific determination of 3-OH fatty acids of lipid A [8]. LPS is a molecule with relatively high chemical and physical stability; however, constant heat treatment normally destroys the biologic activity of the substance. Despite this fact there is one older study proposing the presence of LPS in the smoke of combusted cigarettes after the measurement of smoke extracts with the LAL test. Furthermore, LPS was found in alveolar macrophages of smokers. Therefore, since the presence of LPS and other PAMPs in cigarette smoke has an important impact for understanding smoking-related disease [9], we aimed to detect LPS and bacterial lipoproteins in cigarette smoke by using TLR4-MD2-CD14-transfected HEK293 cells.

---

## 2 Materials

293/mTLR4-MD2-CD14 cells are for studying the activation of TLR4 by LPS. The 293/mTLR2 cells are useful for the detection of TLR2 ligands. Both cell types are designed by stable transfection of Hek293 cells with the pUNO vector. Cells can be purchased at Invivogen (Toulouse, France).

## 2.1 Cell Maintenance and Stimulation

Use all solutions and culture media for preparing the stimulation assay at room temperature.

1. DMEM: 4.5 g/L glucose, L-glutamine, sodium pyruvate, h 3.7 g/L NaHCO<sub>3</sub>.
2. PBS: Dulbecco's Phosphate-Buffered Saline without MgCl<sub>2</sub> and CaCl<sub>2</sub> (Pan-Biotech, Aidenbach, Germany), liquid, sterile-filtered, suitable for cell culture.
3. Blasticidin S hydrochloride 10 mg/mL solution in HEPES buffer. It is required to maintain the plasmids coding for mTLR4 and mTLR2, respectively.
4. Hygromycin B Gold 100 mg/mL solution in HEPES buffer. It is to maintain the plasmid coding for MD2 and CD14.
5. Normocin 50 mg/ml red aqueous solution. It is a formulation of three antibiotics active against mycoplasmas, bacteria, and fungi.
6. Penicillin-Streptomycin: 10,000 U/ml Penicillin, 10 mg/mL Streptomycin.
7. L-Glutamine 200 mM.
8. LPS: *E. coli*, chromatographically purified [10].
9. FSL-1: Synthetic di-acyl lipopeptide binding to the TLR2/6 heterodimer (EMCmicrocollections, Tübingen, Germany) (*see Notes 1 and 2*).
10. Complete Growth Medium: DMEM containing 4.5 g/L glucose, 10% (v/v) fetal bovine serum, 50 U/mL penicillin, 50 µg/mL streptomycin, 100 µg/mL Normocin™, 2 mM L-glutamine, 10 µg/mL Blasticidin, 50 µg/mL of Hygromycin B Gold.
11. Freezing Medium: DMEM, 4.5 g/L glucose, 20% (v/v) fetal bovine serum, 50 U/ml penicillin, 50 µg/ml streptomycin, 100 µg/ml Normocin™, 2 mM L-glutamine, 10% (v/v) DMSO.
12. TC Flask, Cell+ with Vented Cap and TC Plate 96-well Standard F, (Sarstedt, Nümbrecht, Germany).

## 2.2 Measurement of Interleukin-8 in Cell Culture Supernatants

1. 96-well ELISA plates, High Binding, F (Sarstedt, Nümbrecht, Germany).
2. Coating Buffer: 7.13 g NaHCO<sub>3</sub>, 1.59 g Na<sub>2</sub>CO<sub>3</sub>; q.s. to 1.0 L; pH 9.5 with 1 N NaOH.
3. Assay Diluent: PBS with 10% FCS.
4. Washing Buffer: PBS with 0.05% Tween20.
5. Human IL-8 ELISA (OptEIA™ ELISA Development Set, BDbiosciences, Heidelberg, Germany) for human interleukin-8 (IL-8) containing IL-8 catcher antibody, IL-8 recombinant protein, biotinylated IL-8 detector antibody, horse raddish peroxidase coupled to streptavidine.
6. TMB substrate set (BDbiosciences, Heidelberg, Germany).
7. Stop solution 1 M sulfuric acid.

### 2.3 Cigarette and Smoke Extracts

1. Research cigarettes (3R4F) were purchased from the University of Kentucky (Kentucky Tobacco Research & Development Center).
2. Smoke extract: ten cigarettes were combusted by a cigarette smoke generator (DSI, Data science international, St. Paul, Minnesota). Main and side-stream smoke was passed through 70 mL complete cell culture medium in a gas washing bottle.
3. Cigarette extract: the tobacco from ten cigarettes was pulverized in liquid nitrogen with a mortar. Afterward tobacco powder was stirred for 1.5 h in 70 mL 0.05 triethylamine for extraction, followed by the addition of 7 mL 1 M Tris-HCl pH 7.5. Subsequently, extracts were passed through filters with 0.2  $\mu\text{m}$  pore size.

---

## 3 Methods

### 3.1 Cell Maintenance

293/mTLR4-MD2-CD14 cells were cultured in DMEM 10% FCS with Normocin, Hygromycin, Penicillin, and Streptomycin as antibiotics (*see Note 3*). 293/mTLR2 cells were cultured in the same Medium without Hygromycin. Cells were subcultured before reaching confluence by PBS treatment.

1. Do not passage cells more than 20 times to remain fully efficient.
2. Maintain and subculture the cells in Growth Medium supplemented with Normocin™ (100  $\mu\text{g}/\text{mL}$ ), Blasticidin (10  $\mu\text{g}/\text{mL}$ ), and Hygromycin B Gold (50  $\mu\text{g}/\text{mL}$ ).
3. Renew Growth Medium two times a week.
4. Passage cells when a 70–80% confluency is reached; therefore, exchange the cell culture medium against PBS and detach the cells by tapping the flask or by flushing with serological pipette (*see Notes 4 and 5*).
5. Store cells frozen for longer time periods, by exchanging tissue culture medium to freezing medium followed by freezing the cells slowly to  $-80\text{ }^{\circ}\text{C}$  followed by storage in liquid nitrogen.

### 3.2 Stimulation of Transfected 293/mTLR4-MD2-CD14 Hek293 Cells with LPS or Cigarette Extracts

Figure 1 shows an example of determination of LPS in tobacco extracts from 3R4F cigarettes.

1. Prepare the assay not earlier than 48 h after the last passage of the cells (*see Note 6*). Dilute cells  $1 \times 10^6/\text{mL}$ .
2. Use a sterile 96-well tissue culture plate.
3. Generate a twofold serial dilution of LPS starting from the highest LPS concentration of 4 ng/ml in complete cell culture medium to prepare a standard curve of a total of eight points with culture medium (*see Note 7*).
4. Prepare the unknown samples by diluting them in cell culture medium twofold on the same plate. In the example shown in Fig. 1,

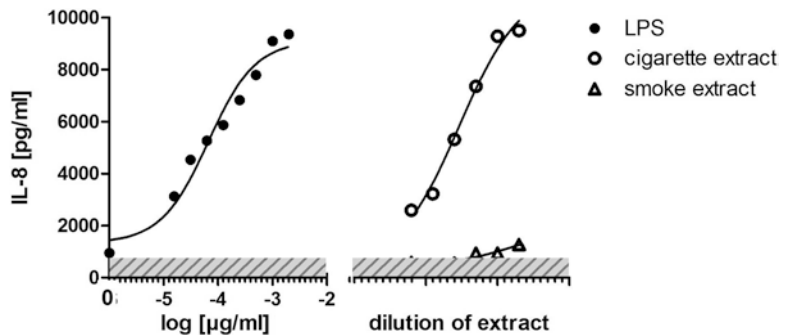
the tobacco extract was serial diluted from 1:500 to 1:16,000, whereas the smoke extract was diluted from 1:4 to 1:128.

5. Add 100  $\mu\text{L}$  culture medium with  $1 \times 10^5$  293/mTLR4-MD2-CD14 cells to the appropriate wells by using a stepper pipette.
6. Place the cells in an incubator at 37 °C in 5%  $\text{CO}_2$  for 24 h.
7. Plates were centrifuged ( $300 \times g$ , 10 min) and supernatants stored at  $-80$  °C.

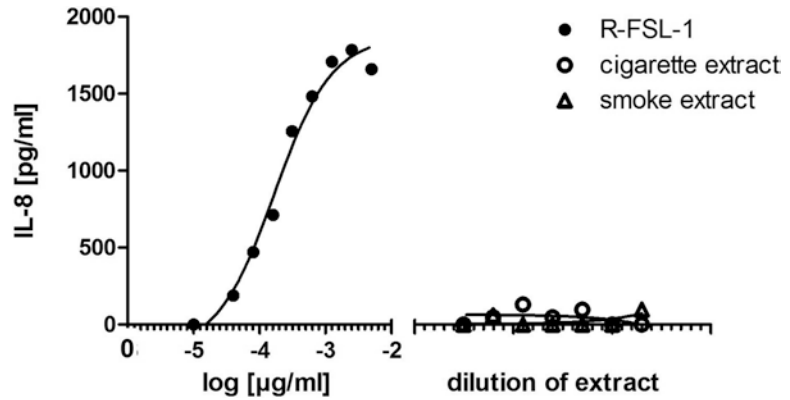
### 3.3 Stimulation of Transfected 293/mTLR2 Cells with FSL-1 or Cigarette Extracts

Figure 2 shows an example of determination of bacterial lipoproteins in tobacco extracts from 3R4F cigarettes.

1. Prepare the assay not earlier than 48 h after the last passage of the cells (*see Note 6*).
2. Use a sterile 96-well cell culture plate.
3. Generate a twofold serial dilution of FSL-1 starting from the highest concentration of 5 ng/ml in complete cell culture medium to prepare a standard curve of a total of eight points with culture medium (*see Note 7*).
4. Prepare the unknown samples by diluting them twofold on the same plate. In the example shown in Fig. 2 the tobacco and the smoke extract were serial diluted from 1:8 to 1:256.
5. Add 100  $\mu\text{L}$  culture medium with  $1 \times 10^5$  293/mTLR2 cells to the appropriate wells by using a stepper pipette.
6. Place the cells in an incubator at 37 °C in 5%  $\text{CO}_2$  for 24 h.
7. Plates were centrifuged ( $470 \times g$ , 10 min) and supernatants stored at  $-20$  °C until measurement of IL-8 is performed.



**Fig. 1** Detection of LPS in tobacco extract. Tobacco from 3R4F cigarettes was extracted with TEA buffer. In addition, smoke of ten cigarettes was passed through complete cell culture medium in a gas-washing bottle. Subsequently, the diluted extracts were evaluated for the presence of LPS. By using the LPS standard curve to compute unknown LPS concentration in cigarettes, we calculated a total amount of 2.5  $\mu\text{g}$  LPS per cigarette. In contrast, the smoke of combusted cigarettes contains amounts of LPS near the detection limit of the test (gray shaded area of the graph, *see Note 8*)



**Fig. 2** Detection of TLR2 binding lipoproteins in tobacco extract. Tobacco from 3R4F cigarettes was extracted with TEA buffer. In addition, smoke of ten cigarettes was passed through cell culture medium in a gas-washing bottle. Subsequently, the extracts were evaluated for the presence of lipoproteins. Both in tobacco and in smoke extracts the lipoprotein concentration is near the detection limit of the test (see **Note 9**)

### 3.4 Determination of IL-8 in Cell Culture Supernatants

A commercial available ELISA development kit for the detection of IL-8 in supernatants was used.

1. Supernatants were thawed and centrifuged to sediment cellular debris ( $470 \times g$ , 10 min).
2. Coat wells with 50  $\mu$ L per well of capture antibody diluted 1/250 (see **Note 10**) in coating buffer.
3. Incubate overnight at 4 °C.
4. Remove liquid from the wells and wash three times with  $\geq 200$   $\mu$ L washing buffer. After the last wash, invert plate and blot on absorbent paper to remove any residual buffer.
5. Block plates with 200  $\mu$ L assay diluent per well. Incubate for 1 h at room temperature.
6. Repeat **step 4**.
7. Prepare the top standard at a concentration of 200 pg/mL in assay diluent. Perform twofold serial dilutions of the top standard to make the standard curve ranging from 200 to 3.1 pg/mL. Pipette 50  $\mu$ L of each dilution.
8. Prepare sample dilutions as well in assay diluent. Pipette 50  $\mu$ L of each sample dilution to a separate well.
9. Incubate for 2 h at room temperature.
10. Repeat **step 4** with a total of five washing cycles.
11. Mix equal volumes of detection antibody diluted 1/250 (see **Note 10**) in assay diluent with the enzyme concentrate diluted 1/250 (see **Note 10**) in assay diluent.
12. Pipette 50  $\mu$ L of the detection reagent prepared in **step 11** to each well.



13. Incubate for 1 h at room temperature.
14. Repeat **step 4** with a total of seven washing cycles.
15. Add 50  $\mu\text{L}$  TMB substrate solution to each well and incubate for 15 min.
16. Add 25  $\mu\text{L}$  stop solution to each well followed by direct measurement of the absorbance at a wavelength of 450 nm in an ELISA plate reader.

### 3.5 Computation of Results

GraphPad Prism Version 5.01 was used for data analysis.

1. Concentration of LPS used for stimulation of cells was entered as  $x$  values and transformed by the equation  $x = \log(x)$ .
2. The corresponding concentrations of IL-8 measured in the cell supernatant by ELISA were entered as  $y$  values.
3. The resulting curve:  $\log(\text{concentration agonist})$  versus  $\text{response}(\text{concentration IL-8})$  was fitted to a nonlinear regression model. From the resulting dose response curve unknown LPS concentration in test samples is interpolated automatically by the software.

---

## 4 Notes

1. In this paper, the diacyl lipopeptide FSL-1 binding to the TLR2/TLR6 heterodimer was used; however, triacyl lipopeptides binding to the TLR2/TLR1 heterodimer work as well (data not shown).
2. For the generation of the standard curve use the best quality PAMPs available. Insufficiently purified PAMPs will greatly influence the performance of the assay.
3. Do not handle the cells cold since it will affect the vitality of the cells. It is important that all buffers and cell culture medium are pre-warmed. Centrifuge the cells at room temperature.
4. The response of the transfected cells can be altered by the action of trypsin. Do not use trypsin to detach the cells. Cells are only loosely adherent; therefore, mechanical detachment is sufficient to harvest them.
5. Do not let the cells grow over 80% confluency. Otherwise, the vitality of the cells will be strongly influenced.
6. Do not use cells to perform the assay that do not adhere to the cell culture flask prior to collection, i.e., when cells look spherical and swim just above the plastic surface.
7. Normally, the detection limit of the test is below 10  $\text{pg/mL}$  LPS and below 40  $\text{pg/mL}$  of bacterial lipopeptides.

8. The TLR4-MD2-CD14 HEK293 cells show background production of IL-8. This IL-8 production is a good indicator for the vitality of these cells. E.g., when working with organic solvents like for instance DMSO it indicates the DMSO dilution needed to be nontoxic for the cells. The TLR2-transfected cells do not show production of IL-8 until stimulated with the ligand.
9. Keep in mind that the amount of biological active PAMPs measured in solution depends on the extraction procedure. Here, we used mild methods to extract the PAMPs from tobacco. However when the total amount of PAMPs in a sample is of interest harsher methods must be employed to release PAMPs that are still bound to microbial debris.
10. Please refer to the manufacturer's protocol since the dilution of these test compounds may vary from lot to lot.

---

## Acknowledgments

We like to thank Prof. Dr. Karl-Heinz Wiesmüller (EMC microcollections, Tübingen, Germany) for providing us with FSL-1. We like to thank Prof. Dr. Ulrich Zähringer (formerly Forschungszentrum Borstel, Germany) for providing us with *E. coli* LPS. We like to thank Dimitri Kasakovski for generating the cigarette and smoke extracts. This work was supported by Deutsche Forschungsgemeinschaft (PE 1813/2-1).

## References

1. Vassallo R, Limper AH (1999) Fungal  $\beta$ -glucan can yield false-positive results with the limulus amebocyte lysate endotoxin assay. *Chest* 116: 583–584
2. Hirano M, Matsumoto T, Kiyohara H, Yamada H (1994) Lipopolysaccharide-independent limulus amebocyte lysate activating, mitogenic and anti-complementary activities of pectic polysaccharides from chinese herbs. *Planta Med* 60:248–252
3. Cooper JF, Weary ME, Jordan FT (1997) The impact of non-endotoxin LAL-reactive materials on Limulus amebocyte lysate analyses. *PDA J Pharm Sci Technol* 51:2–6
4. Ding JL, Ho B (2010) Endotoxin detection— from limulus amebocyte lysate to recombinant factor C. *Subcell Biochem* 53:187–208
5. Lappin DF, Sherrabeh S, Erridge C (2011) Stimulants of Toll-like receptors 2 and 4 are elevated in saliva of periodontitis patients compared with healthy subjects. *J Clin Periodontol* 38:318–325
6. Peters M, Fritz P, Buße A (2012) A bioassay for determination of lipopolysaccharide in environmental samples. *Innate Immun* 18: 694–699
7. Hasday JD, Bascom R, Costa JJ, Fitzgerald T, Dubin W (1999) Bacterial endotoxin is an active component of cigarette smoke. *Chest* 115:829–835
8. Pomorska D, Larsson L, Skórska C, Sitkowska J, Dutkiewicz J (2007) Levels of bacterial endotoxin in air of animal houses determined with the use of gas chromatography-mass spectrometry and Limulus test. *Ann Agric Environ Med* 14:291–298
9. Knobloch J, Schild K, Jungck D, Urban K, Müller K, Schweda EK, Rupp J, Koch A (2011) The T-helper cell type 1 immune response to gram-negative bacterial infections is impaired in COPD. *Am J Respir Crit Care Med* 183: 204–214
10. Güttsches AK, Löseke S, Zähringer U, Sonnenborn U, Enders C, Gatermann S, Buße A (2012) Anti-inflammatory modulation of immune response by probiotic *Escherichia coli* Nissle 1917 in human blood mononuclear cells. *Innate Immun* 18:204–216

## Capillary Electrophoresis Chips for Fingerprinting Endotoxin Chemotypes and Subclasses

Béla Kocsis, Lilla Makszin, Anikó Kilár, Zoltán Péterfi, and Ferenc Kilár

### Abstract

Endotoxins (lipopolysaccharides, LPS; lipooligosaccharides, LOS) are components of the envelope of Gram-negative bacteria. These molecules, responsible for both advantageous and harmful biological activity of these microorganisms, are highly immunogenic and directly involved in numerous bacterial diseases in humans, such as Gram-negative sepsis. The characterization of endotoxins is of importance, since their physiological and pathophysiological effects depend on their chemical structure. The differences among the LPS from different bacterial serotypes and their mutants include variations mainly within the composition and length or missing of their O-polysaccharide chains. Microchip electrophoretic methodology enables the structural characterization of LPS molecules from several bacteria and the quantitative evaluation of components of endotoxin extracts. The improved microchip electrophoretic method is based on the direct labeling of endotoxins by covalent binding of a fluorescent dye. The classification of the S-type LPSs can be done according to their electrophoretic profiles, which are characteristics of the respective bacterial strains. According to the number, distribution, and the relative amounts of components in an endotoxin extract, it is possible to differentiate between the S-type endotoxins from different Gram-negative bacterial strains. The microchip electrophoresis affords high-resolution separation of pure and partially purified (e.g., obtained from whole-cell lysate) *S* and *R* endotoxins. This microchip technique provides a new, standardizable, fast, and sensitive method for the detection of endotoxins and for the quantitative evaluation of components of an endotoxin extract.

**Key words** Endotoxin, Lipopolysaccharide, LPS, Chemotype, Whole-cell lysate, Fluorescent labeling, Microchip electrophoresis, Endotoxin profiles

---

### 1 Introduction

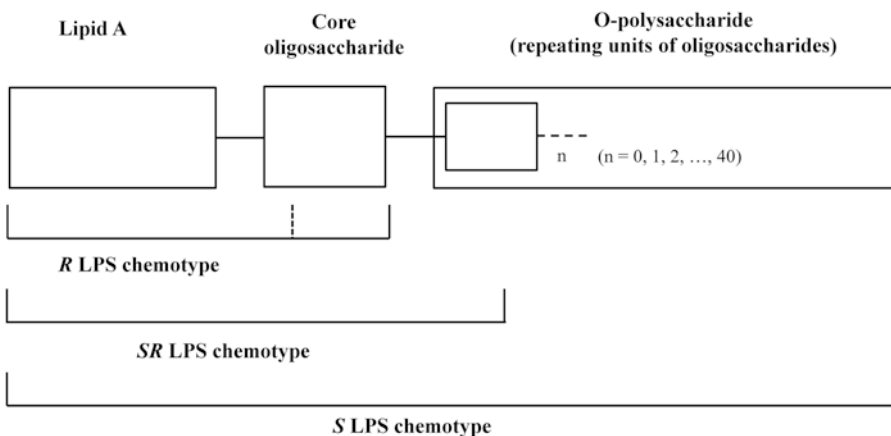
Endotoxins (lipopolysaccharides, LPS; lipooligosaccharides, LOS) are components of the envelope of most Gram-negative bacteria [1]. These molecules, responsible for both advantageous and harmful biological activity of these microorganisms, are highly immunogenic and can be directly involved in numerous bacterial diseases in humans, such as Gram-negative sepsis [2]. The amphiphilic LPS compounds consist of a hydrophobic lipid region (lipid A) covalently substituted by a hydrophilic oligo- or polysaccharide

region [3]. Typically, the polysaccharide region of *S* (smooth) LPS chemotypes consists of a core and an O-polysaccharide chain, whereas the *R* (rough) LPS or LOS chemotypes lack the O-polysaccharide chain and sometimes even the core components (see Fig. 1). The differences among the LPSs from different bacterial serotypes and their mutants include variations mainly within the composition and length or missing of the O-polysaccharide chains. The characterization of endotoxins is of importance, since their physiological and pathophysiological effects depend on their chemical structure.

When a large number of bacterial mutants and their LPS content are to be compared, for instance, in the preparation of vaccines, LPSs are detected directly from bacterial cultures, generally by the relatively short method of Hitchcock and Brown [4]. The procedure involves the enzymatic digestion of whole-cell lysates (by lysozyme and proteinase K enzymes) leading to partially purified, protein-free total cellular LPS. An important feature of this method is that only 1 mL culture volume is necessary for the characterization of LPSs, besides it has a short overall process-time (ca. 40 h).

The analysis of intact LPS molecules and the classification of the chemotypes are routinely checked by sodium dodecyl sulfate-polyacrylamide gel electrophoresis (SDS-PAGE) with silver-staining detection [5].

The fast analyses of Gram-negative bacterial endotoxins with microchip electrophoresis have been described either using noncovalent binding of a fluorescent dye (see the application of the *Agilent Protein 80 LabChip*) [6–8], or using the covalent binding of a fluorescent dye to the ethanolamine groups of the endotoxins (see the application of the *High Sensitivity Protein 250 LabChip*) [8, 9]. The separation is performed with a sieving matrix included in the



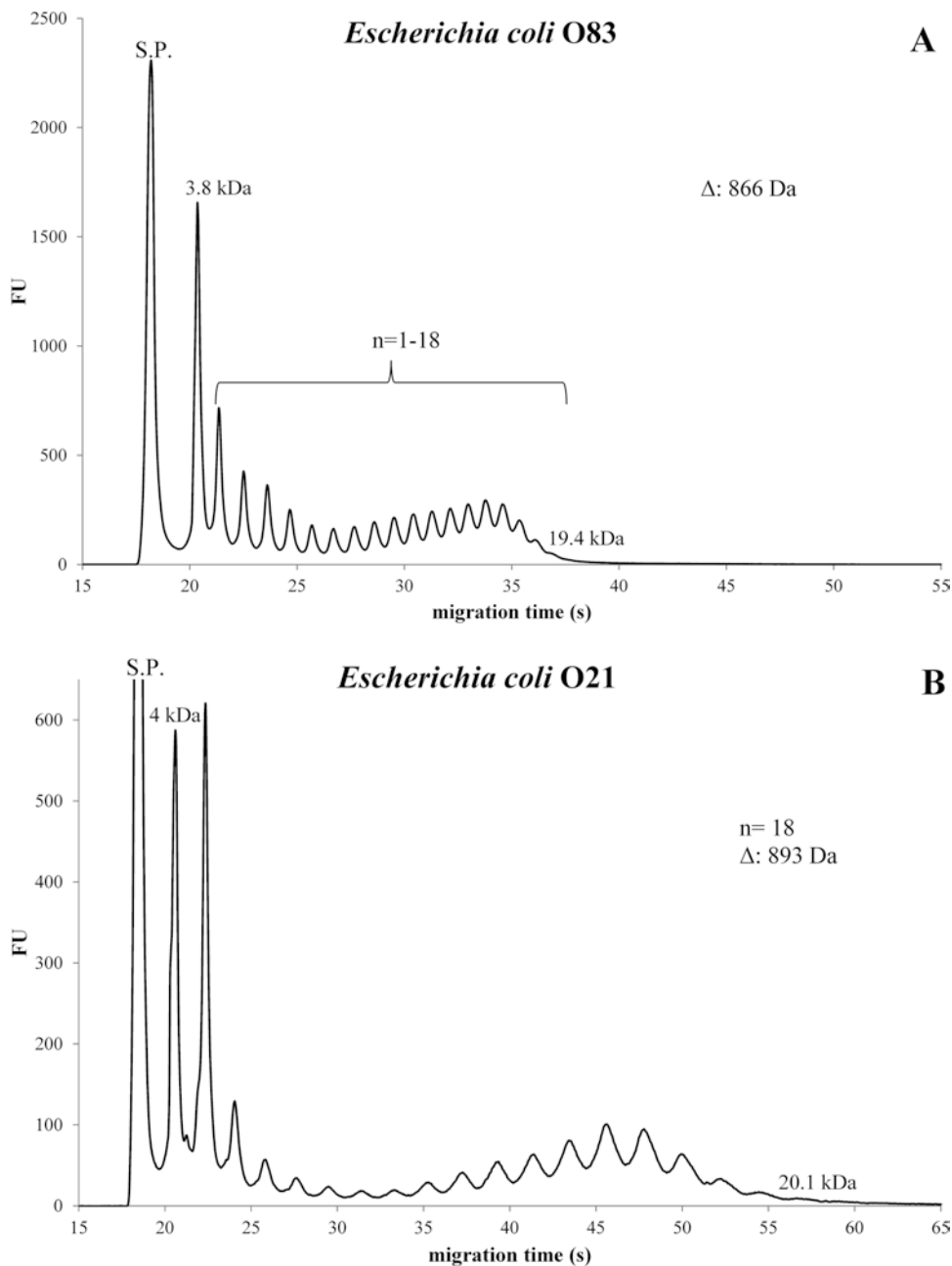
**Fig. 1** Basic structure of endotoxins (lipopolysaccharides, LPSs) from Gram-negative bacteria.  $n$ : the number of repeating units, *R*-type endotoxins (LOS):  $n = 0$ ; *SR*-type endotoxins:  $n = 1$ , *S*-type endotoxins (LPS):  $n > 1$

kits, which provides optimal resolution for the separation of LPS molecules with different compositions, chain-lengths, and concentration. With the use of these microchip analyses 11 endotoxin assignments can be performed within ca. 1 h. Optimization of the experimental conditions (the sample pretreatment, the concentration of the solutions, and the separation time), along with the classification, molecular mass estimation, and quantitative analyses of endotoxin components from purified LPS or partially purified samples from whole-cell lysates, has been made systematically.

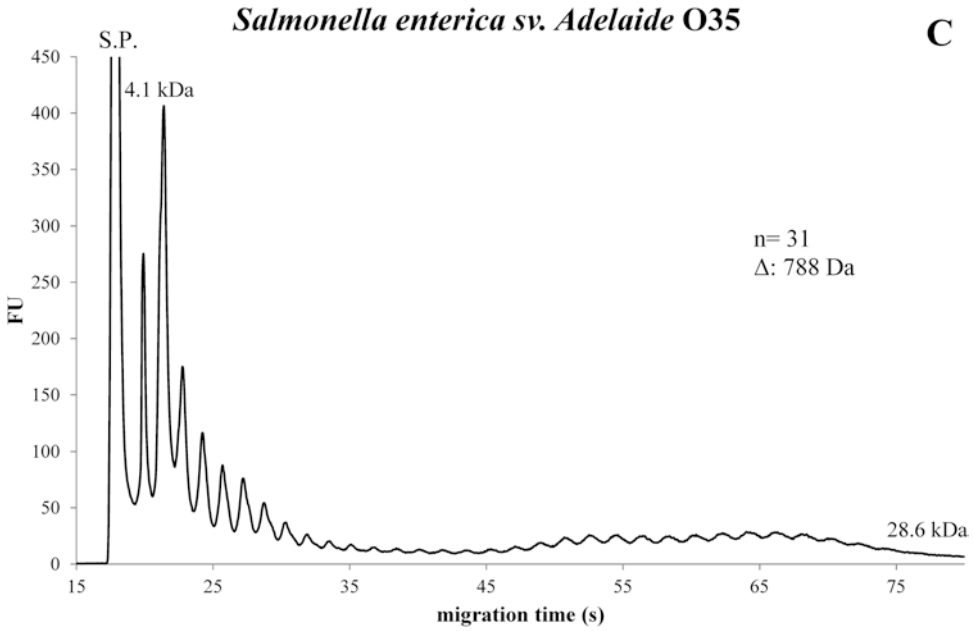
The classification of LPS can be done according to the electrophoretic profiles, which are characteristics of the respective bacterial strains. The LPS components appear as multiple “waves” of peaks. According to the number, distribution, and the relative amounts of components, differentiation of two main groups (*groups 1* and *2*), and within *group 1*, three subgroups (*groups 1a*, *1b*, *1c*) (Fig. 2a–c) can be made. Components with 13 or 15 repeating units, appearing with relatively high amounts, possess molecular masses of ca. 15,500 Da in *group 1a*, or ca. 17,000–18,000 Da in *group 1b*, respectively. In *group 1c*, the relative “maximum” in the quantity distribution appears at components with ca. 23–24,000 Da, corresponding to 18–29 repeating units. The definite decrease in the relative amounts of the LPS components in *group 2* (Fig. 3) up to a molecular mass of ca. 23 kDa is a quite characteristic, while the first endotoxin component (with a molecular mass of 4400 Da) is produced in about 50 times higher amount, compared to the other LPS components.

It is highly important to estimate the molecular masses of endotoxin components. However, the determination of the exact molecular masses in SDS-PAGE is not possible, because molecular mass standards in this technique are available only for proteins. In contrast, the microchip electrophoresis method may be used for molecular mass estimation based on the calculated molecular masses of LPS components with known structures. Constructing the  $\log M$  versus  $1/t$  diagrams, using mass data previously known (e.g., with MS or NMR studies) the molecular masses of the components can be estimated [9] (Fig. 4). It should be noted that endotoxins classified into group 1a have a different  $\log M$ - $1/t$  line compared to the others showing the significant difference in the migration properties of the endotoxin components in group 1a as compared to those in the other groups. For instance, components with 24,000 Da in group 1a are detected at ca. 38 s, while components in the other groups with the same mass migrate much slower (detection time is ca. 58 s) (Fig. 4).

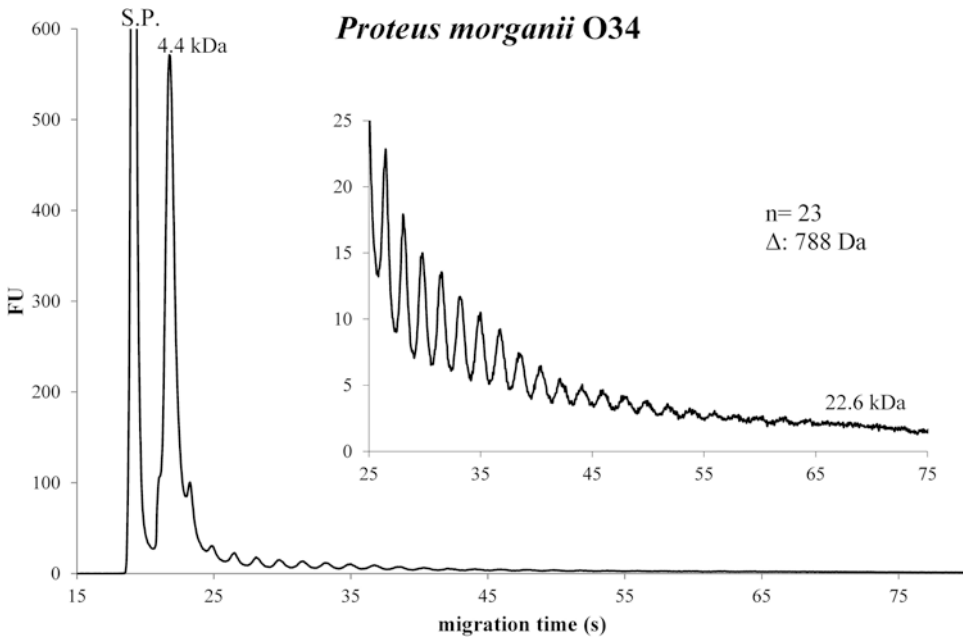
The electrophoretic profiles of purified LOS samples extracted from *Shigella sonnei* 4303 (phase II) and *Salmonella enterica* sv. *Minnesota* (*Salmonella* Minnesota) R595 show only one or two, low-molecular-mass components (Fig. 5). These low molecular



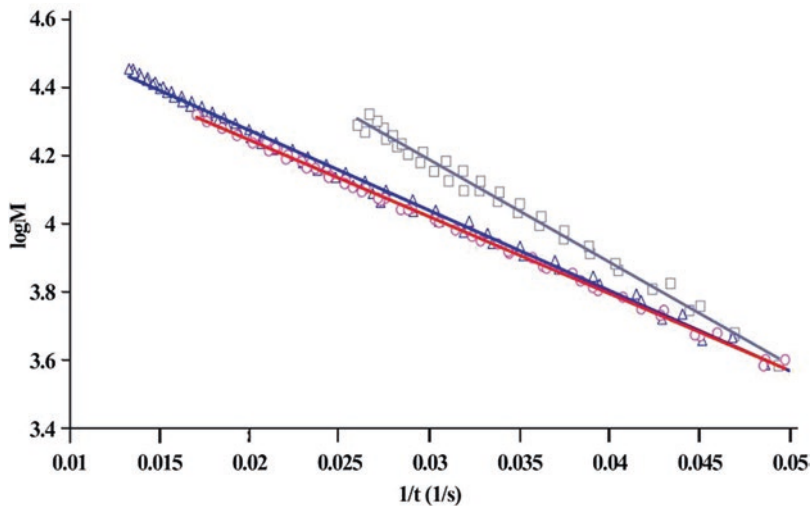
**Fig. 2** Microchip electrophoretic profiles of LPS components prepared from bacteria of (a) *Escherichia coli* O83 (group 1a); (b) *Escherichia coli* O21 (group 1b); and (c) *Salmonella* Adelaide O35 (group 1c). The LPS molecules are visualized by covalently bound fluorescent dye applying the *High Sensitivity Protein 250 LabChip* kit. Experimental conditions: HSP 250 Protein microchip; running buffer, polydimethyl-acrylamide-based linear polymer solution at pH 8 (its adsorption to the capillary wall reduces electroosmotic flow to almost zero, thus the negatively charged LPS-dye-SDS complexes migrate toward the anode); fluorescence detection with 630 nm excitation and 680 emission wavelengths; injection: 80 s at 1000 V; separation: 60 or 90 s at 900 V. The sample concentration applied in the chip wells is 0.1  $\mu\text{g}/\mu\text{L}$ . The first peak corresponds to the system peak (S.P.), i.e., the signal of the nonbound dye, while the subsequent peaks in the electropherogram correspond to LPS components with increasing numbers ( $n$ ) of repeating units in their O-polysaccharide chain (i.e., the first endotoxin peak corresponds to a component built from the lipid A and the core parts). The estimated molecular masses of the first and last sample peaks are indicated.  $\Delta$ : molecular mass of a repeating unit (Da)



**Fig. 2** (continued)



**Fig. 3** Microchip electrophoretic profiles of LPS from *Proteus morganii* O34 prepared from bacteria (group 2). Experimental conditions are the same as in Fig. 2



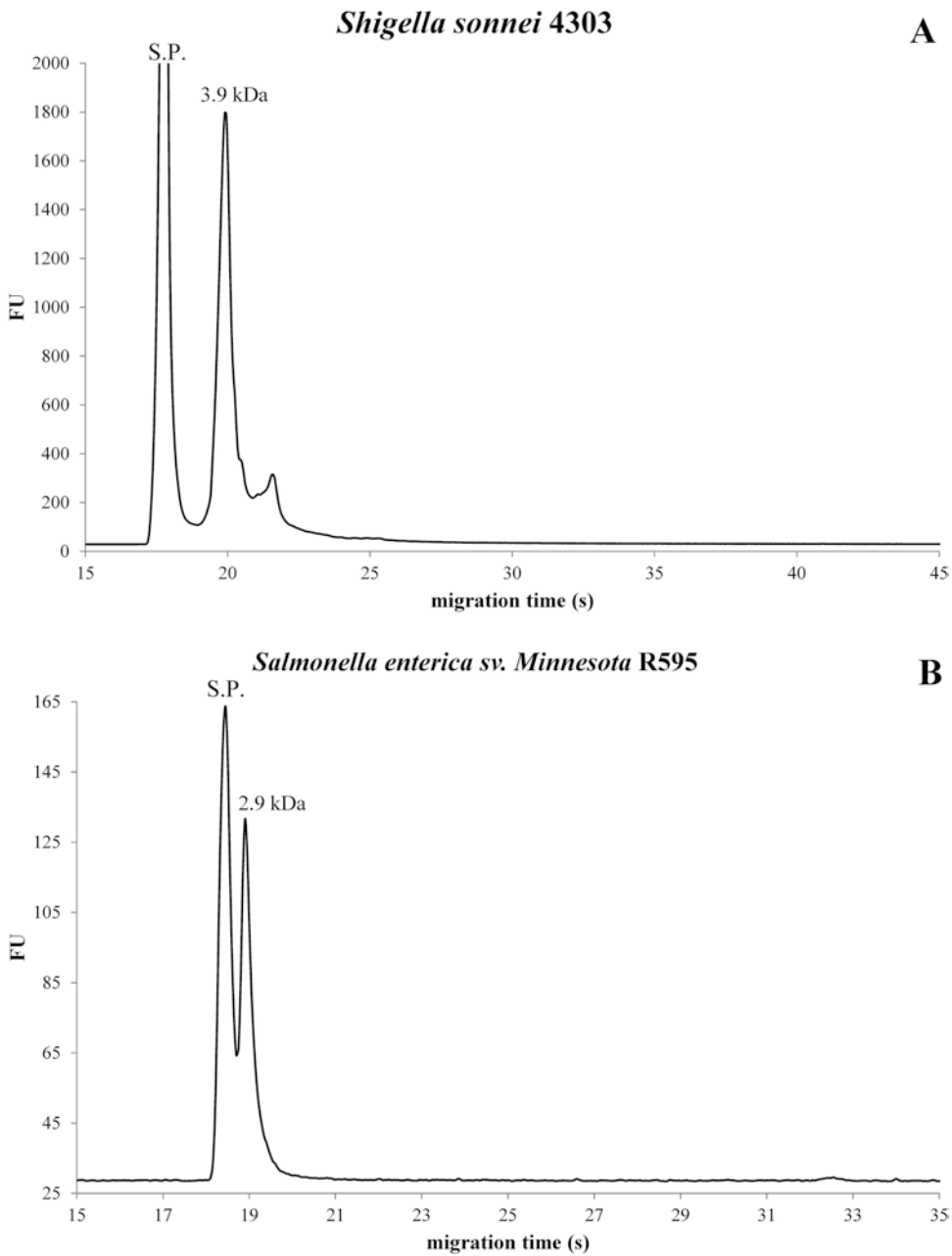
**Fig. 4** The  $\log M$  versus  $1/t$  calibration curves for the endotoxin components. The molecular masses of the LPS known from other studies are used to construct the lines. The calibration lines for *group 1a* (square), *group 1b* (circle), and *group 1c* (triangle) are calculated from the migration data in the electropherograms in Figs. 2 and 3 [9]

components sometimes partially overlap with the system peak (see Fig. 5b).

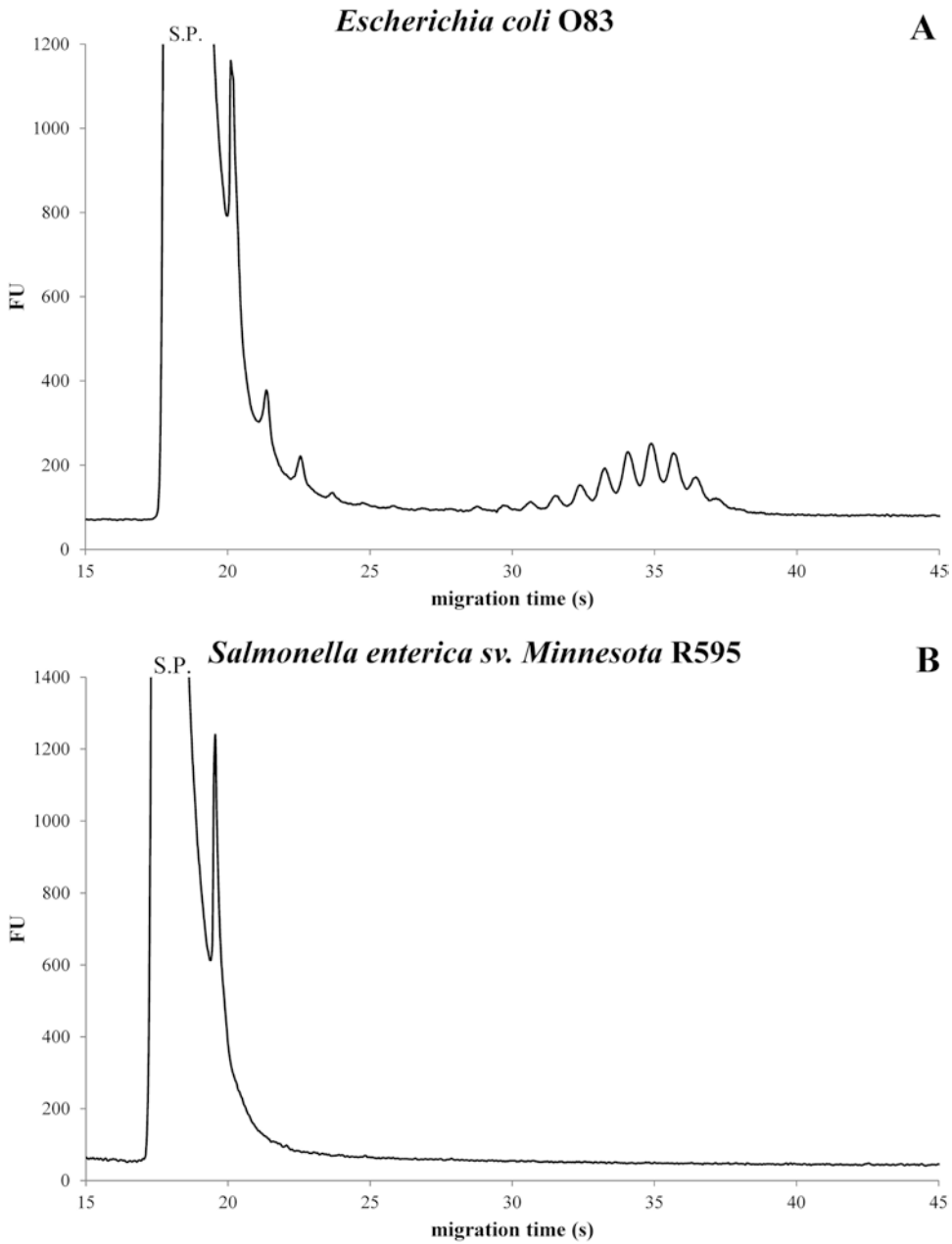
The limits of detection values (at  $S/N = 3$ ), obtained with the covalent labeling of LPS or LOS, are considerably lower (0.43 and 1.13 ng/ $\mu$ L, applying the *High Sensitivity Protein 250 LabChip* analyses for the LPS and LOS, respectively) than those found in the previously developed microchip method using noncovalent labeling of the LPSs (ca. 5 ng/ $\mu$ L LPS with the *Protein 80 LabChip*).

Protein-free LPS samples, obtained from bacterial lysates, can be directly analyzed (without further purification) with the microchip electrophoresis method. Fig. 6a shows the electrophoretic profile of the partially purified LPS in the *E. coli* O83 whole-cell lysate. The “wave-like” pattern of 20 peaks is consistent with the profile in Fig. 2a, although the relative peak area ratios are slightly different in the two patterns. The analysis of an *R*-type partially purified endotoxin sample prepared from the whole-cell lysate of *Salmonella* Minnesota R595 bacteria is shown in Fig. 6b. The electropherogram shows a single-component profile analogue to the purified *R*-chemotype endotoxin in Fig. 5b.





**Fig. 5** Microchip electrophoretic profiles of *R*-type (a) *Sh. sonnei* 4303 and (b) *S. Minnesota* R595 endotoxin components prepared from bacteria. The experimental conditions are the same as in Fig. 2, except for that the *S. Minnesota* R595 sample was diluted 1:200. One (or two) component(s) is (are) found in the LOS. The major sample peak appears as fast-migrating, small-molecular-mass substance after (and in some cases partially overlapping with) the system peak (S.P.)



**Fig. 6** Microchip electrophoretic profiles of partially purified endotoxin samples from whole-cell lysates of (a) S-type *E. coli* O83 and (b) rough R-type *S. Minnesota* R595 bacteria. The experimental conditions are the same as in Fig. 2. Although the electrophoretic profiles of these partially purified LPS are very similar to those of the pure LPS of the same strains (Figs. 2a and 5b, respectively), the relative peak area ratios are slightly different in the two patterns

## 2 Materials

### 2.1 Bacterial Cell Culture and Lysis

1. Bacterial stock is stored at  $-80^{\circ}\text{C}$ .
2. 5 mL Mueller-Hinton broth (Oxoid Ltd., UK): 3.0 g beef extract, 17.5 g acid hydrolysate of casein, 1.5 g starch in 1 L deionized water. Store the broth at  $4^{\circ}\text{C}$ .
3. Dissolve lysozyme in water at 100 mg/mL and store at  $-20^{\circ}\text{C}$ .
4. LPS lysing buffer: 2% (w/v) sodium dodecyl sulfate (SDS), 4% (v/v)  $\beta$ -mercaptoethanol, 10% (w/v) glycerol, 1 M Tris-HCl buffer, pH 6.8, 0.05% (w/v) bromophenol blue. Store at  $25^{\circ}\text{C}$ .
5. Proteinase K enzyme. Store at  $-20^{\circ}\text{C}$ .
6. Ethanol/magnesium-chloride solution: Dissolve magnesium-chloride (3.8 mg) in 50 mL ethanol and store at  $25^{\circ}\text{C}$ . The reagents are of analytical grade.

### 2.2 Preparation of Pure LPS

1. Gram-negative bacterial stock is stored at  $-80^{\circ}\text{C}$ .
2. Extraction of pure S-type LPSs is carried out with the *hot phenol-water extraction* method of Westphal et al. [10]: 110 g phenol and 65 mL distilled water, 100 mg of sodium chloride (per 100 g of wet cells), cold acetone, sodium hydroxide.
3. The R-type pure LPSs are obtained by the phenol-chloroform-light petroleum method of Galanos et al. [11]. Extraction was made in liquid phenol (90 g dry phenol and 11 mL water), chloroform, and light petroleum in a volume ratio of 2:5:8.

### 2.3 LPS Covalently Labeled with Fluorescent Dye

1. 30 mM Tris/HCl buffer, pH 8.5 (store at  $4^{\circ}\text{C}$ ).
2. Sieving matrix: 4.5% polydimethyl-acrylamide-based linear polymer in an SDS-containing buffer, pH 8.0 (this is included in the *Agilent High Sensitivity Protein 250 LabChip* kit).
3. Destaining solution: this solution is included in the *Agilent High Sensitivity Protein 250 LabChip* kit.
4. Sample buffer/DTT solution: Mix 100  $\mu\text{L}$  sample buffer (included in the *Agilent High Sensitivity Protein 250 LabChip kit*) with 3.5% (v/v) 1 M 1,4-dithiothreitol (DTT). Store at  $-20^{\circ}\text{C}$ .
5. Mix the labeling dye (a fluorescent dye included in the *Agilent High Sensitivity Protein 250 LabChip* kit) with DMSO: Add 54  $\mu\text{L}$  DMSO onto the pellet of 1 vial labeling dye and mix until all solid components are completely dissolved (the fluorescent dye reagent needs reconstitution in DMSO, which is known to facilitate the entry of organic molecules into tissues, so it should be used with appropriate care). Prepare a diluted dye solution (2  $\mu\text{L}$  stock solution diluted ten times with 18  $\mu\text{L}$

distilled water) daily for the labeling experiments. Store the dye in the dark (*see* **Note 1**).

6. Ethanolamine (this is corrosive) is stored at  $-20\text{ }^{\circ}\text{C}$ .

#### **2.4 Electrophoresis on Microchip**

1. Microchip developed for protein sizing [12] (e.g., Agilent *High Sensitivity Protein 250* chip from Agilent Technologies).
2. Agilent 2100 Bioanalyzer system equipped with a diode laser for fluorescence detection (Agilent Technologies) and with 2100 Expert software.
3. Syringe priming station for filling the microchip (Agilent Technologies).
4. Electrode cleaner (Agilent Technologies). This is a microchip without capillaries; thus, the space connecting the wells can be filled with ca. 350  $\mu\text{L}$  aqueous solution.

---

### **3 Methods**

These instructions describe the analyses of pure and partially purified endotoxin samples from whole cell lysates of bacteria and assume the use of the Agilent 2100 Bioanalyzer microchip electrophoresis system. The methods are easily adaptable to other microchip formats. It is critical that the molecular mass range of the sieving matrix used for the separation of LPS components is optimal and fluorescent dye is used for labeling and detection.

#### **3.1 Preparation of Pure LPS**

1. Grow the bacteria at  $37\text{ }^{\circ}\text{C}$  in Mueller–Hinton broth in a fermentor (e.g., Biostat U30D, Braun Melsungen, Germany) until the late logarithmic phase (about 10 h) and then collect the cells by centrifugation.
2. Prepare pure LPS by applying the hot phenol–water extraction method [10], by extracting the hydrophilic LPSs from smooth Gram-negative bacteria. Suspend 20 g acetone-dried bacteria in distilled water, mix this bacterial suspension and 90% w/v phenol/water 1:1 (v/v), and heat it up to  $65\text{ }^{\circ}\text{C}$  for 10 min. After the LPS are extracted, let the mixture cool down and centrifuge it at  $4\text{ }^{\circ}\text{C}$ . Collect the water phase that contains the LPS. Repeat the extraction step twice. Dialyze the combined water phases in a tubing (Kalle GmbH, Wiesbaden, Germany) against tap water for 3 days, and against distilled water for another 3 days. Concentrate the dialyzate in a rotary evaporator and ultracentrifuge the crude extract three times for 4 h at  $100,000 \times g$ . Re-suspend the sediment in distilled water and freeze-dry it.
3. Store the endotoxins in lyophilized form, and prepare 2 mg/mL suspensions in phosphate-buffered isotonic saline solution before use.

### 3.2 Preparation of Pure LOS

1. Grow the bacteria at 37 °C in Mueller–Hinton broth in a fermentor until the late logarithmic phase (about 10 h) and then collect the cells by centrifugation.
2. Extract the LOS from acetone-dried bacteria according to [11], which is an efficient extraction method for the hydrophobic LOS (lacking the hydrophilic O-side chains) from rough bacteria. Suspend the bacteria (20 g) in 100 mL phenol-chloroform-light petroleum (2:5:8, v:v:v) and stir for about 20 min. Precipitate the LOS dropwise with distilled water from the phenol extract after evaporation of chloroform and light petroleum in a rotary evaporator. Wash the precipitated LOS with diethyl ether, dry it in a fume hood, dissolve it in water, and centrifuge it at  $100,000 \times g$  for 4 h. Re-suspend the sediment in distilled water and freeze-dry it.
3. Store the LOS in a lyophilized form, and prepare 2 mg/mL solutions in phosphate-buffered isotonic saline solution before use.



### 3.3 Preparation of LPS Samples from Whole-Cell Lysate

1. Streak bacterial stocks on a Mueller-Hinton agar plate and grow overnight at 37 °C in a bacterial incubator.
2. Transfer one colony into 5 mL of Mueller-Hinton broth using a sterile inoculating loop and incubate at 37 °C on a shaker overnight.
3. Collect 1 mL of the cell culture in an Eppendorf tube and wash with 1 mL water once by centrifugation at  $6000 \times g$  for 3 min.
4. Re-suspend the pellets in 1 mL water and heat at 100 °C for 30 min.
5. Transfer 200  $\mu$ L of the cooled suspension to an Eppendorf tube and add 4  $\mu$ L of the lysozyme solution. Incubate the mixture at 37 °C for 30 min. During this process the peptidoglycan layers of the bacterial cell wall are disintegrated.
6. Add 200  $\mu$ L of the LPS lysing buffer to the cooled mixture and incubate the lysates at 100 °C for 10 min. During this step cellular materials, such as proteins, LPS, nucleic acids, cell debris, are released from the bacterial cells.
7. For proteolytic digestion, dissolve Proteinase K at 20  $\mu$ g/ $\mu$ L in water, and add 20  $\mu$ L of this in two portions (10–10  $\mu$ L) to the cell lysate and incubate at 65 °C for 4 h (the second portion is added in the middle of the incubation time, i.e., after 2 h).
8. Precipitate the LPS content by adding 800  $\mu$ L of the ethanol/magnesium-chloride solution and store the mixture at –20 °C overnight.
9. Centrifuge the mixture at  $13,000 \times g$  for 15 min, and suspend the sediment (containing LPS) in 30  $\mu$ L deionized water and sonicate in an ultrasonic bath.

### 3.4 Preparation of LPS Covalently Labeled with Fluorescent Dye

1. Add the LPS samples to the Tris/HCl buffer in 9:1 ratio (*see Note 2*), e.g., 4.5  $\mu\text{L}$  LPS sample and 0.5  $\mu\text{L}$  Tris/HCl buffer.
2. Mix 5  $\mu\text{L}$  of LPS samples in Tris/HCl buffer with 0.5  $\mu\text{L}$  of the fluorescent dye/DMSO solution and incubate for 10 min at room temperature (*see Note 2*).
3. Add 0.5  $\mu\text{L}$  of ethanolamine and incubate for 10 min at room temperature. During this step the excess dye is quenched after reaction with ethanolamine.
4. Dilute the LPS sample mixtures tenfold with deionized water.
5. Combine 4  $\mu\text{L}$  of the labeled and diluted LPS sample mixtures with 2  $\mu\text{L}$  of the sample buffer/DTT solution and incubate at 100 °C for 5 min, then centrifuge (6000  $\times g$ , 15 s).

### 3.5 Loading the Microchip for the Electrophoresis

1. Fill the capillaries of the microchip with sieving matrix. Pipette 12  $\mu\text{L}$  of the sieving matrix (*see Note 3*) in the well marked with  and fill the chip channels hydrodynamically applying the special *syringe priming station*.
2. Adjust the base-plate of the syringe priming station to position “A” and the syringe clip to its middle position.
3. Put the microchip in the priming station and the plunger at 1 mL.
4. Close the syringe priming station and press the plunger until held by the clip.
5. Release the clip after 90 s and slowly pull back the plunger to 1 mL position after 5 s, the priming station is then opened.
6. After the filling, make sure that no bubbles are present in the capillaries. The filling is proper if the capillaries cannot be seen on the backside of the chip.
7. Pipette 12  $\mu\text{L}$  of the sieving matrix (*see Note 3*) in the other three wells marked with “G” and 12  $\mu\text{L}$  of the destaining solution in the well marked with “DS” (*see Note 4*).
8. Load 6  $\mu\text{L}$  of LPS samples onto the sample wells in the microchip, and in the *Ladder well* marked with  (*see Note 5*). Fill all sample wells and the Ladder well of the microchip before the electrophoretic analysis.
9. Place the loaded microchip in the Agilent 2100 Bioanalyzer equipment (*see Note 6*).

### 3.6 Electrophoresis on Microchip Using Agilent 2100 Bioanalyzer

1. Place the loaded chip in the receptacle of the Agilent 2100 Bioanalyzer and carefully close the lid, so the electrodes in the cartridge fit into the wells of the chip.
2. Select the High Sensitivity Protein 250.xsy assay (for the analysis of the covalently labeled LPS samples) from the *Assay* menu

and start the assay immediately by clicking on the start button (*see Note 7*).

3. The analyses of all samples in the microchip are accomplished within 30 min (*see Note 8*). The data procession by the software includes baseline correction, alignment of separated runs in one chip, and the display of the peak data in the microchip electropherograms as gel-like images on a gray scale (this is not shown here). In all samples the peaks corresponding to the LPS components appear directly after the first (relatively big) system peak (*see Note 9*). The LPS appear as multiple “waves” of peaks (LPS components) with a broad molecular mass distribution (containing both, high and low mobility components), according to the number of repeating units in the O-polysaccharide chain, while the LOS contain only one (or two) peak(s) with high mobility (low molecular mass) component(s) since they lack the O-polysaccharide chain. Examples of results are shown in Figs. 2 and 3.
4. Immediately remove the chip from the Agilent 2100 Bioanalyzer when the assay is finished (*see Note 10*).
5. After removing the microchips, apply the electrode cleaner to remove possible contaminants from the electrodes. Slowly fill one of the wells of the electrode cleaner with 350  $\mu\text{L}$  deionized water and then place it in the Agilent 2100 Bioanalyzer. Close the lid and wait for about 10–30 s before the removal of the electrode cleaner.

### **3.7 Determination of the Molecular Masses of the LPS Components**

1. Calculate the molecular masses of LPS components (i.e., lipid A, core region, and repeating units) with known structures from other experiments, such as MS or NMR.
2. For the endotoxins, however, of which all three data are not known, it is possible to construct the  $\log M$  versus  $1/t$  diagrams.
3. Apply the available calibration curves (*see Fig. 4*) for endotoxin components, of which the molecular structures (masses) of one or more constituents are not known, and estimate the molecular masses.

---

## **4 Notes**

1. Remove light covers only when pipetting. The dye contained in the reagents decomposes when exposed to light and this reduces the signal intensity.
2. Use 0.5 mL vials. Using larger vials may lead to poor results, caused by evaporation.

3. Always insert the pipette tip to the bottom of the well when dispensing the liquid. Placing the pipette at the edge of the well may lead to poor results.
4. The unbound fluorescent dye present in the capillary channels is diluted before the detection. The diluting solution consisting of Tris/HCl buffer and SDS without sieving matrix is introduced via a cross-section just before the detection point. This helps to get a better signal-to-noise ratio.
5. The original protein chip kit uses the ladder well for the determination of the molecular masses of proteins. A molecular mass standard mixture would be injected into this ladder well, but—since the protein standards have different migration properties than LPS—the determination of the molecular masses of LPS components cannot be done with the help of those standards. *See* the molecular mass estimation in Subheading 3.6. The ladder well, hence, this well can be used for the analysis of an eleventh sample.
6. Loaded chips should be used within 5 min. Reagents and the sample solutions may undergo evaporation, leading to poor results.
7. The Agilent 2100 Bioanalyzer should not be touched during analysis and should never be placed on a vibrating surface.
8. The analysis starts with the electrophoretic injection into the capillaries for 80 s (the injected volume is ca. 40 pL) and the run times are 60 or 90 s (the collection of the data starts at ca. 10 s after the voltage is applied).
9. The complex of the fluorescent dye and ethanolamine generally appears as a *system peak*. However, this does not disturb the separation of the LPS components. The sensitivity of this method is high, since satisfactory patterns are obtained from 1 mL bacterial cell cultures, which contain ca.  $10^8$  cells and the endotoxin content is less than 1 ng.
10. Leaving the chip for a period longer than 1 h in the Bioanalyzer may cause contamination of the electrodes.

---

## Acknowledgments

The work was supported by the grants TÁMOP 4.2.1/B-10/2/KONV-2010-0002, 4.2.2/B-10/1-0029, OTKA K-100667, and the UNKP-16-4 New National Excellence Program of the Ministry of Human Capacities. Lilla Makszin acknowledges the financial support of the PTE ÁOK-Post-Doc grant.



## References

1. Caroff M, Karibian D (2003) Structure of bacterial lipopolysaccharides. *Carbohydr Res* 338:2431–2447
2. Holst O, Ulmer AJ, Brade H, Flad H-D, Rietschel ET (1996) Biochemistry and cell biology of bacterial endotoxins. *FEMS Immunol Med Microbiol* 16:83–104
3. Magalhaes PO, Lopes AM, Mazzola PG, Rangel-Yagui C, Penna TCV, Pessoa A (2007) Methods of endotoxin removal from biological preparations: a review. *J Pharm Pharm Sci* 10:388–404
4. Hitchcock PJ, Brown TM (1983) Morphological heterogeneity among *Salmonella* lipopolysaccharide chemotypes in silver-stained polyacrylamide gels. *J Bacteriol* 154:269–277
5. Tsai CM, Frasch CE (1982) A sensitive silver stain for detecting lipopolysaccharides in polyacrylamide gels. *Anal Biochem* 119:115–119
6. Kilar A, Péterfi Z, Csorba E, Kilar F, Kocsis B (2008) Capillary electrophoresis chips for screening of endotoxin chemotypes from whole-cell lysates. *J Chromatogr A* 1206:21–25
7. Kilar A, Farkas V, Kovács K, Kocsis B, Kilar F (2008) Novel quantitative electrophoretic analysis of endotoxins on microchips. *Electrophoresis* 29:1713–1722
8. Kocsis B, Kilar A, Makszin L, Kovács K, Kilar F (2011) Capillary electrophoresis chips for fingerprinting endotoxin chemotypes from whole-cell lysates. In: Holst O (ed) *Microbial toxins: methods and protocols*. Springer, NY, pp 89–99
9. Makszin L, Kilar A, Felső P, Péterfi Z, Kocsis B, Kilar F (2012) Quantitative microfluidic analysis of S- and R-type endotoxin components with chip capillary electrophoresis. *Electrophoresis* 33:3351–3360
10. Westphal O, Lüderitz O, Bister F (1952) Über die Extraktion von Bakterien mit Phenol Wasser. *Z Naturforsch B* 7:148–155
11. Galanos C, Lüderitz O, Westphal O (1969) A new method for extraction of R-lipopolysaccharides. *Eur J Biochem* 9:245–249
12. Bousse L, Mouradian S, Minalla A, Yee H, Williams K, Dubrow R (2001) Protein sizing on a microchip. *Anal Chem* 73:1207–1212

## Micromethods for Isolation and Structural Characterization of Lipid A, and Polysaccharide Regions of Bacterial Lipopolysaccharides

Alexey Novikov, Aude Breton, and Martine Caroff

### Abstract

Lipopolysaccharides (LPS) are major components of the external membrane of most Gram-negative bacteria, providing them with an effective permeability barrier. They are essentially composed of a hydrophilic polysaccharide region (PS) linked to a hydrophobic one, termed lipid A. The LPS polysaccharide moiety is divided into the core oligosaccharide (OS) and O-chain repetitive elements. Depending on their individual variable fine structures, LPS may be potent immunomodulators. The lipid A structure is a key determinant for LPS activity. However, the presence of the core region, or at least of the highly charged 3-deoxy-D-*manno*-oct-2-ulosonic acid molecules, is also important for preserving the native lipid A conformation within individual LPS molecules. We describe herein four rapid and practical micromethods for LPS, lipid A, and core OS structural analyses. The first method allows the direct isolation of lipid A from whole bacteria cell mass; the second describes conditions for the sequential release of fatty acids enabling the characterization of their substitution position in the lipid A backbone, to be determined by matrix-assisted laser desorption/ionization mass spectrometry (MALDI-MS). The third one is a microscale procedure for the mass spectra screening of LPS, lipid A, and PS using triethylamine and citric acid. The fourth method is a chromatography procedure for Rough-type LPS on thin-layer-chromatography. These methods were developed to be coupled to mass-spectrometry (e.g., MALDI-MS) but can also be used with other analytical techniques (e.g., chromatography). Examples are given with reference to two major human pathogens: *Bordetella pertussis* and *Pseudomonas aeruginosa*; to one porcine pathogen: *Actinobacillus pleuropneumoniae*; and to commercial samples of *Salmonella* Minnesota Re595 LPS.

**Key words** Gas chromatography, 3-Deoxy-D-*manno*-oct-2-ulosonic acid, Lipooligosaccharide, Lipopolysaccharide, Matrix-assisted laser desorption/ionization mass spectrometry, Polyacrylamide gel electrophoresis, Sodium dodecyl sulfate, Triethylamine, Thin-layer chromatography

---

## 1 Introduction

Endotoxins are major components of the Gram-negative bacterial outer membrane and occur either as lipooligosaccharides (LOS) composed of a lipid A region covalently linked to a core oligosaccharide, or as lipopolysaccharide (LPS) composed of lipid A linked through a core oligosaccharide to a polysaccharide (O-chain),

made of repetitive oligosaccharide subunits. Lipid A is anchored in the outer layer of the external membrane. In some bacteria, it is a powerful immunomodulator, responsible for most of the biological activities of the LPS. Small LPS amounts from such bacteria can have beneficial effects, but larger amounts may cause endotoxic shock.

LPS and lipid A preparations are variably heterogeneous. This is seen in their ladder-like profile on SDS-PAGE or on thin-layer chromatograms (TLC) [1] and in LPS, lipid A, and PS mass spectra [2, 3]. This heterogeneity is due to different levels of biosynthesis related to different numbers of O-chain repetitive units, as well as to variability in other structural elements like fatty acids, phosphate groups, and other specific structural modifications (e.g., methylation, acetylation, substitution with different amino derivatives, etc.). LPS molecular masses range from about 2 to 20 kDa.

Analysis and comparison of the separated structural regions of LPS are usually performed on samples from preparative-scale extractions [2]. However, most commonly used methods for extracting both LPS and LOS are time-consuming and require an appreciable amount of bacteria.

We present here a method for the direct selective separation and extraction of lipids A from bacterial cells, and for their analysis by mass spectrometry (MS) [4]. The method, which is fast and easy, can be applied to  $\mu\text{g}$ -mg quantities of lyophilized bacteria, and is extremely efficient for analysis of bacterial isolates or samples recovered in vivo, as well as for checking modifications as a function of culture conditions for example. Use of the direct lipid A isolation method will be illustrated by MS analysis of *Pseudomonas aeruginosa* lipid A structural modifications induced by transitions between planktonic and biofilm growth styles of these bacteria [3].

Alkaline treatments of lipid A selectively remove ester-linked fatty-acids [5, 6]. Following the kinetics of fatty-acids release, specific to each type (primary or secondary-linked), by MS we obtained more detailed structural information with respect to lipid A acylation patterns. This second method is perfectly compatible with the first one, and can be applied to micro amounts of lipid A directly isolated from bacteria, as illustrated using lipid A and LPS of *Bordetella pertussis*, the agent of whooping cough [7, 8].

A third one, among our methods, consists in the rapid cleavage of LPS and isolation of the lipid A together with the PS moieties for MS screening [9]. The combination of triethylamine (TEA) a well-known lipid A solubilizing agent, and of citric acid, that we described for disaggregation of LPS aggregates [9] was used at a pH value of about 3.4 to 4.4, suitable for LPS mild hydrolysis at 100 °C. The potency of the two components was shown to increase the solubility, to improve desorption/ionization, as well as to preserve LPS labile residues during hydrolysis (amino acids,

phosphates). The screening of lipid A and PS mildly liberated from the crude LPS of different *Actinobacillus pleuropneumoniae* field isolates, a porcine pathogen, together with the comparison of different commercial LOS from *Salmonella* Minnesota Re595 mutant are illustrating here the potency of this method. The *S. Minnesota* deep-rough mutant LOS were selected for being repeatedly described in the literature as the simplest and shortest LOS. This quick description led many biologists to using these LOS as the more common standards for testing biological activities. We show herein by matrix-assisted laser desorption/ionization (MALDI)-MS that the structures of these LOS are not as simple and reproducible as thought, and recommend their characterization by MS before use. TLC analysis also demonstrates the level of heterogeneity and nonreproducibility.

---

## 2 Materials and Techniques

### 2.1 Bacterial Strains and Cultures

1. Grow Gram-negative bacterial cells in required experimental conditions.
2. Before harvesting, kill bacteria by a method appropriate for the species under study, e.g., in cold 2% phenol or by incubation for 40 min at 56 °C and then examine the growth for the absence of viable bacteria.

### 2.2 Chemicals

1. LPS: The three different commercial batches of LPS from Re595 *S. Minnesota*, SmRe595-1: L-9764 55F-4023, SmRe595-2: L-9764 121H4026, and SmRe595-3: L9764 075M4033V were all from Sigma-Aldrich and had been extracted by the phenol-chloroform-light petroleum method.
2. Solvents: Ultra-pure water was obtained with a Millipore Milli-Q® system (resistivity >18 MΩ cm). Chloroform and methanol were of Normapur grade.
3. Acids: Isobutyric acid (synthesis grade) and citric acid (Normapur grade).
4. Bases: Ammonia 28% solution (Normapur grade), methylamine 41% solution (purum grade), triethylamine.
5. MALDI-MS matrix: 2,5-Dihydroxybenzoic acid (DHB, purum grade).

### 2.3 Mass Spectrometry

Matrix-assisted laser desorption/ionization mass spectrometry (MALDI-MS) instructions can be followed using appropriate MALDI-MS system.

The presented MS experiments were performed in the linear mode, with delayed extraction, using a Perseptive Voyager STR (PE Biosystem, France) and/or a Shimadzu Axima Performance

time-of-flight mass spectrometer. The reflectron mode can be used to obtain a better resolution, but it could also lead to underestimation, or even loss, of some fragile molecular species (e.g., lipids A with substituted phosphate groups) due to their fragmentation between the ion-source and the reflector. Lipid A, cores, and LPS mass-spectra are recorded in the negative-ion mode at 20 kV with the adjustment of the extraction delay time to optimized resolution and signal-to-noise ratio. Spectra obtained in the positive-ion mode give important additional fragmentation data, but they will not be presented here [10] (*see Note 1*).

Analyte ions are desorbed from the DHB matrix by pulses from a 337 nm nitrogen laser. Addition of citric acid at a 0.1 M concentration to the matrix solution was found to greatly improve the resolution and signal-to-noise ratio of LPS, cores, and lipid A mass spectra [11]. Citric acid chelates cations, and by insertion between the molecules causes disaggregation of LPS and lipid A micelles, thus improving solubility and cocrystallization of the analyte with the matrix resulting in a better desorption/ionization process (*see Note 2*).

---

### 3 Methods

Isolation of lipid A is effected by mild hydrolysis of the acid-labile link between the proximal Kdo residue of the oligo- or polysaccharide and the lipid moiety of LPS. The most widely used acetic-acid hydrolysis method to liberate free lipid A can also cleave other acid-labile lipid A bonds such as those linking glycosidic phosphate, ethanolamine pyrophosphate, amino sugars {e.g., 4-amino-4-deoxy-L-arabinopyranose (Ara $\beta$ 4N) } or 2-amino-2-deoxy-D-glucopyranose (Glc $\beta$ N) [8] esterifying lipid A phosphate groups}. A later developed mild hydrolytic method using sodium-acetate at pH 4.4 [12] was modified by the addition of 1% SDS, in order to disrupt micelles formed by amphiphilic LPS molecules [13]. The modified method is presented here and used for the comparison with the new micromethod (also presented below) [4]. The latter procedure was found to be as mild as the former SDS-promoted hydrolysis and did not modify, or eliminate, any lipid A native element substitutions.

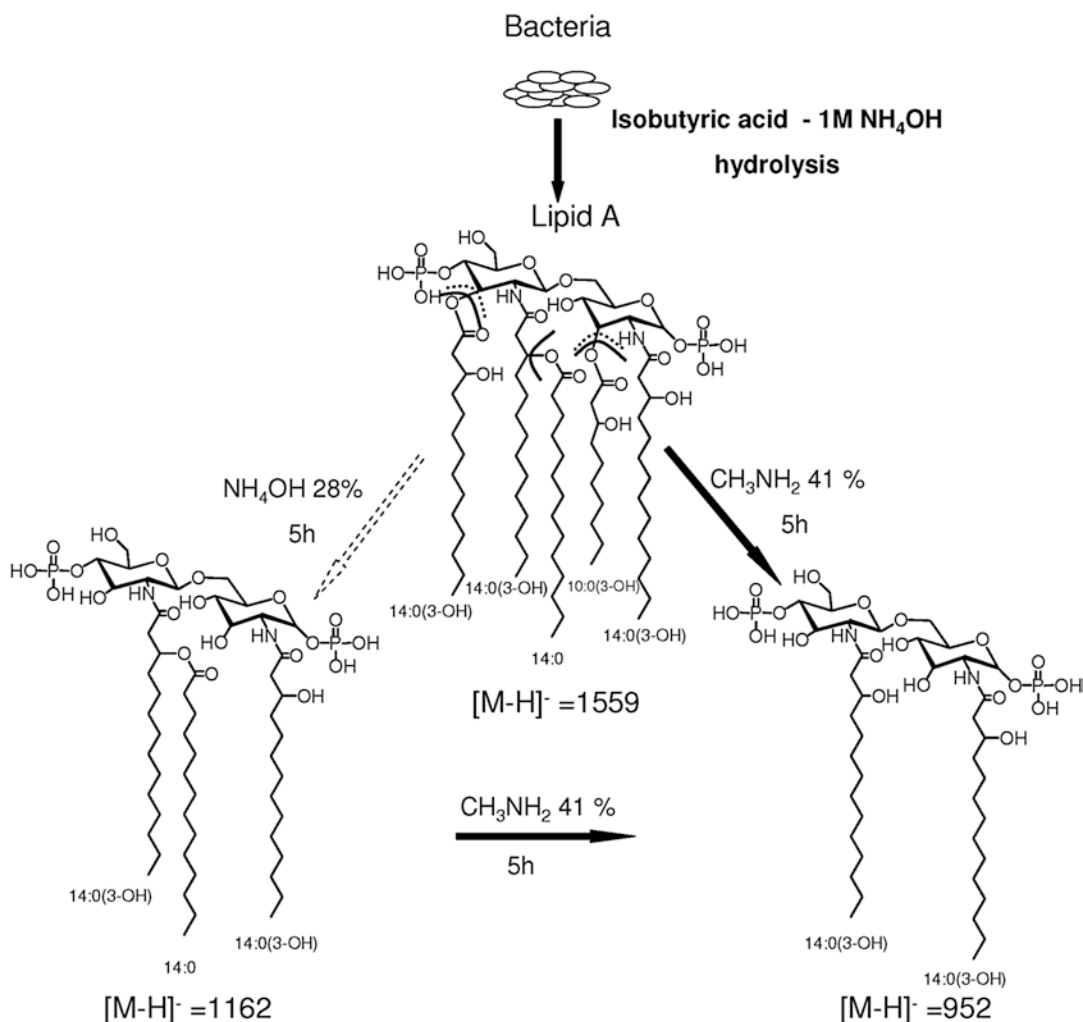
With the biological activities of LPS being intimately related to their structures [14, 15], it was a priority to find methods giving quick information on their structures, their stability and reproducibility with various batches, and their variability with their production under different growth conditions. As lipid A is responsible for most of the biological properties of the LPS molecule, it was necessary to find a new lipid A isolation method that was fast, mild, and applicable to microscale bacterial samples.

These conditions were achieved by hydrolyzing lipid A directly from the bacterial surface and using MALDI-MS for its characterization, i.e., establishing its molecular heterogeneity, degree of acylation, presence of some fatty acids, and other substituents [4]. Our aim was to develop methods for the production of sufficient material for several purposes in addition to direct MS analysis, e.g., analyses by chromatography and application of selective mild-alkaline treatments for the sequential liberation of fatty acids to establish lipid A acylation patterns. The latter is illustrated here with micro quantities of *B. pertussis* lipids A directly isolated from bacterial cells. The lipids A, which were isolated by micro-hydrolysis of the bacteria, can thus be further characterized in a few hours as schematized in Fig. 1 with *B. pertussis* lipid A structure.

The triethylamine-citrate method gives quick data for the structural analysis of lipid A and PS moieties after mild hydrolysis of the native LPS molecules. The method is illustrated with three *A. pleuropneumoniae* (App) field isolates and underlines the variability of core structures for LPS in a single species and even serotype. This method allows, at the same time, the screening of lipids A. In LPS commercial batches, it is indispensable to check the LPS structures present in a given sample as they could vary from one batch to another. The method, illustrated here with *S. Minnesota* Re595 LOS confirms its important role and reliability.

### **3.1 Isolation of Lipid A from LPS/LOS on a Normal Analytical Scale [13] (See Note 3)**

1. Suspend 5 mg of LPS or LOS in 500  $\mu\text{L}$  of a 10 mM sodium-acetate buffer (pH 4.4) containing 1% SDS in a screw-cap tube. Place in an ultrasonic bath to obtain a clear solution (*see* Notes 4 and 5).
2. Heat the sample at 100  $^{\circ}\text{C}$  for 1 h in an Eppendorf<sup>®</sup>-Thermomixer system or similar, under stirring at 1000 rpm. The duration can be adjusted depending on the solubility of the samples.
3. Cool in an ice-water bath and lyophilize the sample with an excess of water to avoid foam formation.
4. Remove SDS by washing with a mixture of 100  $\mu\text{L}$  of water and 500  $\mu\text{L}$  of acidified ethanol (prepared by adding 10  $\mu\text{L}$  of 4 M HCl to 2 mL of 95% ethanol). Centrifuge at 2000  $\times g$  for 10 min (*see* Note 6).
5. Wash the sample twice again with 500  $\mu\text{L}$  of nonacidified ethanol and centrifuge.
6. Extract the lipid A from the dried sample by 500  $\mu\text{L}$  of a mixture of chloroform:methanol:water (3:1.5:0.25; by vol.).
7. Dry the lipid A extract, disperse it in 500  $\mu\text{L}$  of water by sonication, and lyophilize to yield the lipid A as a powder.



**Fig. 1** Schematic representation of the analytical steps used for the analysis of lipid A isolated after hydrolysis of freeze-dried bacteria. The latter were hydrolyzed in a mixture of isobutyric acid-1 M ammonium hydroxide (5:3; by vol.) for 2 h at 100 °C. The *dotted arrow* indicates alkaline treatment for 5 h at 50 °C with 28% ammonium hydroxide leading to partial *O*-deacylation, and the *black arrows* indicate alkaline treatment for 5 h at 37 °C with 41% methylamine, leading to complete *O*-deacylation. The structure displayed is that of *B. pertussis* lipid A

**3.2 Isolation of Lipid A and PS/OS from LPS/LOS: A Rapid MicroScale Method, Using Triethylamine-Citrate, and Preserving Labile Constituents [9]**

This micromethod was aimed at using the TEA-citrate reagent for facilitating MS analysis thanks to its ability to disaggregate LPS molecules as well as to retaining bivalent cations. The method is thus used first for LPS analysis without heating, then for obtaining spectra of the separated lipid A and core constituents. MALDI-TOF is a semiquantitative MS method and it can be used to determine the composition and the predominant LPS species present in each sample (*see* **Notes 3** and **7**).

1. Suspend LPS/LOS samples in an Eppendorf® tube (*see Note 8*) at a concentration of 5 µg/µL for LOS and 10 µg/µL for LPS in 0.01 M TEA-citrate (1:1 molar ratio, pH 3.6). Disperse the suspension by agitation (vortex) and use of ultrasonic bath if available.
2. Dilute the 5–10 µg/µL stock solution to 1–2 µg/µL concentration with 0.01 M TEA-citrate. Sonicate it again. The sample is ready for MALDI-MS analysis as described in Subheading 3.4.
3. Split the lipid A and PS/OS regions by heating the initial sample (5–10 µg/µL) at 100 °C for 1 h in an Eppendorf®-Thermomixer system or similar, under stirring at 1000 rpm (*see Note 9*). The minimal final volume should be kept around 40 µL to avoid evaporation. Cool the samples for 5 min at 4 °C or in an ice-water bath and then perform a short 20 s spin to recover the drops from the top and vortex.
4. Analyze directly the hydrolyzed micro-samples by MS: Dilute the hydrolysate to 1–2 µg/µL concentration with 0.01 M TEA-citrate and sonicate. The sample is ready for MS analysis. Use DHB in 0.1 M aqueous citric acid as the matrix solution. Both lipid A and PS-related molecular ions are expected to be observed (*see Notes 1, 7 and 10*).
5. Lyophilize or desiccate the hydrolyzed samples.
6. Extract the excess of salt with methanol: add methanol at a concentration of 10 µg/µL and suspend the sample by sonication using an ultrasonic bath. Centrifuge the tube at 4 °C, 7000 × *g* for 10 min. Discard the methanol supernatant. Good practice would be to test the methanol supernatant by MALDI-MS to be sure that no specific molecular species are lost (*see Note 6*).
7. Extract the lipid A from the pellet with a mixture of chloroform:methanol:water (3:1.5:0.25; by vol.) at a concentration of 10 µg/µL. Suspend the pellet by sonication. Centrifuge the tube at 4 °C, 7000 × *g* for 10 min. Recover the supernatant.
8. Repeat **step 7** with half a volume of the chloroform:methanol:water mixture. Pool both chloroform:methanol:water supernatants. The sample is ready for lipid A analysis as described in Subheading 3.4.
9. Suspend the pellet in water at 10 µg/µL and homogenize by using vortex and sonication. Centrifuge the tube at 4 °C, 7000 × *g*, during 20 min. Dilute the supernatant containing the PS moiety if necessary, then deposit it on the MALDI sample plate, cover with the matrix solution (10 µg/µL DHB in 0.1 M aqueous citric acid), and let it dry as described in Subheading 3.4.



A quick version of the method also gives good results by testing native LPS samples suspended in TEA-Citrate as described. Then compare it to a sample of the same mixture directly after treatment at 100 °C. In this case, there is no need to remove salts; they were selected for direct use. The longer version of the method presented above is only necessary when samples have never been studied, when masses are not already known, and when superposed lipid A and core peaks cannot be sorted out. The quick method is very convenient for rapid comparison between different batches, growth conditions, species, or kinetics of hydrolysis (*see* **Notes 3, 4, 5, and 9**).

**3.3 Isolation of Lipid A from Whole Cells: A Micro Method [4] (See Note 3)**

1. After collecting a culture pellet, wash the cells with a buffer or water, only if necessary as it could fragilize LPS molecules, and lyophilized it.
2. Suspend 10 mg of lyophilized bacteria in 400  $\mu\text{L}$  of a mixture of isobutyric acid:1 M ammonium hydroxide (5:3; by vol.) under the hood, in a screw-cap tube and heat for 2 h at 100 °C with stirring (*see* **Notes 4 and 8**).
3. Cool the sample to 4 °C, and centrifuge at  $2000 \times g$  for 15 min.
4. Dilute the supernatant with water (1:1; by vol.) and lyophilize it.
5. Wash the material obtained twice with 400  $\mu\text{L}$  of methanol and centrifuge ( $2000 \times g$  for 15 min).
6. Extract the insoluble lipid A twice with 100  $\mu\text{L}$  of chloroform:methanol:water (3:1.5:0.25; by vol.). This extract can be used directly for MALDI-MS (*see* **Notes 1 and 7**).

**3.4 MALDI-Mass Spectrometry of Isolated LPS, Lipid A, and Core moieties [11]**

1. Take up LPS at 1  $\mu\text{g}/\mu\text{L}$  in water. Desalt the solution with a few grains of Dowex 50 W-X8 ( $\text{H}^+$ ) (*see* **Note 1**).
2. Take up lipid A in a mixture of chloroform:methanol:water (3:1.5:0.25; by vol.) at 1  $\mu\text{g}/\mu\text{L}$  or use directly the lipid A extract obtained in Subheading 3.2. Desalt the solution with a few grains of Dowex 50 W-X8 ( $\text{H}^+$ ) (*see* **Notes 1 and 10**).
3. Take up core and/or PS moieties at 1  $\mu\text{g}/\mu\text{L}$  in water. Desalt the solution with a few grains of Dowex 50 W-X8 ( $\text{H}^+$ ) (*see* **Notes 1 and 10**).
4. Drop 0.5–1  $\mu\text{L}$  of the different solutions on the target.
5. Add 0.5–1  $\mu\text{L}$  of the matrix solution (DHB dissolved at 10  $\mu\text{g}/\mu\text{L}$  in the same solvent for lipid A, or in 0.1 M citric acid in water for LPS and PS) and dry. Different ratios between sample and matrix have to be tested for defining the best concentrations (0.5:1/1:1/1:0.5).
6. Submit the sample on the target to MALDI-MS analysis, as described in Subheading 2.3 (*see* **Notes 1 and 7**).

### 3.5 Sequential Liberation of Ester-Linked Fatty Acids of LPS, or Lipid A, by Mild Alkali Treatment for Analysis by Mass Spectrometry

Sequential fatty-acid release by mild-alkali treatment was found to be useful in establishing lipid A acylation patterns [5, 6]. Fatty acids being ester-linked in direct acylation of the di-glucosamine backbone (primary acylation) were released more readily than those bound to the hydroxyl groups of other fatty acids (secondary acylation). We set up experimental conditions for breaking: (1) only primary ester fatty acid bonds and (2) all fatty acid ester bonds. The conditions were established from our experience with numerous samples and proved that the technique can be scaled down if LPS or lipid A supply is limiting (*see Note 3*).

1. Dry under a stream of nitrogen, lipid A solutions (50  $\mu\text{L}$ ), obtained in Subheadings 3.2 and 3.3, or the equivalent amount of LPS in an Eppendorf<sup>®</sup> tube (*see Note 8*).
2. *In order to only liberate primary ester-linked fatty acids*, add 50  $\mu\text{L}$  of 28% ammonium hydroxide, sonicate, then close the tube, and stir for 5 h at 50 °C in a Thermomixer-system or in a simple thermostated bath using magnetic stirring (*see Notes 5 and 9*).
3. Dry the sample under a stream of nitrogen.
4. Take up the modified lipid A into 50  $\mu\text{L}$  of a mixture of chloroform:methanol:water (3:1.5:0.25; by vol.) or into 50  $\mu\text{L}$  of water when a LPS sample is treated. This sample is ready to be analyzed by MS, as described in Subheading 3.4 (*see Notes 1, 7 and 10*).
5. *In order to liberate both the primary and secondary ester-linked fatty acids*, repeat the above **steps 1–4** replacing ammonium hydroxide by 41% methylamine and keeping the mixture for 5 h at 37 °C under stirring.
6. If necessary, the liberated fatty acids can be recovered by extraction and tested by GC/MS.

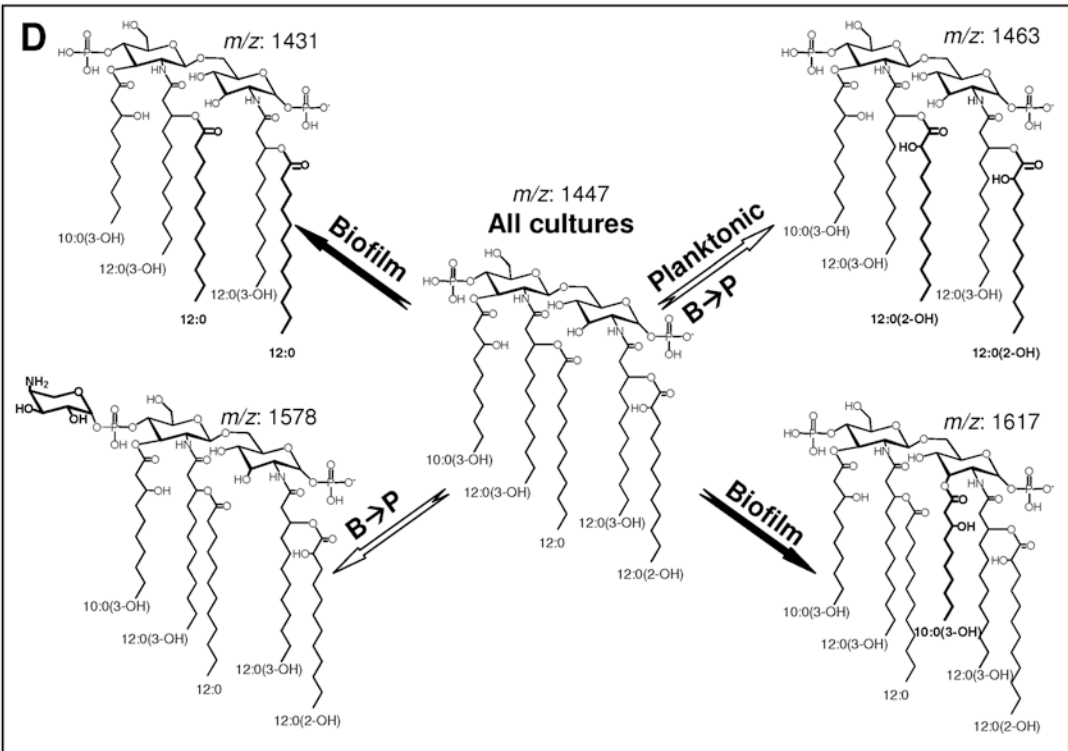
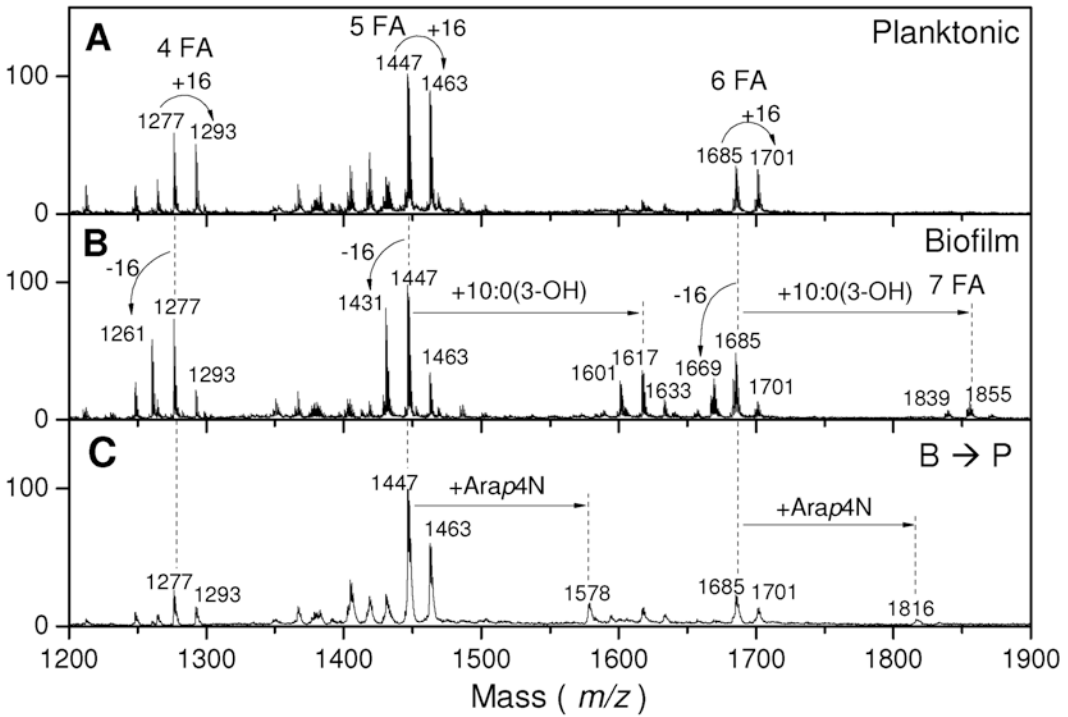
---

## 4 Examples of Analysis

### 4.1 Illustration of *P. aeruginosa* Lipid A Structural Modifications Induced by the Switch Between Planktonic and Biofilm Lifestyles [3]

The micro-method for lipid A isolation, directly from bacterial cells, is particularly useful for comparing the lipid A structures of different species and strains of a genus, as well as for the same bacteria grown under different culture conditions (e.g., media, temperature, oxygen tension, salt stress, bivalent ions concentration, etc.), or colonizing different niches (e.g., environmental isolates versus clinical isolates) (*see Note 3*).

Here, we give the example of lipids A isolated from *P. aeruginosa* strain PAO1 grown in planktonic culture, in biofilm, then in planktonic culture inoculated by biofilm-isolated bacteria (hereafter assigned as “B  $\rightarrow$  P” culture). Mass spectra of the lipids A, extracted by the micro-method from ~4 mg samples of dried bacteria cultured in these three ways, are presented in Fig. 2a–c, the corresponding structures are presented in Fig. 2d. The observed modifications contribute to higher inflammatory response in human monocytes [2].



**Fig. 2** Negative-ion MALDI mass-spectra of lipids A isolated (a) from a planktonic culture of PAO1 bacteria, (b) from biofilm ones, and (c) from Biofilm to planktonic cultures. 4 FA four fatty acids, 5 FA five fatty acids, 6 FA six fatty acids, 7 FA seven fatty acids. (d) Structures of the major hexa-acyl lipid A species appearing at  $m/z$  1617 and of the different penta-acyl lipid A species appearing at  $m/z$  1431, 1447, 1463, and 1578. Comparison of MALDI mass-spectra shows an important decrease of the 12:0(2-OH) content, and an increase of 12:0 content in the lipid A of biofilm cultured bacteria

## 4.2 Fatty Acids

### Positioning

### on the Di-GlcN

### Backbone,

### by Sequential Alkaline

### Treatment [6]:

### Example

### of *B. pertussis* Lipid A

The kinetics of esterified fatty acid liberation from lipid A samples was shown to be dependent on the substitution pattern, and could be used to determine the fatty-acid linkage. We first showed that liberation of primary ester-linked fatty acid (at C3 and C3') was much faster than that of the fatty acids in secondary ester linkages (at C2 and C2' acyloxyacyls), thus allowing a distinction between them by the application of the two-steps protocol described in Subheading 3.5 [6]. Furthermore, we observed that following kinetics of primary fatty-acid liberation, we could discriminate between the fatty acids located at the C3 and C3' positions.

The kinetics presented in Fig. 3a was obtained from *B. pertussis* Tohama I LPS sample [8] selected for its basically single lipid A molecular-species composition. In the initial mass spectrum ( $T = 0$ ), only one lipid A major peak is observed at  $m/z$  1559, corresponding to the structure displayed in Fig. 1. We followed the evolution of the mass spectra as a function of time, during the alkaline treatment (28% ammonium hydroxide at 50 °C). Mass spectra were recorded after treatment times of 8 min, 15 min, 30 min, 1 h, and 2 h. Drastic differences in the fatty-acid-releasing times were observed that related to their linkage position. Thus, at C3, the 10:0(3-OH) is completely liberated only after 8–15 min, transforming the initial penta-acyl lipid A into a tetra-acyl one ( $m/z$  1389), while at C3', the 14:0(3-OH) is only released after 1–2 h, leading to disappearance of the peak at  $m/z$  1389, and to the consecutive appearance of the one at  $m/z$  1163. The time of release of the acyloxyacyl 14:0 at C2' is again much longer. In fact, to completely cleave this bond requires the use of stronger hydrolysis conditions, as described in Subheading 3.5. Only after this second treatment, the peak at  $m/z$  953 remains in the spectrum, corresponding to a di-acyl lipid A with amide-linked 14:0(3-OH) fatty acids at C2 and C2' (data not shown). Similar kinetics was obtained from a lipid A sample (Fig. 3b). In this case, we used lipid A from *B. pertussis* 1414 strain that was obtained by direct hydrolysis of dried bacterial cells. Two major molecular species were present in the initial spectrum at  $m/z$  1559 (penta-acyl lipid A) and at  $m/z$  1333 (tetra-acyl lipid A with a free position at C3'). In conclusion, twice as long treatments were necessary to liberate the same fatty acids from the lipid A sample compared to LPS, probably owing to solubility differences between the two samples.

## 4.3 Illustration

### of the TEA-Citrate

### Method with

### *A. pleuropneumoniae*:

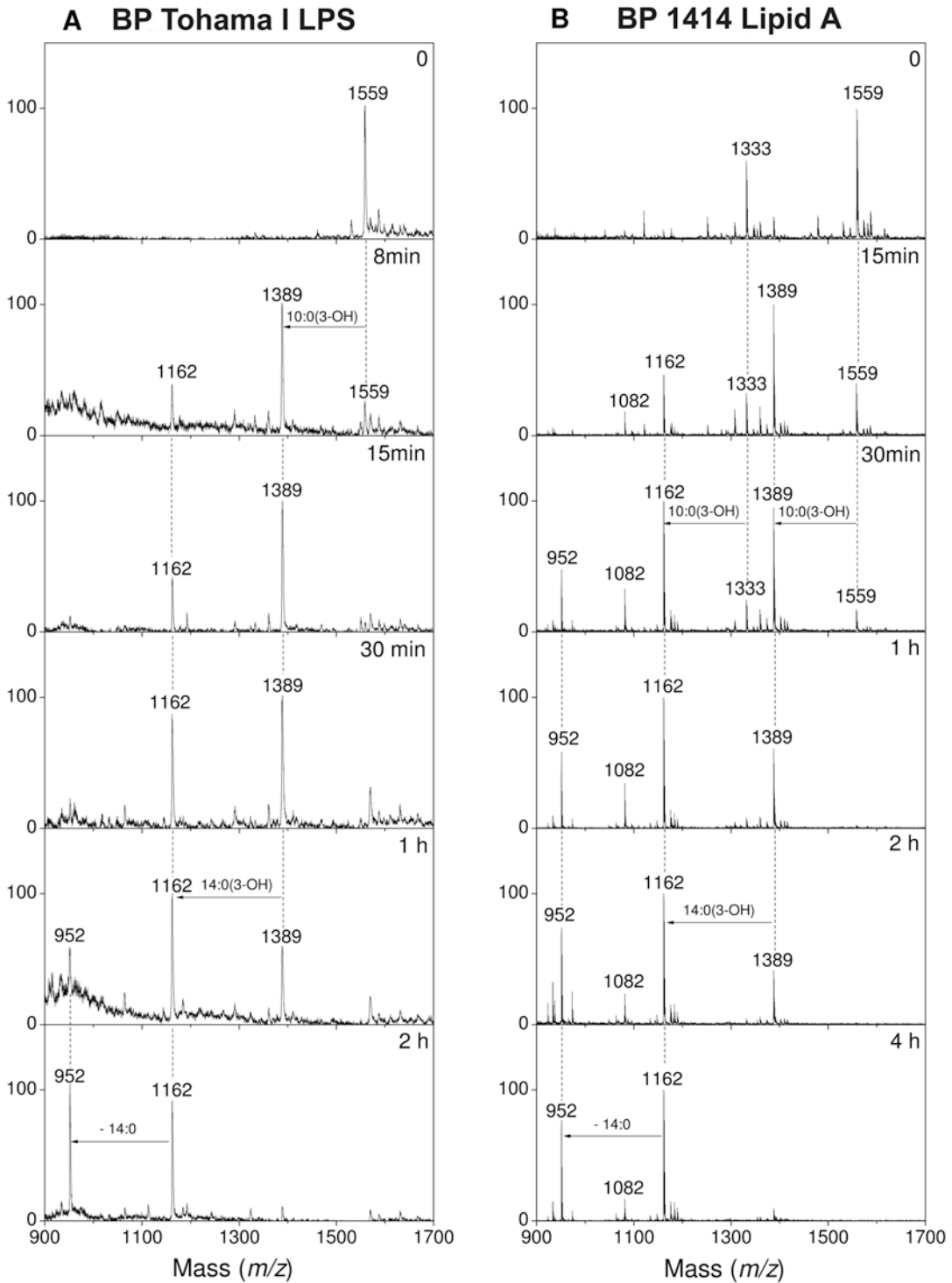
### Core and Lipid

### A Screening

### Among Three Field

### Isolates

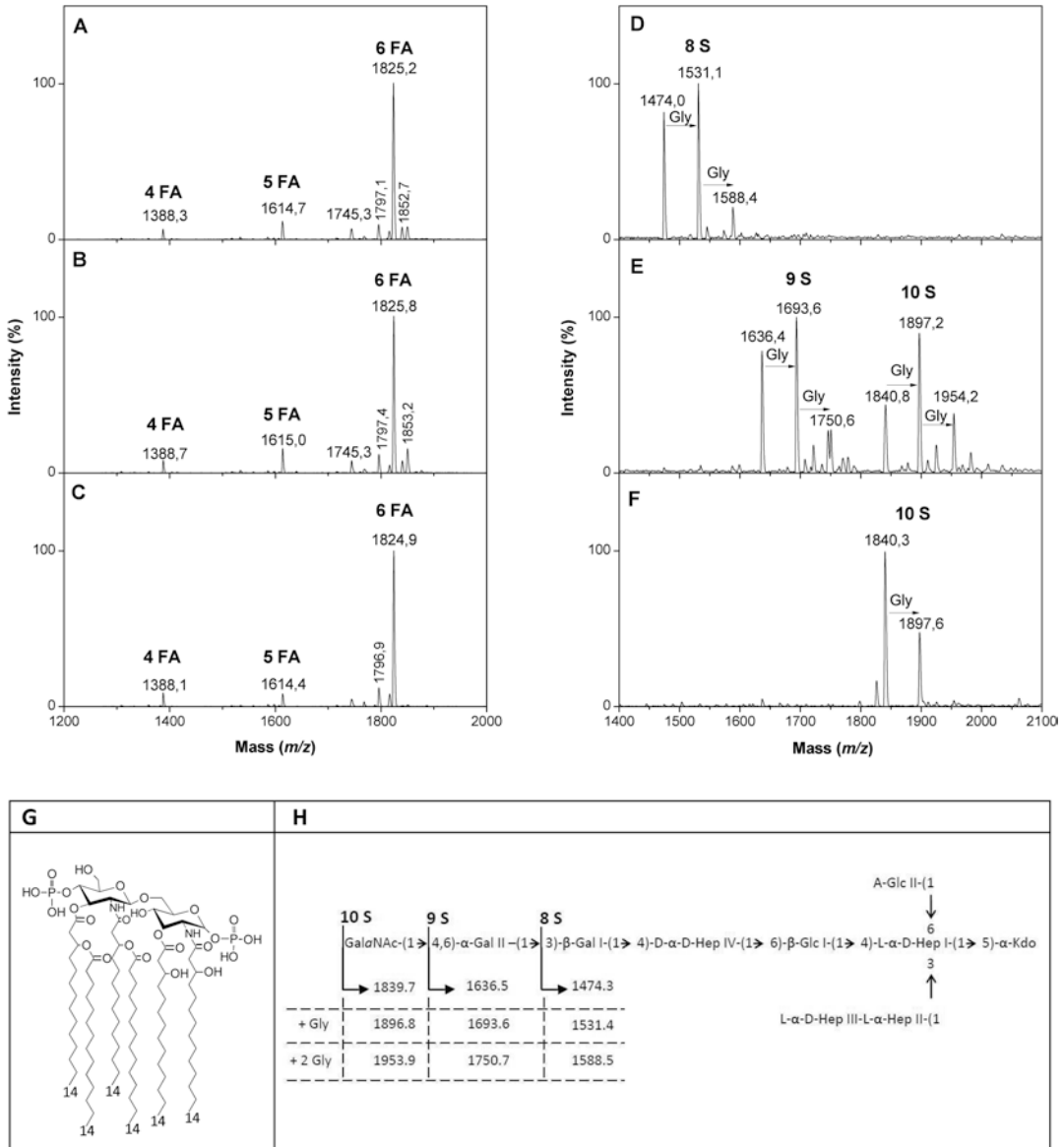
Cultures of three field isolates studied in this work were obtained from Professor Gottschalk laboratory, Montreal University, Faculty of Veterinary Medicine. The isolates were denoted as FMV94-9216, 00-7025 and 13-007 by the furnisher. All the three samples were of serotype 1 according to the structure of their capsular polysaccharides (*see Note 3*). Preliminary analyses of LPS by SDS-PAGE confirmed Smooth-type phenotypes to be similar to that of a reference serotype 1 strain [16, 17].



**Fig. 3** Negative-ion MALDI mass spectra of lipid A obtained from: (a) *B. pertussis* strain Tohama I LPS, and (b) *B. pertussis* strain BP1414 lipid A. The corresponding time of hydrolysis with 28% ammonium hydroxide at 50 °C is given in each spectrum. A clear difference is observed for fatty-acids release between the two samples, due to differences in solubility. Both strains also display different natural degrees of heterogeneity

Crude LPS were extracted from lyophilized bacteria [18]. TEA-citrate hydrolysis was applied to these samples as described in Subheading 3.2. MALDI-MS was performed as described in Subheading 3.4 (see Notes 1, 7, 8, and 10).

The lipid A profiles of the three isolates are very similar (Fig. 4a–c), with a major hexa-acyl molecular species appearing at



**Fig. 4** MALDI-MS analysis of lipid A and core OS regions of LPS from three *A. pleuropneumoniae* serotype 1 field isolates. (a, b, c) Lipid A negative-ion mass-spectra obtained respectively for isolates FMV94-9216, 00-7025, and 13-007. (d, e, f) Core OS negative-ion mass-spectra obtained respectively for isolates FMV94-9216, 00-7025 and 13-007. (g) Structure of the major hexa-acyl lipid A molecular species from *A. pleuropneumoniae*. (f) Complete and incomplete core OS structures of *A. pleuropneumoniae* serotype 1, observed for the three field isolates under study. S Sugar

$m/z$  1825 (Fig. 4g). Minor penta- and tetra-acyl molecular species are observed at  $m/z$  1615 and at  $m/z$  1389 respectively.

First, it should be noted that all core-OS peaks correspond to their anhydrous form. This is consistent with the fact reported earlier [17] that the only Kdo residue present is phosphorylated at the C4 position. As shown earlier [19], this substitution is lost during acid hydrolysis, by beta-elimination. Absence of satellite peaks at +18 mass units corroborates the fact that the Kdo molecule is 100% phosphorylated (*see Note 5*).

The core-oligosaccharide structure described for serotype 1 App [17] represents a deca-saccharide (Kdo + 4 Hep + 2 Glc + 2 Gal + GalNAc). The anhydrous form of this classical structure is observed at  $m/z$  1840 (*see Fig. 4e* and f). It is observed for the field isolates 13-007 and 00-7025 (Fig. 4f and e respectively). Isolate 00-7025 reveals the presence of nona-saccharides in which the terminal GalNAc residue is missing ( $m/z$  1636, Fig. 4e), and isolate FMV94-9216 reveals major octa-saccharide missing the terminal GalNAc-Gal disaccharide ( $m/z$  1474, Fig. 4d).

For all the tree isolates core-OS molecular species are observed substituted with one or two Gly residues at +57 or +114 mass units [9]. For isolate 13-007 (Fig. 4f) major molecular species correspond to nonsubstituted deca-saccharide with a smaller peak corresponding to one Gly substitution. For 00-7025 and FMV94-9216 isolates, the major peaks correspond to species substituted with one Gly residue ( $m/z$  1897, 1693, and 1531) as well as with two Gly residues ( $m/z$  1954, 1750, and 1588).

The LPS core moieties of this porcine pathogen were shown to be responsible for adhesion to respiratory tract cells and mucus [20]. The presence of Gly was reported to influence the vaccine capacities of the corresponding structures [21].

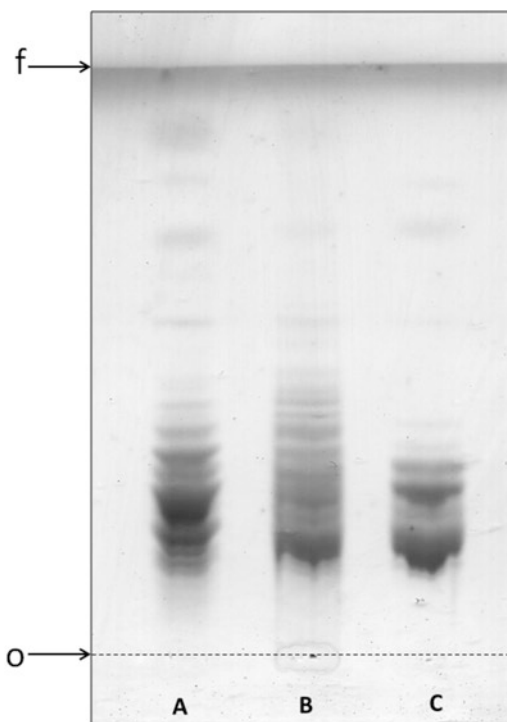
#### 4.4 Lipid A Screening of Three Commercial LOS Batches from *S.* Minnesota Re595

##### 4.4.1 TLC

It has been described in the early 90s [1] that different proportions of isobutyric acid-1 M ammonium hydroxide could be used as mobile phase for TLC analysis of LPS, lipid A, and core oligosaccharides. Here, a new ratio between the two components was shown to be efficient for comparing the three Re595 deep-rough mutants by HPTLC.

1. Deposit the solutions (2  $\mu$ L) of the three Re595 mutant LPS batches (25  $\mu$ g/ $\mu$ L in water) in lanes of 0.5 cm on the baseline of HPTLC Silica-gel-coated glass-plates.
2. Develop for 1.5 h for separating the different molecular species in the solvent mixture made of isobutyric acid:1 M ammonium hydroxide, (5:2; by vol.) (*see Note 4*).
3. Reveal the spots by charring (10% sulfuric acid in ethanol).

As shown in Fig. 5, the three LPS HPTLC profiles are fairly different and too much complicated for representing the well-known simplest LPS structure with lipid A and two Kdo molecules, they are often referred to. Sample A contains at least 8–10 molecular species,



**Fig. 5** HPTLC migration of the three samples (a) 50  $\mu\text{g}$  SmRe595-1, (b) 60  $\mu\text{g}$  SmRe595-2, (c) 30  $\mu\text{g}$  SmRe595-3 in isobutyric acid: 1 M ammonia (5:2; by vol.). The three samples display different profiles of migration indicating structural diversity and heterogeneity between them

sample B at least about the same number but with different types, and with differences in the relative intensity of each type. Sample C revealed to be the less heterogeneous, with 4–6 molecular species. To better characterize the structural heterogeneity of each sample, we performed a comparative MALDI-MS analysis of the three samples, as presented below.

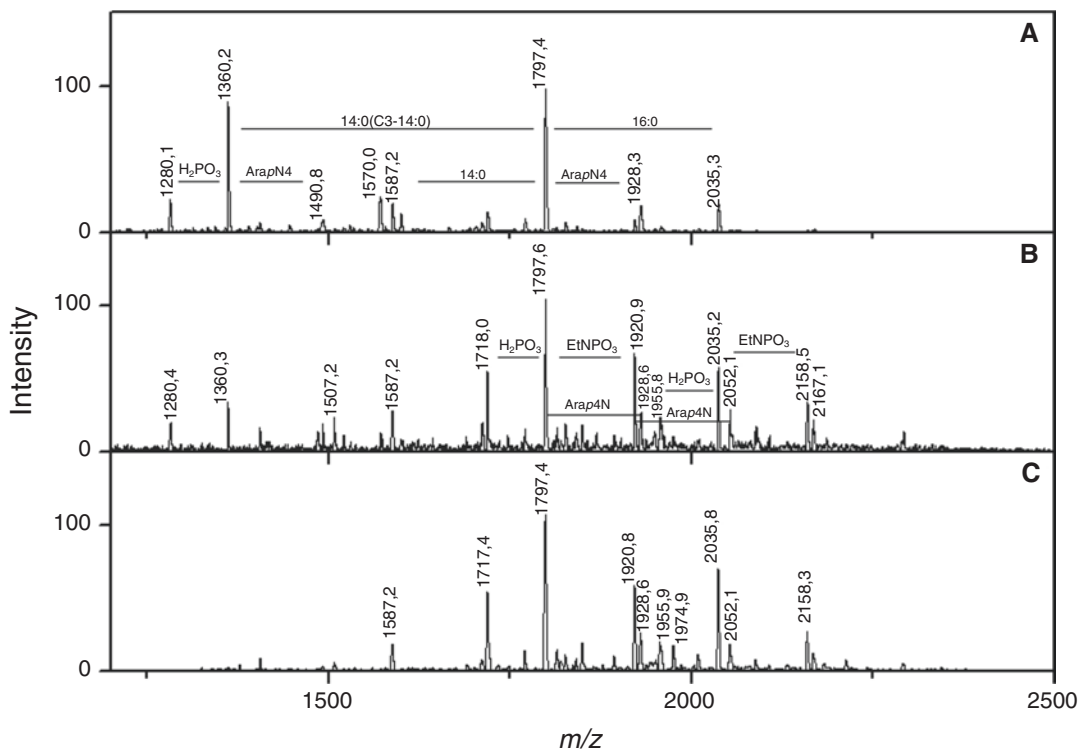
4.4.2 TEA-Citrate  
Hydrolysis of the Three  
TLC-Tested Commercial S.  
Minnesota Re595 LPS  
Followed by MALDI-MS  
Analysis of Their Lipids A

The TEA-citrate treatment was used to quickly compare the structures present in the three commercial LPS samples (*see Note 3*).

The lipid A is generally composed of six fatty acids: 14:0(3-OH) linked at C-2 and C-3, 14:0[3-O(12:0)] linked at C-2', and 14:0[3-O(14:0)] at C-3'. Posttranslational modifications often appear with, for example, esterification of the 14:0(3-OH) at C2 by a 16:0. The phosphate groups on Glc $p$ N I or II could be substituted by phosphoethanolamine (PEA) or Arap $4$ N residues [22]. As shown in Fig. 6, and expected after the TLC results, the three lipid A spectra showed differences and behaved differently upon hydrolysis (*see Notes 1, 7, 8, and 10*):

- For the three samples, the major peak appears at  $m/z$  1797 and corresponds to a hexa-acylated molecule. The dephosphorylated associated molecule ( $m/z$ ) is present in different amounts





**Fig. 6** Negative-ion MALDI mass-spectra of lipid A after TEA-Citrate treatment. (a) SmRe595-1, 45 min of treatment; (b) SmRe595-2, 20 min of treatment; (c) SmRe595-3, 45 min of treatment. *EtNPO3* ethanolamine phosphate, *H2PO3* phosphate group

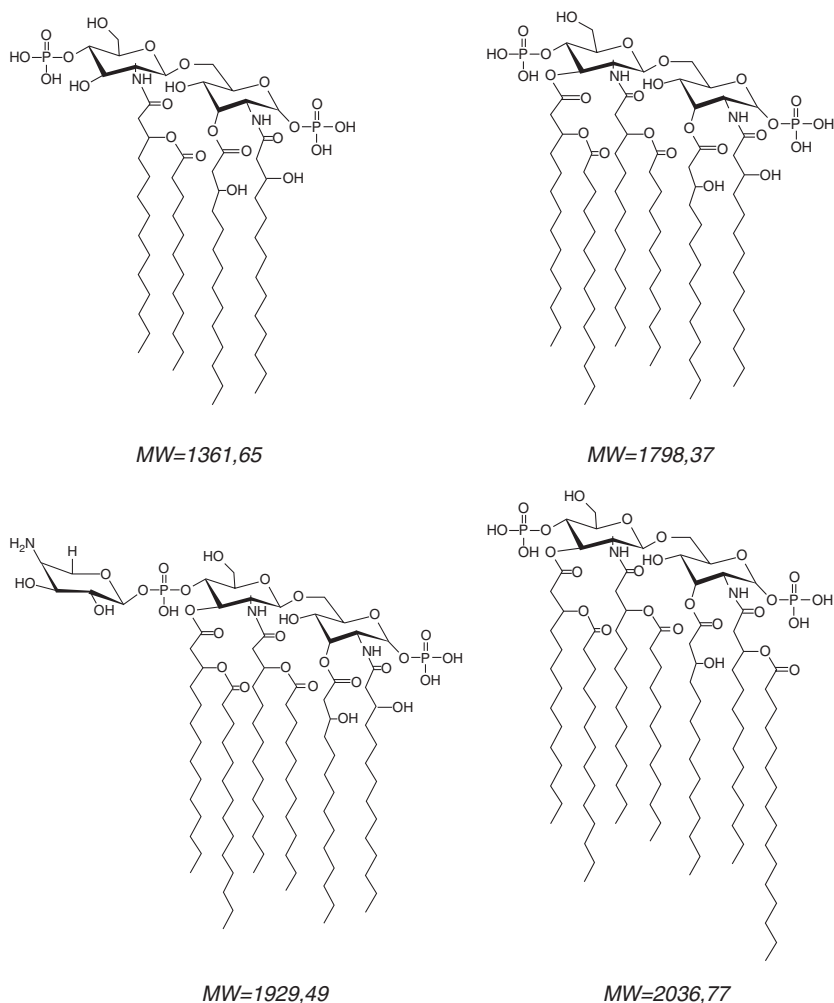
depending on the batch. Batch 2, which was submitted to a shorter time of hydrolysis (20 min. vs 45 min. For the two other samples), already presents the highest level of dephosphorylation, followed by batch 3 at 45 min. Batch 1 only displays a negligible peak of monophosphoryl lipid A. These results demonstrate that some important dephosphorylation can take place, even under very mild hydrolysis conditions. From the huge dephosphorylation level observed just after 20 min of treatment in sample 2, we have to consider that the preparation of this very sample leads to important physico-chemical differences, and this impacts the experiments, at the structural, and therefore biological level (*see Note 9*).

- The peak at  $m/z$  1920 corresponds to a hexa-acylated molecular species substituted with a PEA group. It is hardly detected in batch 1.
- The peak at  $m/z$  1928 corresponds to the 1797 molecular species substituted with an Arap4N residue. This substitution is present in the three batches.
- Lipid A molecular species containing 16:0 (corresponding to peaks at  $m/z$  2035) vary in intensity from one to another batch, and batches 2 and 3 display this palmitoylated form, also substituted with PEA ( $m/z$  2158).

- The penta-acylated lipid A molecular species are observed in the three batches at  $m/z$  1587 (with their dephosphorylated equivalent molecular species at  $m/z$  1507 for batch 2). Proportions vary greatly depending on each batch.
- The tetra-acylated lipid A molecular species appears as a major peak in the batch 1 spectrum, and such structures are known for their antagonist activity. It is present at a much smaller proportion in Batch 2 and absent from batch 3.

The corresponding described lipid A structures are given in Fig. 7. The influence of the number and nature of fatty acids in biological studies has already been stressed [23].

Different commercial batches from a single supplier, or from different ones, cannot be considered identical, just by referring to their name.



**Fig. 7** Structure of the predominant lipid A molecular species present in each sample. (a) SmRe595-1, (b) SmRe595-2, (c) SmRe595-3

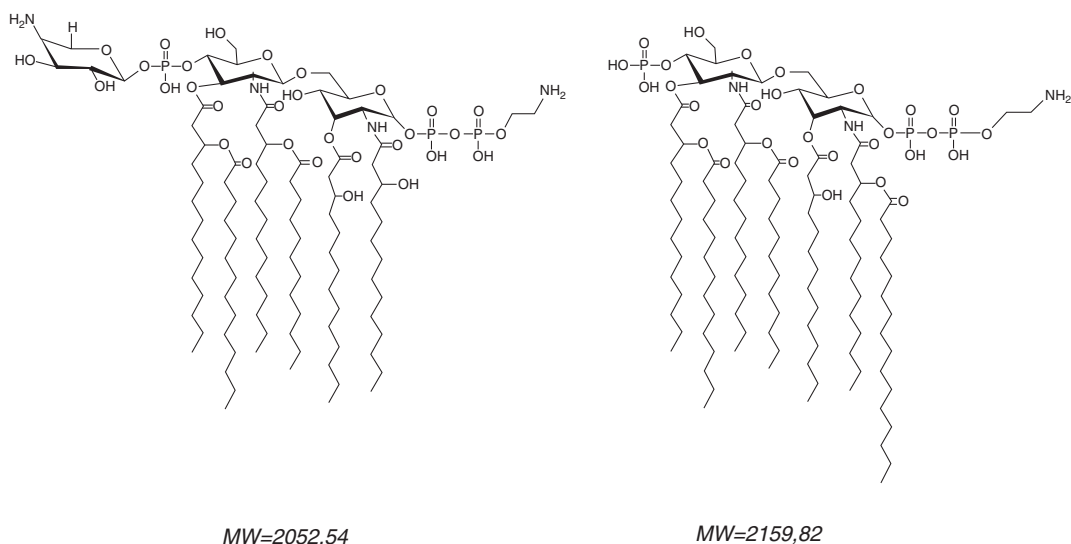


Fig. 7 (continued)

## 5 Notes

1. MALDI-MS is a very convenient MS process; however, depending on the temperature, humidity, or other variables the crystallization can be a critical step and has to be repeated if a spectrum is weak or absent.
2. Other MS methods can be successfully performed, but they are often more dependent on the presence of salt and other contaminants, thus requiring further purification steps.
3. The methods presented here are rapid, facile, and effective procedures for the analysis of microscale samples and for following the evolution and biosynthesis of lipid A structures under different growth conditions, as illustrated. The method can also be readily adapted to the verification of quality and reproducibility of the bacterial production.
4. Each method can be experimentally adapted to the starting material and to the amount of bacterial sample.
5. A phosphorylated terminal Kdo unit can render the glycosidic bond less labile [24]. Depending on the mass ratio between the glycosidic and lipid moieties, the degree of acylation of the lipid A, as well as the presence of polar groups, the solubility of the samples can be highly variable. As with all methods, adjustments in the experimental conditions are sometimes required.
6. In the large-scale LPS hydrolysis method (Subheading 3.1), the ethanol supernatant should remain clear during the SDS extraction step; otherwise, some lipid A might be lost in this fraction. If this is the case, ethanol should be concentrated and

added back to the sample before *re-extraction*, and the centrifugation step should be performed at a higher speed and lower temperature. The same applies to any “washing steps.”

7. During MS analysis, different ratios between sample and matrix volumes should be tested to obtain the best-quality spectra with respect to signal-to-noise ratio and to the resolution of the peaks.
8. Polypropylene screw cap Eppendorf® tubes can be used for all stages of microscale sample preparation. Preliminary tested and certified by the manufacturer tubes should be used. Use of tubes of unknown origin and poor plastic quality can lead to appearance in mass-spectra of plastic related artifact peaks (a polymer with 44 mass units repeating pattern is putatively attributed to polyethylene glycol). It is therefore recommended to test all new batches.
9. Each hydrolysis time is given as the optimum for the large amount of different LPS samples tested; however if some dephosphorylation is observed in the spectra, the acid hydrolysis time should be reduced and adjusted for a given LPS.
10. The desalting process performed with the Dowex resin before MS analysis is a crucial step. It can be easily effected by the deposition of a drop of water on a piece of Parafilm® on which a few grains of resin are added and mixed. Mixtures with chloroform are desalted in an Eppendorf® tube.

---

## Acknowledgments

Aude Breton is a recipient of a CIFRE grant in collaboration with the LPS-BioSciences company. We thank Pr. Gottschalk for his kind exchanges and expertise with App strains and isolates.

## References

1. Caroff MGL, Karibian D (1990) Several uses for isobutyric acid-ammonium hydroxide solvent in endotoxin analysis. *Appl Environ Microbiol* 56:1957–1959
2. Caroff M, Brisson JR, Martin A, Karibian D (2000) Structure of the *Bordetella pertussis* 1414 endotoxin. *FEBS Lett* 477:8–14
3. Ciornei CD, Novikov A, Beloin C, Fitting C, Caroff M, Ghigo JM, Cavaillon JM, Adib-Conquy M (2010) Biofilm-forming *Pseudomonas aeruginosa* bacteria undergo lipopolysaccharide structural modifications and induce enhanced inflammatory cytokine response in human monocytes. *Innate Immun* 16:288–301
4. El Hamidi A, Tirsoaga A, Novikov A, Hussein A, Caroff M (2005) Microextraction of bacterial lipid A: easy and rapid method for mass spectrometric characterization. *J Lipid Res* 46:1773–1778
5. Aussel L, Therisod H, Karibian D, Perry MB, Bruneteau M, Caroff M (2000) Novel variation of lipid A structures in strains of different *Yersinia* species. *FEBS Lett* 465:87–92
6. Tirsoaga A, El Hamidi A, Perry MB, Caroff M, Novikov A (2007) A rapid, small-scale procedure for the structural characterization of lipid A applied to *Citrobacter* and *Bordetella* strains: discovery of a new structural element. *J Lipid Res* 48:2419–2427

7. Caroff M, Deprun C, Richards JC, Karibian D (1994) Structural characterization of the lipid A of *Bordetella pertussis* 1414 endotoxin. *J Bacteriol* 176:5156–5159
8. Marr N, Tirsoaga A, Blanot D, Fernandez R, Caroff M (2008) Glucosamine found as a substituent of both phosphate groups in *Bordetella* lipid A backbones: role of a BvgAS-activated ArnT ortholog. *J Bacteriol* 190:4281–4290
9. Chafchaoui-Moussaoui I, Novikov A, Bhrada F, Perry MB, Filali-Maltouf A, Caroff M (2011) A new rapid and micro-scale hydrolysis, using triethylamine citrate, for lipopolysaccharide characterization by mass spectrometry. *Rapid Commun Mass Spectrom* 25:2043–2048
10. Karibian D, Brunelle A, Aussel L, Caroff M (1999) 252Cf-plasma desorption mass spectrometry of unmodified lipid A: fragmentation patterns and localization of fatty acids. *Rapid Commun Mass Spectrom* 13:2252–2259
11. Therisod H, Labas V, Caroff M (2001) Direct microextraction and analysis of rough-type lipopolysaccharides by combined thin-layer chromatography and MALDI mass spectrometry. *Anal Chem* 73:3804–3807
12. Rosner MR, Tang J, Barzilay I, Khorana HG (1979) Structure of the lipopolysaccharide from an *Escherichia coli* heptose-less mutant: I. Chemical degradations and identification of products. *J Biol Chem* 254:5906–5917
13. Caroff M, Tacken A, Szabo L (1988) Detergent-accelerated hydrolysis of bacterial endotoxins and determination of the anomeric configuration of the glycosyl phosphate present in the “isolated lipid A” fragment of the *Bordetella pertussis* endotoxin. *Carbohydr Res* 175:273–282
14. Caroff M, Karibian D (2003) Structure of bacterial lipopolysaccharides. *Carbohydr Res* 338:2431–2447
15. Caroff M, Karibian D, Cavaillon JM, Haeffner-Cavaillon N (2002) Structural and functional analyses of bacterial lipopolysaccharides. *Microbes Infect* 4:915–926
16. Altman E, Brisson JR, Perry MB (1986) Structure of the O-chain of the lipopolysaccharide of *Haemophilus pleuropneumoniae* serotype 1. *Biochem Cell Biol* 64:1317–1325
17. Caroff M (2004) Novel method for isolating endotoxins. PCT WOO4062690, 2005
18. Michael FS, Brisson JR, Larocque S, Monteiro M, Li J, Jacques M, Perry MB, Cox AD (2004) Structural analysis of the lipopolysaccharide derived core oligosaccharides of *Actinobacillus pleuropneumoniae* serotypes 1, 2, 5a and the genome strain 5b. *Carbohydr Res* 339:1973–1984
19. Lebbar S, Haeffner-Cavaillon N, Karibian D, Le Beyec Y, Caroff M (1995) 252Cf-plasma desorption mass spectrometry analysis of lipids A obtained by an elimination reaction under mild conditions. *Rapid Commun Mass Spectrom* 9:693–696
20. Ramjeet M, Deslandes V, St Michael F, Cox AD, Kobisch M, Gottschalk M, Jacques M (2005) Truncation of the lipopolysaccharide outer core affects susceptibility to antimicrobial peptides and virulence of *Actinobacillus pleuropneumoniae* serotype 1. *J Biol Chem* 280:39104–39114
21. Gamian A, Mieszala M, Lipiński T, Zielińska-Kuźniarz K, Gawlik-Jędrzyak M, Dzierzba K, Pietkiewicz J, Szeja W (2011) O-aminoacylation of bacterial glycoconjugates: from native structure to vaccine design. *Curr Pharm Biotechnol* 12:1781–1791
22. Karibian D, Deprun C, Caroff M (1993) Comparison of lipids A of several *Salmonella* and *Escherichia* strains by 252Cf plasma desorption mass spectrometry. *J Bacteriol* 175:2988–2993
23. Heine H, Rietschel ET, Ulmer AJ (2001) The biology of endotoxin. *Mol Biotechnol* 19:279–296
24. Caroff M, Lebbar S, Szabó L (1987) Do endotoxins devoid of 3-deoxy-d-manno-2-octulosonic acid exist? *Biochem Biophys Res Commun* 143:845–847

# Chapter 17

## Mass Spectrometry for Profiling LOS and Lipid A Structures from Whole-Cell Lysates: Directly from a Few Bacterial Colonies or from Liquid Broth Cultures

Béla Kocsis, Anikó Kilár, Szandra Péter, Ágnes Dörnyei, Viktor Sándor, and Ferenc Kilár

### Abstract

Lipopolysaccharides (LPSs, endotoxins) are components of the outer cell membrane of most Gram-negative bacteria and can play an important role in a number of diseases of bacteria, including Gram-negative sepsis. The hydrophilic carbohydrate part of LPSs consists of a core oligosaccharide (in the case of an R-type LPS or lipooligosaccharide, LOS) linked to an O-polysaccharide chain (in the case of an S-type LPS), which is responsible for O-specific immunogenicity. The hydrophobic lipid A anchor is composed of a phosphorylated diglucosamine backbone to which varying numbers of ester- and amide-linked fatty acids are attached and this part of the LPSs is associated with endotoxicity. The detailed chemical characterization of endotoxins requires long-lasting large-scale isolation procedures, by which high-purity LPSs can be obtained. However, when a large number of bacterial samples and their LPS content are to be compared promptly, small-scale isolation methods are used for the preparation of endotoxins directly from bacterial cell cultures. The purity of the endotoxins extracted by these methods may not be high, but it is sufficient for analysis.

Here, we describe a fast and easy micromethod suitable for extracting small quantities of LOS and a slightly modified micromethod for the detection of the lipid A constituents of the LPSs from bacteria grown in different culture media and evaluate the structures with mass spectrometry. The cellular LOS and lipid A were obtained from crude isolates of heat-killed cells, which were then subjected to matrix-assisted laser desorption/ionization mass spectrometry analysis. The observed ions in the 10-colony samples were similar to those detected for purified samples. The total time for the sample preparation and the MS analysis is less than 3 h.

**Key words** Crude cell lysate, Lipid A isolation, Matrix-assisted laser desorption/ionization mass spectrometry, Microextraction, LOS

---

## 1 Introduction

Lipopolysaccharides (LPSs) are components of the outer cell membrane of most Gram-negative bacteria. They are also called endotoxins, as they may possess a distinctive range of biological effects including lethal toxicity, typically by the intense activation of the

complement and cytokines system, leading to septic shock [1]. The basic structure of a *smooth* or S-type LPS molecule comprises three covalently linked regions: the “lipid A” phosphoglycolipid, the “oligosaccharide core,” and the “O-polysaccharide chain” (or “O-antigen”). A second type of LPSs, called *rough* or R-type LPS, or more correctly lipooligosaccharide, LOS, consists of only the lipid A and core moieties. Toxicity is associated with the lipid A moiety of LPSs and strongly depends on the acylation and phosphorylation patterns.

The development of techniques for the isolation of LPSs from the bacterial outer membrane is important with respect to investigations of LPS structure and function. Highly purified LPSs can be obtained by large-scale extraction and long-lasting (5–10 days) purification processes, such as the phenol–chloroform–light petroleum [2] or the hot phenol–water [3] methods. However, during the isolation procedure the LPSs might undergo degradation through loss of phosphate (P), phosphoethanolamine (PEtN), and/or fatty acyl chains, which are important in the host–pathogen interactions [4]. Several scaled-down analytical procedures have been developed in an effort to determine native LPS [5, 6] and particularly lipid A structures [7–9] as quick as possible from small numbers of bacterial cells. Routine and easy methods are essential, for instance, to determine structural variations resulting from varied cell growth conditions, or to compare LPSs from laboratory strains and clinical isolates, or in the quality control of endotoxins prepared for human vaccines.

Matrix-assisted laser desorption ionization (MALDI) mass spectrometry is widely used for the structural characterization of native LOS and chemically hydrolyzed lipid A from different bacteria, whereas the elucidation of intact LPS (containing several O-repeating units) with MS is often difficult [10].

Here, we present two extremely simple, small-scale isolation methods: one for LOS and another for the lipid A part of either LOS or LPS obtained directly from crude lysates of whole bacterial cells, followed by their MALDI-TOF MS analysis [11]. The micro-methods are based on the disruption of the intact cells—taken directly from agar plate cell cultures or liquid culture media—by the application of heat (100 °C) to release LPS or LOS from the cell membrane, and the partial purification by washing the culture pellets with pure water to remove intracellular components (nucleic acid, proteins) and other water-soluble cell wall materials. The lipid A constituents of the LPS/LOS are hydrolyzed directly from the heat-killed cells of R- or S-type bacteria with aqueous citric acid solution at elevated temperature (100 °C). The resulting LOS and lipid As are found in partially purified forms in the culture pellet, which can be isolated with centrifugation and directly subjected to MALDI-MS analysis without further purification or freeze-drying. The entire procedure, including sample preparation and MS analy-

sis, can be completed in less than 3 h, and it is probably the easiest procedure for preparing LOS or lipid A, practically free from protein and nucleic acid, although some bacterial contaminants (e.g., lipid co-extractives) may be present.

This quick and simple approach could provide a rapid and efficient way to give preliminary information on the LOS and lipid A structures from small quantities of cells, as illustrated analyzing the LOS of two model bacteria, *Salmonella Minnesota* R595 (Fig. 1) and *Shigella sonnei* R41 (Fig. 2), and the lipid A parts of two *Escherichia coli* bacteria (Fig. 3). The observed ions in the whole-cell lysate LOS samples were essentially similar to those detected for the purified samples. Due to the mild conditions of this method, biologically important but labile substituents (such as PEtN), which were not previously reported, have been detected (Fig. 2). Also, some dephosphorylation was observed in the purified R-LPS samples, as shown in their mass spectra.

---

## 2 Materials

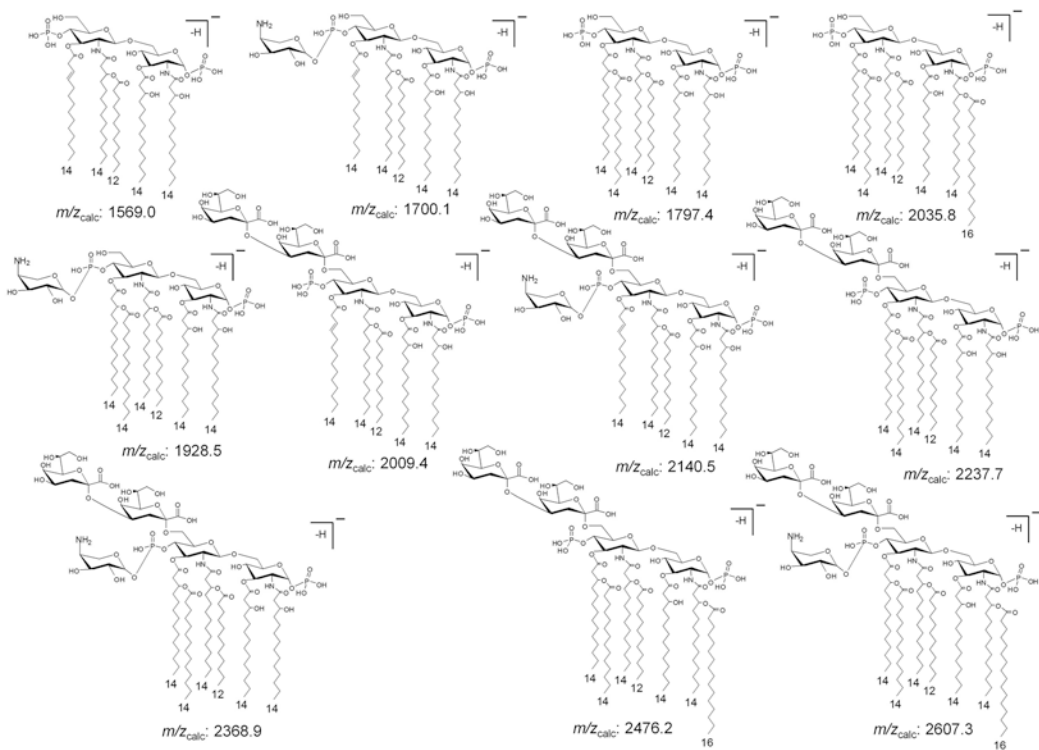
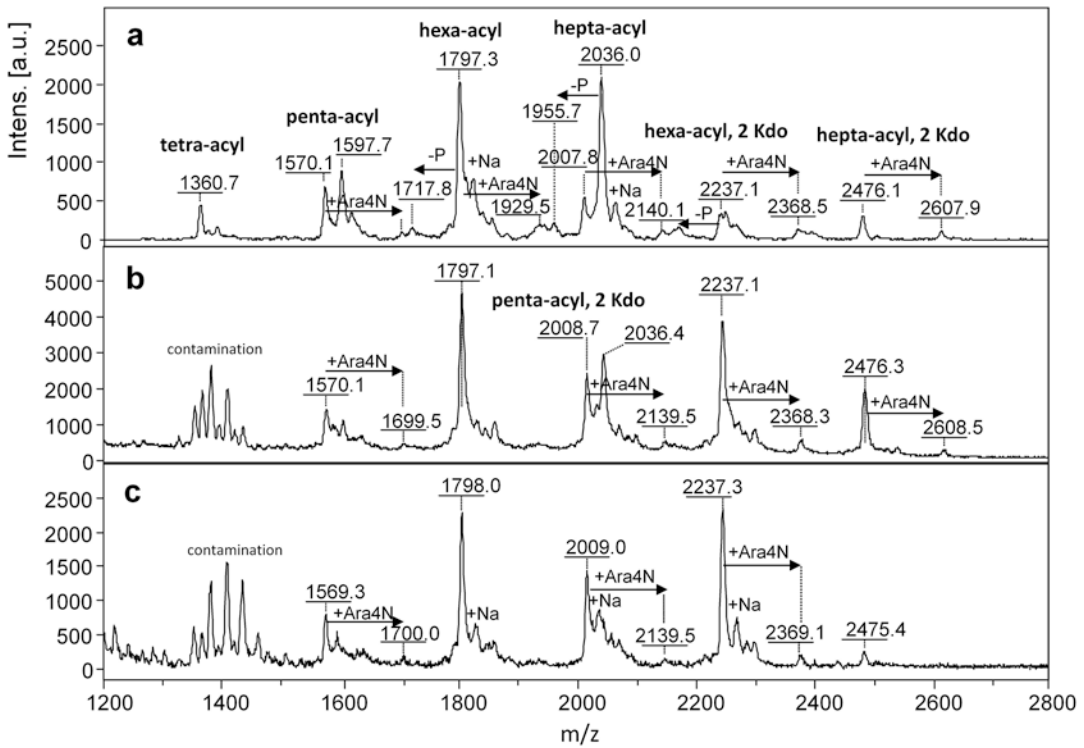
### 2.1 Preparation of Pure LOS

1. Gram-negative bacterial stock is stored at  $-80\text{ }^{\circ}\text{C}$ .
2. Distilled water and diethyl ether.
3. Rotary evaporator and flask.
4. Ultracentrifuge and rotors.
5. Lyophilizator (freeze-dryer).
6. Extraction of pure LOS is carried out with the phenol-chloroform-light petroleum [2]. For extraction, mix liquid phenol (90 g dry phenol and 11 mL water), chloroform, and light petroleum in a volume ratio of 2:5:8.

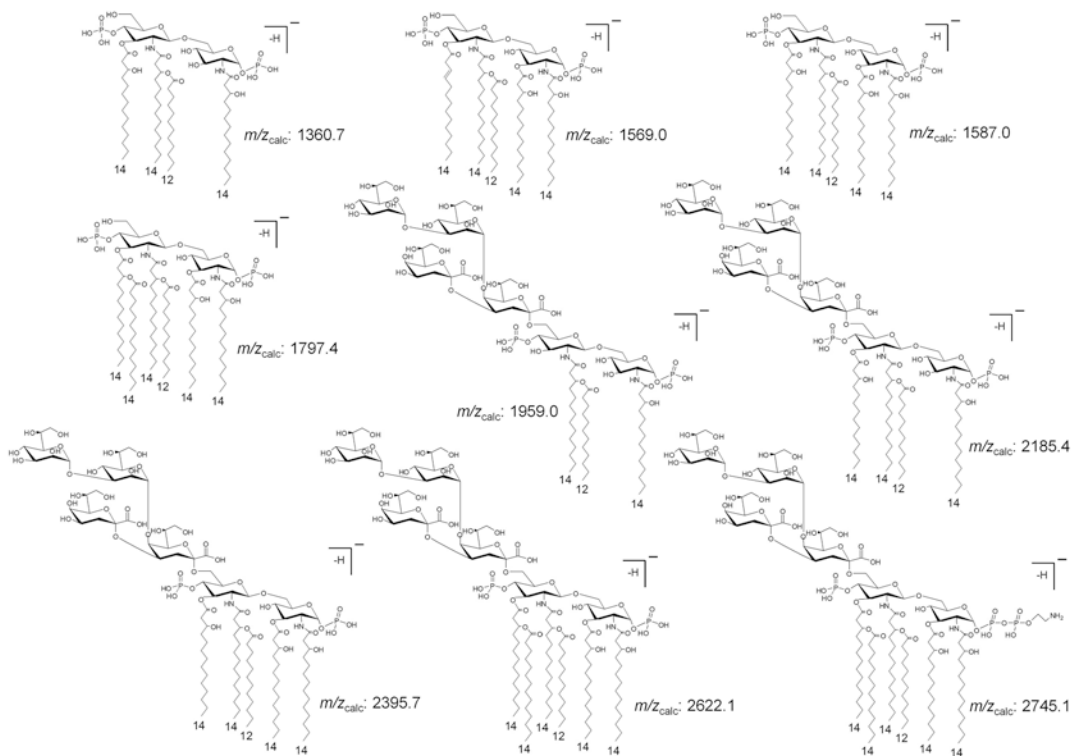
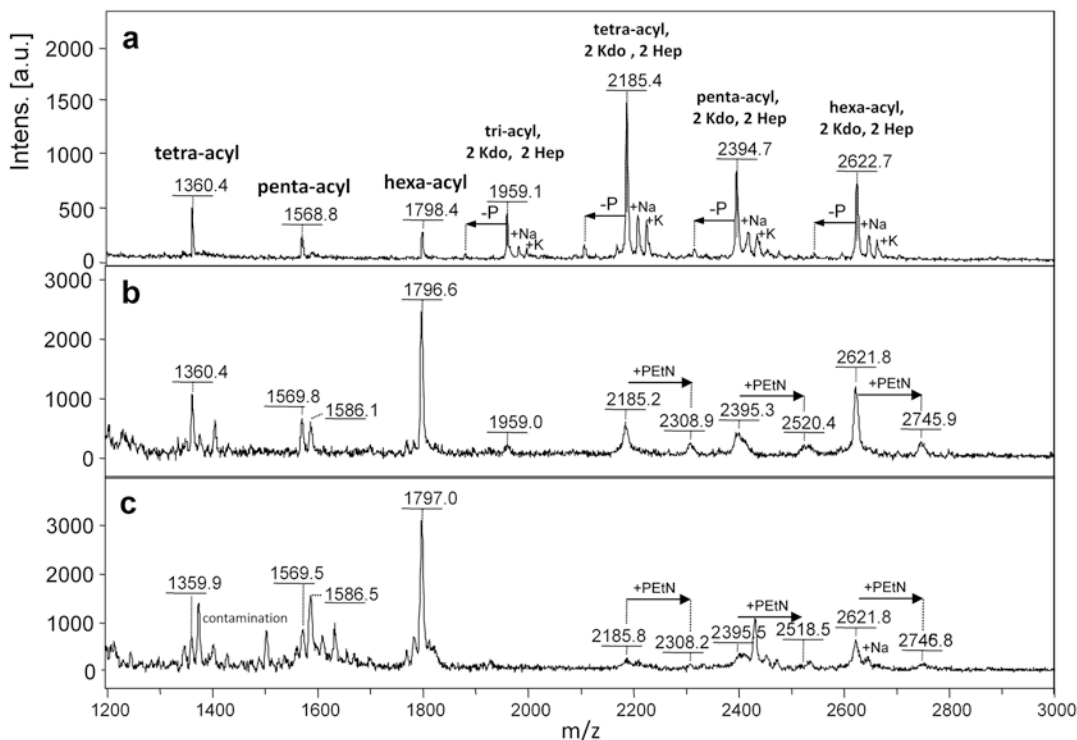
### 2.2 Bacterial Cell Culture and Lysis

1. Store Gram-negative bacterial stocks at  $-80\text{ }^{\circ}\text{C}$ . The following strains are used for the analyses of LOS with known structures: *S. Minnesota* R595, *S. sonnei* R41; and for the lipid A analysis: *E. coli* O55 and ATCC 25922.
2. Mueller-Hinton agar plates.
3. 3 mL Mueller-Hinton broth: 3.0 g Beef extract, 17.5 g casein acid hydrolysate, 1.5 g starch in 1 L deionized water. Store the broth at  $4\text{ }^{\circ}\text{C}$ .
4. High-purity water (LC-MS Chromasolv grade), citric acid.
5. Shaker incubator for maintaining cultures at  $37\text{ }^{\circ}\text{C}$ .
6. Microcentrifuge containing rotor for 1.5–2.0 mL microcentrifuge tubes.
7. Vortex mixer.

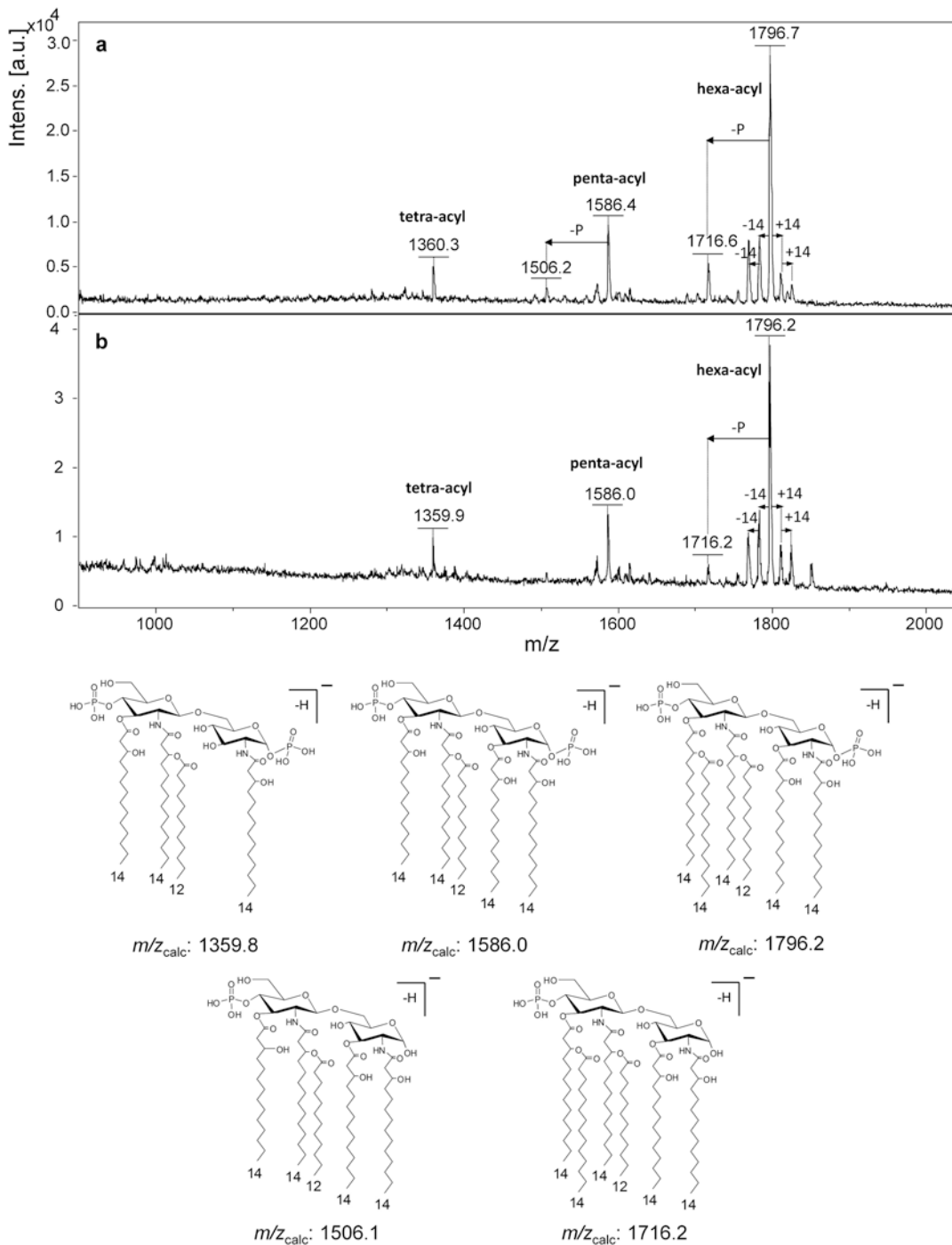




**Fig. 1** Negative-ion, linear mode MALDI-TOF mass spectra of purified LOS from *S. Minnesota* R595 (**a**) and R-type LPSs isolated from crude cell lysates of the *S. Minnesota* R595 bacterium grown in liquid medium (**b**) or on agar plate (**c**). DHB was used in (**a**) and (**c**), and THAP matrix in (**b**). +Na indicates a sodium adduct. The predicted structures for the detected  $[M-H]^-$  ions are shown. The full structure of the R-LPS from *S. Minnesota* R595 has been reported earlier [12]



**Fig. 2** Negative-ion, linear mode MALDI-TOF mass spectra of purified LOS from *S. sonnei* R41 (a) and LOS isolated from crude cell lysates of the *S. sonnei* R41 bacterium grown in liquid medium (b) or on agar plate (c). As MALDI matrix THAP was used. +Na and +K indicate a sodium and a potassium adduct, respectively. The predicted structures for the detected  $[M-H]^-$  ions are shown. The full structure of the LOS from *S. sonnei* R41 has been reported earlier [13]. The phosphate group (for instance at C1) could provide an attachment site for the PeiN moiety



**Fig. 3** Negative-ion, reflectron mode MALDI-TOF mass spectra of lipid A isolated from crude cell lysates of *E. coli* O55 (**a**) and *E. coli* ATCC 25922 bacteria (**b**) grown on agar plate. As MALDI matrix DHB was used. The predicted structures for the detected  $[M-H]^-$  ions are shown. Fatty acid alkane chain length heterogeneities for the major hexa-acylated ion at  $m/z$  1796 are indicated by the mass differences of  $\pm 14$  u ( $-\text{CH}_2-$  group)

### 2.3 MS

1. Dowex 50WX8-200 (H<sup>+</sup>) cation-exchange resin that has been converted into its ammonium form (*see Note 1*).
2. Ammonium-hydroxide solution, high-purity water.
3. Ultrasonic bath sonicator.
4. THAP matrix: saturated (ca. 20 mg/mL) solution of 2',4',6'-trihydroxyacetophenone monohydrate in acetonitrile:water (1:1, v/v) prepared in a microcentrifuge tube. Mix and bath-sonicate for 20 min. Vortex for 1 min and centrifuge at 12,000 × *g* for 5 min before use.
5. DHB matrix: saturated (ca. 10 mg/mL) solution of 2,5-dihydroxybenzoic acid in 0.1 M citric acid aqueous solution prepared in a microcentrifuge tube. Mix and bath-sonicate for 20 min. Vortex for 1 min and centrifuge at 12,000 × *g* for 5 min before use.
6. Peptide Calibration standard mixture (Bruker Daltonics, Bremen, Germany).
7. MALDI plate (stainless-steel target).
8. Mass spectrometer: e.g., Autoflex II MALDI-TOF MS instrument (Bruker Daltonics, Bremen, Germany) equipped with a 1.2 m drift tube and a nitrogen laser (337 nm) using a 50 Hz firing rate.
9. Flex Analysis 2.4 software packages (Bruker Daltonics, Bremen, Germany).

---

## 3 Methods

### 3.1 Preparation of Pure LOS

1. Grow the bacteria at 37 °C in Mueller–Hinton broth in a fermentor (e.g., Biostat U30D, Braun Melsungen, Germany) until the late logarithmic phase (about 10 h) and then collect the cells by centrifugation.
2. Extract LOS in pure form from acetone-dried bacteria according to the method of Galanos et al. [2], which is an efficient extraction method for LOS from rough bacteria. Suspend the bacteria (20 g) in 100 mL phenol-chloroform-light petroleum (2:5:8, v/v/v) and stir for 20 min. Precipitate the LOS by adding dropwise distilled water from the phenol phase which is obtained after the evaporation of chloroform and light petroleum in a rotary evaporator. Wash the precipitated LOS with diethyl ether, then dry in a fume hood, dissolve in distilled water, and centrifuge at 100,000 × *g* ultracentrifugation for 4 h. Re-suspend the sediment in distilled water and freeze-dry.
3. Store the LOS in lyophilized form, and prepare 1 mg/mL aqueous suspensions before use.

### 3.2 Isolation of LOS from Whole Cells

#### 3.2.1 Isolation of LOS from Cells Grown in Liquid Medium

1. Streak bacterial stocks on a Mueller-Hinton agar plate and grow overnight at 37 °C in a bacterial incubator.
2. Transfer one colony into 3 mL of culture medium (Mueller-Hinton broth) using a sterile inoculating loop and incubate at 37 °C on a shaker overnight.
3. Transfer the cell culture into an Eppendorf tube in two portions (1.5–1.5 mL) and centrifuge at  $6000 \times g$  for 3 min (transfer the second portion into the same Eppendorf tube after the supernatant from the first portion has been discarded). Discard the supernatant.
4. Re-suspend the pellets with 1 mL of water with a vortex and centrifuge at  $6000 \times g$  for 3 min. Discard the supernatant. Repeat this step two times.
5. Re-suspend the pellets with 1 mL of water and incubate at 100 °C for 30 min.
6. After cooling at room temperature, centrifuge the sample at  $12,000 \times g$  for 5 min. Discard the supernatant, and the sediment (ca. 10  $\mu$ L) containing LOS is ready to use.

#### 3.2.2 Isolation of LOS from Cells Grown on Agar Plate

1. Streak bacterial stocks on a Mueller-Hinton agar plate and grow overnight at 37 °C in a bacterial incubator.
2. Transfer ten colonies (about 1.5 mg) with a sterile inoculating loop into an Eppendorf tube containing 150  $\mu$ L of water and mix by repeatedly pipetting the suspension up and down.
3. Incubate the cell suspension at 100 °C for 30 min.
4. After cooling at room temperature, centrifuge the sample at  $12,000 \times g$  for 5 min. Discard the supernatant, and the sediment (ca. 10  $\mu$ L) containing the LOS is ready to use.

### 3.3 Isolation of Lipid A from Whole Cells

1. Streak bacterial stocks on Mueller-Hinton agar plate and grow overnight at 37 °C in a bacterial incubator.
2. Transfer ten colonies (about 1.5 mg) with a sterile inoculating loop into an Eppendorf tube containing 1 mL of 0.1 M citric acid aqueous solution (*see Note 2*).
3. Mix the cell suspension by vortexing and incubate at 100 °C for 90 min.
4. After cooling at room temperature, centrifuge the samples at  $12,000 \times g$  for 5 min. Discard the supernatant, and the sediment (ca. 10  $\mu$ L) containing free lipid A is ready to use.

### 3.4 Sample Preparation for Mass Spectrometry

1. Mix 10  $\mu$ L of pure LPS or LPS or lipid A from cell lysate suspensions with 10  $\mu$ L of 0.1 M citric acid solution in an Eppendorf tube and sonicate for 10 min (*see Note 3*).
2. Desalt 5  $\mu$ L of the sample suspension with some grains (ca. 5  $\mu$ L suspension) of Dowex 50WX8-200 ( $\text{NH}_4^+$ ) cation-exchange beads (*see Note 4*).

3. Deposit 0.5–1  $\mu\text{L}$  from this sample suspension onto a spot of the MALDI plate (*see Note 5*) and mix gently (*see Note 6*) with 0.5–1  $\mu\text{L}$  of the saturated solution of the DHB matrix (dissolved in 0.1 M citric acid solution) or the THAP matrix (dissolved in acetonitrile–water mixture (1:1, v/v)) (*see Note 7*) and analyze immediately after drying (*see Notes 8–10*).
4. Submit the sample on the target to MALDI–MS analysis and acquire spectra by scanning the sample for optimal ion signals.

### 3.5 Determination of Purified and Whole-Cell Lysate LOS and Lipid A Samples with MALDI-TOF Mass Spectrometry

The presented MS experiments were done in linear or reflectron modes (*see Note 11*). Acquire mass spectrometry data in the negative ionization mode at 19 kV, using pulsed ion extraction (allowing 120 ns delay between generation and extraction/acceleration of the ions). Adjust the laser power between 65% and 85% of its maximal intensity (*see Note 12*). Record the mass spectra of the LOS over the  $m/z$  range 900–5000, and of the lipid A over the  $m/z$  range 900–2500. One spectrum was the sum of 500 laser shots on a sample spot. Perform the calibration of the instrument externally using a peptide calibration standard. Identify the LOS and lipid A components according to the molecular mass of their quasimolecular  $[\text{M}-\text{H}]^-$  ions.

Examples of analysis are given for two LOS samples from *S. Minnesota* R595 (Fig. 1) and *S. sonnei* R41 (Fig. 2) with known structures [12, 13], and for two lipid A samples from *E. coli* O55 and ATCC 25922 (Fig. 3). In all cases, a complex pattern of ions was obtained in the mass spectra due to natural sample heterogeneity and in-source fragmentation [10]. Fine structural variations were attributable to different degrees of lipid A acylation and phosphorylation, as well as the presence of phosphate substituents [e.g., 4-amino-4-deoxy-L-arabinopyranose (Ara<sub>4</sub>N) or ethanolamine]. The high-intensity signals for the individual LOS components from the cell lysates were of the same  $m/z$ , as observed in the spectra of the high-purity LPS analogs. However, some differences could be seen in the relative signal intensities, the appearance of dephosphorylation products in the purified samples, and the detection of an additional PEtN substituent in the whole-cell lysate LOS sample of *S. sonnei* R41 (Fig. 2).

The mass spectra of the two *E. coli* lipid As (Fig. 3) isolated from whole cells displayed all the expected mass spectral peaks—with high signal-to-noise ratio—of an *E. coli*-type lipid A.

---

## 4 Notes

1. The Dowex 50WX8-200 ( $\text{H}^+$ ) cation-exchange resin has to be converted into its ammonium form suitable for sample desalting. Wash about 5 mL of the protonated form of the commercial resin two times with 25 mL of 1 M  $\text{NH}_4\text{OH}$  solution for

10 min, and once with 10 mL of 0.1 M  $\text{NH}_4\text{OH}$  solution for 10 min, with continuous stirring. Then, wash the resin five to six times with 10 mL of distilled water, until the supernatant is neutral and store in distilled water for usage.

2. By boiling the sample in 0.1 M citric acid (pH 2.9), the lipid part is cleaved from the terminal Kdo (3-deoxy-D-manno-oct-2-ulosonic acid) residue of the oligo- or polysaccharide part. We have obtained similar results by applying 1% (v/v) acetic acid (pH 3.5), the most widely used mild-acid hydrolysis method to liberate free lipid A from purified LPS [14]. However, with both procedures there is a risk of partially losing other acid-labile linkages, such as phosphate, phosphoethanolamine, amino sugars (e.g., Ara $\text{p}4\text{N}$ ), or ester-linked fatty acid.
3. Citric acid chelates the divalent cations (e.g.,  $\text{Ca}^{2+}$  or  $\text{Mg}^{2+}$ ) present in the sample, and promotes disaggregation of LPS and lipid A micelles by insertion between the molecules, thus improving solubility.
4. The presence of contaminating alkali metal ions (primarily  $\text{Na}^+$  and  $\text{K}^+$ ) can lead to adduct ion formation  $\{[M + n\text{Na} + m\text{K} - (n + m + 1)\text{H}]^-, n, m = 0, 1, 2, \dots\}$ . Multiple peaks (e.g.,  $M + 23 - 2$ ,  $M + 39 - 2$ ) provide complicated mass spectra and decrease sensitivity. The effect of alkali metal cations can be substantially reduced by rapid desalting with a cation exchange resin in the  $\text{NH}_4^+$  form. This desalting process can be carried out by the deposition of the resin suspension on the top of a small piece of Parafilm on which the same volume of sample suspension is added and mixed by repeatedly pipetting the suspension up and down. However, if the salts are not removed completely, small adduct signals could still be observed in the MALDI mass spectra.
5. Care must be taken not to pipette any Dowex beads along with the sample suspension onto the MALDI target, as they could disturb the matrix crystallization and/or analyte incorporation.
6. The matrix-sample suspension is mixed on the sample plate by repeatedly pipetting the suspension up and down. Putting the sample first, followed by the matrix layer onto the MALDI plate, does not change the quality of the MALDI spectra. However, the premixing of the sample and matrix solutions in a tube should be avoided as—in our case—this resulted in poor quality of the spectra.
7. In general, the selection of matrix is empirical. Even though DHB or THAP have proven to be the most efficient for the ionization of LPS-derived samples, other matrices such as ATT (6-aza-2-thiothymine) or CMBT (5-chloro-2-mercapto-benzothiazole)—this latter applied only for lipid A samples—are also commonly used for MALDI-TOF MS analysis in endotoxin research.

8. Allow the plate to air dry in an area where it will not be exposed to contaminants. The solvent evaporation using the DHB matrix from aqueous solution takes usually less than 5 min, while for the THAP matrix prepared in a volatile solvent takes usually less than 2 min.
9. After the rapid solvent evaporation, the matrix-sample mixture forms a crystalline precipitate. The DHB preparations result in a finely dispersed homogeneous matrix-sample layer with very dense, thick crystals, occasionally showing a white crust ring. By contrast, the THAP preparations show a heterogeneous spatial distribution with long crystals.
10. The crystallization can be a critical step and has to be repeated if a spectrum is not obtained. The best ion formation occurs from particular spots, called “hot spots,” a factor strongly increasing measurement times. It is therefore important to acquire and average many single-shot spectra from several positions (usually 10–20) within a given sample spot to gain representative sample data. One reason for hot spot formation could be the heterogeneous incorporation of the analyte into the co-crystallized matrix-sample complex.
11. The linear mode gives higher sensitivity but the resolution is more improved in the reflectron mode. Masses obtained with linear mode conditions are average masses, whereas in reflectron mode, the isotopic patterns of the molecules are resolved, so the mass values determined correspond to monoisotopic masses. Because of the lower resolution power of the TOF analyzer in linear mode, the peaks are broader compared to the measurements with reflectron mode conditions. The linear mode is used for the intact R-type LPS endotoxins and the reflectron mode is used for the lipid A samples.
12. As fluctuation of the laser power also contributes to the variable signal intensities of the samples, it should be adjusted to limit the acceptable analyte signal intensity above background noise before the spectra are averaged.

---

## Acknowledgments

The work was supported by the grants OTKA K-100667, OTKA K-106044 and UNKP-16-4-III New National Excellence Program of the Ministry of Human Capacities. Á.D. acknowledges the financial support of the János Bolyai Research Scholarship (Hungarian Academy of Sciences).



## References

1. Rietschel ET, Brade H (1992) Bacterial endotoxins. *Sci Am* 267:54–61
2. Galanos C, Lüderitz O, Westphal O (1969) A new method for extraction of R-lipopolysaccharides. *Eur J Biochem* 9:245–249
3. Westphal O, Lüderitz O, Bister F (1952) Über Die Extraktion Von Bakterien Mit Phenol Wasser. *Z Naturforsch B* 7:148–155
4. Nummila K, Kilpeläinen I, Zähringer U, Vaara M, Helander IM (1995) Lipopolysaccharides of polymyxin B-resistant mutants of *Escherichia coli* are extensively substituted by 2-aminoethyl pyrophosphate and contain aminoarabinose in lipid A. *Mol Microbiol* 16:271–278
5. Hitchcock PJ, Brown TM (1983) Morphological heterogeneity among *Salmonella* lipopolysaccharide chemotypes in silver-stained polyacrylamide gels. *J Bacteriol* 154:269–277
6. Thérisod H, Labas V, Caroff M (2001) Direct microextraction and analysis of rough-type lipopolysaccharides by combined thin-layer chromatography and MALDI mass spectrometry. *Anal Chem* 73:3804–3807
7. Yi EC, Hackett M (2000) Rapid isolation method for lipopolysaccharide and lipid A from Gram-negative bacteria. *Analyst* 125:651–656
8. El Hamidi A, Tirsoaga A, Novikov A, Hussein A, Caroff M (2005) Microextraction of bacterial lipid A: easy and rapid method for mass spectrometric characterization. *J Lipid Res* 46:1773–1778
9. Zhou P, Chandan V, Liu X, Chan K, Altman E, Li J (2009) Microwave assisted sample preparation for rapid and sensitive analysis of *H. pylori* lipid A applicable to a single colony. *J Lipid Res* 50:1936–1944
10. Kilar A, Dörnyei Á, Kocsis B (2013) Structural characterization of bacterial lipopolysaccharides with mass spectrometry and on- and off-line separation techniques. *Mass Spectrom Rev* 32:90–117
11. Kilar A, Péter Sz, Dörnyei Á, Sándor V, Kocsis B, Kilar F (2016) Structural analysis of endotoxins from bacterial culture suspensions. *J Mass Spectrom*—submitted for publication
12. Brandenburg K, Wagner F, Müller M, Heine H, Andrä J, Koch MHJ, Zähringer U, Seydel U (2003) Physicochemical characterization and biological activity of a glyco-glycerolipid from *Mycoplasma fermentans*. *Eur J Biochem* 270:3271–3279
13. Kilar A, Dörnyei Á, Bui A, Szabó Z, Kocsis B, Kilar F (2011) Structural variability of endotoxins from R-type isogenic mutant of *Shigella sonnei*. *J Mass Spectrom* 46:61–70
14. Wilkinson SG (1996) Bacterial lipopolysaccharides—themes and variations. *Prog Lipid Res* 35:283–343

# INDEX

## A

- Actinobacillus pleuropneumoniae* ..... 169, 171, 177–180
- Agarose gel ..... 41, 43–45, 128–129
- Analysis
  - multivariate ..... 120
  - principal component ..... 120, 121
- Aptamer ..... 9–21, 61–67, 134
- Assay
  - fluorescence ..... 31
  - toxicity ..... 10, 29, 33, 38, 187

## B

- Bacillus anthracis* ..... 61, 81
- Bacillus cereus* ..... 61–67, 81
- Bacillus thuringiensis* ..... 61, 67, 81
- Bacteriophage
  - F8 ..... 108
  - HAP1 ..... 108
  - T4 ..... 108, 110
- Bioconjugate probes ..... 133–141
- Biosensing
  - electrochemical ..... 17–19
- Biosensors ..... 9–21, 134, 143
- Bloom ..... 85, 91
- Bordetella pertussis* ..... 168, 171, 172, 177, 178
- Botulism
  - protein ..... 9–21

## C

- Chitosan
  - hydrogel ..... 128, 129, 132
  - LPS complex ..... 129, 130, 132
- Cholera ..... 1–7
- Cigarette extract ..... 144, 146–148
- Clostridia* ..... 38
- Clostridium tetani* ..... 37–45
- Colistin ..... 128–129, 131, 132, 134
- C-18 silane ..... 133–141

## D

- 3-Deoxy-D-*manno*-oct-2-ulosonic acid (Kdo) ..... 196

## E

- Electrochemical DNA (E-DNA) ..... 9–11
- Electropolymerization ..... 51, 54, 58
- EndoLysa test ..... 108, 110, 111
- Endotoxin
  - profiles ..... 153–156, 158, 168
  - removal ..... 65, 85–93, 107–112, 138, 163
  - unit (EU) ..... 107
- Enzyme-linked immunosorbent assay (ELISA) ..... 1, 5, 50, 95, 108, 134, 143, 145, 148
- Escherichia coli* ..... 30, 33, 107–112, 135, 144, 145, 154, 156, 158, 189, 192, 195

## F

- Fatty acids
  - ester-linked ..... 168, 175, 177, 196
  - positioning ..... 177
  - sequential liberation ..... 171, 175
- Fealden software ..... 12, 14, 15, 20
- Food
  - pathogen ..... 61
  - poisoning ..... 61
- Fourier transform infrared spectroscopy (FTIR)
  - acquisition ..... 116–118, 122
  - amide I/II region ..... 114
  - fatty acid region ..... 114
  - fingerprint ..... 114, 121, 151–164
  - frequencies ..... 18, 19, 114, 123
  - mixed region ..... 114
  - pre-processing ..... 118, 119
  - wavenumber region ..... 113, 114, 123

## G

- Gold
  - colloidal ..... 95–97, 102
  - electrode ..... 10, 12, 14, 15
- Gram-negative ..... 107, 113, 133, 151, 152, 159, 160, 167, 169, 187, 189
- Gram-positive ..... 37, 61

**H**

Hek293 cells  
TLR-transfected.....144  
Hemocytometer..... 31, 90

**I**

Immunoaffinity .....70  
Immuno-sensors.....49–58  
Interleukin-8 .....145

**L**

Laser interferometry.....125–132  
Limulus amoebocyte lysate (LAL) ..... 108–111, 134, 143, 144  
Lipid A  
isolation ..... 168, 170, 172, 175, 192  
screening.....177–183  
Lipooligosaccharide (LOS) ..... 114, 151, 167, 188  
Lipopolysaccharide (LPS) ..... 152, 158, 159, 188  
aggregates ..... 50, 140, 168  
chemotype .....151–164  
immobilization .....138–140  
molecular mass determination ..... 153, 156, 163, 168  
R-type preparation .....152, 156, 157, 159, 188, 190, 197  
S-type preparation ..... 152, 158, 159, 188  
Lipoprotein  
FSL-1 .....145, 147–148  
Liquid chromatography .....29, 30, 93  
*Listeria monocytogenes*  
detection ..... 49, 51–53, 55–56  
Listeriosis .....49  
Loop-mediated isothermal amplification assay (LAMP) ..... 1, 38, 41–42, 45

**M**

Magnetic beads  
antibody-coated .....75–76  
aptamer-linked ..... 62, 64, 67  
nanosilicate platelets (MNSP)  
preparation..... 17, 62, 64, 87–90, 96–98, 109, 159–162, 168, 185, 189  
Mass spectrometry  
MALDI-TOF ..... 70, 172, 188, 190, 191, 193, 195  
tandem..... 65, 72, 77, 78  
Microarray  
antibody.....50  
Microchip electrophoresis  
covalent binding .....80, 152  
fluorescent dye .....152, 154, 159–160, 162, 164  
noncovalent binding .....152

*Microcystis aeruginosa*  
growth inhibition test ..... 87, 90–91  
settling enhancement test .....85–93  
Microscopy  
cytofluorometry .....27  
Monolayers  
self-assembled (SAM) .....133–141  
MTS assay .....25, 28  
Mycotoxins ..... 5, 65, 92–93, 144  
microcystin LR  
adsorption test .....92–93  
quantification..... 5, 65, 93, 144  
ochratoxin A .....95–104  
zearalenone .....95–104

**N**

Nanoparticles  
gold..... 95, 97, 134, 135  
magnetic labeling.....50  
Neurotoxin  
botulinum ..... 10, 12, 13

**P**

Pathogen-associated molecular patterns (PAMP) .....143, 144  
Piranha solution ..... 135, 138, 140  
Polymerase chain reaction (PCR)  
amplification ..... 1, 38–44, 50, 66  
FLASH based .....38, 44  
real-time .....10, 50, 52, 61–67, 126  
sequencing ..... 40–41, 43, 72  
Polymyxin B ..... 108, 136  
Proteomics ..... 70, 75, 80  
*Proteus mirabilis* ..... 113–123  
*Pseudomonas aeruginosa*  
biofilm ..... 127, 168, 175–177  
exotoxin A .....29, 34  
planktonic .....168, 175–177  
Pyrrole-NHS ..... 50–51, 53–54, 56

**Q**

Quickfold module.....20

**R**

Refractive index..... 58, 125, 126  
Ricin protein  
preparation.....13, 17

**S**

*Salmonella*  
*enterica* sv. *Minnesota* .....153  
*Minnesota* .....153, 156–158, 169, 171, 180–183, 189, 190, 195

SDS-PAGE  
 silver staining.....152  
 Selected reaction monitoring (SRM) .....70  
*Shigella sonnei*.....153, 157, 189, 191, 195  
 Smoke extract ..... 144, 146–148  
 Spore  
     lysis .....62, 65  
     trapping .....61–67  
 Surface enhance raman scattering (SERS) .....50  
 Surface plasmon resonance (SPR)  
     imaging (SPRI) .....50–58

**T**

Test strip  
     immunochromatographic ..... 1–7, 95–104  
 Tetanospasmin.....39  
 Tetanus .....37–39, 45  
 TetR gene .....39  
 TetX gene .....38–45  
 Thin-layer chromatography (TLC).....168  
 Toll-like receptor (TLR) ..... 134, 144, 149, 150

Toxin

AB .....25–35  
 cholera .....1–7  
 detection .....1–7  
 diphtheria .....29, 34  
 inhibitors ..... 26, 29–32, 34  
 shiga .....27

**V**

Vero cell..... 26, 27, 31–33  
*Vibrio cholerae*.....1–6  
 Voltammetry.....12, 15, 16, 18, 19

**W**

Whole-cell lysate..... 152, 153, 156, 158, 161, 187–197

**Y**

*Yersinia pestis*  
     inactivation .....71, 77  
     protein extraction.....71, 77